

# Development of Novel *Mycobacterium tuberculosis* Enoyl Acyl Carrier Protein Reductase Inhibitors

**THESIS**

Submitted in partial fulfilment  
of the requirements for the degree of  
**DOCTOR OF PHILOSOPHY**

by

**PEDGAONKAR GANESH SITARAM**

**ID No 2011PHXF431H**

Under the Supervision of  
**D. SRIRAM**



**BITS Pilani**

Pilani | Dubai | Goa | Hyderabad

**BIRLA INSTITUTE OF TECHNOLOGY AND SCIENCE, PILANI**

**2014**

# **BIRLA INSTITUTE OF TECHNOLOGY AND SCIENCE, PILANI**

## **CERTIFICATE**

This is to certify that the thesis entitled “**Development of Novel *Mycobacterium tuberculosis* Enoyl Acyl Carrier Protein Reductase Inhibitors**” and submitted by **PEDGAONKAR GANESH SITARAM** ID No. **2011PHXF431H** for award of Ph.D. of the Institute embodies original work done by him under my supervision.

Signature of the Supervisor:

Name in capital letters : **D. SRIRAM**

Designation : **Professor**

Date:

## Acknowledgement

---

*It is a moment of gratification and pride to look back with a sense of contentment at the long travelled path, to be able to recapture some of the fine moments and to be able to thank the infinite number of people, some of whom were with me from the beginning, some who joined me at some stage during the journey, whose rally round kindness, love and blessings have brought me to this day. I wish to thank each and every one of them with all my heart.*

*Foremost, I would like to express my sincere gratitude to my advisor **Prof. D. Sriram** for the continuous support of my Ph.D. study and research, for his patience, motivation, enthusiasm, and immense knowledge. His guidance helped me in all the time of research and writing of this thesis. I could not have imagined having a better advisor and mentor for my Ph.D. study.*

*I deeply acknowledge and my heartfelt thanks to **Prof. P. Yogeewari**, Department of Pharmacy, BITS, Pilani-Hyderabad campus, for her valuable suggestions, guidance and precious time which she offered me throughout my research.*

*I gratefully acknowledge my DAC member **Dr. A. Sajeli Begum** for her understanding, encouragement and personal attention which have provided good and smooth basis for my Ph.D. tenure.*

*I take this opportunity to thank **Prof. Bijendra Nath Jain**, Vice-Chancellor (BITS) and Director **Prof. V.S. Rao** (Hyderabad campus), for allowing me to carry out my doctoral research work in the institute.*

*I am thankful to **Prof. S.K. Verma**, Dean, Academic Research Division, BITS-Pilani and **Dr. Vidya Rajesh**, Associate Dean, Academic Research Division, BITS-Pilani, Hyderabad campus for their co-operation and encouragement at every stage of this research work.*

*I would like to express my gratitude to **Dr. Shrikant Y. Charde**, Head of the department, Pharmacy, for providing me with all the necessary laboratory facilities and for having helped me at various stages of my research work.*

*I sincerely acknowledge the help rendered by **Dr. V. Vamsi Krishna**, and other faculty members at the BITS-Pilani, Hyderabad campus. It's my pleasure to acknowledge their constant moral support.*

*I owe a great deal of appreciation and gratitude to **Dr. Vinay Kumar Nandicoori**, Scientist, and his group at National Institute of Immunology, New Delhi, India for providing Mycobacterium tuberculosis InhA clone.*

*I take this opportunity to sincerely acknowledge the Department of Science & Technology (DST), Government of India, New Delhi, for providing financial assistance in the form of INSPIRE Fellowship which buttressed me to perform my work comfortably. Also, I thank Aditya Birla Science & Technology Company Limited Mumbai, India for funding the project.*

*It's my fortune to gratefully acknowledge the support of some special individuals. Words fail me to express my appreciation to all my friends **Jean, S. Ganesh, Manoj, Bobesh, Renuka, Shalini, Brindha, Sridevi, Brahmam, Ram, Mahibalan, Patrisha, Mallika, Madhubabu, Praveen, Suman, Poorna, Gangadhar, Saketh, Srikanth, Venkat, Radhika, S. Reshama, S. Priyanka, Anup, Omkar and P. Santosh** for the time they had spent for me and making my stay at campus a memorable one. I take this opportunity to thank one and all for their help directly or indirectly.*

*I express my thanks to our laboratory assistants, **Mr. Srinivas, Mrs. Saritha, Mr. Rajesh, Mr. Ramu**, also **Mrs. Rekha and Mr. G. Ganesh**.*

*Most importantly to my wife, **Amruta**. You have supported me in the darkest times and believed in me even when I did not believe in myself. Your tireless effort enabled me to take the time necessary to complete this work. I've always loved your joyful spirit and this spirit provided the boost that made even the longest hours enjoyable. This would not have been possible without you. No words can express how grateful I am for your love and support and how very much I love and appreciate you.*

*I would like to begin by dedicating this piece of work to **my parents**, whose dreams had come to life with me getting the highest degree in education. I owe my doctorate degree to my parents who kept with their continuous care, support and encouragement my morale high. Thanks are due if I don't dedicate this thesis to my brother **Satish** and sister **Surekha**, and other family members, whose constant and continuous support, love and affection made me reach this height. Also, the most little and adorable family members Aaditi, Yash and youngest of all, Radha kept the delight of life ignited.*

*Lastly, and above all, I would like to thank the God Almighty; for all that he has given to me.*

*To those I may have Wronged,*

*I ask Forgiveness.*

*To those I may have Helped,*

*I wish I did More.*

*To those I Neglected to help,*

*I ask for Understanding.*

*To those who helped me,*

*I sincerely Thank you*

*So much...*

***Date:***

***Pedgaonkar Ganesh Sitaram***

## Abstract

---

In the present study we focused on achieving promising antimycobacterial cellular potency through developing potential *Mycobacterium tuberculosis* InhA (2-*trans*-enoyl-acyl carrier protein reductase) direct inhibitors.

Utilizing the moderately active hits identified by our research group earlier *via* virtual screening efforts, four different chemo-types of inhibitors were selected as initial InhA leads. The obtained leads were taken up for hit expansion by chemical synthesis and library of a total 123 molecules from 4 different series/leads as InhA inhibitors was synthesized that displayed considerable *in vitro* enzyme efficacy and bactericidal activity against *Mycobacterium tuberculosis* H37Rv strain. Compound **PR\_15** (1-(1,5-dimethyl-3-oxo-2-phenyl-2,3-dihydro-1H-pyrazol-4-yl)-3-(4-methoxyphenyl)urea) emerged as the most potent molecule displaying 93.12 % inhibition of *Mycobacterium tuberculosis* InhA at 10  $\mu$ M with an IC<sub>50</sub> of 2.96  $\mu$ M, inhibited drug sensitive *Mycobacterium tuberculosis* with MIC of 8.86  $\mu$ M and was non-cytotoxic at 50  $\mu$ M. Compounds **RD\_21** (2-(5-(4-(Benzyloxy)benzylidene)-4-oxo-2-thioxothiazolidin-3-yl)-N-(3,4-dichlorophenyl)acetamide) and **RD\_37** (3-(5-(Benzo[*d*][1,3]dioxol-5-ylmethylene)-4-oxo-2-thioxothiazolidin-3-yl)-N-(2-chloro-5-(trifluoromethyl)phenyl)propanamide) were considered to be most potent antimycobacterial compounds with *Mycobacterium tuberculosis* MIC of 0.37 and 0.38  $\mu$ M respectively in the presence of efflux pump inhibitor piperine. The ability of potent ligands to stabilize the catalytic domain of the InhA protein was re-ascertained biophysically through differential scanning fluorimetry experiments wherein the thermal stability of the catalytic domain of InhA native protein and of the protein bound with the ligand was measured. The safety profile of synthesized compounds was evaluated by checking their *in vitro* cytotoxicity against RAW 264.7 cell line (mouse leukemic monocyte macrophage) by 3-(4,5-dimethylthiazol-2-yl)-2,5-diphenyltetrazolium bromide (MTT) assay. Also, all the synthesized derivatives were further evaluated for their predicted ADMET properties using the QikProp3.5 module of Schrodinger software wherein most of the drugs exhibited drug-like characteristics of a promising drug candidate from pharmaceutical point of view.

With new anti-tubercular agents desperately needed, we believe that the present class of inhibitors reported in this work would be interesting as initial leads for further chemical optimization as potential anti-tubercular agents.

# Table of contents

---

| Contents   | Page No.   |
|--|------------|
| <i>Certificate</i>   | <i>i</i>   |
| <i>Acknowledgements</i>  | <i>ii</i>  |
| <i>Abstract</i>  | <i>v</i>   |
| <i>List of Tables</i>  | <i>vi</i>  |
| <i>List of Figures</i>   | <i>vii</i> |
| <i>Abbreviations</i>   | <i>xii</i> |
| <b>Chapter 1 - Introduction</b>  | 1-9        |
| 1.1 The etiological agent of TB - <i>Mycobacterium tuberculosis</i>    | 2          |
| 1.2 Development of current TB drug chemotherapy                        | 3          |
| 1.3 The emergence of drug resistance to current anti-tubercular agents | 4          |
| 1.3.1 Multidrug-resistant TB (MDR-TB)                                  | 6          |
| 1.3.2 Extensively drug-resistant TB (XDR-TB)                           | 6          |
| 1.3.3 Totally drug-resistant TB (TDR-TB)                               | 7          |
| 1.4 Current TB drug development pipeline                               | 7          |
| <b>Chapter 2 - Literature review</b>                                   | 10-36      |
| 2.1 Mycolic acid biosynthesis  | 10         |
| 2.2 InhA as an anti-tubercular drug discovery platform                 | 14         |
| 2.3 InhA indirect inhibitors   | 14         |
| 2.3.1 Isoniazid (INH) and Ethionamide (ETH)                            | 14         |
| 2.4 InhA direct inhibitors   | 16         |
| 2.4.1 NAD analogues  | 16         |
| 2.4.2 Azaisoindolinones  | 17         |
| 2.4.3 Triclosan (TCN) and Alkyl diphenyl ethers                        | 18         |
| 2.4.4 Indole-5-amides and Pyrazoles                                    | 25         |
| 2.4.5 Pyrrolidine carboxamides   | 26         |
| 2.4.6 Arylamides   | 29         |
| 2.4.7 Imidazopiperidines   | 30         |

---

| Contents   | Page No.     |
|--|--------------|
| 2.4.8 Pyrrole hydrazines   | 31           |
| 2.4.9 Methyl thiazoles   | 32           |
| 2.4.10 Discovery of novel miscellaneous leads as InhA direct inhibitors using<br>Virtual screening           | 34           |
| <b>Chapter 3 - Objectives and Plan of work</b>   | <b>37-39</b> |
| 3.1 Objectives   | 37           |
| 3.2 Plan of work   | 37           |
| 3.2.1 Synthesis and characterization   | 38           |
| 3.2.2 <i>In vitro</i> enzyme inhibitory potency  | 38           |
| 3.2.3 Evaluation of protein interaction and stability using biophysical<br>characterization technique        | 38           |
| 3.2.4 <i>In vitro Mycobacterium tuberculosis</i> activity studies  | 38           |
| 3.2.5 <i>In vitro</i> cytotoxicity screening   | 39           |
| 3.2.6 ADMET Properties   | 39           |
| <b>Chapter 4 - Materials and Methods</b>   | <b>40-51</b> |
| 4.1 Design of novel <i>Mycobacterium tuberculosis</i> InhA direct inhibitors                                 | 40           |
| 4.2 Synthesis and characterization   | 43           |
| 4.2.1 Synthesis of 2-(2-oxobenzo[d]oxazol-3(2H)-yl)acetamide derivatives                                     | 43           |
| 4.2.2 Synthesis of 2-(4-oxoquinazolin-3(4H)-yl)acetamide derivatives   | 44           |
| 4.2.3 Synthesis of 4-amino-1,5-dimethyl-2-phenyl-1H-pyrazol-3(2H)-one<br>derivatives                         | 46           |
| 4.2.4 Synthesis of 5-arylalkylidene-2-(4-oxo-2-thioxothiazolidin-3-<br>yl)acetamide/ propanamide derivatives | 47           |
| 4.3 Enzyme inhibition studies  | 47           |
| 4.3.1 InhA protein expression, isolation and purification  | 47           |
| 4.3.2 <i>Mycobacterium tuberculosis</i> InhA inhibition assay  | 48           |
| 4.4 Biophysical characterization   | 48           |
| 4.5 Bacterial growth inhibition with <i>Mycobacterium tuberculosis</i> H37Rv strain                          | 49           |
| 4.6 Cytotoxicity studies   | 49           |
| 4.7 Molecular docking studies  | 50           |



---

| Contents   | Page No.      |
|--|---------------|
| 4.8 ADMET Properties   | 50            |
| <b>Chapter 5 - Results and Discussion</b>  | <b>52-181</b> |
| 5.1 Development of 2-(2-oxobenzo[ <i>d</i> ]oxazol-3(2 <i>H</i> )-yl)acetamide derivatives as potential <i>Mycobacterium tuberculosis</i> InhA inhibitors          | 52            |
| 5.1.1 Chemical synthesis and characterization  | 53            |
| 5.1.2 Experimental protocol utilised for synthesis   | 54            |
| 5.1.3 Characterization of synthesized compounds  | 58            |
| 5.1.4 <i>In vitro</i> <i>Mycobacterium tuberculosis</i> InhA inhibition assay, antimycobacterial potency and cytotoxicity studies of the synthesised molecules     | 70            |
| 5.1.5 Evaluation of protein interaction and stability using biophysical characterization experiment  | 73            |
| 5.1.6 Discussion   | 74            |
| 5.1.7 Highlights of the study  | 83            |
| 5.2 Development of 2-(4-oxoquinazolin-3(4 <i>H</i> )-yl)acetamide derivatives as potential <i>Mycobacterium tuberculosis</i> InhA inhibitors                       | 85            |
| 5.2.1 Chemical synthesis and characterization  | 85            |
| 5.2.2 Experimental protocol utilised for synthesis   | 87            |
| 5.2.3 Characterization of synthesized compounds  | 93            |
| 5.2.4 <i>In vitro</i> <i>Mycobacterium tuberculosis</i> InhA inhibition assay, antimycobacterial potency and cytotoxicity studies of the synthesised molecules     | 106           |
| 5.2.5 Evaluation of protein interaction and stability using biophysical characterization experiment  | 109           |
| 5.2.6 Discussion   | 110           |
| 5.2.7 Highlights of the study  | 122           |
| 5.3 Development of 4-amino-1,5-dimethyl-2-phenyl-1 <i>H</i> -pyrazol-3(2 <i>H</i> )-one derivatives as potential <i>Mycobacterium tuberculosis</i> InhA inhibitors | 123           |
| 5.3.1 Chemical synthesis and characterization  | 123           |
| 5.3.2 Experimental protocol utilised for synthesis   | 125           |
| 5.3.3 Characterization of synthesized compounds  | 130           |

---

---

| <b>Contents</b>  | <b>Page No.</b> |
|--|-----------------|
| 5.3.4 <i>In vitro Mycobacterium tuberculosis</i> InhA inhibition assay, antimycobacterial potency and cytotoxicity studies of the synthesised molecules                | 139             |
| 5.3.5 Evaluation of protein interaction and stability using biophysical characterization experiment  | 142             |
| 5.3.6 Discussion   | 143             |
| 5.3.7 Highlights of the study  | 147             |
| 5.4 Development of 5-arylalkylidene-2-(4-oxo-2-thioxothiazolidin-3-yl)acetamide/propanamide derivatives as potential <i>Mycobacterium tuberculosis</i> InhA inhibitors | 148             |
| 5.4.1 Chemical synthesis and characterization  | 148             |
| 5.4.2 Experimental protocol utilised for synthesis   | 149             |
| 5.4.3 Characterization of synthesized compounds  | 154             |
| 5.4.4 <i>In vitro Mycobacterium tuberculosis</i> InhA inhibition assay, antimycobacterial potency and cytotoxicity studies of the synthesised molecules                | 170             |
| 5.4.5 Evaluation of protein interaction and stability using biophysical characterization experiment  | 174             |
| 5.4.6 Discussion   | 174             |
| 5.4.7 Highlights of the study  | 180             |
| <b>Chapter 6 - Summary and Conclusion</b>  | 182-184         |
| <b>Future perspectives</b>   | 185             |
| <b>References</b>  | 186-202         |
| <b>Appendix</b>  | 203-205         |
| List of publications and presentations   | 203             |
| Biography of the candidate   | 204             |
| Biography of the supervisor  | 205             |

---

## List of Tables

---

| <b>Table No.</b> | <b>Description</b>   | <b>Page No.</b> |
|------------------|--|-----------------|
| Table 5.1        | Physicochemical properties of synthesized compounds <b>BX_04 – BX_21</b> and <b>BX_23 – BX_31</b>  | 57              |
| Table 5.2        | <i>In vitro</i> biological evaluation of the synthesized derivatives <b>BX_04 – BX_21</b> and <b>BX_23 – BX_31</b>                           | 71              |
| Table 5.3        | QikProp analysis of the ADMET properties of the synthesized derivatives <b>BX_04 – BX_21</b> and <b>BX_23 – BX_31</b>                        | 83              |
| Table 5.4        | Physicochemical properties of synthesized compounds <b>QN_04 – QN_11</b> , <b>QN_16 – QN_23</b> and <b>QN_25 – QN_36</b>                     | 92              |
| Table 5.5        | <i>In vitro</i> biological evaluation of the synthesized derivatives <b>QN_04 – QN_11</b> , <b>QN_16 – QN_23</b> and <b>QN_25 – QN_36</b>    | 107             |
| Table 5.6        | QikProp analysis of the ADMET properties of the synthesized derivatives <b>QN_04 – QN_11</b> , <b>QN_16 – QN_23</b> and <b>QN_25 – QN_36</b> | 121             |
| Table 5.7        | Physicochemical properties of synthesized compounds <b>PR_04 – PR_31</b>   | 128             |
| Table 5.8        | <i>In vitro</i> biological evaluation of the synthesized derivatives <b>PR_04 – PR_31</b>  | 140             |
| Table 5.9        | QikProp analysis of the ADMET properties of the synthesized derivatives <b>PR_04 – PR_31</b>   | 146             |
| Table 5.10       | Physicochemical properties of synthesized compounds <b>RD_03 - RD_42</b>   | 151             |
| Table 5.11       | <i>In vitro</i> biological evaluation of the synthesized derivatives <b>RD_03 – RD_42</b>  | 171             |
| Table 5.12       | QikProp analysis of the ADMET properties of the synthesized derivatives <b>RD_03 – RD_42</b>   | 179             |

## List of Figures

---

| Figure No.  | Description   | Page No. |
|-------------|---|----------|
| Figure 1.1  | Stages of <i>Mycobacterium tuberculosis</i> infection   | 2        |
| Figure 1.2  | Current global pipeline of TB drug development  | 8        |
| Figure 1.3  | Mechanism of action of new anti-tubercular drugs in development   | 9        |
| Figure 2.1  | Model of the mycobacterial cell wall  | 11       |
| Figure 2.2  | Fatty acid/mycolic acid biosynthesis in mycobacteria  | 13       |
| Figure 2.3  | Reduction mechanism of InhA   | 14       |
| Figure 2.4  | Mechanism of action of INH in <i>Mycobacterium tuberculosis</i>   | 15       |
| Figure 2.5  | The development of NAD analogues  | 16       |
| Figure 2.6  | Structures of INH-NAD adducts and truncated analogues   | 17       |
| Figure 2.7  | Modifications effected around azaisoindolinone framework and chemical structure of most active azaisoindolinones                                  | 18       |
| Figure 2.8  | Triclosan and its derivatives   | 19       |
| Figure 2.9  | Structures of triclosan bound to the <i>E. coli</i> FabI and InhA   | 20       |
| Figure 2.10 | Superposition of InhA complexes with Triclosan and C <sub>16</sub> -NAC   | 21       |
| Figure 2.11 | Chemical structure of class I and class II triazoles and most potent compound <b>26</b>   | 23       |
| Figure 2.12 | Chemical structure of diaryl ether scaffold and modifications effected around it  | 24       |
| Figure 2.13 | General structure of diphenyl ether derivatives   | 25       |
| Figure 2.14 | Chemical structure of representative Indole-5-amide and Pyrazole  | 26       |
| Figure 2.15 | Development of pyrrolidine carboxamides   | 27       |
| Figure 2.16 | Chemical structure of most potent antimycobacterial compounds <b>d12</b> and <b>p67</b>   | 28       |
| Figure 2.17 | General structure of 3-(9 <i>H</i> -fluoren-9-yl)pyrrolidine-2,5-dione derivatives (left) and structure of most potent compound <b>4b</b> (right) | 29       |

| Figure No.  | Description  | Page No. |
|-------------|--|----------|
| Figure 2.18 | General structure of compounds identified in initial high-throughput screening (left) and, most potent arylamide identified by microtiter synthesis and <i>in situ</i> screening (right) | 29       |
| Figure 2.19 | General structure of Imidazopiperidines (left) and most potent compound <b>9b</b> (right)  | 30       |
| Figure 2.20 | Docked region and structure-activity relationship for pyrrole hydrazones   | 31       |
| Figure 2.21 | Chemical structure of reported potent InhA inhibitor <b>4</b> (PT70), methyl thiazole scaffold <b>7</b> and general structure of methyl thiazole analogues of present series (right)     | 32       |
| Figure 2.22 | InhA catalytic site I interactions   | 33       |
| Figure 2.23 | Substrate site binding regions of InhA. Protein complexes of <b>7</b>  | 34       |
| Figure 2.24 | Three positions for optimization in target compound <b>7</b> and structure of optimized lead compound <b>65</b>  | 36       |
| Figure 4.1  | Virtual screening work flow  | 40       |
| Figure 4.2  | Analysis of top active compound ( <b>UPS 1</b> )   | 41       |
| Figure 4.3  | Selected hits from virtual screening and their <i>Mycobacterium tuberculosis</i> InhA inhibition activity measured at 10 $\mu$ M   | 42       |
| Figure 4.4  | Chemical structure of selected hits as lead molecules for further optimization   | 43       |
| Figure 4.5  | Synthetic scheme 1 utilised for synthesis of 2-(2-oxobenzodioxazol-3(2 <i>H</i> )-yl)acetamide derivatives   | 43       |
| Figure 4.6  | Synthetic scheme 2 utilised for synthesis of 2-(2-oxobenzodioxazol-3(2 <i>H</i> )-yl)acetamide derivatives   | 44       |
| Figure 4.7  | Synthetic scheme 1 utilised for synthesis of 2-(4-oxoquinazolin-3(4 <i>H</i> )-yl)acetamide derivatives  | 44       |
| Figure 4.8  | Synthetic scheme 2 utilised for synthesis of 2-(4-oxoquinazolin-3(4 <i>H</i> )-yl)acetamide derivatives  | 45       |
| Figure 4.9  | Synthetic scheme 3 utilised for synthesis of 2-(4-oxoquinazolin-3(4 <i>H</i> )-yl)acetamide derivatives  | 45       |
| Figure 4.10 | Synthetic scheme utilised for synthesis of 4-amino-1,5-dimethyl-   | 46       |

| <b>Figure No.</b> | <b>Description</b>  | <b>Page No.</b> |
|-------------------|---|-----------------|
|                   | 2-phenyl-1 <i>H</i> -pyrazol-3(2 <i>H</i> )-one derivatives   |                 |
| Figure 4.11       | Synthetic scheme utilised for synthesis of 5-arylalkylidene-2-(4-oxo-2-thioxothiazolidin-3-yl)acetamide/propanamide derivatives   | 47              |
| Figure 5.1        | Chemical structure of lead molecule <b>UPS 14</b>   | 53              |
| Figure 5.2        | Synthetic protocol utilized for synthesis of compounds <b>BX_04</b> – <b>BX_21</b>  | 54              |
| Figure 5.3        | Synthetic protocol utilized for synthesis of compounds <b>BX_23</b> – <b>BX_31</b>  | 54              |
| Figure 5.4        | DSF experiment for compound <b>BX_25</b> showing an increase in thermal stability between the native InhA protein (pink) and InhA protein-compound <b>BX_25</b> complex (green) | 73              |
| Figure 5.5        | Superimposition of docked pose of the reported reference inhibitor (Yellow) to the original pose of the reference inhibitor (Red)   | 74              |
| Figure 5.6        | Binding pose and interaction pattern of lead molecule <b>UPS 14</b>   | 75              |
| Figure 5.7        | Binding pose and its interaction pattern of the compound <b>BX_23</b>   | 76              |
| Figure 5.8        | Binding pose and its interaction pattern of the compound <b>BX_19</b>   | 77              |
| Figure 5.9        | Binding pose and its interaction pattern of the compound <b>BX_24</b> and <b>BX_27</b>  | 78              |
| Figure 5.10       | Binding pose and its interaction pattern of the compound <b>BX_05</b>   | 79              |
| Figure 5.11       | Binding pose and its interaction pattern of the compound <b>BX_25</b> , <b>BX_28</b> and <b>BX_15</b>   | 80              |
| Figure 5.12       | Binding pose and its interaction pattern of the compound <b>BX_12</b>   | 80              |
| Figure 5.13       | Chemical structure and biological activity of the most active compound <b>BX_25</b>   | 84              |
| Figure 5.14       | Chemical structure of lead molecule <b>UPS 17</b>   | 85              |
| Figure 5.15       | Synthetic protocol utilized for synthesis of compounds <b>QN_04</b> – <b>QN_11</b>  | 86              |
| Figure 5.16       | Synthetic protocol utilized for synthesis of compounds <b>QN_16</b> – <b>QN_23</b>  | 87              |
| Figure 5.17       | Synthetic protocol utilized for synthesis of compounds <b>QN_25</b> –   | 87              |

| <b>Figure No.</b> | <b>Description</b>   | <b>Page No.</b> |
|-------------------|--|-----------------|
|                   | <b>QN_36</b>   |                 |
| Figure 5.18       | DSF experiment for compound <b>QN_07</b> (protein-ligand complex, green) showing an increase in the thermal shift of 2.2 °C compared with the native InhA protein (pink) | 109             |
| Figure 5.19       | Superimposition of docked pose of the reference inhibitor (Yellow) to the original pose of the reference inhibitor (Red)   | 111             |
| Figure 5.20       | Binding pose and its interaction pattern of lead molecule <b>UPS 17</b>  | 112             |
| Figure 5.21       | Binding pose and its interaction pattern of the compound <b>QN_33</b> in the active site of the InhA protein   | 113             |
| Figure 5.22       | Interacting pattern of the compound <b>QN_10</b> in the active site of the InhA protein  | 113             |
| Figure 5.23       | Binding pose and its interaction pattern of the compound <b>QN_09</b> in the active site of the InhA protein   | 115             |
| Figure 5.24       | Interacting pattern of the compound <b>QN_34</b> in the active site of the InhA protein  | 115             |
| Figure 5.25       | Interacting pattern of the compound <b>QN_22</b> in the active site of the InhA protein  | 116             |
| Figure 5.26       | Interacting pattern of the compound <b>QN_27</b> in the active site of the InhA protein  | 117             |
| Figure 5.27       | Interacting pattern of the compound <b>QN_17</b> at the active site of the InhA protein  | 118             |
| Figure 5.28       | Binding pose and its interaction pattern of the compound <b>QN_28</b> in the active site of the InhA protein   | 118             |
| Figure 5.29       | Chemical structure and biological activity of the most active compound <b>QN_17</b>  | 122             |
| Figure 5.30       | Chemical structure of lead molecule <b>UPS 1</b>   | 123             |
| Figure 5.31       | Synthetic protocol utilized for synthesis of compounds <b>PR_04 – PR_31</b>  | 124             |
| Figure 5.32       | DSF experiment for compound <b>PR_12</b> (protein-ligand complex, green) showing an increase in the thermal shift of 0.9 °C compared with the native InhA protein (pink) | 143             |

| <b>Figure No.</b> | <b>Description</b>   | <b>Page No.</b> |
|-------------------|--|-----------------|
| Figure 5.33       | Binding pose and its interaction pattern of compound <b>PR_15</b>  | 144             |
| Figure 5.34       | Chemical structure and biological activity of the most active compound <b>PR_15</b>  | 147             |
| Figure 5.35       | Chemical structure of lead molecule <b>UPS 8</b>   | 148             |
| Figure 5.36       | Synthetic protocol utilized for synthesis of compounds <b>RD_03 – RD_42</b>  | 149             |
| Figure 5.37       | DSF experiment for compound <b>RD_13</b> (protein-ligand complex, green) showing an increase in the thermal shift of 0.5 °C compared with the native InhA protein (pink) | 174             |
| Figure 5.38       | Binding pose and interaction pattern of most active compound <b>RD_13</b>  | 177             |
| Figure 5.39       | Chemical structure and biological activity of the most active compound <b>RD_13</b>  | 181             |



## List of Abbreviations

---

|                     |   |  |
|---------------------|---|--|
| $\mu\text{g}$       | : | Microgram  |
| $\mu\text{M}$       | : | Micromolar   |
| $^{13}\text{C}$ NMR | : | Carbon Nuclear Magnetic Resonance                              |
| $^1\text{H}$ NMR    | : | Proton Nuclear Magnetic Resonance                              |
| 3D                  | : | Three Dimensional  |
| ACP                 | : | Acyl Carrier Protein   |
| ADMET               | : | Absorption, Distribution, Metabolism, Elimination and Toxicity |
| AMK                 | : | Amikacin   |
| ATP                 | : | Adenosine Triphosphate   |
| CAP                 | : | Capreomycin  |
| $\text{CDCl}_3$     | : | Chloroform deuterated  |
| CDI                 | : | 1,1'-Carbonyldiimidazole                                       |
| CoA                 | : | Coenzyme A   |
| CoMFA               | : | Comparative Molecular Field Analysis                           |
| d                   | : | Doublet  |
| DCM                 | : | Dichloromethane  |
| DD-CoA              | : | 2- <i>trans</i> -decenoyl-CoA                                  |
| DMF                 | : | <i>N,N</i> -Dimethylformamide                                  |
| DMSO                | : | Dimethyl sulfoxide   |
| $\text{DMSO-d}_6$   | : | Dimethyl sulphoxide deuterated                                 |
| DNA                 | : | Deoxyribonucleic acid  |
| DOTS                | : | Directly Observed Treatment, Short course                      |
| EDC                 | : | 1-Ethyl-3-(3-dimethylaminopropyl)carbodiimide                  |
| EDTA                | : | Ethylene diamine tetra acetic acid                             |
| EMB                 | : | Ethambutol   |
| ETH                 | : | Ethionamide  |
| FAS-I               | : | Fatty acid synthase-I pathway                                  |
| FAS-II              | : | Fatty acid synthase-II pathway                                 |
| hERG                | : | human Ether-a-go-go-Related Gene                               |
| HIV                 | : | Human Immuno Deficiency Virus                                  |
| HOBT                | : | Hydroxybenzotriazole   |

|                  |   |   |
|------------------|---|---|
| IC <sub>50</sub> | : | Half Maximal Inhibitory Concentration                       |
| INH              | : | Isoniazid   |
| InhA             | : | 2- <i>trans</i> -enoyl-acyl carrier protein reductase       |
| IPTG             | : | Isopropyl-β-D-thiogalactopyranoside                         |
| <i>J</i>         | : | Coupling constant   |
| KAN              | : | Kanamycin   |
| K <sub>i</sub>   | : | Inhibitor constant  |
| LCMS             | : | Liquid chromatography–Mass Spectrometry                     |
| m                | : | Multiplet   |
| M.p              | : | Melting point   |
| MDCK             | : | Madin-Darby canine kidney (MDCK) epithelial cell line       |
| MDR-TB           | : | Multidrug-Resistant <i>Mycobacterium tuberculosis</i>       |
| mg               | : | Milligram   |
| MIC              | : | Minimum Inhibitory Concentration                            |
| mL               | : | Milliliter  |
| mmol             | : | Millimole   |
| MTT              | : | (4,5-Dimethylthiazol-2-yl)-2,5-diphenyltetrazolium bromide  |
| NADH             | : | Nicotinamide Adenine Dinucleotide                           |
| nM               | : | Nanomolar   |
| PAS              | : | <i>para</i> -Aminosalicylic acid                            |
| PCR              | : | Polymerase Chain Reaction                                   |
| PDB              | : | Protein Data Bank   |
| PMSF             | : | Phenylmethanesulfonyl fluoride                              |
| ppm              | : | Parts per million   |
| PTH              | : | Prothionamide   |
| PZA              | : | Pyrazinamide  |
| RIF              | : | Rifampicin  |
| RNA              | : | Ribonucleic acid  |
| rRNA             | : | Ribosomal Ribonucleic acid                                  |
| rt               | : | Room temperature  |
| s                | : | Singlet   |
| SAR              | : | Structure Activity Relationship                             |
| SDS-PAGE         | : | Sodium Dodecyl Sulphate- Polyacrylamide Gel Electrophoresis |

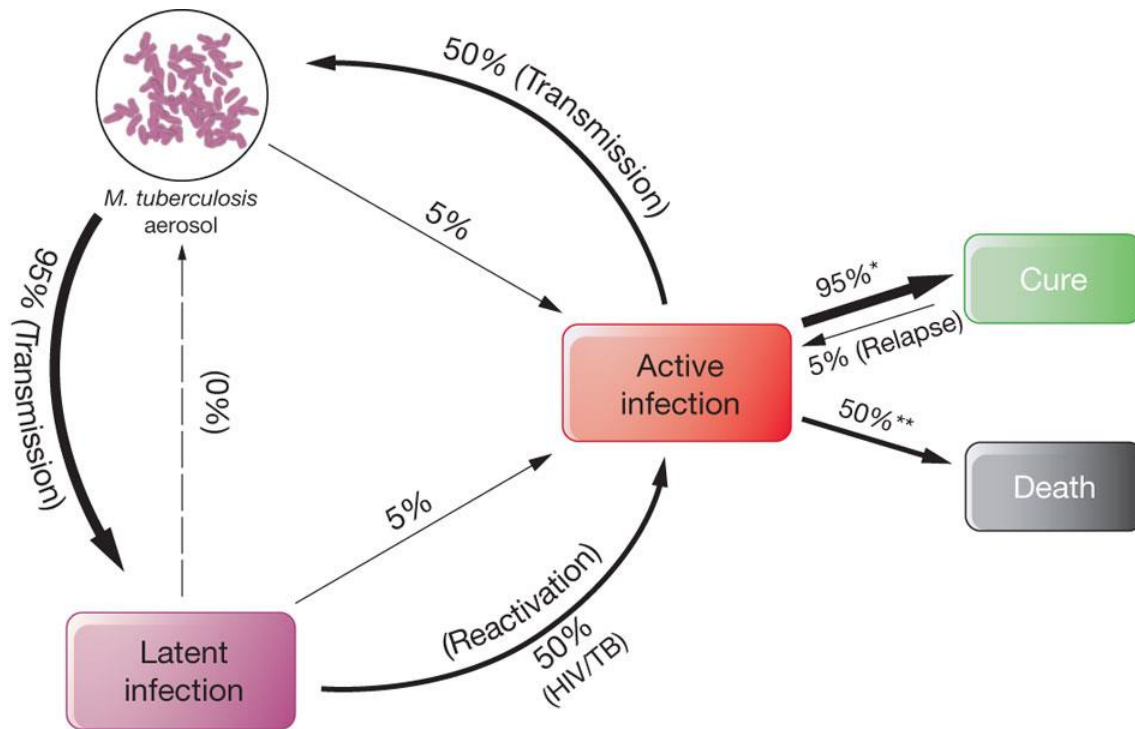
|                |   |  |
|----------------|---|--|
| STM            | : | Streptomycin   |
| t              | : | Triplet  |
| TB             | : | Tuberculosis   |
| TCN/TRC        | : | Triclosan  |
| TDR-TB         | : | Totally Drug-Resistant <i>Mycobacterium tuberculosis</i>     |
| TEA            | : | Triethylamine  |
| TFA            | : | Trifluoroacetic acid   |
| THF            | : | Tetrahydrofuran  |
| TLC            | : | Thin-layer chromatography                                    |
| T <sub>m</sub> | : | Melting temperature  |
| WHO            | : | World Health Organisation                                    |
| XDR-TB         | : | Extensively Drug-Resistant <i>Mycobacterium tuberculosis</i> |
| XP             | : | Extra Precision  |
| δ              | : | Chemical shift   |

If the importance of a disease for mankind is measured from the number of fatalities which are due to it, then tuberculosis must be considered much more important than those most feared infectious diseases, plague, cholera, and the like. Statistics have shown that 1/7 of all humans die of tuberculosis.

- *Die Ätiologie der Tuberculose, Robert Koch (1882)*

Tuberculosis (TB) is a disease of antiquity which is more prevalent in the world today than at any other time in human history. It is the leading cause of morbidity and mortality among the infectious diseases. The disease is transmitted via the respiratory route as a highly infectious aerosol, whose exposure outcome ranges from immediate organism destruction by the host's immune system to infected individuals developing active primary TB disease [Flynn J.L. *et al.*, 2001]. However, the majority of individuals infected with *Mycobacterium tuberculosis*, the pathogen responsible for TB, have a non-contagious, clinically latent infection with 5-10% risk of developing active TB disease during their lifetime (**Figure 1.1**) [Clark-Curtiss J.E. and Haydel S.E., 2003]. The rapid emergence of drug resistant TB-strains and HIV co-infection, which compromises host defence mechanism, further complicates the effective control of the disease [Corbett E.L. *et al.*, 2003].

In 1993, the World Health Organization (WHO) declared TB a global public health emergency due to the steady global increase in disease cases. TB still remains one of the major health hazards which cause maximum deaths from a single microorganism. According to WHO, in 2012, 8.6 million people developed TB and 1.3 million died from the disease (including 320 000 deaths among HIV-positive people) with majority of these cases in the South-East Asia (29%), African (27%) and Western Pacific (19%) regions. India and China alone accounted for 26% and 12% of total cases, respectively [WHO Global Tuberculosis Report, 2013]. Globally, approximately one third of the world's population has been infected with *Mycobacterium tuberculosis* and given the vast number of individuals who succumb to the disease each year; long-term actions must be aimed at reducing global mortality and eliminating the disease at the earliest.



**Figure 1.1:** Stages of *Mycobacterium tuberculosis* infection [Koul A. *et al.*, 2011]. *Mycobacterium tuberculosis* aerosol transmission and progression to infectious TB or non-infectious (latent) disease. A sizeable pool of latently infected people may relapse into active TB, years after their first exposure to the bacterium. Latent TB is commonly activated by immune suppression, as in the case of HIV. In cases of drug-susceptible (denoted by an asterisk), 95% of patients recover upon treatment, whereas 5% relapse. If untreated (denoted by two asterisks), high mortality results.

### 1.1 The etiological agent of TB - *Mycobacterium tuberculosis*

In 1882, Robert Koch discovered *Mycobacterium tuberculosis*, an acid-fast, obligate aerobic bacillus which divides at an extremely slow rate as the causative agent of TB [Koch R., 1882]. *Mycobacterium tuberculosis* is an obligate intracellular pathogen which can survive up to decades in a phenotypically non-replicating state, primarily in hypoxic granulomas in the lung [Murphy D.J. and Brown J.R., 2007]. It has outstanding mechanisms to escape from elimination and a high degree of intrinsic resistance to most antibiotics, chemotherapeutic agents and immune eradication [Coker R.J., 2004]. One major obstacle for host defence mechanisms and therapeutic intervention is robust, mycolic acid-rich cell wall, which is unique among prokaryotes [Brennan P.J. and Nikaido H., 1995]. Mycolic acids are the primary constituent of the mycobacterial cell wall which contributes to the outer membrane

permeability and integrity as well as virulence [Dubnau E. *et al.*, 2000]. This contributes to the chronic nature of the disease, imposes lengthy treatment regimens and represents a formidable obstacle for researchers [Cole S.T. *et al.*, 1998].

## **1.2 Development of current TB drug chemotherapy**

Most of the drugs used today as the first-line agents were discovered during the 1950's and the 60's [Villemagne B. *et al.*, 2012]. The discovery of streptomycin (STM), the first effective anti-tubercular agent, in 1944 brought much excitement and hope to the world [Jones D. *et al.*, 1944]. This aminoglycoside antibiotic interferes with protein biosynthesis through an interaction with the small 30S subunit of the ribosome [Carter A.P. *et al.*, 2000]. This was quickly followed by the discovery of *para*-aminosalicylic acid (PAS) in 1946 and later in 1952 isoniazid (INH), one of today's most active anti-tubercular drugs was introduced to the TB chemotherapy [Fox W. *et al.*, 1999; Bernstein J. *et al.*, 1952]. The target of PAS is still subject of investigations, whereas INH inhibits mycolic acids biosynthesis, one of the essential components of the mycobacterial cell wall [Timmins G.S. and Deretic V., 2006]. The use of pyrazinamide (PZA) first introduced in 1954, was a great success as it allowed shortening the duration of the TB therapy to current 6 months than initial 9 months [Malone L. *et al.*, 1952]. It was possible because of ability of PZA to inhibit semi-dormant bacilli residing in acidic environments such as found in the TB lesions [Palomino J.C. *et al.*, 2014].

Ethambutol (EMB) was discovered in 1961, which exerts bacteriostatic effect against multiplying bacilli interfering with the biosynthesis of arabinogalactan in the cell wall of mycobacteria [Takayama K. and Kilburn J.O., 1989]. Finally, rifampin (RIF) appeared as a drug of choice for TB treatment around 1970, which is one of the most effective anti-tubercular antibiotics and together with INH constitutes the basis of the combination therapy for TB [Wehrli W., 1983]. It is active against growing and slow metabolizing bacilli and inhibits bacterial RNA synthesis by binding to the  $\beta$ -subunit of the DNA-dependent polymerase [McClure W.R. and Cech C.L., 1978].

Despite the efficiency of these drugs alone, a significant improvement in management of TB was obtained with combined therapy in order to limit the emergence of resistant strains. The Directly Observed Treatment, Short course (DOTS) strategy by the WHO consists of a broad TB control effort which focuses four principal elements [Haydel S.E., 2010]: (i) proper case detection with microbiological laboratory support, (ii) standard chemotherapeutic treatment

with patient support and supervision including directly observed therapy, (iii) consistent availability of TB drugs, and (iv) standard monitoring and evaluation system with impact measurements.

First-line anti-tubercular antibiotics target actively replicating *Mycobacterium tuberculosis* cells in the lung and significantly reduce transmission rates to other persons within the first two months of treatment. The INH and RIF are active against dividing cells with RIF also having activity against dormant bacteria, thus accounting for sterilizing properties during the short-course antibiotic regimen [Hafner R. *et al.*, 1997; Dickinson J.M. *et al.*, 1981]. PZA exhibits greatest activity against dormant organisms localized within macrophages or the acidic environment of the pulmonary lesion [Girling D.J., 1984]. Inclusion of EMB in the first-line drug regimen is recommended to prevent RIF's resistance when INH resistance is suspected.

Second-line agents are introduced into treatment regimens when resistance to primary antibiotics develops [Dorman S.E. and Chaisson R.E., 2007]. However, second-line agents exhibit lower potency and/or greater toxicity. The fluoroquinolone, aminoglycoside, and capreomycin (CAP) antibiotics target DNA replication and protein synthesis, and offer the greatest effectiveness of the second-line anti-tubercular drugs [Mukherjee J.S. *et al.*, 2004]. The remaining antibiotics exhibit bacteriostatic activity and are considerably less potent, more toxic, and more expensive [Dorman S.E. and Chaisson R.E., 2007].

### **1.3 The emergence of drug resistance to current anti-tubercular agents**

*Mycobacterium tuberculosis* is intrinsically resistant to many antibiotics due to the low permeability of its mycolic acid-rich waxy cell envelope, the action of efflux pumps [Banerjee S.K. *et al.*, 1996; Silva P.E. *et al.*, 2001; Singh M. *et al.*, 2011], and the presence of chromosomally encoded resistance genes. The major mechanisms of acquired drug resistance in *Mycobacterium tuberculosis* are categorised by Green K.D. and Garneau-Tsodikova S. in a recent publication as: (i) mutations or modifications of the drug targets (RIF, EMB, kanamycin (KAN), amikacin (AMK), CAP, and the fluoroquinolones), (ii) the inability in prodrugs activation (INH, PZA and Ethionamide (ETH)) due to mutations which leads to a loss of function, and (iii) enzymatic inactivation of the drug (KAN) [Green K.D. and Garneau-Tsodikova S., 2013].

The most common mechanism of resistance in *Mycobacterium tuberculosis* is the alteration of the target's binding site through the accumulation of mutations which decrease the binding affinity of the drug to its target. This mechanism is used by *Mycobacterium tuberculosis* to develop resistance against RIF, EMB and fluoroquinolones by altering the binding site of their respective targets: the  $\beta$ -subunit of RNA polymerase [Campbell E.A. *et al.*, 2001], a glycosyltransferase [Telenti A. *et al.*, 1997], and DNA gyrase [Takiff H.E. *et al.*, 1994]. Similarly, ribosomal mutations (e.g., A1401G) in the 16S rRNA has been found to confer resistance to AMK, KAN, and CAP [Wachino J. *et al.*, 2010]. An alternative mode of resistance in *Mycobacterium tuberculosis* is the inactivation of rRNA methyltransferase enzymes which has been linked to resistance to CAP and viomycin [Johansen S.K. *et al.*, 2006].

Three anti-tubercular agents, INH, PZA and ETH, are prodrugs that must be metabolized to its active form against *Mycobacterium tuberculosis*. INH is activated by the catalase-peroxidase, KatG enzyme and produces isonicotinic-acyl radicals that react with NADH to form an INH-NADH adduct. The adduct binds its main target InhA, and inhibits mycolic acid biosynthesis [Timmins G.S. and Deretic V., 2006]. ETH is a structural analogue of INH and is activated by the monooxygenase EthA, which oxidizes ETH to its active form, 2-ethyl-4-amidopyridine which targets InhA and blocks mycolic acid biosynthesis similarly to INH [Vannelli T.A. *et al.*, 2002]. PZA is activated by pyrazinamidase/nicotinamidase, PncA, to pyrazinoic acid whose exact mechanism of action still remains unclear [Zhang Y. and Mitchison D., 2003]. Resistance to any of such prodrugs can arise due to reduced metabolism by their corresponding activator. Structural mutations that lower or abolish the enzymatic activity of KatG [Ramaswamy S.V. *et al.*, 2003; Hazbon M.H. *et al.*, 2006], EthA [Baulard A.R. *et al.*, 2000; Debarber A.E. *et al.*, 2000; Morlock G.P. *et al.*, 2003], and PncA [Stoffels K. *et al.*, 2012; Rajendran V. and Sethumadhavan R., 2013] were found to lead to INH, ETH, and PZA resistance, respectively.

Drug modification is perhaps the most prevalent mechanism of resistance exploited by bacteria. *Mycobacterium tuberculosis* naturally has a chromosomally encoded class A  $\beta$ -lactamase, BlaC, which provides intrinsic resistance to Penicillin [Hugonnet J.E. and Blanchard J.S., 2007]. One mechanism of acquired resistance to aminoglycosides, such as KAN and AMK, is their modification and inactivation by a set of enzymes known as



aminoglycoside modifying enzymes [Ramirez M.S. and Tolmasky M.E., 2010; Labby K.J. and Garneau-Tsodikova S., 2013].

Recently three major strategies have been proposed by Green K.D. and Garneau-Tsodikova S. to overcome resistance in TB: (i) identification of novel drugs for well-established targets, (ii) identification and characterization of novel compounds that target unexplored vital cell processes or enzymes, and (iii) identification of compounds that behave synergistically with current anti-tubercular drugs [Green K.D. and Garneau-Tsodikova S., 2013].

### **1.3.1 Multidrug-resistant TB (MDR-TB)**

Strains of *Mycobacterium tuberculosis* resistant to both INH and RIF, regardless of profiles of sensitivity/resistance to other drugs, have been termed as “multidrug-resistant (MDR)”. MDR-TB is a major concern due to the associated high risk of death. Globally in 2012, data from drug resistance surveys and continuous surveillance among notified TB cases suggest that 3.6% of newly diagnosed TB cases and 20% of those previously treated for TB had MDR-TB. The highest levels of MDR-TB are found in eastern Europe and central Asia, where in some countries more than 20% of new TB cases and more than 50% of those previously treated for TB have MDR-TB. India and China, the world’s two most populated countries, account for more than 50% of the world’s MDR-TB cases [WHO Global Tuberculosis Report, 2013].

While resistance to either drug may be managed with other first-line agents, MDR-TB requires treatment with second-line agents under DOTS-Plus programme which are less effective and more toxic [Zignol M. *et al.*, 2006]. The WHO currently recommends the use of a regimen including AMK, ETH, a fluoroquinolone (such as moxifloxacin), and PZA to treat MDR-TB [Veziris N. *et al.*, 2003].

### **1.3.2 Extensively drug-resistant TB (XDR-TB)**

XDR-TB is defined as MDR-TB resistant to any fluoroquinolone, and at least one of the injectable second-line antibiotics used in TB treatment (CAP, KAN, and AMK). At least one case of extensively drug-resistant TB (XDR-TB) had been reported by 92 countries by the end of 2012. On an average, an estimated 9.6% of MDR-TB cases have XDR-TB [WHO Global Tuberculosis Report, 2013].

Considering that XDR-TB is resistant to powerful first-line and second-line antibiotics, patients must be treated with more expensive, less effective second-line antibiotics, resulting in a longer treatment course for a minimum of 18-24 months, lower cure rates, and significantly increased healthcare costs [Chan E.D. *et al.*, 2008]. Moreover, second-line therapeutic treatment requires strict patient monitoring, supervision, counselling, and support to prevent further drug resistance that could potentially render the disease untreatable [Hopewell P.C. *et al.*, 2006].

### **1.3.3 Totally drug-resistant TB (TDR-TB)**

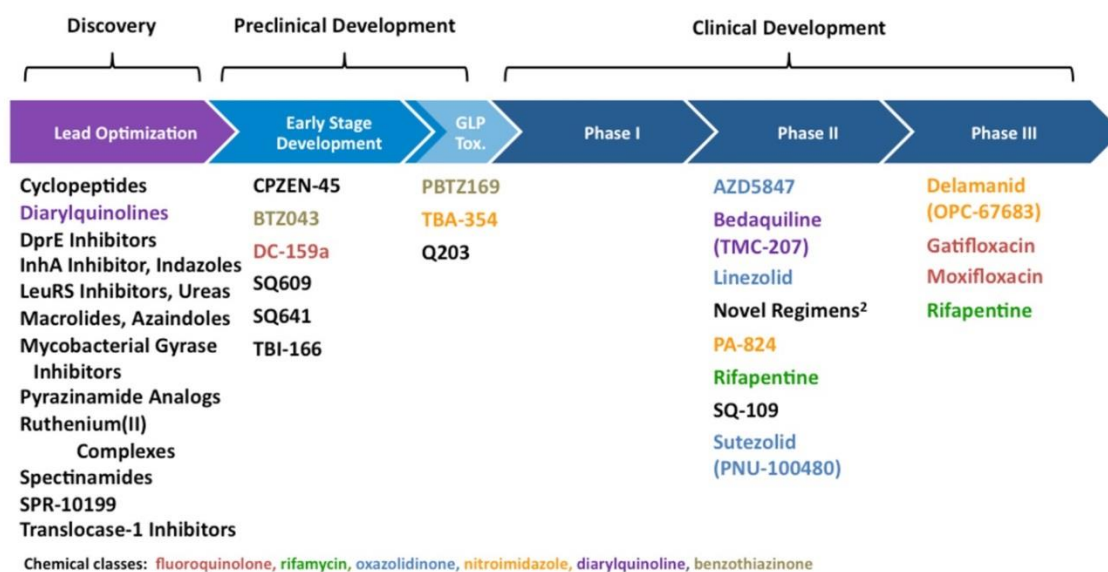
Totally drug-resistant TB (TDR-TB) refers to *Mycobacterium tuberculosis* clinical strains exhibiting *in vitro* resistance to all first- and second-line agents tested. The presence of TDR-TB was first observed in Italy in 2003 [Migliori G.B. *et al.*, 2007] and subsequently in Iran [Velayati A.A. *et al.*, 2009] and India [Udwadia Z.F. *et al.*, 2012].

Recently, Bedaquiline (TMC-207), Delamanid (OPC-67683) and Linezolid, three new drugs approved by the US-Food and Drug Administration and the European Medicines Agency, may offer therapeutic solutions for TDR-TB. With more new anti-tubercular agents in the pipeline, there is hope of identifying drugs that may be bactericidal or bacteriostatic in TB treatment and challenge the TDR-TB terminology [Parida S.K. *et al.*, 2014].

## **1.4 Current TB drug development pipeline**

Substantial progress has been made in last 40 years and a promising portfolio of new anti-tubercular drugs is on the horizon (**Figure 1.2**). Some have the potential to become the cornerstone of future TB treatment. Bedaquiline, a novel adenosine triphosphate synthase inhibitor has been recently been granted license by the U. S. Food and Drug Administration under its accelerated approval procedure for treatment of MDR-TB patients, as a part of new combination therapy when other alternatives have failed [Cohen J., 2013]. European Medicines Agency has recently approved Delamanid, a member of the nitroimidazole which has entered phase 3 trials for the treatment of MDR-TB.

The most rapid progress in the expansion of anti-tubercular drugs portfolio has been made through re-purposing or re-dosing known anti-tubercular drugs such as rifamycins (RIF, rifapentine) and fluoroquinolones (moxifloxacin and gatifloxacin). These drugs have all entered advanced phase 3 studies [Zumla A.I. *et al.*, 2014].

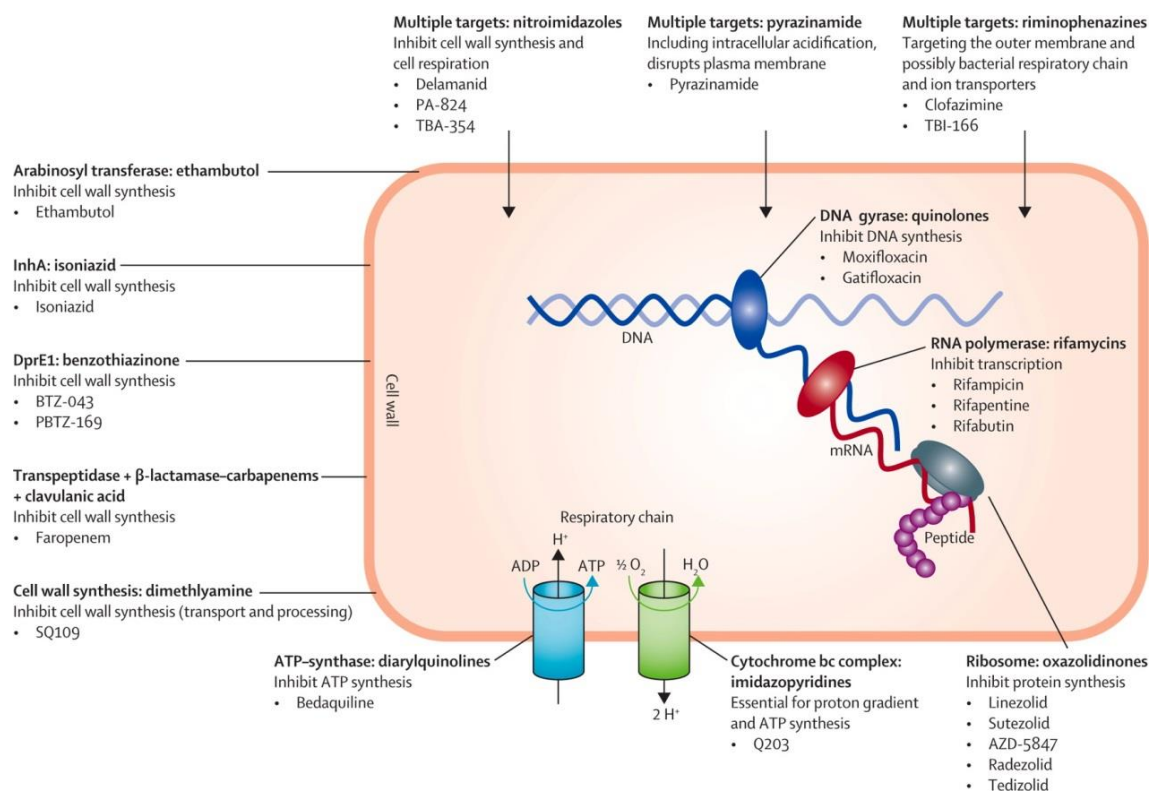


**Figure 1.2:** Current global pipeline of TB drug development [Source: Stop TB Partnership Working Group on New Drugs <http://www.newtbdrugs.org/pipeline-discovery.php>]

The discovery of novel compounds still remains challenging. Whole bacteria cell screening achieved significant success and identified diarylquinolines (bedaquiline) [Andries K. *et al.*, 2005], benzothiazines (BTZ-043 and PBTZ-169) [Makarov V. *et al.*, 2009], and imidazopyridine amide (Q-203) [Pethe K. *et al.*, 2013]. TBA-354, a second-generation nitroimidazole shows similar *in vitro* anti-tubercular activity as that of delamanid, but better activity than PA-824 [Zumla A.I. *et al.*, 2014]. Riminophenazines, exemplified by clofazimine, originally a dye- showed potential to shorten treatment of MDR-TB, but skin colouration due to accumulation in fatty tissue and organs remained major side effect. To reduce discolouration, TBI-166 was selected from 69 riminophenazine derivatives whose preclinical data suggested similar antimycobacterial properties [Zhang D. *et al.*, 2012].

Q203 is an optimised imidazopyridine, a new class of drugs that inhibit mycobacterial growth by blocking the respiratory cytochrome bc1 complex-essential to maintain the proton gradient and ATP synthesis. Although the drug has a similar target as bedaquiline, it inhibits ATP synthesis more potently in both aerobic and hypoxic conditions, and active against both MDR-TB and XDR-TB [Pethe K. *et al.*, 2013]. Two benzothiazinones, PBTZ-169 and BTZ-043, are in late stage clinical development which uses a novel mechanism of action that inhibits the enzyme decaprenylphosphoryl- $\beta$ -D-ribose 2'epimerase (DprE1) in *Mycobacterium tuberculosis*. Inhibition of this enzyme prevents the formation of decaprenyl phosphoryl arabinose, which results in cell lysis and bacterial death [Zumla A.I. *et al.*, 2014].

The most successful approach to yield novel drugs has been to re-engineer old antibacterial drug classes and improve their antimycobacterial potencies [Lechartier B. *et al.*, 2014]. Examples of such redesigned scaffolds are the nitroimidazoles (delamanid, PA-824, and TBA-354) and 1,2-ethylenediamine (SQ109). Oxazolidinones such as linezolid were developed for Gram-positive bacterial infections and were later shown to have anti-tubercular activity. Four modified versions of oxazolidinone derivatives (sutezolid, AZD-5847, radezolid, and tedizolid) might have improved activity against *Mycobacterium tuberculosis* and avoid myelosuppression- a problem with linezolid [Sotgiu G. *et al.*, 2012]. **Figure 1.3** summarises the mechanism of action of such new anti-tubercular drugs currently in various phases of development.



**Figure 1.3:** Mechanism of action of new anti-tubercular drugs in development [Zumla A.I. *et al.*, 2014]

Combinations of these new drugs with existing anti-tubercular therapies can lead to shorter and better tolerated regimens, and have lesser drug-drug interactions compared with existing regimens. Since anti-tubercular drugs need to be given in combination to prevent drug resistance, trials are underway with companion drugs to simplify, improve, or shorten treatment regimens for drug-sensitive and resistant TB-strains.

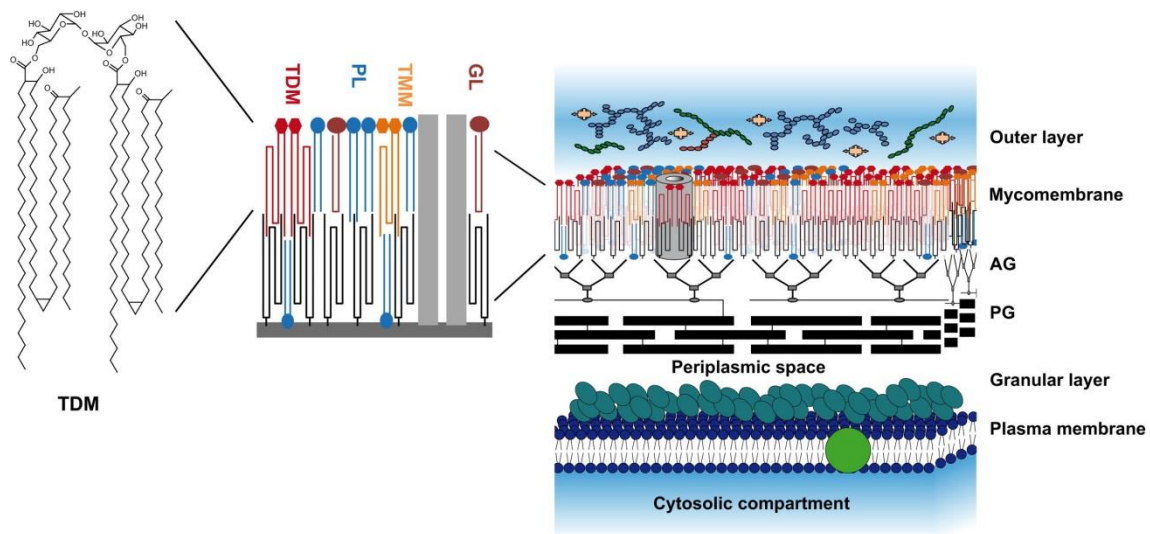
The rise in drug-resistant *Mycobacterium tuberculosis* and the relatively few candidates in drug development pipeline signify the urgent need for novel anti-tubercular agents, ideally with clinical efficiency in MDR, XDR, and TDR isolates. Recent years have seen an enormous increase in efforts to discover new lead compounds using both whole-cell screening and target-based biochemical approaches, although progress in validating new targets has been slower than expected. Many efforts currently focus on revisiting and optimizing existing inhibitors (of validated targets in FAS-II) through rational drug design and structure activity relationship studies. Since the discovery that mycolic acid biosynthesis is one of the primary effects of the frontline and most efficient anti-tubercular drug INH, much interest has been devoted to deciphering the chemistry and biosynthesis of mycolic acids. This metabolic pathway represents a valuable source for recruiting potential targets for the development of new antimycobacterial drugs in the alarming context of the emergence of MDR, XDR, and TDR-TB [Marrakchi H. *et al.*, 2014].

### 2.1 Mycolic acid biosynthesis

The distinctive cell envelope produced by *Mycobacterium tuberculosis* is associated with the physiology and pathogenicity of mycobacteria [Daffe M. and Draper P., 1998]. The outer layer of the mycobacterial cell wall is mainly comprised of mycolic acids, which are long-chain (C<sub>60</sub>-C<sub>90</sub>)  $\alpha$ -alkyl  $\beta$ -hydroxy fatty acids, important for the *Mycobacterium tuberculosis* to live and replicate inside macrophages [Pan P. and Tonge P.J., 2012].

Mycolic acids are found either unbound, extractable with organic solvents such as esters of trehalose or glycerol, or esterifying the terminal pentaarabinofuranosyl units of arabinogalactan; which together with peptidoglycan forms the cell wall skeleton [Daffe M. and Draper P., 1998; McNeil M. *et al.*, 1991]. Both forms are crucial for the extraordinary design and impermeability of the mycobacterial cell envelope, and participate in formation of outer membrane called as “mycomembrane”, recently visualized by electron microscopy [Sani M. *et al.*, 2010; Hoffmann C. *et al.*, 2008; Zuber B. *et al.*, 2008]. The arabinogalactan-mycolate [Crick D.C. *et al.*, 2001] covalently linked with peptidoglycan and mycomembrane;

provide a thick layer that protects the tubercle bacillus from general antibiotics and the host's immune system (**Figure 2.1**) [Takayama K. *et al.*, 2005].



**Figure 2.1:** Model of the mycobacterial cell wall [Marrakchi H. *et al.*, 2014]. The outer layer is mainly composed of glucan and proteins, with only a tiny amount of lipid. The mycomembrane corresponds to the permeability barrier. Its inner leaflet is formed by a parallel arrangement of mycolic acid chains (in black) linked to arabinogalactan (AG) that in turn is covalently attached to peptidoglycan (PG); the inner leaflet of the mycomembrane is presumably composed of free lipids that include trehalose dimycolates (TDM) (in red), trehalose monomycolates (TMM) (in orange), various glycolipids (GL, in brown), and phospholipid (PL, in blue). [Adapted from Zuber B. *et al.*, 2008]. A representation of TDM shows the very-long chain of MAs that have to pack after folding at the site of the motifs (here mycolic unit, cyclopropane, and keto group) to fit in a conventional membrane of 7-8 nm in thickness. The granular layer above the plasma membrane is composed of proteins; these proteins may precipitate upon treatments of bacteria before the observation by transmission electron microscopy and yield a thicker appearance to the outer leaflet of the plasma membrane [see Zuber B. *et al.*, 2008].

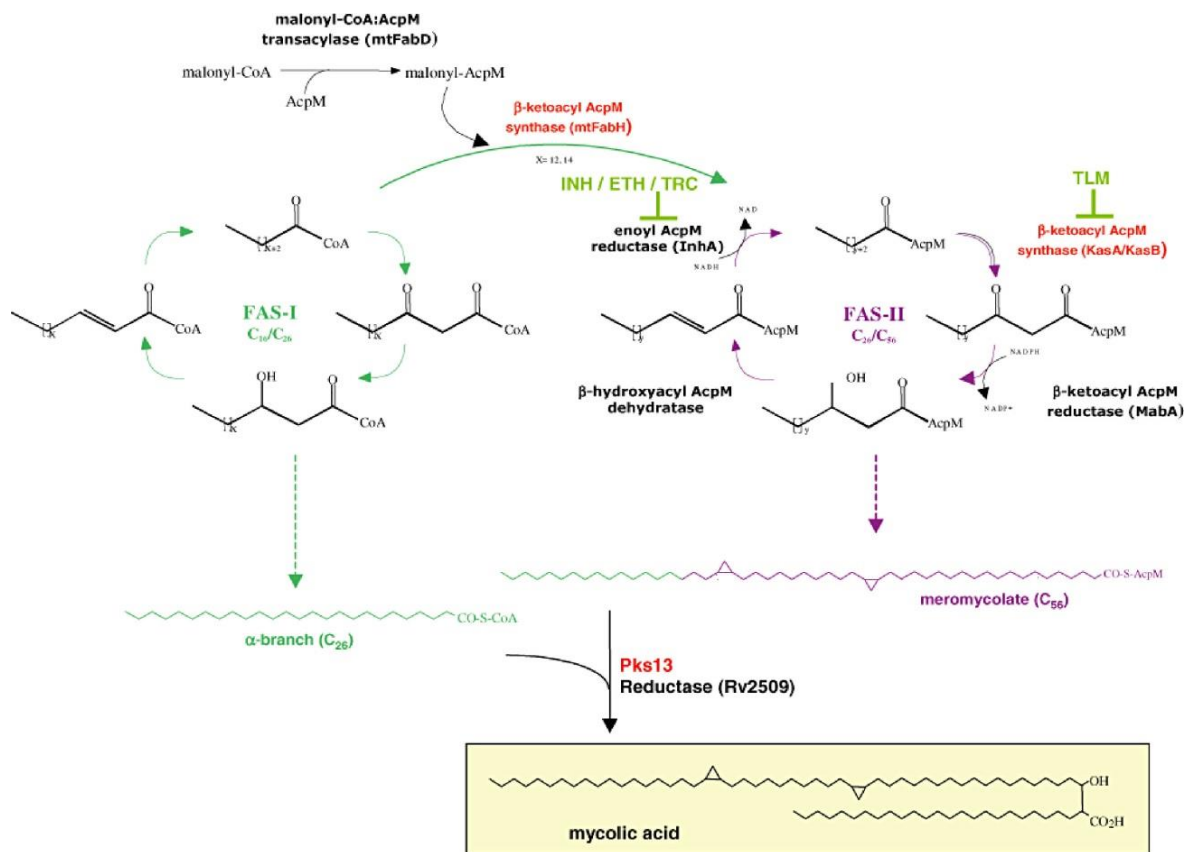
The biosynthetic pathway of mycolic acid involves type I and type II fatty acid synthases, FAS-I and FAS-II respectively. The eukaryotic-like FAS-I catalyses the *de novo* synthesis of fatty acids from acetyl-CoA. In contrast, FAS-II is similar to systems found in bacteria, apicomplexa parasites and plants, and is composed of four dissociable enzymes that act successively and repetitively to elongate the growing acyl chain. Acyl-primers are continually

activated *via* a thioester linkage to the prosthetic group of coenzyme A (CoA) for FAS-I, or of an acyl carrier protein (ACP) for FAS-II [Bhatt A. *et al.*, 2007].

The mycolic acid biosynthesis involves five discrete stages, as explained in a review by Takayama K. *et al.* and are illustrated in **Figure 2.2**: (i) the synthesis of the C<sub>26</sub> saturated straight chain fatty acids by FAS-I to provide the  $\alpha$ -alkyl branch of the mycolic acids, (ii) the synthesis of the C<sub>56</sub> fatty acids by FAS-II providing the meromycolate backbone, (iii) the introduction of functional groups to the meromycolate chain by numerous cyclopropane synthases, (iv) the condensation reaction catalysed by the polyketide synthase Pks13 between the  $\alpha$ -branch and the meromycolate chain before a final reduction to generate the mycolic acid, and (v) the transfer of mycolic acids to arabinogalactan and other acceptors such as trehalose *via* the Antigen 85 complex [Takayama K. *et al.*, 2005].

Mycolic acids give rise to important characteristics, including resistance to chemical injury, resistance to dehydration, low permeability to hydrophobic antibiotics, virulence [Dubnau E. *et al.*, 2000; Glickman M.S. *et al.*, 2000; Glickman M.S. and Jacobs W.R. Jr., 2001], acid-fast staining [Bhatt A. *et al.*, 2007], biofilm formation [Ojha A. *et al.*, 2005] and the ability to persist within the host [Daffe M. and Draper P., 1998; Yuan Y. *et al.*, 1998; Glickman M.S. *et al.*, 2000; Bhatt A. *et al.*, 2007].

It's interesting to note that mammals do not synthesize mycolic acids and thus compounds that antagonize the enzymes involved in mycolic acid biosynthesis are promising leads for developing novel anti-tubercular agents. Many efforts currently focus on revisiting and optimizing existing inhibitors of validated drug targets in FAS-II, particularly because it can remove much of the uncertainty surrounding new drug targets and *in vivo* clinical efficacy.



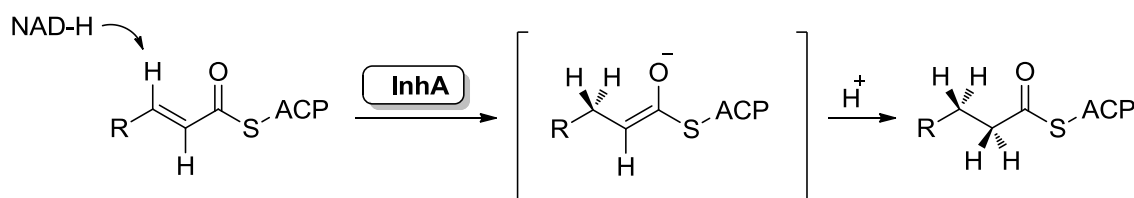
**Figure 2.2:** Fatty acid/mycolic acid biosynthesis in mycobacteria [Bhatt A. *et al.*, 2007]. FAS-I is involved in the synthesis of C<sub>16</sub> and C<sub>26</sub>. The C<sub>16</sub> acyl-CoA product acts as a substrate for the synthesis of meromycolic acids by FAS-II, whereas the C<sub>26</sub> fatty acid constitutes the α-branch of the final mycolic acid. MtFabH has been proposed to be the link between FAS-I and FAS-II by converting C<sub>14</sub>-CoA generated by FAS-I to C<sub>16</sub>-AcpM, which is channelled into the FAS-II cycle. This latter comprises four enzymes which will act successively and repeatedly to ensure fatty acid elongation, ultimately leading to meromycolates (C<sub>56</sub>). These enzymes are the condensing enzymes KasA and KasB, the keto-reductase MabA, an unidentified dehydratase, and the enoyl-reductase InhA. Finally, the polyketide synthase Pks13 catalyses the condensation of the α-branch and the meromycolate to produce mycolic acids. Targets for the action of activated INH, ethionamide (ETH), triclosan (TRC), or thiolactomycin (TLM) are indicated. FAS-II enzymes are labelled in black, excepted the condensing enzymes, which are indicated in red. The relative contribution of FAS-I and FAS-II activities in fatty acid/mycolic acid biosynthesis is represented in green and purple respectively.



## 2.2 InhA as an anti-tubercular drug discovery platform

In the past decade, beginning with the discovery that the first-line and most efficient anti-tubercular drug INH suppress mycolic acid biosynthesis through the inhibition of InhA (2-*trans*-enoyl-acyl carrier protein reductase), there have been several efforts to develop novel and potent InhA inhibitors as leads for novel TB chemotherapeutics.

InhA encoded by the *Mycobacterium tuberculosis* gene *inhA*, catalyses the final enzymatic step in the elongation cycle of the FAS-II pathway [Banerjee A. *et al.*, 1994; Dessen A. *et al.*, 1995]. It is a NADH-dependent reductase that exhibits specificity for long chain enoyl thioester substrates, and its reduction mechanism is shown in **Figure 2.3**.



**Figure 2.3:** Reduction mechanism of InhA [Lu X.Y. *et al.*, 2010].

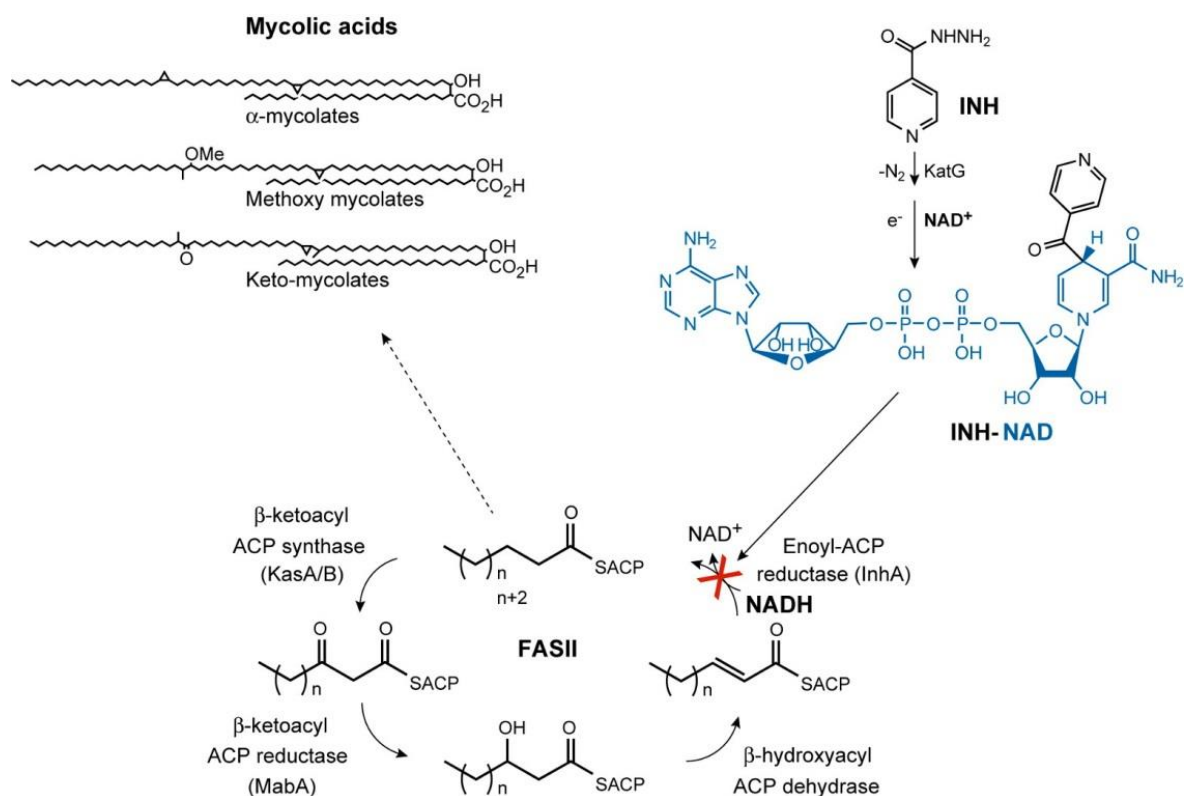
InhA enzyme inhibition leads to the inhibition of mycolic acid biosynthesis, accumulation of long-chain fatty acids [Takayama K. *et al.*, 1972; Winder F.G. and Collins P.B., 1971], and ultimately to cell death [Vilcheze C. *et al.*, 2000; Wang F. *et al.*, 2007].

## 2.3 InhA indirect inhibitors

### 2.3.1 Isoniazid (INH) and Ethionamide (ETH)

Isoniazid, one of the oldest known anti-tubercular and structurally simplest drugs, was found to have an exquisite activity against *Mycobacterium tuberculosis* more than 50 years ago, yet its precise mechanism of action could not be illuminated until genetic tools were developed. The combination of genetic, biochemical, and X-ray crystallographic studies [Banerjee A. *et al.*, 1994; Dessen A. *et al.*, 1995; Rozwarski D.A. *et al.*, 1998] provided a consistent model indicating that INH is activated by the catalase-peroxidase KatG to form an adduct with nicotinamide adenine dinucleotide (NAD) that inhibits the *inhA*-encoded NADH-dependent InhA enzyme of FAS-II. The addition of the isonicotinoyl radical to position 4 of the nicotinamide ring can result in two stereoisomers, in which only 4(S) isomer of INH-NAD

adduct possesses potent antimycobacterial activity [Stigliani J.L. *et al.*, 2008]. The mechanism of action of INH is illustrated in **Figure 2.4**.



**Figure 2.4:** Mechanism of action of INH in *Mycobacterium tuberculosis* [Vilcheze C. and Jacobs W.R. Jr., 2007]. INH is activated by KatG to form the INH-NAD adduct. This adduct inhibits InhA of the FASII, which synthesizes mycolic acids (representation of three mycolic acid classes). This inhibition results in the inhibition of mycolic acid biosynthesis and ultimately cell death.

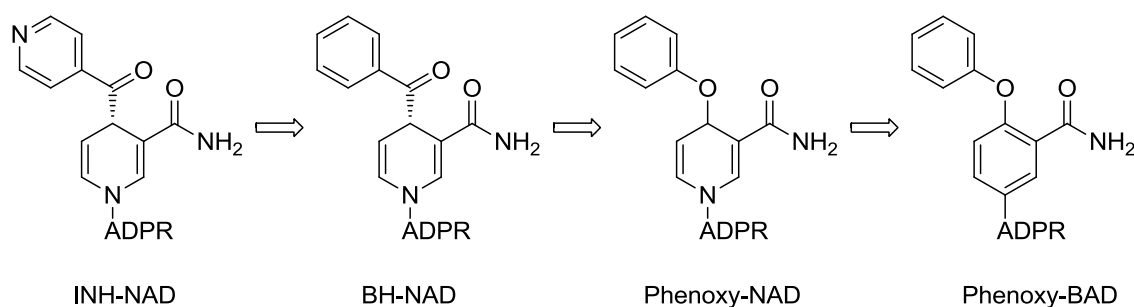
Similar to INH, Ethionamide (ETH) is a prodrug (also Prothionamide (PTH), an analogue of ETH,) and is activated in *Mycobacterium tuberculosis* by EthA, a flavin monooxygenase, to form a covalent ETH-NAD adduct that inhibits InhA [Morlock G.P. *et al.*, 2003; Wang F. *et al.*, 2007]. INH and ETH are highly specific and effective, and being prodrugs, mutations in the activators KatG and EthA have been correlated to most of the clinical resistance in the cases of drug-resistant TB [Hazbon M.H. *et al.*, 2006; Morlock G.P. *et al.*, 2003]. Therefore one should be able to attain the same clinical efficacy as INH and avoid much of the current resistance to INH and ETH by bypassing the requirement for KatG activation and directly inhibiting InhA.

## 2.4 InhA direct inhibitors

### 2.4.1 NAD analogues

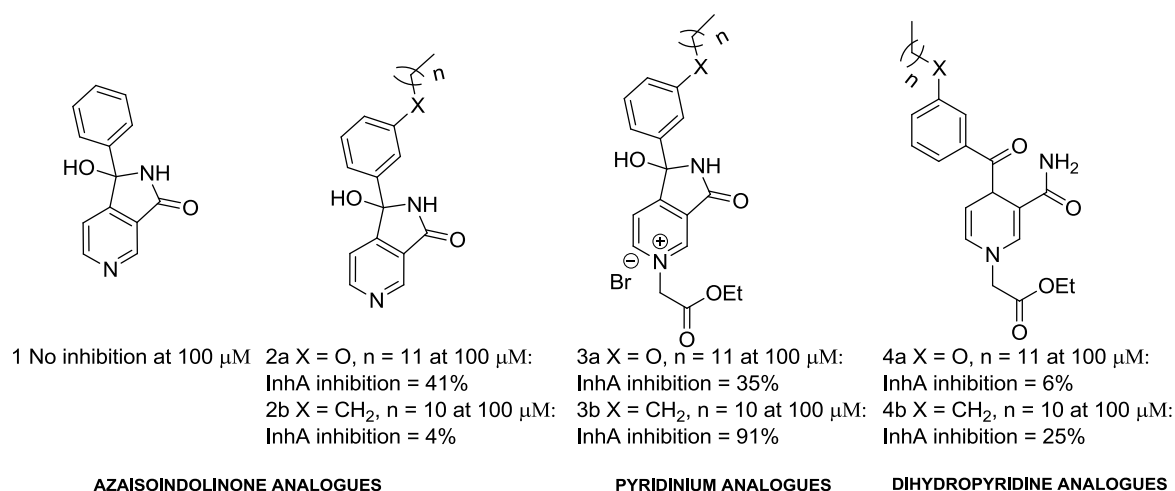
The discovery of the mechanism of INH activation brought a new enthusiasm to design of novel inhibitors to mimic INH-NAD adduct, that do not require activation by KatG for combating resistant-TB strains. Therefore, several studies were focused on the synthetic formation of INH-NAD adduct [Nguyen M. *et al.*, 2002; Broussy S. *et al.*, 2005; Argyrou A. *et al.*, 2007; Delaine T. *et al.*, 2007]. It was found that the benzoylhydrazine-NAD adduct (BH-NAD) formed *via* the reaction of the activated benzoic acid hydrazide and NAD competes with INH-NAD for binding to InhA [Rawat R. *et al.*, 2003], which encouraged scientists to investigate benzoyl and isonicotinoylnicotinamide analogues.

However, under biomimetic conditions three major structures (open keto-amide, cyclized hemiamidal and oxidized hemiamidal) rather than INH-NAD adducts exist due to poor stability [Nguyen M. *et al.*, 2002; Wilming M. and Johnsson K., 1999], that lack InhA inhibitory potency [Wilming M. and Johnsson K., 1999, Broussy S. *et al.*, 2003]. Considering such factors, Bonnac L. *et al.* redesigned the INH-NAD adduct at position 4, and used 4-phenoxy substitution of NAD instead of INH [Bonnac L. *et al.*, 2007]. They also replaced the nitrogen of nicotinamide ring with carbon in previous studies because of the glycosidic bond instability of INH-NAD adduct [Zatorski A. *et al.*, 1996; Pankiewicz K.W. *et al.*, 1997], to provide 4-phenoxy-substituted BAD analogues. The IC<sub>50</sub> value of 27  $\mu$ M confirmed the idea that simple aromatic mimics of the INH-NAD adduct can also inhibit InhA. The development of NAD analogues is illustrated in **Figure 2.5**. Although these NAD analogues do not need KatG activation, they were unable to overcome the resistance found in clinical strains caused by InhA (S94A) mutant.



**Figure 2.5:** The development of NAD analogues [Lu X.Y. *et al.*, 2010].

In 2010, Delaine T. *et al.* synthesized three series (pyridine, pyridinium and 1,4-dihydropyridines) of potential *Mycobacterium tuberculosis* InhA inhibitors that were structurally simplified analogues of INH-NAD adduct, the active form of INH (**Figure 2.6**). The incorporation of a lipophilic component into the nicotinamide hemiamidal framework provided more active derivatives. The dihydropyridine-based analogues **4** were too unstable for further development despite of their inhibitory activity towards InhA, owing to oxidation of dihydropyridine ring and loss of the N-substituent. The presence of the positive charge in the pyridinium series may represent an obstacle to the membrane crossing and responsible for their limitation to be regarded as hit molecules. In contrast, the stable azaisoindolinone compound **2a** showed InhA inhibitory activity along with promising antimicrobial profile compared to INH. Encouraged by these results, azaisoindolinone **2a** was selected as a hit compound for further optimization studies on targeting InhA [Delaine T. *et al.*, 2010].



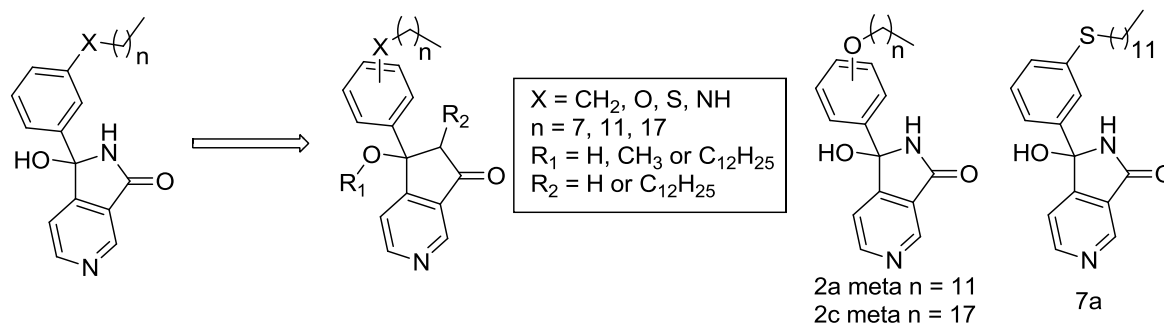
**Figure 2.6:** Structures of INH-NAD adducts and truncated analogues [Delaine T. *et al.*, 2010].

### 2.4.2 Azaisoindolinones

In 2011, Deraeve C. *et al.* reported a series of azaisoindolinones embedding a lipophilic chain based on the previous work done by Delaine T. *et al.* in 2010, and demonstrated for the first time that aryl azaisoindolinone framework undergoes epimerization at the C<sub>7</sub> carbon probably *via* a cycle opening pathway. The structure-activity relationship analysis, carried out around the parent azaisoindolinone scaffold **2a** helped to understand the pharmacophore elements (**Figure 2.7**). The following modifications resulted into the best molecular interaction with the InhA enzyme: (i) the attachment of lipophilic chain through the phenyl ring to the

azaisoindolinone scaffold, (ii) 12 or 18 carbons long chain bound to oxygen or sulphur atom to the *meta* position of the phenyl ring, and (iii) a free tertiary hydroxyl at C<sub>7</sub> position [Deraeve C. *et al.*, 2011].

The improvements made in the InhA inhibitory activity of azaisoindolinone through structural modifications were also well correlated with inhibitory potency of the growth of *Mycobacterium tuberculosis*. Compounds **2c** and **7a** displayed better InhA inhibitory potency (67 and 66% InhA inhibition at 100  $\mu$ M respectively) and better activity against *Mycobacterium tuberculosis* (MIC of 25 and 12.5  $\mu$ M respectively) than the lead molecule **2a** (27% InhA inhibition at 100  $\mu$ M and MIC of 156  $\mu$ M) (**Figure 2.7**). In contrast, some structural modifications led to a loss of InhA inhibitory activity and still associated with capacity to inhibit *Mycobacterium tuberculosis* growth. The cytotoxicity of these compounds towards eukaryote cells still impedes their further optimisation and development [Deraeve C. *et al.*, 2011].

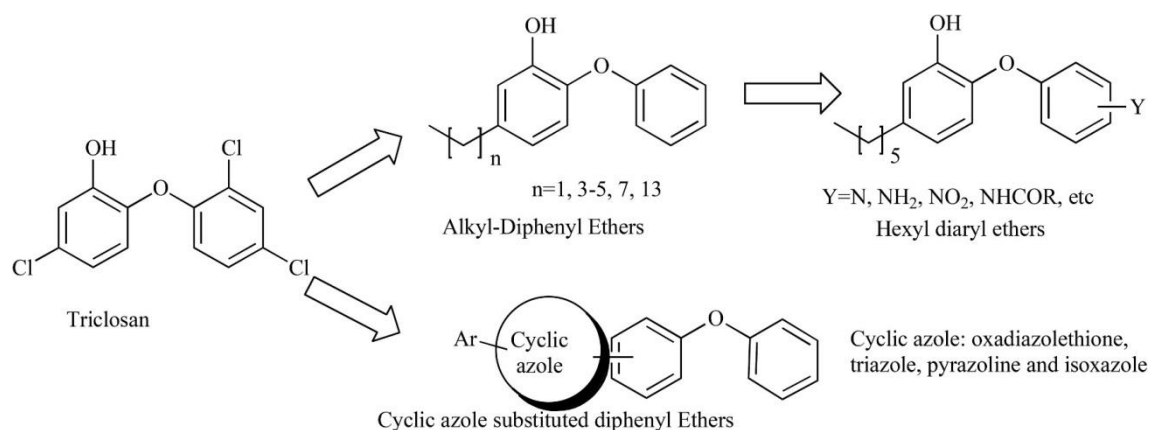


**Figure 2.7:** Modifications effected around azaisoindolinone framework of Delaine T. *et al.* (2010) and chemical structure of most active azaisoindolinones [Deraeve C. *et al.*, 2011].

### 2.4.3 Triclosan (TCN) and Alkyl diphenyl ethers

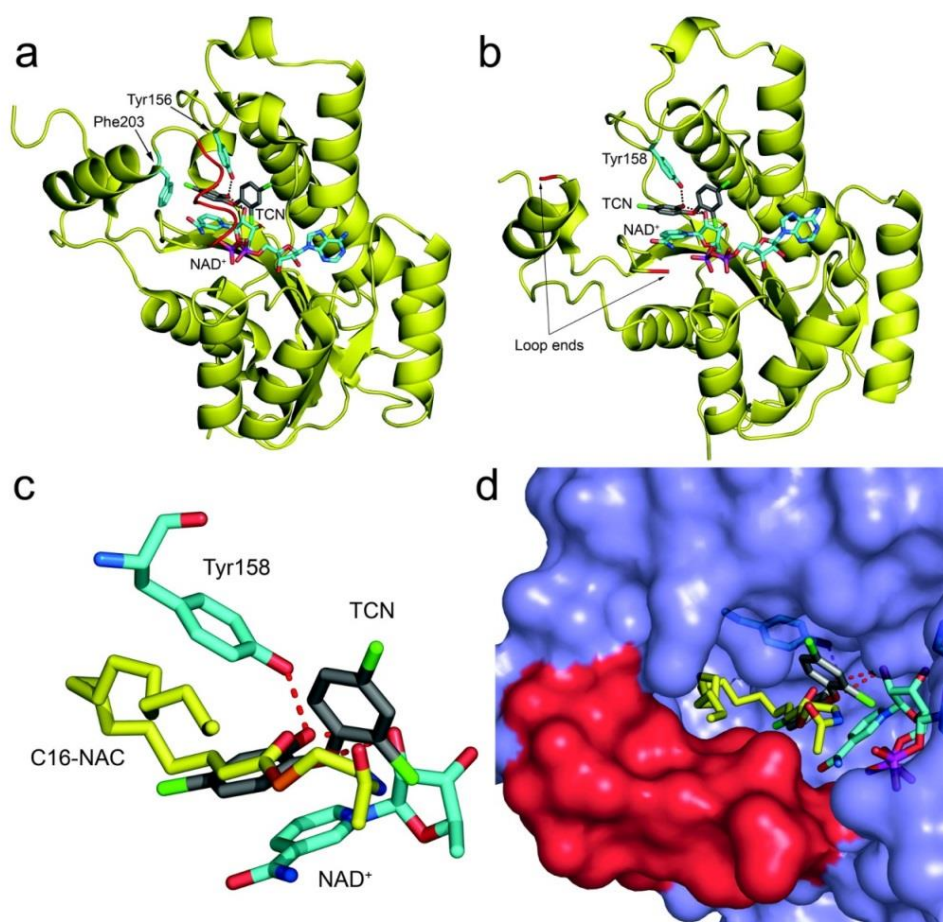
Triclosan was known to inhibit the synthesis of fatty acids in *Escherichia coli*, *Staphylococcus aureus* and other bacterium, by directly targeting enoyl-acyl carrier protein reductase (ENR or FabI) (**Figure 2.8**) [McMurry L.M. *et al.*, 1998; Roujeinikova A. *et al.*, 1999; Levy C.W. *et al.*, 1999]. Previous studies shown that TCN acts as an uncompetitive and site-directed inhibitor of ecFabI which forms a stable FabI-NAD<sup>+</sup>-TCN ternary complex through non-covalent interactions with amino acids [Heath R.J. *et al.*, 1999]. TCN is a picomolar inhibitor ( $K_i = 7$  pM) of the ecFabI which mimics its natural substructure [Roujeinikova A. *et al.*, 1999]. Earlier experiments have shown that TCN inhibits

*Mycobacterium tuberculosis* InhA [Parikh S.L. *et al.*, 2000], as a submicromolar uncompetitive inhibitor ( $K_i = 0.2 \mu\text{M}$ ) and the mode of action of InhA-TCN was quite different from that of INH, which not only avoids KatG activation but also combats InhA (S94A) mutant resistance. In addition, some gene dosage and selection experiments suggested that TCN is an intracellular InhA inhibitor [McMurry L.M. *et al.*, 1999]; with only moderate bactericidal activity against *Mycobacterium tuberculosis*, with an  $\text{MIC}_{99}$  value of 12.5 mg/mL (43 mM) [Sullivan T.J. *et al.*, 2006].



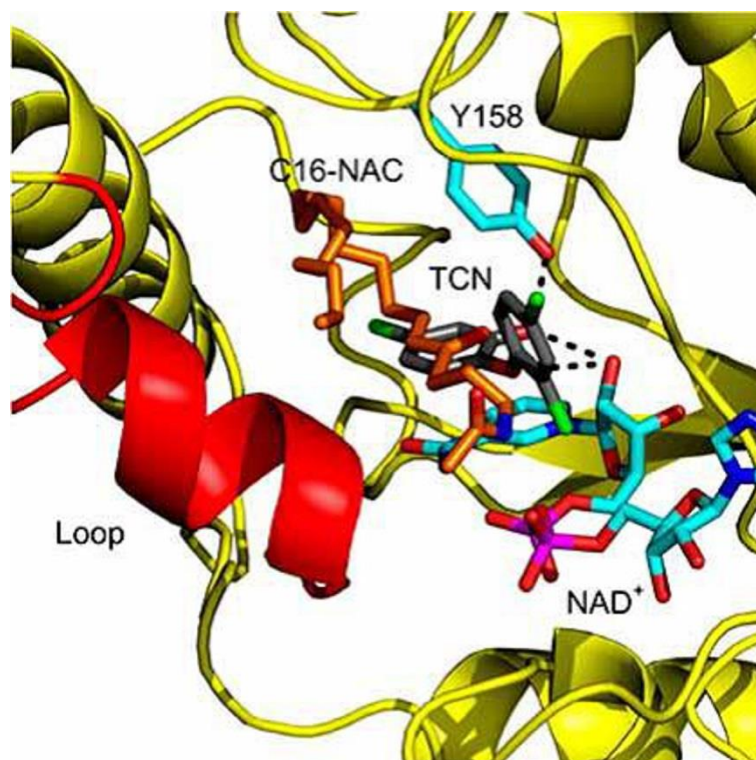
**Figure 2.8:** Triclosan and its derivatives [Lu X.Y. *et al.*, 2010].

In order to understand the activity difference (30000 fold) in the affinity of TCN with ecFabI and InhA, Tonge P.J. *et al.* determined the structure of TCN with InhA, which had one TCN molecule in the active site and was different from crystal structure determined by Kuo *et al.* [Kuo M.R. *et al.*, 2003]. There was a difference between ordering of the substrate binding loop of ecFabI-TCN and InhA-TCN complexes, wherein residues 195-200 were ordered when TCN binds to ecFabI and residues 197-211 were disordered in the InhA-TCN complex (**Figure 2.9**) [Sivaraman S. *et al.*, 2003].



**Figure 2.9:** Structures of triclosan bound to the *E. coli* FabI and InhA. Structures of triclosan (TCN; gray molecule) in complex with NAD<sup>+</sup> (blue molecule) and a) the *E. coli* FabI (PDB ID: 1QSG) and b) InhA. In the FabI-triclosan complex, the active site loop is ordered (coloured red) and residue Phe203 (blue) is shown adjacent to the loop, while in the InhA-triclosan complex, the loop is disordered (loop ends coloured red). In panels c and d, the InhA-triclosan structure has been overlaid with the structure of the C<sub>16</sub>-N-acetylcytseamine substrate (C<sub>16</sub>-NAC; yellow) bound to InhA and NAD<sup>+</sup> (PDB ID: 1BRV) [Rozwarski D.A. *et al.*, 1999]. In the C<sub>16</sub>-NAC complex, the active site loop (red surface) is ordered [Sullivan T.J. *et al.*, 2006].

To cause substrate binding loop of InhA to be ordered and improve the affinity of InhA, Tonge P.J. *et al.* superimposed the C<sub>16</sub>-NAC on the InhA-TCN complex and found that the substrate binding loop is ordered in the InhA-C<sub>16</sub>-NAC complex (**Figure 2.10**). Thus, a series of diphenyl ethers was designed by replacing chlorine atom on the phenol ring of TCN with various alkyl groups based on structure-based drug design strategies (**Figure 2.8**).



**Figure 2.10:** Superposition of InhA complexes with Triclosan and C<sub>16</sub>-NAC. The structure of triclosan (TCN) (grey) bound to InhA was superimposed with that of C<sub>16</sub>-NAC (gold) bound to InhA determined by Sacchettini J.E. *et al.* (PDB ID: 1BVR) [Rozwarski D.A. *et al.*, 1999]. Both complexes contain NAD<sup>+</sup> (cyan). Hydrogen bonds between triclosan, tyrosine158 and the NAD<sup>+</sup> ribose are shown in black dots. InhA from the C<sub>16</sub>-NAC structure is shown in ribbon format (yellow) and the substrate binding loop, which is ordered in this structure, is coloured red [Tonge P.J. *et al.*, 2007].

In 2006, Sullivan T.J. synthesized a series of alkyl diphenyl ethers and determined their IC<sub>50</sub> and Ki values for InhA inhibition (**Figure 2.8**). Among the synthesized compounds, 5-octyl-2-phenoxyphenol (8PP, diphenyl ether with octyl substituent at position 5) emerged as the most potent compound with a Ki value of 1.1 nM for InhA [Sullivan T.J. *et al.*, 2006]. As the length of alkyl substituent was increased from 2 to 8 carbons, a corresponding decrease in IC<sub>50</sub> value was observed. 14PP (diphenyl ether with tetradecyl substituent at position 5) was much less potent than 8PP with a Ki value of 30.3 nM for InhA. In order to observe the interactions of the alkyl diphenyl ethers with InhA, 5PP (diphenyl ether with pentyl substituent at position 5) and 8PP were co-crystallized with InhA. The results indicated that these compounds bind in a similar manner compared to TCN, namely, hydrogen bonds with Tyr158 and 2'-hydroxyl group of NAD<sup>+</sup>, and alkyl substituted phenol ring stacks with the

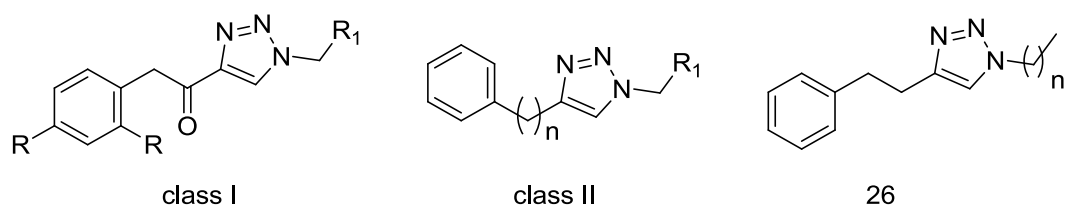


nicotinamide ring of NAD<sup>+</sup>. The hydrophobic pocket was a major site of interaction for side chains of the alkyl diphenyl ethers binding to InhA according to the studies. The *in vivo* studies showed that 6PP (diphenyl ether with hexyl substituent at position 5) and 8PP exhibited higher affinity for InhA and lower cytotoxicity than TCN, but still had limited bioavailability [Boyne M.E. *et al.*, 2007].

During their efforts to improve bioavailability of these alkyl diphenyl ethers, am Ende *et al.*, modified the phenyl ring with various heterocycles including nitrogen atom or phenyl ring substituted with nitro, amino, amide and piperazine groups at the *ortho*, *meta* or *para* positions as shown in **Figure 2.8**. Most of the derivatives showed significantly improved ClogP values (ClogP < 5) but decreased InhA inhibition activity. These results indicated that the introduction of a bulky substituent at the *ortho*, *meta* or *para* positions of the phenyl ring, or the incorporation nitrogen atom into the phenyl ring reduces InhA inhibitory potency [am Ende C.W. *et al.*, 2008].

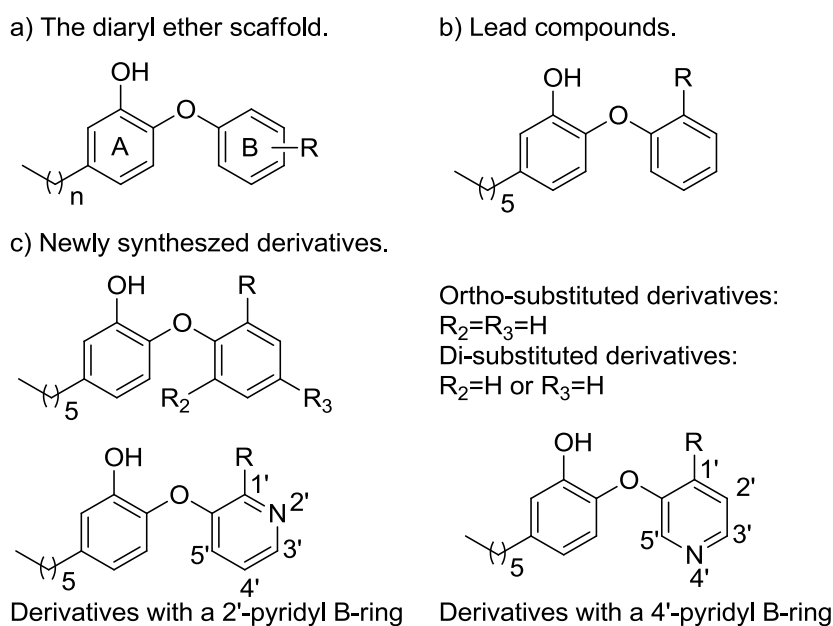
In 2008, Kini *et al.* reported a series of novel cyclic azole substituted diphenyl ether derivatives based on TCN backbone for anti-tubercular activity as shown in **Figure 2.8**. The compounds exhibited high activity against the H37Rv with MIC value in the range of 2.4 - 3.7  $\mu$ M, which was comparable to the standard drugs such as INH and RIF. Molecular modelling studies showed that the cyclic azole substituted derivatives occupied a larger binding domain than TCN [Kini S.G. *et al.*, 2009].

In 2011, Menendez C. *et al.* reported the design, synthesis and evaluation of potential InhA inhibitors by replacing the phenolic moiety (ring B) in TCN derivatives with 1,4-disubstituted triazole using click chemistry (**Figure 2.11**). They exploited copper-catalysed [3+2] cycloaddition between alkynes and different azides to afford two different classes of 1,2,3-triazoles. Class I had  $\alpha$ -ketotriazole moiety as a central fragment whereas, class II was investigated as a 1,4-dialkyl-substituted triazole to verify the contribution of the carbonyl group in the binding site of InhA. All the molecules were evaluated as inhibitors against InhA and for their anti-tubercular activity against *Mycobacterium tuberculosis* H37Rv strain. Inhibition studies showed that  $\alpha$ -ketotriazoles were poor inhibitors of InhA compared to class II compounds, particularly those bearing C<sub>8</sub>- or C<sub>9</sub>-alkyl chain, which were found to be good inhibitors of InhA. Compound **26** showed the best inhibitory activity as well as an MIC below 2 mg/mL [Menendez C. *et al.*, 2011].



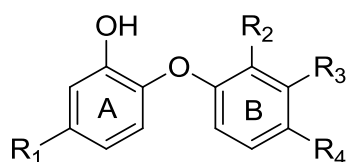
**Figure 2.11:** Chemical structure of class I and class II triazoles and most potent compound **26** [Menendez C. *et al.*, 2011].

The studies of Lu H. *et al.* on the enoyl-ACP reductase enzymes in other pathogens revealed that the *in vivo* efficacy of diaryl ether inhibitors correlates with their residence time on the enzyme target but not with their binding affinity values for enzyme inhibition ( $K_i$ ) or their *in vitro* antibacterial MIC values [Lu H. and Tonge P.J., 2008]. Based on this hypothesis, Luckner S.R. *et al.* developed long residence time inhibitors of InhA and discovered PT070 [Luckner S.R. *et al.*, 2010], the first slow-onset diaryl ether inhibitor which showed a 430-fold increase in binding affinity to InhA compared with PT004 (**Figure 2.12**). PT070 had a residence time of 24 min on InhA and was found to bind the enzyme through a two-step induced-fit mechanism, in which the rapid formation of the initial EI complex is followed by the slow formation of the final enzyme-inhibitor complex (EI\*). By using PT004 and PT070 as lead molecules, Pan P. *et al.* synthesized a series of twenty compounds with a hexyl-substituted A-ring and various modifications to the B-ring (**Figure 2.12**). All synthesized compounds were evaluated for InhA enzyme inhibition and cell-based antibacterial activity against *Mycobacterium tuberculosis*. It was found that the activity of the diaryl ether compounds was highly sensitive to the size of the *ortho* substituent/s on the B-ring. Introduction of groups on both *ortho* positions resulted in a loss of activity that, according to docking studies, leads to a conformation having unfavourable van der Waals interactions with the enzyme. The *ortho, para*-di-substituted compound PT107 showed similar activity to that of the parent compound, suggesting that *para* groups on the B-ring were well tolerated. The results showed that 2'-N pyridyl B-rings had significantly better activity than the 4'-N analogues, and the pyridyl B-ring was a better scaffold than the phenyl B-ring. It was shown that in case of diaryl ether compounds, slow-onset inhibitors always had higher binding affinity than rapid reversible inhibitors [Pan P. *et al.*, 2014].



**Figure 2.12:** Chemical structure of diaryl ether scaffold and modifications effected around it. a) The general structure of the diaryl ether scaffold. The diaryl ethers share a scaffold consisting of an alkyl phenol A-ring and a B-ring with various substituents. b) Lead compounds for structure-activity relationship studies described here. c) Newly synthesized derivatives including *ortho*-substituted derivatives, di-substituted derivatives, and derivatives with heterocyclic B-rings (2'-pyridyl or 4'-pyridyl) [Pan P. *et al.*, 2014].

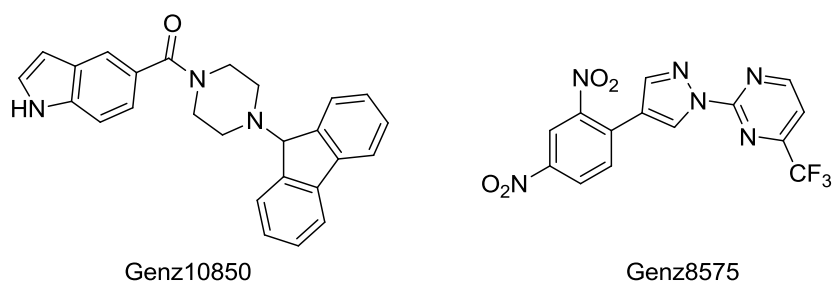
Recently, Kamsri P. *et al.* investigated the key structural features critical for the *Mycobacterium tuberculosis* InhA inhibition by 3D-QSAR CoMSIA models, constructed based on available experimental binding properties of diphenyl ether inhibitors. A set of four representative compounds was subjected to molecular dynamics simulations of inhibitor-InhA complexes to gain deeper insight into a fundamental basis of structural behaviour, inhibitor-InhA interactions and thermodynamic properties. The results showed that substitution with bulky groups as  $R_1$  substituent on the phenyl A ring of the inhibitors favoured hydrophobic pocket of InhA, whereas; small substituents with hydrophilic property were important at the  $R_3$  and  $R_4$  positions of the phenyl B rings to form hydrogen bonds with protein (**Figure 2.13**). In case of substitution at  $R_2$  position, small substituents with simultaneous hydrophilic or hydrophobic properties were preferred for interaction with the pyrophosphate moiety of  $NAD^+$  and the methyl side chain of Ala198, respectively. These findings provided structural guidance for the design of new and potent diphenyl ether-based inhibitors with high inhibitory potency against *Mycobacterium tuberculosis* InhA [Kamsri P. *et al.*, 2014].



**Figure 2.13:** General structure of diphenyl ether derivatives [Kamsri P. *et al.*, 2014].

#### 2.4.4 Indole-5-amides and Pyrazoles

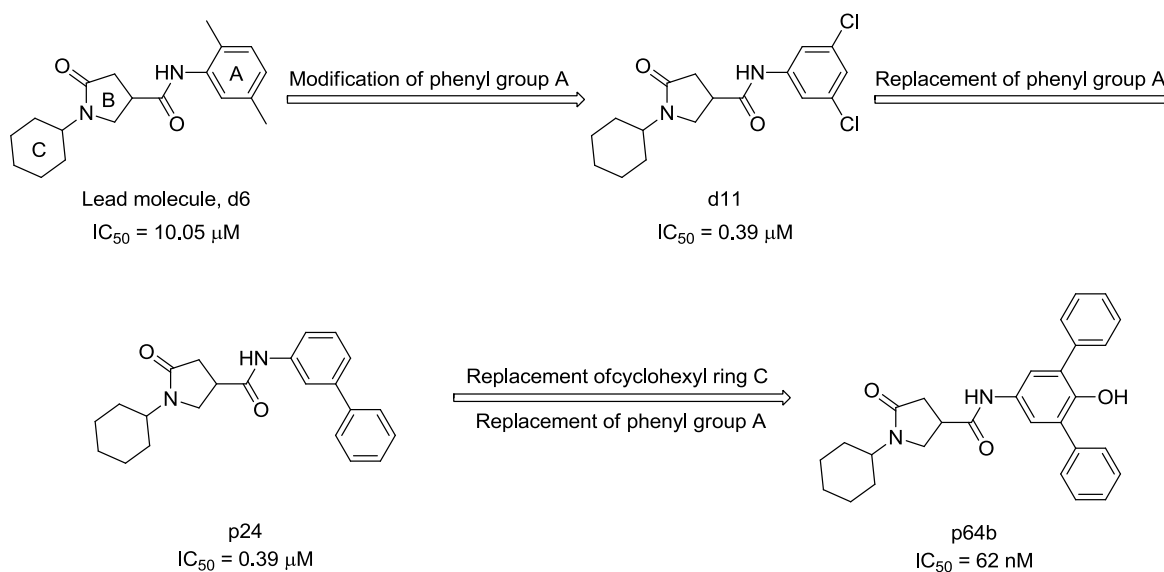
During their efforts to discover direct InhA inhibitors based on detailed understanding of the mechanism of TCN against InhA, Kuo M.R. *et al.* identified two novel series of direct InhA inhibitors using high-throughput screening of ~500000 combinatorial library compounds, which were shown to be effective against MDR-TB. Two representative compounds, one from each series are Genz10850 and Genz8575, with  $IC_{50}$  values of 0.16  $\mu$ M and 0.24  $\mu$ M against InhA, respectively (**Figure 2.14**). The structure-activity relationship of Genz10850 analogues showed that carbon position 2 or 3 of the piperazine ring was very crucial owing to the steric clash with the Phe149 of the protein. Indole nitrogen formed hydrogen bonds with the phosphate oxygen of NAD<sup>+</sup> and should not be alkylated or acylated. Kinetic studies indicated that both compounds are competitive with the C<sub>16</sub>-NAC substrate. The crystal structure of InhA-Genz10850 revealed the binding mode of Genz10850 to InhA. The piperazine and indole groups of Genz10850 overlaid the phenol ring and the dichlorophenyl ring of TCN, respectively. The carbonyl group of the Genz10850 formed hydrogen bonds with catalytic residue Tyr158 and 2'-hydroxyl group of NAD<sup>+</sup>, whereas bulky fluorenyl group occupied the long acyl chain of C<sub>16</sub>-NAC binding site with van der Waals interactions. This hydrophobic interaction was shown to be essential for high affinity of InhA. Several analogues of pyrazole were also prepared based on the screening results, among which Genz8575 displayed 91 % inhibition of InhA at 40  $\mu$ M. Replacing the trifluoromethylpyrimidine group of Genz8575 with other substituted aromatic rings caused a significant decrease in activity, suggesting importance of trifluoromethylpyrimidine group for the high affinity of InhA [Kuo M.R. *et al.*, 2003].



**Figure 2.14:** Chemical structure of representative Indole-5-amide and Pyrazole [Kuo M.R. *et al.*, 2003].

### 2.4.5 Pyrrolidine carboxamides

In 2006, He *et al.* identified pyrrolidine carboxamides as a novel class of InhA inhibitors through high throughput screening of a library comprising of around 30000 molecules and microarray parallel synthesis methods. These compounds were classified into 13 structurally diverse groups and substantial scaffold differences among the inhibitor groups suggested a high tolerance of the InhA binding pocket. Among them, a pyrrolidine carboxamide **d6**, showed an  $IC_{50}$  of 10.05  $\mu$ M. Initial *in silico* analysis of this compound into the InhA active site suggested the formation of a hydrogen-bonding network between **d6**, enzyme active site residues, and the NAD<sup>+</sup> cofactor that probably serves as the key feature that governs the orientation of the compound within the active site. The dual hydrogen bonding network involved the oxygen atom on the pyrrolidine carbonyl group, InhA catalytic residue Tyr158, and the NAD<sup>+</sup>. This hydrogen bonding network seemed to be a conserved feature among all the InhA-inhibitor complexes identified so far. Since the molecular modelling study suggested a central role of the ketopyrrolidine core B in formation of the hydrogen bonding network, it was kept unchanged while the molecule was further optimized by replacing the phenyl ring A and cyclohexyl ring C with other groups (**Figure 2.15**) [He X. *et al.*, 2006].

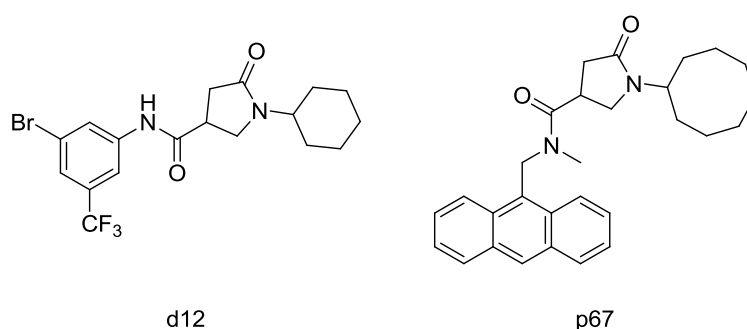


**Figure 2.15:** Development of pyrrolidine carboxamides [Lu X.Y. *et al.*, 2010].

Modification of pyrrolidine carboxamides by various substitutions at phenyl ring A resulted in compounds with significant activity. Compound **d11** emerged as most potent molecule with symmetric 3- and 5-chloro atoms on the phenyl ring with IC<sub>50</sub> of 0.39 μM against InhA (**Figure 2.15**). The oxygen of the carbonyl group of ketopyrrolidine formed hydrogen bonds with the hydroxyl group of Tyr158 and with 2'-hydroxyl moiety of the nicotinamide in the crystal structure of compound **d11** bound with InhA. Replacement of phenyl ring A of pyrrolidine carboxamides with various aromatic and aliphatic rings indicated that increase in the size of aromatic ring can improve the activity due to the hydrophobic interactions. Based on these results, He *et al.* further modified the phenyl ring A of pyrrolidine carboxamides and this time with substituted phenyl rings and other saturated rings. The SAR results suggested that the hydrophobic interactions between the large phenyl ring and the active site of InhA were essential for the activity. Compound **p24** showed an IC<sub>50</sub> of 0.39 μM and the most potent inhibitor **p64b** displayed promising IC<sub>50</sub> of 62 nM. A 160 fold gain in potency was thus realized through library optimization (**Figure 2.15**) [He X. *et al.*, 2006].

Pyrrolidine carboxamide classes are racemic and the InhA inhibitory potency is exhibited by R-enantiomers only. The inhibitory potency of R-enantiomers was 10-fold higher than S-enantiomers. Unfortunately, compounds with good enzyme inhibition potency do not exhibit equally correlating activity against *Mycobacterium tuberculosis* H37Rv strain. The most potent MIC value of 62.5 μM was displayed by compounds **d12** and **p67** which may be limited due to poor membrane permeability of pyrrolidine carboxamides. Nevertheless, these

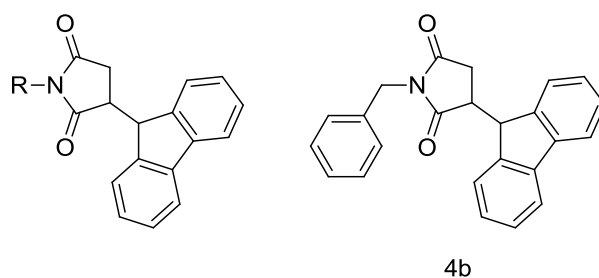
novel pyrrolidine carboxamides provided a good foundation for the discovery of direct InhA inhibitors (**Figure 2.16**) [He X. *et al.*, 2006].



**Figure 2.16:** Chemical structure of most potent antimycobacterial compounds **d12** and **p67** [He X. *et al.*, 2006].

In 2008, Kumar A. and Siddiqi M.I. performed comparative molecular field analysis (CoMFA) studies and subsequent *de novo* ligand design using the LeapFrog program on reported selective *Mycobacterium tuberculosis* InhA inhibitors belonging to the class of pyrrolidine carboxamides. In order to rationalize the structure-activity relationship of pyrrolidine carboxamides and they proposed thirteen new pyrrolidine carboxamide analogues, based on the information derived from the CoMFA contour maps. Structurally, the designed molecules differed from the previously reported molecules with addition of bulky substituents in region A (aromatic substitution toward the amide linkage) and maintained the similar steric bulk at region B (substitution toward the pyrrolidine ring). In some cases addition of substituents at the central core resulted in increased activity [Kumar A. and Siddiqi M.I., 2008].

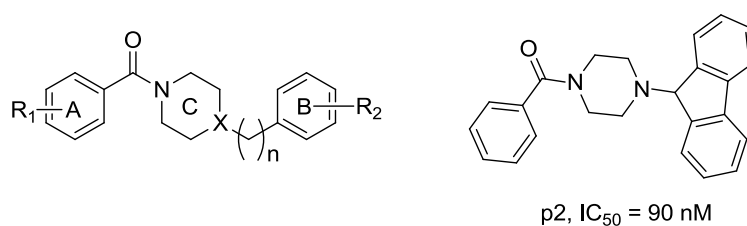
Recently, Matviiuk T. *et al.* reported the discovery, synthesis and screening results of a series of 3-(9*H*-fluoren-9-yl)pyrrolidine-2,5-dione derivatives as a novel class of potent inhibitors of *Mycobacterium tuberculosis* H37Rv strain as well as the InhA enzyme (**Figure 2.17**). The replacement of the piperazine ring of Genz-10850 with a succinimide core resulted in increased activity against *Mycobacterium tuberculosis* H37Rv strain. Compound **4b** emerged as most potent molecule with 56 % inhibition of InhA at 50  $\mu$ M and *Mycobacterium tuberculosis* MIC of 91.4  $\mu$ M. The ability of these novel compounds to strongly inhibit InhA and/or *Mycobacterium tuberculosis* growth presented them as new leads for the development of candidate drugs [Matviiuk T. *et al.*, 2013].



**Figure 2.17:** General structure of 3-(9H-fluoren-9-yl)pyrrolidine-2,5-dione derivatives (left) and structure of most potent compound **4b** (right) [Matviiuk T. *et al.*, 2013].

### 2.4.6 Arylamides

Arylamides are the novel class of direct InhA inhibitors identified by He *et al.* from the high-throughput screening [He X. *et al.*, 2007]. The library was synthesized using microtiter library synthesis followed by *in situ* screening, which enabled the rapid discovery of more potent InhA inhibitors. In an InhA-inhibitor complex, the amide carbonyl group oxygen displayed formation of hydrogen bonds with Tyr158 and 2'-hydroxyl of the nicotinamide ribose, a conserved feature previously seen in all crystal structures of InhA complexed with various direct inhibitors. The unsubstituted phenyl ring was located inside the hydrophobic site with van der Waals interactions. This hydrophobic site was sufficiently large that additional space was still available to accommodate other hydrophobic groups by analysing the complex. By using bulky hydrophobic groups instead of the initial phenyl ring, most of the compounds exhibited excellent activity against InhA. Among the synthesized analogues, one compound with a fluorenyl group attached to piperazine ring exhibited an  $IC_{50}$  of 90 nM (**Figure 2.18**) [He X. *et al.*, 2007].



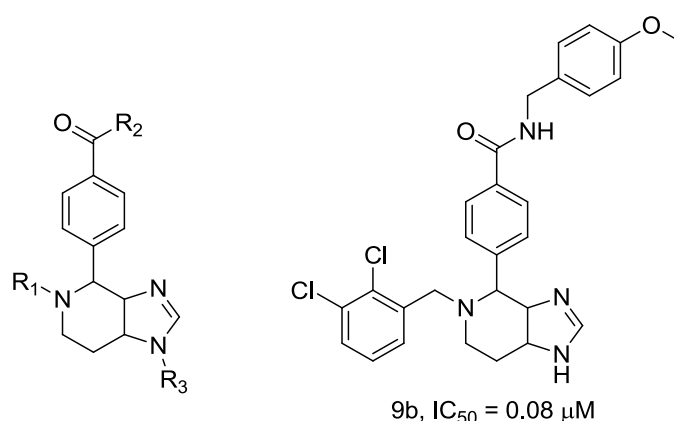
**Figure 2.18:** General structure of compounds identified in initial high-throughput screening (left) and most potent arylamide identified by microtiter synthesis and *in situ* screening (right) [He X. *et al.*, 2007].



However, similar to pyrrolidine carboxamide series, arylamides do not exhibit good *in vitro* anti-tubercular activity. Most of the compounds showed MIC values higher than 125  $\mu\text{M}$ , and only one compound displayed *Mycobacterium tuberculosis* MIC of 62.5  $\mu\text{M}$ . These results suggested that arylamides may have poor membrane permeability or are easily extruded by efflux pumps.

### 2.4.7 Imidazopiperidines

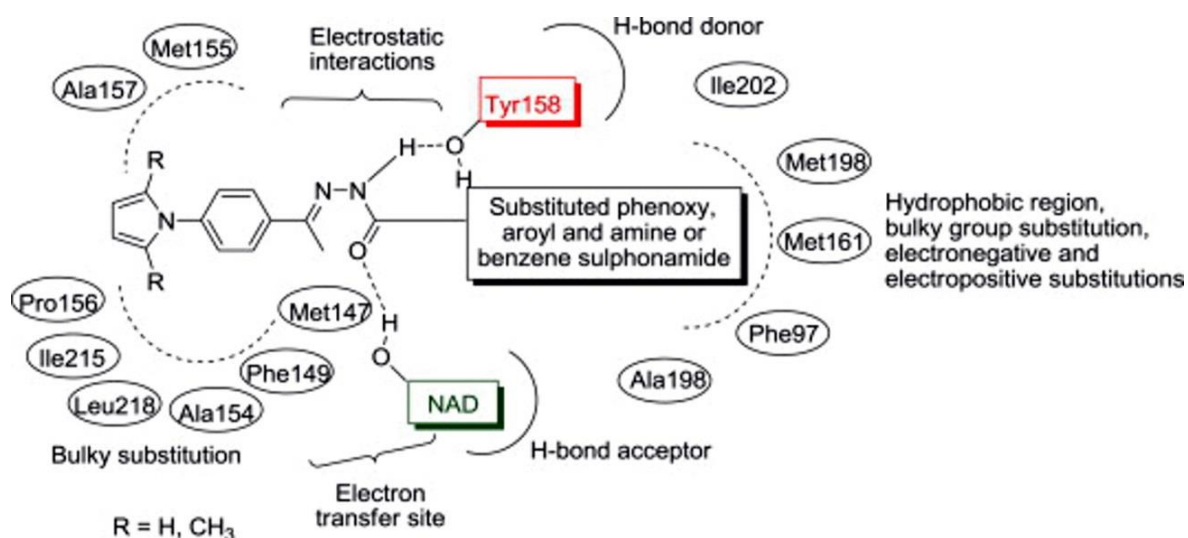
Researchers at *GlaxoSmithKline* described a new series of Imidazopiperidines as non-covalent inhibitors of InhA from screening [Wall M.D. *et al.*, 2007]. Compound **9b** exhibited the most potent InhA inhibitory potency with  $\text{IC}_{50}$  of 0.08  $\mu\text{M}$  (**Figure 2.19**). Previous studies suggested that, it was suitable to use solid phase synthesis for carrying out the optimization on the carbonyl and piperidine positions due to the specificity of the imidazopiperidine structure [Stocker F.B. and Evans A.J., 1990]. The results of initial screening showed that, (i) substitutions at the carbonyl and piperidine positions are critical for activity, (ii) *para*-position of benzylamine group with electron donating group at the carbonyl position and mono or dichloro benzyl group at the piperidine displayed good potency, (iii) replacement the imidazole group with a phenyl group leads to a complete loss of activity. The mechanism of action of imidazopiperidines still remains unclear, yet it was suggested that a non-specific mechanism may exist, based on the lack of broad-spectrum antibacterial activity compared to TCN.



**Figure 2.19:** General structure of Imidazopiperidines (left) and most potent compound **9b** (right) [Wall M.D. *et al.*, 2007].

## 2.4.8 Pyrrole hydrazines

Recently, More U.A. *et al.* synthesized and screened a novel series of 52 pyrrole hydrazine derivatives against *Mycobacterium tuberculosis* InhA. The binding mode of the highly active compounds at the active site of InhA explored using surflex-docking method displayed hydrogen bonding interactions with Tyr158 and NAD<sup>+</sup> in the same manner as TCN. The promising activity of these compounds was attributed to the incorporation of heterocyclic moieties *viz.*, substituted pyridine, pyrrole and aromatic compounds substituted with methyl-, hydroxyl-, chloro-, bromo-, nitro-, acetamide- and amine- groups. The electron donating groups attached to phenyl ring, and methyl substituted pyrrole exhibited a solubilizing effect on the compound. The halogen substituted aromatic compounds improved the lipophilic nature of the molecules, whereas the methoxy substituted compounds enacted as electron donor. In addition, the presence of -C=NNH- moiety and -C=O group on hydrazine bridge were essential for hydrogen bonding with the receptor, while hydroxyl group at the 4<sup>th</sup> position of phenyl ring resulted in improved solubility [More U.A. *et al.*, 2014].



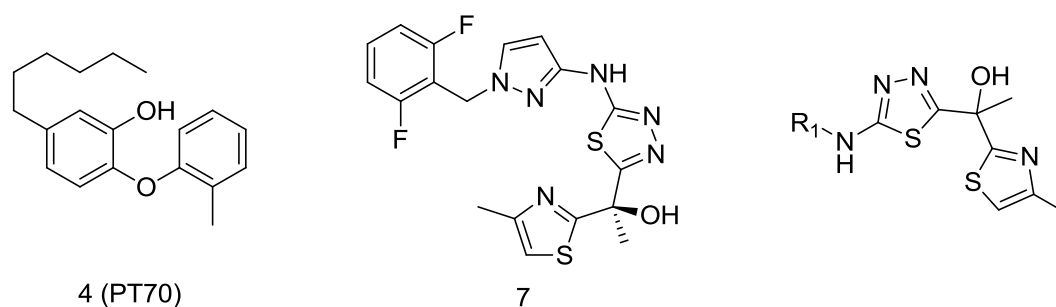
**Figure 2.20:** Docked region and structure-activity relationship for pyrrole hydrazones. Green residue represents hydrogen bond acceptor, red residues hydrogen bond donors, and black residues form the hydrophobic pocket [More U.A. *et al.*, 2014].

The combined results of anti-tubercular activity, docking studies and 3D-QSAR suggested that (**Figure 2.20**): (i) the hydrazone moiety, which occupied the middle part of pocket in the InhA active site, made a contribution (NH<sup>+</sup>⋯OH (Tyr158), C=O<sup>+</sup>⋯HO (NAD<sup>+</sup>) to hydrogen bonding) to the selectivity making it a suitable scaffold for InhA, (ii) pyrrole, aroyloxy, aroyl,

benzenesulphonamide and hydrazone bridge with appropriate substitutions might be useful to design new molecules with enhanced selectivity towards InhA enzyme [More U.A. *et al.*, 2014].

#### 2.4.9 Methyl thiazoles

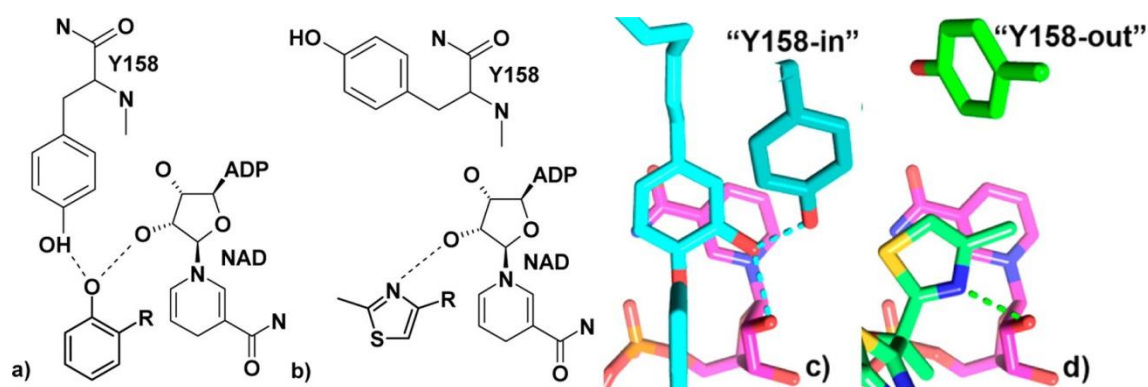
Several unsuccessful efforts in past to achieve promising mycobacterial cellular potency (MIC) through potent inhibition ( $IC_{50}$ ) of FASII enzymes such as InhA, led to belief that there is disconnect between enzyme inhibition and cellular potency. But in 2011, researchers at GlaxoSmithKline published series of methyl thiazoles, wherein they showed that mycobacterial cellular potency indeed can be achieved with potent enzyme inhibition. It was demonstrated that the potent enzyme inhibition (InhA  $IC_{50} = 0.003 \mu M$ ) by a direct InhA inhibitor methyl thiazole scaffold **7** was successfully translated into cellular potency (*Mycobacterium tuberculosis* MIC =  $0.19 \mu M$ ) (**Figure 2.21**) [Ballell Pages L. *et al.*, 2010; Castro Pichel J. *et al.*, 2012].



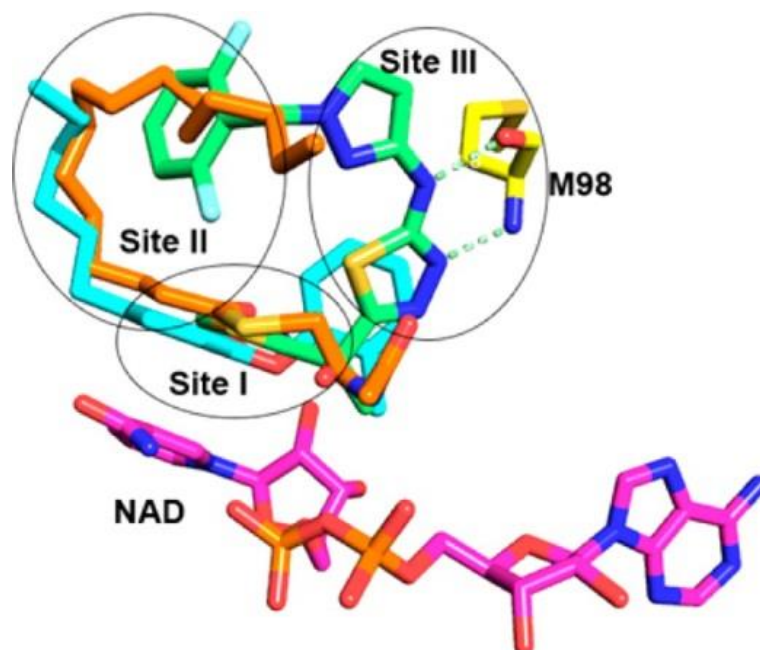
**Figure 2.21:** Chemical structure of reported potent InhA inhibitor **4** (PT70) [Pan P. and Tonge P.J., 2012], methyl thiazole scaffold **7** [Ballell Pages L. *et al.*, 2010; Castro Pichel J. *et al.*, 2012] and general structure of methyl thiazole analogues of present series (right) [Shirude P.S. *et al.*, 2013].

Encouraged by these results, a group of scientists at AstraZeneca elucidated the molecular mode of action of this series and the properties that drive cellular potency [Shirude P.S. *et al.*, 2013]. They identified for the first time a mechanism of InhA inhibition which showed a previously unknown neutrally charged “warhead” being accommodated in the “Y158-out” conformation at site I of the InhA protein (**Figure 2.22** and **Figure 2.23**). Notably, these compounds showed preferential binding to the NADH-bound form of the enzyme as opposed to the NAD<sup>+</sup> bound form of the enzyme which might reflect the charge complementarity between the site I group and NADH (*i.e.*, both neutral). Additionally, their studies indicated

that novel hydrophilic interactions with protein residue M98 at site III lead to favourable physicochemical properties, resulting in cellular activity (**Figure 2.23**). On the basis of this mechanism, new analogues were synthesized with potent enzyme inhibition, attractive cellular potency, improved CYP inhibition, and safety profile as compared to the previously reported methyl-thiazole lead molecule **7** (**Figure 2.21**). Based on these results, it was proposed that the aspects of the binding mode and molecular mode of inhibition of this series are transferable to other series, which are capable of opening up new avenues of medicinal chemistry against this important and clinically validated TB target [Shirude P.S. *et al.*, 2013].



**Figure 2.22:** InhA catalytic site I interactions: (a,b) diagrammatic representation of chemical structures and (c,d) stick representations of X-ray crystal structures representing two classes of catalytic site interactions. Substrate competitive inhibitors have been categorized into two types by their interactions at site I according to the conformation of tyrosine residue 158; “Y158-in” (a,c) as demonstrated by **4** [Luckner S.R. *et al.*, 2010] and a previously unreported “Y158-out” conformation (b,d) as demonstrated by the complex of **7** with InhA [Shirude P.S. *et al.*, 2013].



**Figure 2.23:** Substrate site binding regions of InhA. Protein complexes of **7** (PDB ID: 4bpq) [Shirude P.S. *et al.*, 2013], **4** (PDB ID: 2x23) [Luckner S.R. *et al.*, 2010] and C<sub>16</sub> fatty acyl substrate (PDB ID: 1bvr) [Rozwarski D.A. *et al.*, 1999] are overlaid. The figure highlights three regions within the substrate binding site: site I, the catalytic site; site II, the hydrophobic pocket; site III, also termed the size-limited region [Pan P. and Tonge P.J., 2012]. Proteins atoms have been removed for clarity, except for M98 from the InhA-NADH-7 complex which is drawn with carbon atoms in yellow. **7** is shown as sticks with green carbon atoms, **4** is shown with cyan carbon atoms, and C<sub>16</sub> fatty acyl substrate is shown with orange carbon atoms. NAD is shown as sticks with pink carbon atoms. Both the phenolic ring of **4** and the methyl thiazole ring of **7** occupy a similar positioning, allowing  $\pi$ -stacking with the nicotinamide ring of the cofactor NAD [Shirude P.S. *et al.*, 2013].

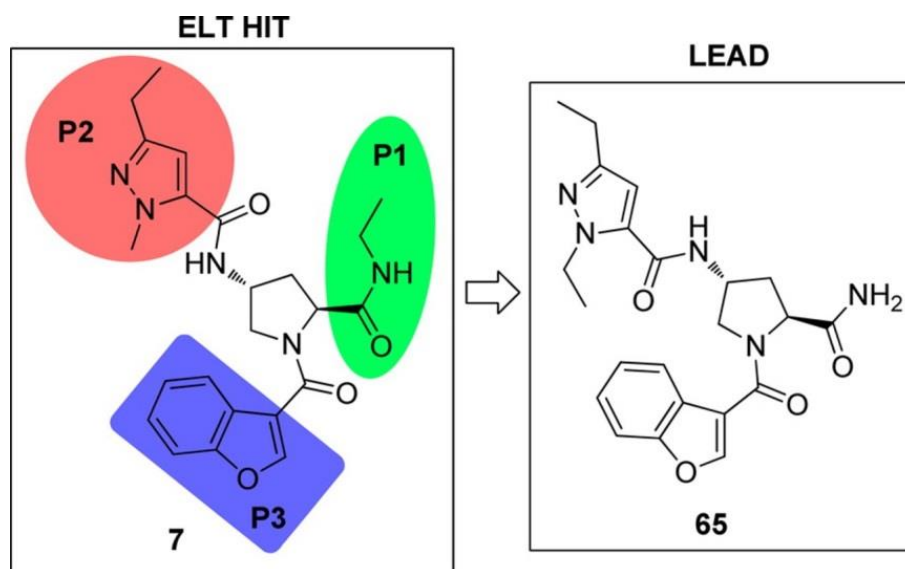
#### 2.4.10 Discovery of novel miscellaneous leads as InhA direct inhibitors using Virtual screening

Pauli I. *et al.* in 2013 used two different virtual-ligand-screening approaches to identify new InhA inhibitors from a library of ligands selected from the ZINC database. In their efforts to identify new chemo-types that could serve as a starting point for the design of chemically novel and patentable drug candidates in drug discovery, two distinct *in silico* approaches were adopted: (i) the development of a 3D pharmacophore model for ligands of *Mycobacterium tuberculosis* InhA followed by a pharmacophore-based virtual screening, and (ii) a virtual screening using a combination of four docking programs that employ distinct

search algorithms. The use of these methodologies resulted in the identification of compounds having satisfactory *in vitro* *Mycobacterium tuberculosis* InhA inhibitory activity with IC<sub>50</sub> values ranging from 24 to 83 μM. In addition, it was suggested that the *Mycobacterium tuberculosis* InhA substrate-binding cavity is large enough to accommodate, simultaneously, both substrate and inhibitor [Pauli I. *et al.*, 2013].

In their efforts to identify new leads against TB, Shanthi V. and Ramanathan K. in 2013, performed virtual screening from Drug bank database by utilizing INH-NAD adduct as search query. Initially, virtual compounds were subjected to molinspiration program and screening was carried out by restricting the number of rotatable bonds to a maximum of 12. Subsequently, physiochemical properties such as toxicity, solubility, drug-likeness and drug score were analysed for the filtered set of compounds, and final data reduction was performed by means of molecular docking and normal mode docking analysis. The results indicated that DB04362, adenosine diphosphate-5-(betaethyl)-4-methyl-thiazole-2-carboxylic acid displayed strong binding affinity towards both the native and mutant type InhA, and can be used as a starting point for designing of anti-tubercular lead molecules [Shanthi V. and Ramanathan K., 2013].

Recently, Encinas L. *et al.* identified a class of potent and selective *Mycobacterium tuberculosis* direct InhA inhibitors by means of the application of DNA encoded library technology wherein a large collection of chemo-typically diverse DNA-encoded small molecule libraries were screened for affinity towards InhA. This screening yielded compound **7** with *Mycobacterium tuberculosis* InhA IC<sub>50</sub> of 34 nM and MIC of 8 μM. In order to improve anti-tubercular potency, they introduced one modification at a time in compound **7** around the three possible positions (**Figure 2.24**). The combined results of these efforts showed that: (i) P<sub>3</sub> position was most flexible in terms of SAR manipulations and nature of the substitution at this position was of key importance for potent enzymatic activity, (ii) the substitution with diethylpyrazole moiety at P<sub>2</sub> position was most suitable for improving anti-tubercular potency of compounds, and (iii) nature of substitution at P<sub>1</sub> position was critical in determining physicochemical and ADME properties. This feature combination resulted in identification of optimized lead compound **65** (with *Mycobacterium tuberculosis* InhA IC<sub>50</sub> of 4 nM and MIC of 0.5 μM) which despite its good balance between InhA inhibition, anti-tubercular potency, and pharmacokinetic profile, was found to be inactive *in vivo* against a murine TB acute infection model [Encinas L. *et al.*, 2014].



**Figure 2.24:** Three positions for optimization in target compound **7** and structure of optimized lead compound **65** [Encinas L. *et al.*, 2014].

The popularity of InhA as a screening target may derive from the facts that screens may usually lead to hits and at least two commercially useful compounds act by inhibiting it. Based on this basic viewpoint, some novel classes of InhA direct inhibitors have been identified using various strategies. Despite the structural diversity in the different InhA inhibitor classes, two generalizations arise from an analysis of the data. Firstly, in almost every case the inhibitors bind to the enzyme in the presence of the oxidized and/or reduced cofactor, albeit in the case of INH and the diazaborines as covalent adducts of the cofactor [Lu H. and Tonge P.J., 2008]. And secondly, high affinity inhibition is often coupled to ordering of the ‘substrate binding loop’ that is located close to the active site [Lu H. and Tonge P.J., 2008].

The search for new TB drugs remains challenging albeit vitally important task. The failing effectiveness of current anti-tubercular drugs to combat infection signifies urgent need to identify new and potent agents.

### 3.1 Objectives

The global pandemic of drug sensitive TB as well as the increasing threat from various drug-resistant forms of TB drives the quest for newer, safer, more effective TB treatment options. A thorough review of literature available enlightened the importance of mycobacterial type II fatty acid biosynthesis pathway and particularly *Mycobacterium tuberculosis* InhA enzyme which is an essential but underexploited target for TB drug discovery. The present study, thus focus on achieving promising mycobacterial cellular potency through developing potential *Mycobacterium tuberculosis* InhA direct inhibitors.

The main objectives of the proposed work are:

1. To synthesize novel *Mycobacterium tuberculosis* InhA inhibitors with a view to improve antimycobacterial activity.
2. To evaluate the inhibitory potency of the synthesized compounds by *in vitro* InhA inhibition assay.
3. To evaluate the protein interaction and stability of synthesized compounds using biophysical characterization technique.
4. To undertake *in vitro* antimycobacterial screening of the synthesized compounds against *Mycobacterium tuberculosis*, and
5. To perform the *in vitro* cytotoxicity studies of the synthesized compounds.

### 3.2 Plan of work

The plan of work was classified into the following categories:

#### 3.2.1 Synthesis and characterization

In 2013, our research group demonstrated a virtual screening strategy to develop novel inhibitors against *Mycobacterium tuberculosis* InhA [Kumar U.C. *et al.*, 2013]. The strategy



resulted in identification of several hits which exhibited InhA inhibitory activity in enzymatic studies. Thus, we decided to take these moderately active hits as lead molecules for further optimization of their enzyme inhibition potency. Based on this and inputs from protein-ligand interactions observed in the structure of InhA with lead molecules, further modifications (and combinations thereof) were explored in a ligand expansion step. The designed molecules were further synthesized in our laboratory utilizing previously reported methodology available in literature for structurally related molecules. All reactions were monitored using thin layer chromatography and LCMS. The synthesized compounds were fully characterized using modern analytical techniques. LCMS, <sup>1</sup>H-NMR and <sup>13</sup>C-NMR were recorded and analysed to confirm the structure of the compounds. Purity of the compounds was evaluated by elemental analysis.

### **3.2.2 *In vitro* enzyme inhibitory potency**

The synthesized compounds were evaluated for their InhA inhibitory potency by *in vitro* *Mycobacterium tuberculosis* InhA inhibition assay.

### **3.2.3 Evaluation of protein interaction and stability using biophysical characterization technique**

The ability of some active compounds to stabilize the catalytic domain of the InhA protein was assessed utilizing the differential scanning fluorimetry (DSF) technique by which the thermal stability of the catalytic domain of InhA native protein and of the protein bound with the ligand was measured.

### **3.2.4 *In vitro* *Mycobacterium tuberculosis* activity studies**

All the synthesized compounds were further screened for their *in vitro* antimycobacterial activity against *Mycobacterium tuberculosis* H37Rv (ATCC27294) by using agar dilution method.

### **3.2.5 *In vitro* cytotoxicity screening**

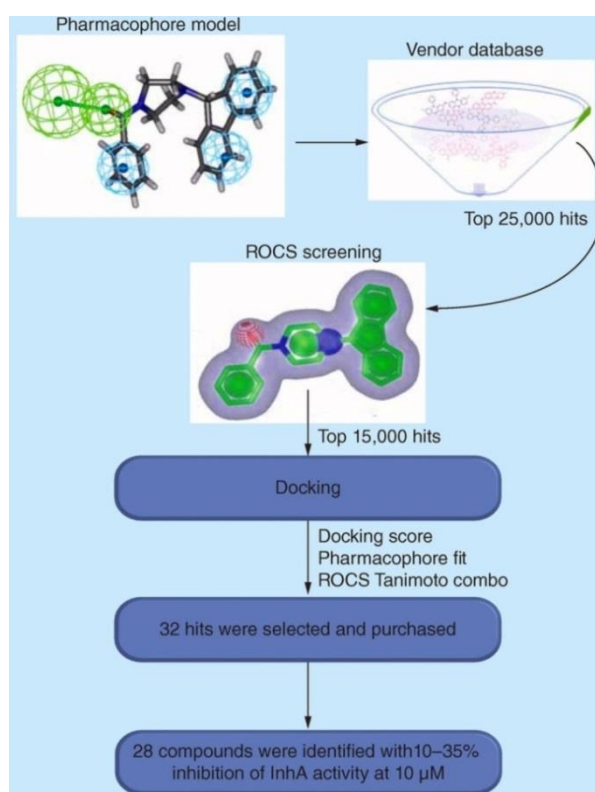
All the synthesized compounds were also screened for their *in vitro* cytotoxicity against RAW 264.7 cell line (mouse leukemic monocyte macrophage) using 3-(4,5-dimethylthiazol-2-yl)-2,5-diphenyltetrazolium bromide (MTT) assay.

### **3.2.6 ADMET Properties**

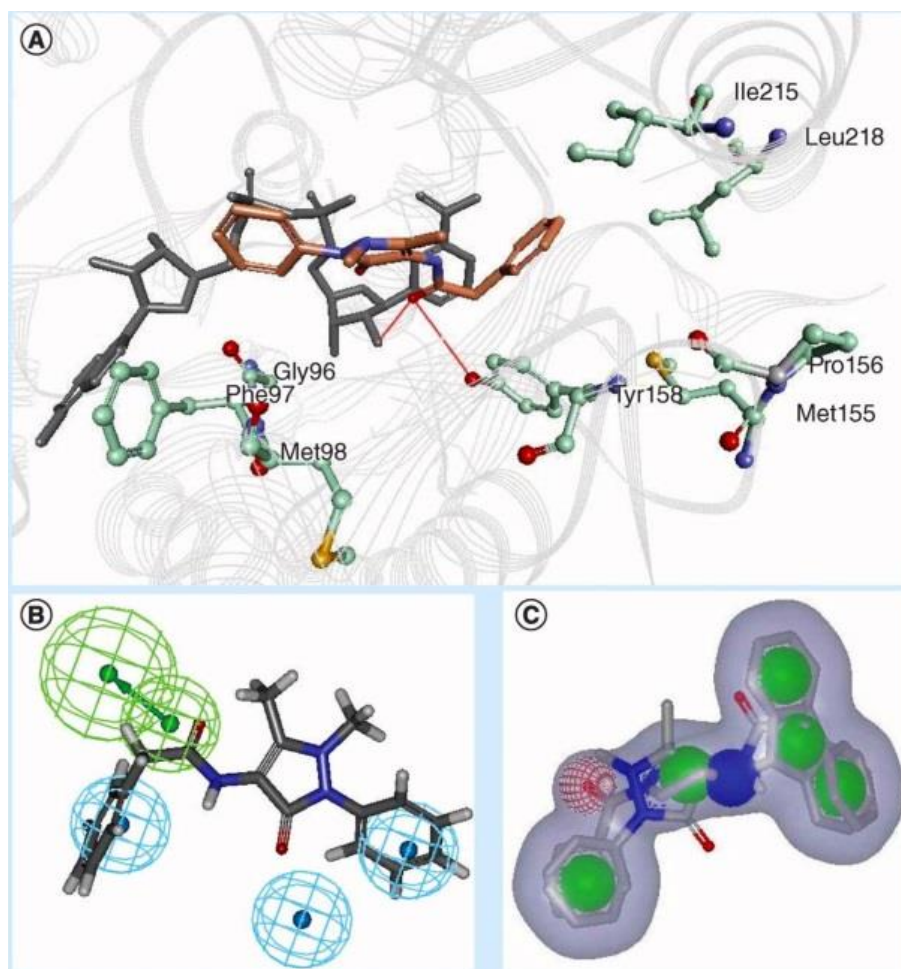
All the synthesized derivatives were further evaluated for their predicted ADMET properties using the QikProp3.5 module of Schrodinger software to determine their drug-likeness characteristics of a promising drug candidate from pharmaceutical point of view.

#### 4.1 Design of novel *Mycobacterium tuberculosis* InhA direct inhibitors

In 2013, our research group demonstrated a virtual screening strategy to develop novel inhibitors against *Mycobacterium tuberculosis* InhA [Kumar U.C. *et al.*, 2013]. Quantitative pharmacophore models were generated and validated using known set of reported *Mycobacterium tuberculosis* InhA inhibitors. The validated pharmacophore model was used as a query to screen an in-house/commercial database of 400,000 compounds and 25,000 hits were retrieved (**Figure 4.1**). These hits were further ranked based on its shape and feature similarity with potent *Mycobacterium tuberculosis* InhA inhibitor using rapid overlay of chemical structures (ROCS) and subsequent hits were subjected for docking to identify the binding conformation of the hits in the active site of the protein. It was found that, the carbonyl group of the top hit (UPS 1) formed a hydrogen bond with the side chain of Tyr158 and the ribose hydroxyl group of NAD<sup>+</sup> correlating with the protein-inhibitor complex interactions outlined in InhA crystal structure (PDB ID: 2H7M) (**Figure 4.2**).

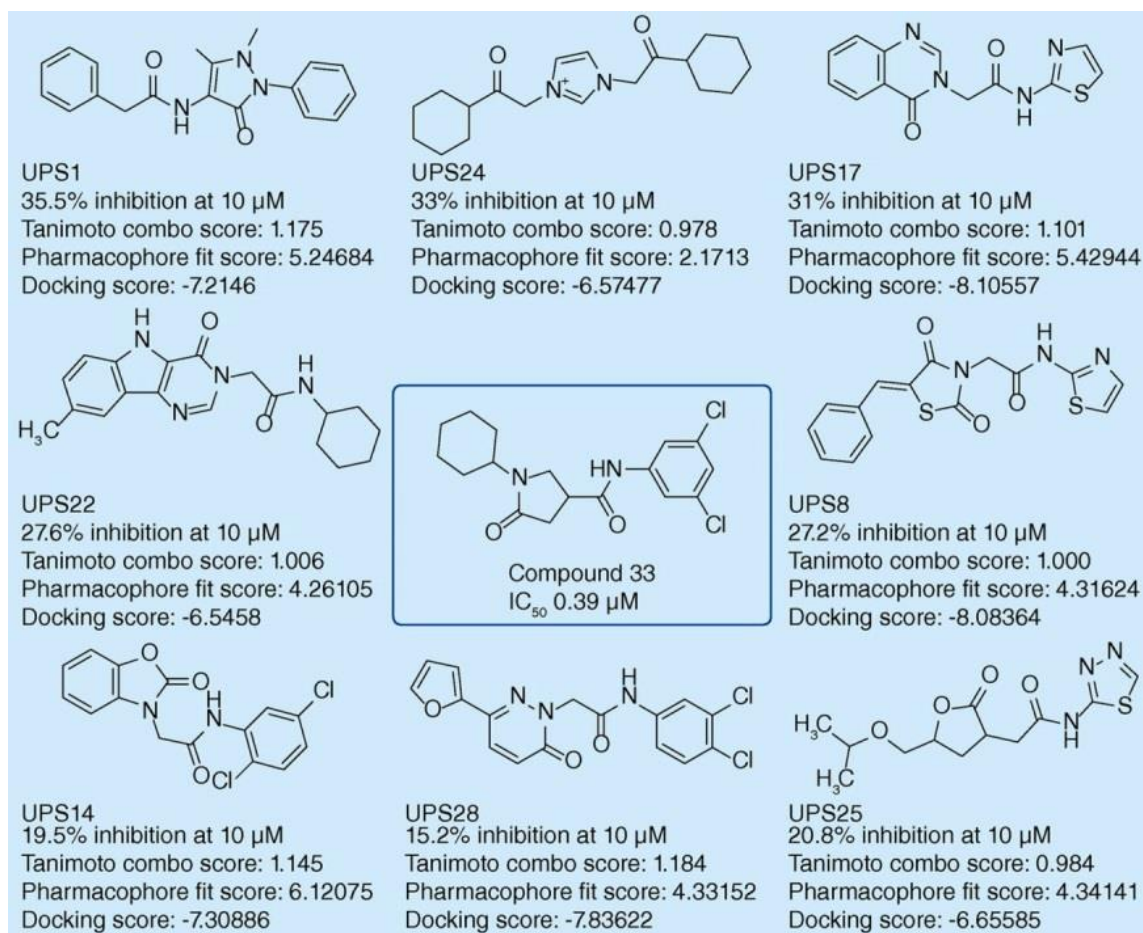


**Figure 4.1:** Virtual screening work flow [Kumar U.C. *et al.*, 2013].



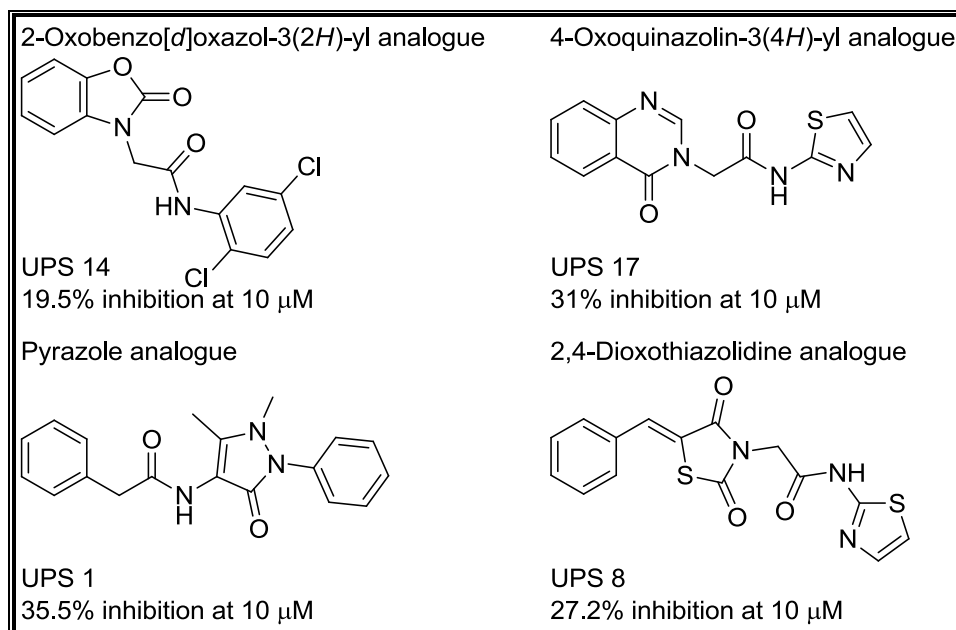
**Figure 4.2:** Analysis of top active compound (**UPS 1**). (A) Predicted bound conformation of the top active compound (**UPS 1**) from the screening. (B) Pharmacophore-mapped and (C) rapid overlay of chemical structures model-aligned conformation of the top active compound (**UPS 1**) [Kumar U.C. *et al.*, 2013].

The main advantage of this virtual screening strategy could be attributed to the ROCS model, as the compounds were screened against a highly active compound taken as reference and hits were scored based on a similarity index, such as the Tanimoto Combo Score. Based on the pharmacophore, ROCS model and docking interactions, 32 compounds were selected and assayed for InhA inhibitory potency where 90% of the hits (28 compounds belonging to eight different chemo-types) exhibited inhibitory activity against InhA in enzymatic studies (**Figure 4.3**) [Kumar U.C. *et al.*, 2013].



**Figure 4.3:** Selected hits from virtual screening and their *Mycobacterium tuberculosis* InhA inhibition activity measured at 10  $\mu\text{M}$  [Kumar U.C. *et al.*, 2013].

Our quest for more potent molecules encouraged us to utilize these moderately active hits as a structural framework for further optimization in order to improve their InhA inhibition potency (**Figure 4.4**). Based on this and inputs from protein-ligand interactions observed in the structure of InhA with lead molecules, further modifications (and combinations thereof) were explored in a ligand expansion step for developing a strong structure-activity relationship (SAR) profile and also to understand the ideal site for introducing chemical diversity.

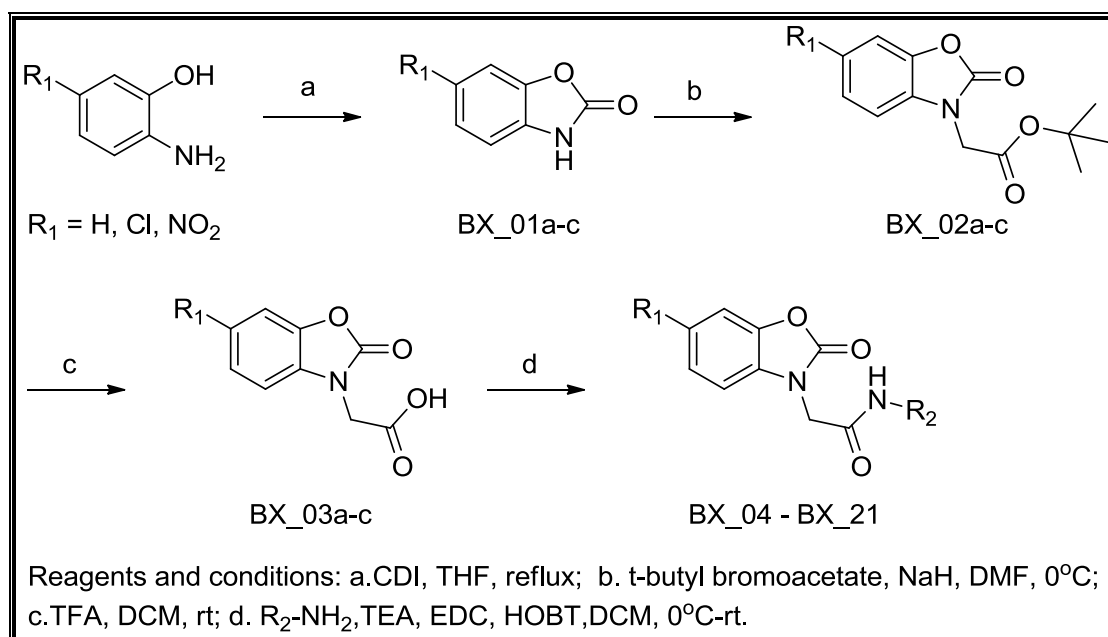


**Figure 4.4:** Chemical structure of selected hits as lead molecules for further optimization.

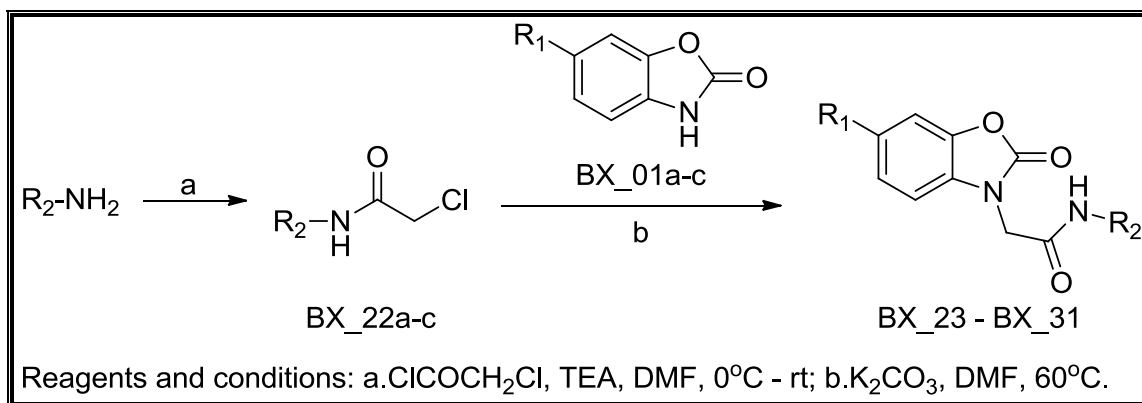
## 4.2 Synthesis and characterization

Hit expansion of the selected four lead molecules (**Figure 4.4**) was achieved using the following synthetic protocols.

### 4.2.1 Synthesis of 2-(2-oxobenzo[*d*]oxazol-3(2*H*)-yl)acetamide derivatives

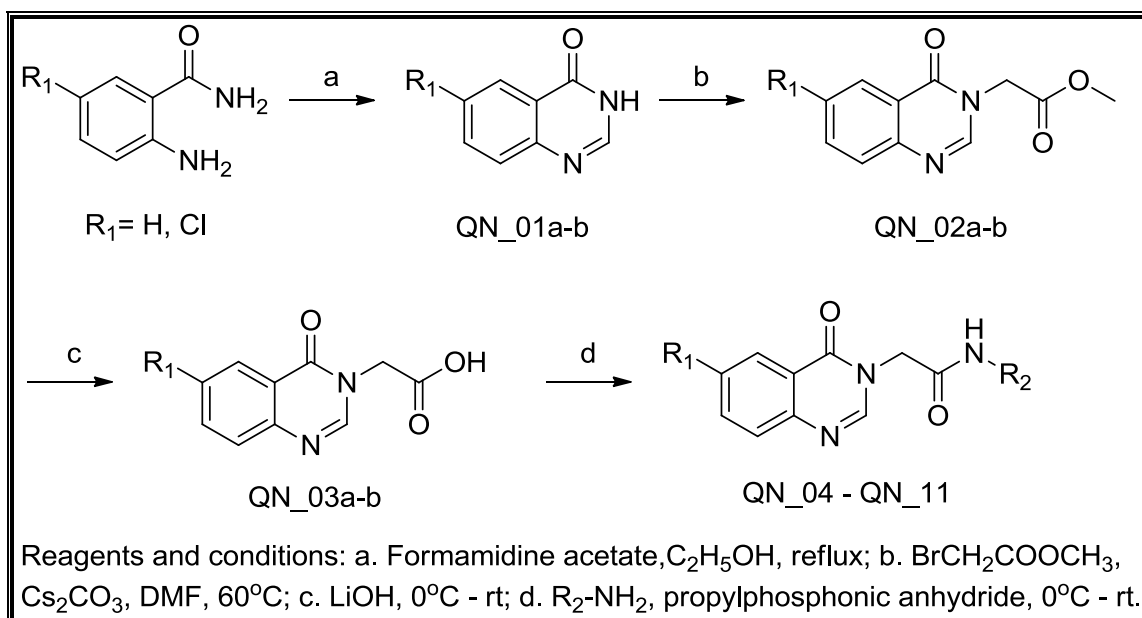


**Figure 4.5:** Synthetic scheme 1 utilised for synthesis of 2-(2-oxobenzo[*d*]oxazol-3(2*H*)-yl)acetamide derivatives.

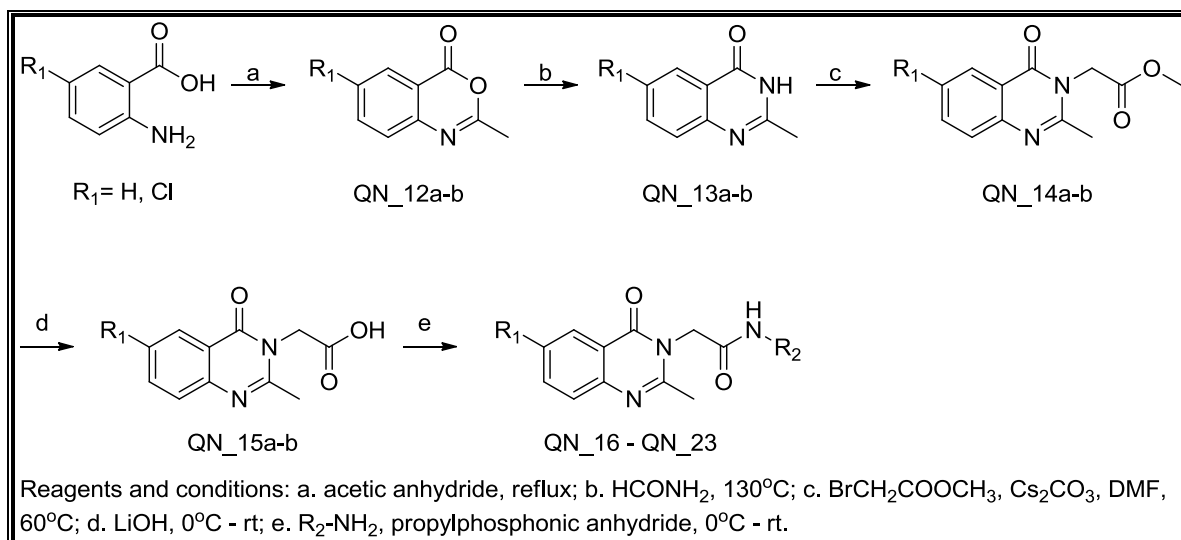


**Figure 4.6:** Synthetic scheme 2 utilised for synthesis of 2-(2-oxobenzo[*d*]oxazol-3(2*H*)-yl)acetamide derivatives.

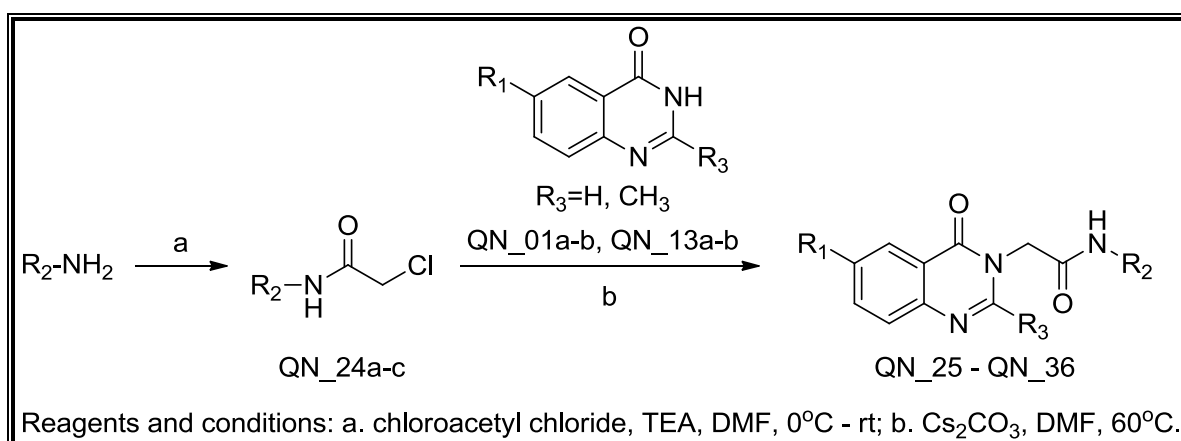
#### 4.2.2 Synthesis of 2-(4-oxoquinazolin-3(4*H*)-yl)acetamide derivatives



**Figure 4.7:** Synthetic scheme 1 utilised for synthesis of 2-(4-oxoquinazolin-3(4*H*)-yl)acetamide derivatives.



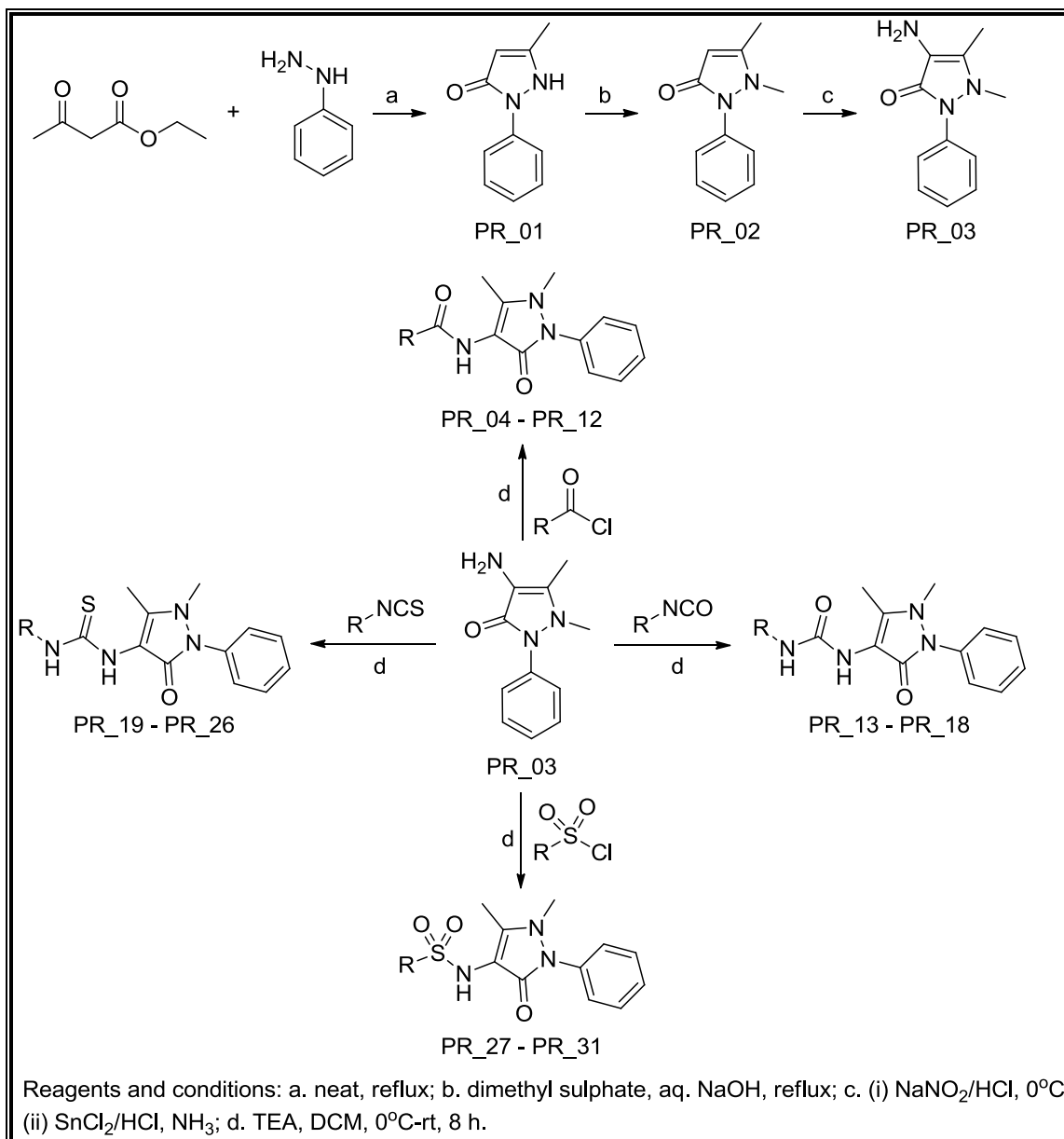
**Figure 4.8:** Synthetic scheme 2 utilised for synthesis of 2-(4-oxoquinazolin-3(4H)-yl)acetamide derivatives.



**Figure 4.9:** Synthetic scheme 3 utilised for synthesis of 2-(4-oxoquinazolin-3(4H)-yl)acetamide derivatives.

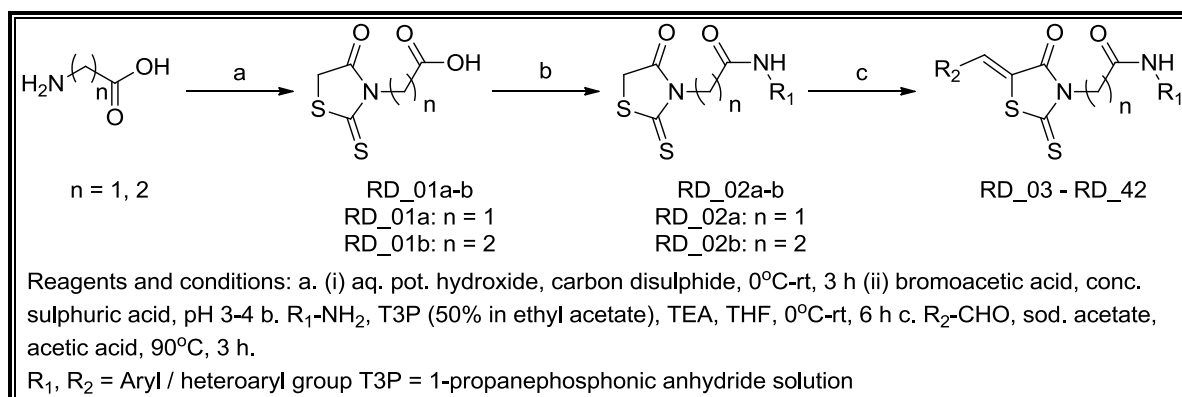


### 4.2.3 Synthesis of 4-amino-1,5-dimethyl-2-phenyl-1*H*-pyrazol-3(2*H*)-one derivatives



**Figure 4.10:** Synthetic scheme utilised for synthesis of 4-amino-1,5-dimethyl-2-phenyl-1*H*-pyrazol-3(2*H*)-one derivatives.

#### 4.2.4 Synthesis of 5-arylalkylidene-2-(4-oxo-2-thioxothiazolidin-3-yl)acetamide/propanamide derivatives



**Figure 4.11:** Synthetic scheme utilised for synthesis of 5-arylalkylidene-2-(4-oxo-2-thioxothiazolidin-3-yl)acetamide/propanamide derivatives.

The melting points were determined by capillary melting point apparatus and are not corrected. Homogeneity of the compounds was monitored by thin layer chromatography (TLC) on silica gel 60 F<sub>254</sub> coated on aluminium plates, visualized by UV light and KMnO<sub>4</sub> treatment. <sup>1</sup>H and <sup>13</sup>C NMR spectra were recorded on a Bruker AM-300 (300.12 MHz, 75.12 MHz) NMR spectrometer, Bruker BioSpin Corp, Germany. Chemical shifts were reported in ppm (δ) with reference to the internal standard TMS. Molecular weights of the synthesized compounds were checked by SHIMADZU LCMS-2020 series in ESI mode. Elemental analyses were carried out on elemental vario MICRO CUBE, CHN Analyser. All commercially available chemicals and solvents were used without further purification.

### 4.3 Enzyme inhibition studies

#### 4.3.1 InhA protein expression, isolation and purification

*Mycobacterium tuberculosis inhA* gene which encodes InhA was cloned and transformed into *E. coli* BL21 (DE3) cells [Khan S. *et al.*, 2010]. The transformed colonies were grown in LB broth at 37 °C with constant aeration, in the presence of 100 µg/ml of ampicillin. Later, the transformed colonies were grown at 37 °C to reach an optical density of 0.6 (A595). Exponentially growing cultures were induced with 0.1 mM IPTG (isopropyl-β-D-thiogalactopyranoside) and further the cells were grown at 18 °C for 12-16 h. Cells were harvested and lysed by sonication in lysis buffer containing 50 mM Tris-HCl, 200 mM NaCl, 0.05 % β-mercaptoethanol, 0.1 mM PMSF (phenylmethanesulfonyl fluoride) and 8 %

glycerol, pH-7.5. The cell lysate containing His 6-fusion protein was equilibrated with Ni-NTA affinity resins for 3-4 h, and washed with wash buffer containing 50 mM Tris-HCl, 200 mM NaCl, 20 mM imidazole and 8 % glycerol. Later the tagged proteins were eluted with buffer containing different concentration of imidazole ranging from 100 to 300 mM. Fractions were pooled and the InhA protein isolated was identified using sodium dodecyl sulphate- polyacrylamide gel electrophoresis (SDS-PAGE).

#### **4.3.2 *Mycobacterium tuberculosis* InhA inhibition assay**

The substrate *2-trans*-decenoyl-CoA (DD-CoA) was synthesized from *2-trans*-decenoic acid using the mixed anhydride method and purified according to the procedure described by Goldman and Vagelos [Goldman P. and Vagelos P.R., 1961]. The absorption of each reaction mixture was determined with a PerkinElmer VICTOR X3 spectrophotometer. The Kinetic assays using DD-CoA and wild-type InhA were performed as described [Delaine T. *et al.*, 2010]. For the inhibition assays with InhA the pre-incubation reactions were performed in 80  $\mu$ l (total volume) of 30 mM PIPES buffer, 150 mM NaCl, pH 6.8 at 25 °C containing 70 nM InhA and inhibitor (at 10  $\mu$ M). DMSO was used as co-solvent and its final concentration was 0.5 %. After 2h of pre-incubation, the addition of 35 mM substrate (DD-CoA) and 200 mM cofactor (NADH) initiated the reaction which was followed at 340 nm (oxidation of NADH) and at 25 °C using PerkinElmer VICTOR X3 spectrophotometer. Control reactions were carried out under the same conditions as described above but without ligands. The inhibitory activity of each compound tested was expressed as the percentage inhibition of InhA activity (initial velocity of the reaction) with respect to the control experiments. All activity assays were performed in triplicate.

#### **4.4 Biophysical characterization**

The stabilization of protein complex with some of active ligand was evaluated by measuring fluorescence of the native protein and the protein-ligand complex in the presence of a fluorescent dye (sypro orange) whose fluorescence increases when exposed to non-polar residues of the protein and reaches a maximum when the protein denatures. In brief, the native protein (7.5  $\mu$ L (1.5 mg/mL) of protein + 3.5  $\mu$ L of buffer [50 mM Tris (pH 7.4), 1 mM EDTA, 5 mM DTT]) was subjected to stepwise heating in a PCR instrument (Bio-Rad iCycler5) from 25 to 100 °C with an increment of 0.1 °C/min in the presence of the fluorescent dye sypro orange [2.5  $\mu$ L (1:100); Sigma, St Louis, MO]. As the temperature

increases, the stability of the protein decreases and becomes zero at equilibrium, where the concentrations of folded and unfolded protein become equal. This temperature was noted as the melting temperature ( $T_m$ ). The dye exhibited maximum fluorescence at this point as it was exposed to the hydrophobic portion of the protein as a result of protein denaturing. A higher or positive shift in  $T_m$  of the protein-ligand complex compared with the native protein signifies better stabilization of the protein-ligand complex, which in turn is a reflection of inhibitor binding [Niesen F.H. *et al.*, 2007].

#### **4.5 Bacterial growth inhibition with *Mycobacterium tuberculosis* H37Rv strain**

All the synthesized compounds were evaluated for anti-mycobacterial screening as per previously reported procedure [Franzblau S.G. *et al.*, 1998]. Two-fold serial dilutions of each test compound/drug were prepared and incorporated into Middlebrook 7H11 agar medium with oleic acid, albumin, dextrose, and catalase (OADC) growth supplement to get final concentrations of 50, 25, 12.5, 6.25, 3.13, 1.56, 0.78, 0.39 and 0.195  $\mu\text{g}/\text{mL}$ . Inoculum of *Mycobacterium tuberculosis* H37Rv ATCC 27294 was prepared from fresh Middlebrook 7H11 agar slants with OADC (Difco) growth supplement adjusted to 1 mg/mL (wet weight) in Tween 80 (0.05%) saline diluted to  $10^{-2}$  to give a concentration of  $\sim 10^7$  cfu/mL. Five microliters of this bacterial suspension was spotted onto 7H11 agar tubes containing different concentrations of the drug as discussed above. The tubes were incubated at 37 °C, and final readings (as MIC in mg/mL) were determined after 28 days. This method is similar to that recommended by the National Committee for Clinical Laboratory Standards for the determination of MIC in triplicate. Also, the synthesized compounds were screened for their bacterial growth inhibition in *Mycobacterium tuberculosis* H37Rv in the presence of reported efflux pump inhibitor/s piperine (8  $\mu\text{g}/\text{mL}$ ) and/or verapamil (50  $\mu\text{g}/\text{mL}$ ) [Alibert S. and Pages J-M., 2007].

#### **4.6 Cytotoxicity studies**

All the synthesized compounds were further examined for cytotoxicity in a RAW 264.7 cell line (mouse leukaemic monocyte macrophage) at concentrations of 50 and/or 100  $\mu\text{M}$ . After 48 h of exposure, viability was assessed on the basis of cellular conversion of MTT into a formazan product using the Promega Cell Titer 96 non-radioactive cell proliferation assay [Gerlier D. and Thomasset N., 1986]. We selected this macrophage cell line to test the toxicity as naturally *Mycobacterium tuberculosis* resides inside the macrophages and the drug

molecules should not possess any toxicity against these macrophages. The RAW 264.7 cells were grown in RPMI medium supplemented with 10 % fetal bovine serum (FBS), 10,000 units' penicillin and 10 mg streptomycin per ml in T25 flasks to attain 80-90 % confluence. Cells were scraped and seeded into wells as 5,000 cells per well in poly-L-lysine coated plates. The microtiter plates were incubated at 37 °C, 5 % CO<sub>2</sub>, 95 % air and 100 % relative humidity for 24 h prior to addition of synthesized compounds. Each compound at 50 and/or 100 µM concentration was then added to cells and incubated at 37 °C for 72 h, later 10 µL of 10 mg/ml concentration of MTT was added and incubated for 3 h at 37 °C. At the end of incubation formazan crystals were formed, the media from microtiter plates were removed. Later, the bound crystals were subsequently dissolved by adding 100 µL DMSO. Absorbance was then read on plate reader at a wavelength of 595 nm. The percent growth was calculated for each well relative to the control wells. The percentage inhibition was calculated from the following formula:

$$\text{Percentage inhibition} = \frac{100 - \text{mean OD sample}}{\text{mean OD day 0}}$$

#### **4.7 Molecular docking studies**

Glide XP (extra precision) module of Schrödinger 9.2 (Glide, version 5.7, Schrödinger, LLC, New York, NY, 81 2011) was utilized for docking. The crystal structure of *Mycobacterium tuberculosis* InhA complexed with 1-cyclohexyl-N-(3,5-dichlorophenyl)-5-oxopyrrolidine-3-carboxamide (PDB ID:2H7M) having resolution of 1.62 Å was retrieved from the Protein Data Bank ([www.rcsb.org](http://www.rcsb.org)) and further used for docking of synthesized compounds. The reported crystal structure is a monomer, having only one chain A with the inhibitor bound to it. The protein was prepared using protein preparation wizard and glide energy grids were generated for prepared protein complex. The binding site was defined by a rectangular box surrounding the X-ray ligand. Ligand was refined using the “Refine” option in Glide, and the option 70 to output Glide XP descriptor information was chosen (Glide 71 v5.7, Schrodinger, LLC, New York, NY).

#### **4.8 ADMET Properties**

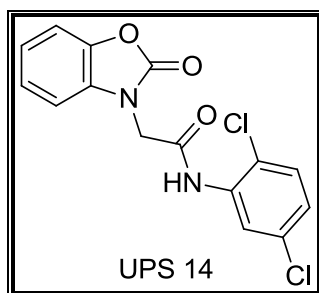
All the synthesized derivatives were further evaluated for their predicted ADMET properties using the QikProp3.5 module of Schrodinger software. The physically significant and pharmaceutically relevant properties such as QPlogPo/w (predicted octanol/water partition

coefficient logP), QPlogHERG (predicted IC<sub>50</sub> value for blockage of hERG K<sup>+</sup> channels), QPPCaco (predicted apparent Caco-2 cell permeability in nm/sec), QPlogBB (predicted brain/blood partition coefficient), QPPMDCK (predicted apparent MDCK cell (model for blood-brain barrier) permeability in nm/s), percent human oral absorption, and rule of five (mol\_MW < 500, QPlogPo/w < 5, donorHB ≤ 5, accptHB ≤ 10) were predicted. These predicted pharmacokinetic parameters provides an idea about the drug-like characteristics of a promising drug candidate to be worked for further development from pharmaceutical point of view.

The *Mycobacterium tuberculosis* InhA enzyme has been demonstrated to be the target of first-line agent INH, validating it as a remarkable anti-tubercular drug target. As a prodrug, INH must first get activated by KatG to form an active INH-NAD adduct which then functions as potent inhibitor of InhA. Clinical studies demonstrated that most INH-resistant strains arise from KatG-associated mutations. Consequently, inhibitors targeting InhA directly without prerequisite for activation would be promising candidates for development of new anti-tubercular agents. Thus in present study we focus on achieving promising mycobacterial cellular potency through developing potential *Mycobacterium tuberculosis* InhA direct inhibitors.

### 5.1 Development of 2-(2-oxobenzo[d]oxazol-3(2H)-yl)acetamide derivatives as potential *Mycobacterium tuberculosis* InhA inhibitors

Virtual screening efforts of our research group in the quest of anti-tubercular drug discovery resulted in the identification of one of the lead *N*-(2,5-dichlorophenyl)-2-(2-oxobenzo[d]oxazol-3(2H)-yl)acetamide (**UPS 14**) displaying *Mycobacterium tuberculosis* InhA IC<sub>50</sub> of 22.12±0.8 µM [Kumar U.C. *et al.*, 2013]. Based on this and inputs from protein-ligand interactions observed in the structure of InhA with lead molecules, further modifications (and combinations thereof) were explored as a ligand expansion step. The lead molecule **UPS 14** enabled us convenient structure-activity relationship (SAR) investigations at both 6<sup>th</sup> and N-1 positions of benzo[d]oxazol-2(3H)-one nucleus. Investigation of benzoxazolone pharmacophore has recently generated significant interest from a medicinal chemistry point of view and their synthesis has been well explored in the literature. The synthetic pathway used to achieve the lead modifications is delineated in **Figure 5.2** and **Figure 5.3**. A library of twenty seven derivatives was synthesized (compound **BX\_04** – **BX\_21** and **BX\_23** – **BX\_31**, **Table 5.1**) and evaluated for their ability to inhibit InhA enzyme as step towards the derivation of SAR and hit optimization.

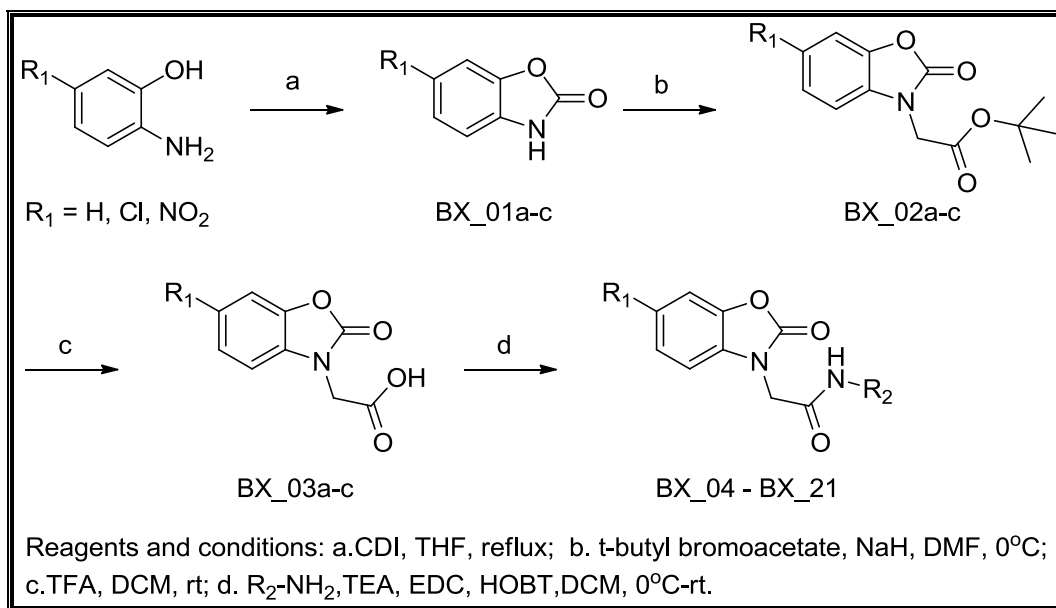


**Figure 5.1:** Chemical structure of lead molecule **UPS 14**.

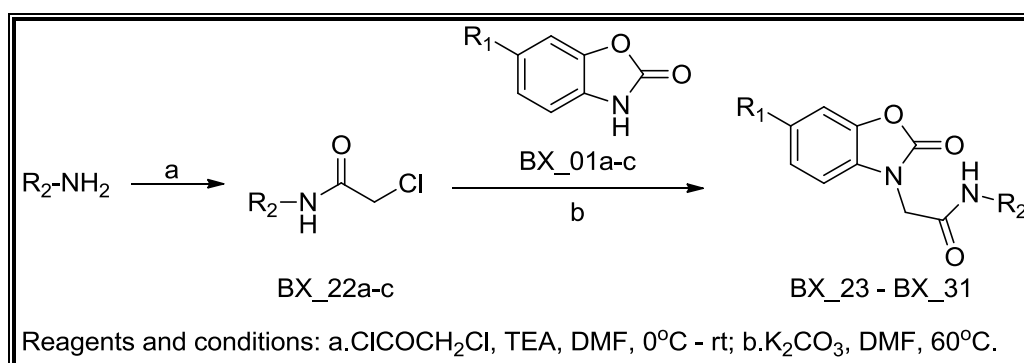
### 5.1.1 Chemical synthesis and characterization

Construction of the target molecule was achieved by first treating the commercially available 2-aminophenol with 1,1'-carbonyldiimidazole (CDI) in refluxing tetrahydrofuran (THF) to afford the corresponding benzoxazolone (**BX\_01a-c**) in good yield. This benzoxazolone (**BX\_01a-c**) was further alkylated at the N-1 position with *tert*-butyl bromoacetate in presence of sodium hydride as base to give the corresponding acetate (**BX\_02a-c**) in quantitative yield, which when subjected to acidic hydrolysis using trifluoroacetic acid (TFA) afforded the corresponding acid (**BX\_03a-c**). The final library was synthesized by condensing this key intermediate acid derivative (**BX\_03a-c**) with various substituted amines. Selection of amino substituents at N-1 position was based on our previous research experience in TB, in an effort to improve the anti-tubercular potency of these molecules. The final coupling was achieved by using EDC/HOBT as coupling agents. Though the reaction went smoothly for aromatic amines giving the desired products in good yield, a similar conversion was not observed in the case of heterocyclic amines especially with 2-amino-5-nitrothiazole, 2-aminobenzothiazole and 2-amino-6-nitrobenzothiazole, probably due to their low nucleophilicity and solubility issues. Hence, an alternative strategy was designed as depicted in **Figure 5.3**, wherein the corresponding amine was first treated with chloroacetyl chloride in presence of triethylamine (TEA) as base to give the corresponding 2-chloro-*N*-(aryl/heteroaryl)acetamide (**BX\_22a-c**). This on further alkylation with the corresponding benzoxazolone derivative (**BX\_01a-c**) gave the desired amide derivative in good yield and purity (**BX\_23 – BX\_31**).





**Figure 5.2:** Synthetic protocol utilized for synthesis of compounds **BX\_04 – BX\_21**.



**Figure 5.3:** Synthetic protocol utilized for synthesis of compounds **BX\_23 – BX\_31**.

### 5.1.2 Experimental protocol utilised for synthesis

#### Procedure for the synthesis of 6-substituted benzo[d]oxazol-2(3H)-ones (**BX\_01a-c**)

To a stirred solution of appropriate aminophenol (1 mmol) in dry THF (20 mL) was added CDI (1.1 mmol) at room temperature (rt). The solution was refluxed for about 4 h (monitored by TLC & LCMS for completion), and solvent evaporated under reduced pressure [Bell I.M. *et al.*, 2012]. The residue was further diluted with water (20 mL) and ethyl acetate (20 mL) and the layers separated. The organic layer was washed with 2 N hydrochloric acid (15 mL), water (10 mL), dried over anhydrous sodium sulphate and evaporated under reduced pressure. The residue was purified by silica gel column chromatography using hexane: ethyl acetate as eluent to give the corresponding benzoxazolone (**BX\_01a-c**) in good yield.

**Procedure for the synthesis of 6-substituted *tert*-butyl 2-(2-oxobenzo[*d*]oxazol-3(2*H*)-yl)acetate (BX\_02a-c)**

To a well stirred suspension of sodium hydride (60% dispersion in mineral oil, 1.2 mmol) in *N,N*-dimethylformamide (DMF) (10 mL) at 0 °C was added dropwise a solution of the corresponding benzoxazolone (BX\_01a-c) (1 mmol) in DMF (10 mL), followed by *tert*-butyl bromoacetate (1.1 mmol). The solution was slowly warmed to rt and stirred at rt for about 1 h (monitored by TLC & LCMS for completion), quenched with saturated ammonium chloride solution (15 mL) and concentrated under reduced pressure. The residue was partitioned between ethyl acetate (20 mL) and water (10 mL) and the organic layer was dried over anhydrous sodium sulphate and concentrated under reduced pressure. The crude product was purified by silica gel column chromatography using hexane: ethyl acetate as eluent to give the corresponding product (BX\_02a-c).

**Procedure for the synthesis of 6-substituted 2-(2-oxobenzo[*d*]oxazol-3(2*H*)-yl)acetic acids (BX\_03a-c)**

TFA (2 mmol) was added dropwise over 5 min to a stirred solution of corresponding 6-substituted *tert*-butyl 2-(2-oxobenzo[*d*]oxazol-3(2*H*)-yl)acetate (BX\_02a-c) (1 mmol) in anhydrous dichloromethane (DCM) (15 mL) under nitrogen at 0 °C. The solution was slowly warmed to the rt and stirred at rt for about 4 h (monitored by TLC & LCMS for completion) and concentrated under reduced pressure. The residue was dissolved in toluene and concentrated under reduced pressure (twice), and finally triturated with ether to give a corresponding product (BX\_03a-c).

**Procedure for the synthesis of substituted 2-(2-oxobenzo[*d*]oxazol-3(2*H*)-yl)acetamides (BX\_04 – BX\_21)**

A solution of corresponding 2-(2-oxobenzo[*d*]oxazol-3(2*H*)-yl)acetic acid (BX\_03a-c) (1 mmol), substituted amine (1.2 mmol), 1-ethyl-3-(3-dimethylaminopropyl)carbodiimide (EDC) (1.2 mmol), *N*-hydroxybenzotriazole (HOBT) (1.2 mmol), and TEA (2.2 mmol) were stirred for 6 h at rt in DCM (4 mL) (monitored by TLC & LCMS for completion). The reaction mixture was further diluted with water (10 mL) and DCM (10 mL), and the layers separated. The organic layer was dried over anhydrous sodium sulphate and concentrated under reduced pressure. The crude product was purified by silica gel column chromatography

using hexane: ethyl acetate as eluent to give the corresponding product (**BX\_04 – BX\_21**). The physicochemical properties of synthesized derivatives are shown in **Table 5.1**.

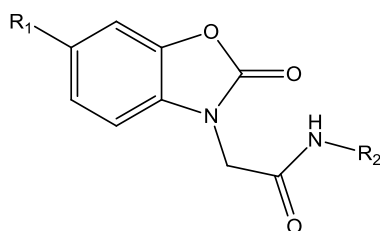
#### **Procedure for the synthesis of 2-chloro-*N*-(aryl/heteroaryl)acetamides (**BX\_22a-c**)**

Chloroacetyl chloride (2 mmol) was added dropwise to a well stirred suspension of corresponding amine (1 mmol) and TEA (3 mmol) in DMF (15 mL) at 0 °C. The reaction mixture was then slowly warmed to rt and stirred at rt for about 3 h (monitored by TLC & LCMS for completion). The solvent was then evaporated under reduced pressure and the residue was further diluted with water (20 mL) and ethyl acetate (30 mL), and the layers separated. The aqueous layer was re-extracted with ethyl acetate (2 × 30 mL) and the combined organic layer was washed with brine (20 mL), dried over anhydrous sodium sulphate and evaporated under reduced pressure. The residue was then purified by silica column chromatography using hexane: ethyl acetate as eluent to give corresponding product (**BX\_22a-c**).

#### **Procedure for the synthesis of substituted 2-(2-oxobenzo[*d*]oxazol-3(2*H*)-yl)acetamides (**BX\_23 – BX\_31**)**

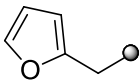
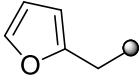
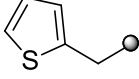
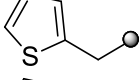
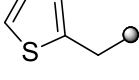
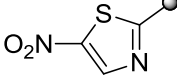
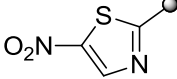
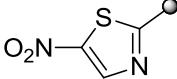
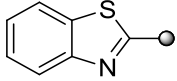
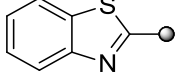
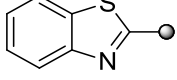
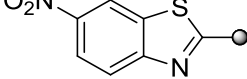
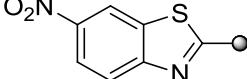
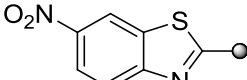
To a solution of corresponding 2-chloro-*N*-(aryl/heteroaryl)acetamides (**BX\_22a-c**) (1.2 mmol) in DMF (3 mL) was added anhydrous potassium carbonate (1.5 mmol) and corresponding benzo[*d*]oxazol-2(3*H*)-one (**BX\_01a-c**) (1 mmol). The reaction mixture was heated at 60 °C for 3 h (monitored by TLC & LCMS for completion). The residue was further diluted with water (10 mL) and ethyl acetate (20 mL) and the layers separated. The aqueous layer was re-extracted with ethyl acetate (2 x 15 mL) and the combined organic layer was washed with brine (15 mL), dried over anhydrous sodium sulphate and evaporated under reduced pressure and the residue was purified by silica column chromatography using hexane: ethyl acetate as eluent to give the desired product (**BX\_23 – BX\_31**). The physicochemical properties of synthesized derivatives are shown in **Table 5.1**.

**Table 5.1:** Physicochemical properties of synthesized compounds **BX\_04** – **BX\_21** and **BX\_23** – **BX\_31**.



| Comp         | R <sub>1</sub>  | R <sub>2</sub> | Yield (%) | Melting point (°C) | Molecular formula   | Molecular weight |
|--------------|-----------------|----------------|-----------|--------------------|---|------------------|
| <b>BX_04</b> | H               |                | 66.6      | 190-191            | C <sub>15</sub> H <sub>12</sub> N <sub>2</sub> O <sub>3</sub>                               | 268.27           |
| <b>BX_05</b> | Cl              |                | 73.2      | 181-183            | C <sub>15</sub> H <sub>11</sub> ClN <sub>2</sub> O <sub>3</sub>                             | 302.71           |
| <b>BX_06</b> | NO <sub>2</sub> |                | 73.3      | 222-223            | C <sub>15</sub> H <sub>11</sub> N <sub>3</sub> O <sub>5</sub>                               | 313.26           |
| <b>BX_07</b> | H               |                | 69.6      | 157-159            | C <sub>16</sub> H <sub>10</sub> ClF <sub>3</sub> N <sub>2</sub> O <sub>3</sub>              | 370.71           |
| <b>BX_08</b> | Cl              |                | 74.3      | 139-140            | C <sub>16</sub> H <sub>9</sub> Cl <sub>2</sub> F <sub>3</sub> N <sub>2</sub> O <sub>3</sub> | 405.16           |
| <b>BX_09</b> | NO <sub>2</sub> |                | 78.5      | 127-129            | C <sub>16</sub> H <sub>9</sub> ClF <sub>3</sub> N <sub>3</sub> O <sub>5</sub>               | 415.71           |
| <b>BX_10</b> | H               |                | 68.2      | 221-223            | C <sub>14</sub> H <sub>11</sub> N <sub>3</sub> O <sub>3</sub>                               | 269.26           |
| <b>BX_11</b> | Cl              |                | 65.3      | 243-245            | C <sub>14</sub> H <sub>10</sub> ClN <sub>3</sub> O <sub>3</sub>                             | 303.70           |
| <b>BX_12</b> | NO <sub>2</sub> |                | 67.1      | 253-255            | C <sub>14</sub> H <sub>10</sub> N <sub>4</sub> O <sub>5</sub>                               | 314.25           |
| <b>BX_13</b> | H               |                | 65.2      | 162-164            | C <sub>15</sub> H <sub>13</sub> N <sub>3</sub> O <sub>3</sub>                               | 283.28           |
| <b>BX_14</b> | Cl              |                | 64.4      | 182-184            | C <sub>15</sub> H <sub>12</sub> ClN <sub>3</sub> O <sub>3</sub>                             | 317.73           |
| <b>BX_15</b> | NO <sub>2</sub> |                | 66.7      | 187-189            | C <sub>15</sub> H <sub>12</sub> N <sub>4</sub> O <sub>5</sub>                               | 328.28           |
| <b>BX_16</b> | H               |                | 72.2      | 110-112            | C <sub>14</sub> H <sub>12</sub> N <sub>2</sub> O <sub>4</sub>                               | 272.26           |

Contd...

| Comp         | R <sub>1</sub>  | R <sub>2</sub>  | Yield (%) | Melting point (°C) | Molecular formula   | Molecular weight |
|--------------|-----------------|---|-----------|--------------------|---|------------------|
| <b>BX_17</b> | Cl              |    | 73.4      | 142-144            | C <sub>14</sub> H <sub>11</sub> ClN <sub>2</sub> O <sub>4</sub>   | 306.70           |
| <b>BX_18</b> | NO <sub>2</sub> |    | 73.2      | 165-167            | C <sub>14</sub> H <sub>11</sub> N <sub>3</sub> O <sub>6</sub>     | 317.25           |
| <b>BX_19</b> | H               |    | 74.4      | 128-130            | C <sub>14</sub> H <sub>12</sub> N <sub>2</sub> O <sub>3</sub> S   | 288.32           |
| <b>BX_20</b> | Cl              |    | 72.3      | 166-168            | C <sub>14</sub> H <sub>11</sub> ClN <sub>2</sub> O <sub>3</sub> S | 322.77           |
| <b>BX_21</b> | NO <sub>2</sub> |    | 74.7      | 220-222            | C <sub>14</sub> H <sub>11</sub> N <sub>3</sub> O <sub>5</sub> S   | 333.32           |
| <b>BX_23</b> | H               |    | 72.2      | 193-195            | C <sub>12</sub> H <sub>8</sub> N <sub>4</sub> O <sub>5</sub> S    | 320.28           |
| <b>BX_24</b> | Cl              |    | 70.9      | 268-270            | C <sub>12</sub> H <sub>7</sub> ClN <sub>4</sub> O <sub>5</sub> S  | 354.73           |
| <b>BX_25</b> | NO <sub>2</sub> |    | 73.6      | 273-275            | C <sub>12</sub> H <sub>7</sub> N <sub>5</sub> O <sub>7</sub> S    | 365.28           |
| <b>BX_26</b> | H               |   | 67.9      | 250-252            | C <sub>16</sub> H <sub>11</sub> N <sub>3</sub> O <sub>3</sub> S   | 325.34           |
| <b>BX_27</b> | Cl              |  | 68.4      | 267-269            | C <sub>16</sub> H <sub>10</sub> ClN <sub>3</sub> O <sub>3</sub> S | 359.79           |
| <b>BX_28</b> | NO <sub>2</sub> |  | 67.6      | 256-258            | C <sub>16</sub> H <sub>10</sub> N <sub>4</sub> O <sub>5</sub> S   | 370.34           |
| <b>BX_29</b> | H               |  | 64.8      | >280               | C <sub>16</sub> H <sub>10</sub> N <sub>4</sub> O <sub>5</sub> S   | 370.34           |
| <b>BX_30</b> | Cl              |  | 65.7      | 269-271            | C <sub>16</sub> H <sub>9</sub> ClN <sub>4</sub> O <sub>5</sub> S  | 404.78           |
| <b>BX_31</b> | NO <sub>2</sub> |  | 68.1      | 265-267            | C <sub>16</sub> H <sub>9</sub> N <sub>5</sub> O <sub>7</sub> S    | 415.34           |

### 5.1.3 Characterization of synthesized compounds

Both analytical and spectral data (<sup>1</sup>H NMR, <sup>13</sup>C NMR and mass spectra) of all the synthesized compounds were in full agreement with the proposed structures.

#### Benzo[*d*]oxazol-2(3*H*)-one (**BX\_01a**)

The compound was synthesized according to the general procedure using 2-aminophenol (2.0 g, 18.32 mmol) and CDI (3.2 g, 20.15 mmol) to afford **BX\_01a** (1.9 g, 76.7 %) as white

solid. M.p: 139-141 °C. <sup>1</sup>H NMR (DMSO-d<sub>6</sub>): δ<sub>H</sub> 8.18 (s, 1H), 7.47 – 6.91 (m, 4H). <sup>13</sup>C NMR (DMSO-d<sub>6</sub>): δ<sub>C</sub> 155.3, 144.6, 129.8, 125.4, 124.6, 110.1, 109.6. ESI-MS *m/z* 136 (M+H)<sup>+</sup>. Anal. Calcd. for C<sub>7</sub>H<sub>5</sub>NO<sub>2</sub>: C, 62.22; H, 3.73; N, 10.37; Found: C, 62.25; H, 3.70; N, 10.40.

#### **6-Chlorobenzo[*d*]oxazol-2(3*H*)-one (BX\_01b)**

The compound was synthesized according to the general procedure using 2-amino-5-chlorophenol (2.0 g, 13.93 mmol) and CDI (2.4 g, 15.32 mmol) to afford **BX\_01b** (1.8 g, 78.4 %) as white solid. M.p: 193-195 °C. <sup>1</sup>H NMR (DMSO-d<sub>6</sub>): δ<sub>H</sub> 8.25 (s, 1H), 7.83 – 7.41 (m, 3H). <sup>13</sup>C NMR (DMSO-d<sub>6</sub>): δ<sub>C</sub> 155.6, 140.3, 131.7, 128.5, 125.9, 123.2, 122.8. ESI-MS *m/z* 168 (M-H)<sup>-</sup>. Anal. Calcd. for C<sub>7</sub>H<sub>4</sub>ClNO<sub>2</sub>: C, 49.58; H, 2.38; N, 8.26; Found: C, 49.61; H, 2.40; N, 8.29.

#### **6-Nitrobenzo[*d*]oxazol-2(3*H*)-one (BX\_01c)**

The compound was synthesized according to the general procedure using 2-amino-5-nitrophenol (2.0 g, 12.97 mmol) and CDI (2.3 g, 14.27 mmol) to afford **BX\_01c** (1.8 g, 79.3 %) as pale yellow solid. M.p: 250-252 °C. <sup>1</sup>H NMR (DMSO-d<sub>6</sub>): δ<sub>H</sub> 8.29 (s, 1H), 8.31 – 8.01 (m, 3H). <sup>13</sup>C NMR (DMSO-d<sub>6</sub>): δ<sub>C</sub> 155.7, 144.0, 140.1, 136.6, 121.1, 117.5, 115.1. ESI-MS *m/z* 179 (M-H)<sup>-</sup>. Anal. Calcd. for C<sub>7</sub>H<sub>4</sub>N<sub>2</sub>O<sub>4</sub>: C, 46.68; H, 2.24; N, 15.55; Found: C, 46.65; H, 2.21; N, 15.58.

#### ***tert*-Butyl 2-(2-oxobenzo[*d*]oxazol-3(2*H*)-yl)acetate (BX\_02a)**

The compound was synthesized according to the general procedure using benzo[*d*]oxazol-2(3*H*)-one (**BX\_01a**) (1.5 g, 11.10 mmol) and *tert*-butyl bromoacetate (2.3 g, 12.21 mmol) to afford **BX\_02a** (1.9 g, 69.4 %) as white solid. M.p: 150-152 °C. <sup>1</sup>H NMR (DMSO-d<sub>6</sub>): δ<sub>H</sub> 8.15 – 7.42 (m, 4H), 4.27 (s, 2H), 1.39 (s, 9H). <sup>13</sup>C NMR (DMSO-d<sub>6</sub>): δ<sub>C</sub> 169.7, 154.8, 139.2, 132.5, 125.7, 124.6, 116.3, 116.0, 83.1, 53.6, 28.2. ESI-MS *m/z* 250 (M+H)<sup>+</sup>. Anal. Calcd. for C<sub>13</sub>H<sub>15</sub>NO<sub>4</sub>: C, 62.64; H, 6.07; N, 5.62; Found: C, 62.58; H, 6.04; N, 5.65.

#### ***tert*-Butyl 2-(6-chloro-2-oxobenzo[*d*]oxazol-3(2*H*)-yl)acetate (BX\_02b)**

The compound was synthesized according to the general procedure using 6-chlorobenzo[*d*]oxazol-2(3*H*)-one (**BX\_01b**) (1.5 g, 8.84 mmol) and *tert*-butyl bromoacetate (1.8 g, 9.73 mmol) to afford **BX\_02b** (1.37 g, 82.1 %) as white solid. M.p: 197-199 °C. <sup>1</sup>H NMR (DMSO-d<sub>6</sub>): δ<sub>H</sub> 7.87 – 7.31 (m, 3H), 4.23 (s, 2H), 1.34 (m, 9H). <sup>13</sup>C NMR (DMSO-d<sub>6</sub>):

$\delta_C$  169.6, 154.7, 140.5, 131.7, 130.1, 125.9, 123.6, 122.8, 82.3, 53.2, 28.5. ESI-MS  $m/z$  284 (M+H)<sup>+</sup>. Anal. Calcd. for C<sub>13</sub>H<sub>14</sub>ClNO<sub>4</sub>: C, 55.04; H, 4.97; N, 4.94; Found: C, 55.07; H, 4.99; N, 4.96.

#### ***tert*-Butyl 2-(6-nitro-2-oxobenzo[*d*]oxazol-3(2*H*)-yl)acetate (BX\_02c)**

The compound was synthesized according to the general procedure using 6-nitrobenzo[*d*]oxazol-2(3*H*)-one (BX\_01c) (3.0 g, 16.65 mmol) and *tert*-butyl bromoacetate (3.5 g, 18.32 mmol) to afford BX\_02c (2.1 g, 68.6 %) as white solid. M.p: 182-184 °C. <sup>1</sup>H NMR (DMSO-*d*<sub>6</sub>):  $\delta_H$  8.28 – 7.98 (m, 3H), 4.31 (s, 2H), 1.37 (s, 9H). <sup>13</sup>C NMR (DMSO-*d*<sub>6</sub>):  $\delta_C$  169.5, 154.5, 144.2, 140.3, 138.6, 123.1, 121.2, 117.5, 82.0, 53.6, 28.4. ESI-MS  $m/z$  295 (M+H)<sup>+</sup>. Anal. Calcd. for C<sub>13</sub>H<sub>14</sub>N<sub>2</sub>O<sub>6</sub>: C, 53.06; H, 4.80; N, 9.52; Found: C, 53.09; H, 4.78; N, 9.49.

#### **2-(2-Oxobenzo[*d*]oxazol-3(2*H*)-yl)acetic acid (BX\_03a)**

The compound was synthesized according to the general procedure using *tert*-butyl 2-(2-oxobenzo[*d*]oxazol-3(2*H*)-yl)acetate (BX\_02a) (1.5 g, 6.0 mmol), and TFA (1.3 g, 12.0 mmol) to afford BX\_03a (0.9 g, 83.1 %) as white solid. M.p: 226-228 °C. <sup>1</sup>H NMR (DMSO-*d*<sub>6</sub>):  $\delta_H$  11.17 (s, 1H), 7.82 – 7.18 (m, 4H), 4.12 (s, 2H). <sup>13</sup>C NMR (DMSO-*d*<sub>6</sub>):  $\delta_C$  176.6, 154.7, 139.2, 132.5, 125.9, 124.8, 116.4, 116.1, 56.1. ESI-MS  $m/z$  192 (M-H)<sup>-</sup>. Anal. Calcd. for C<sub>9</sub>H<sub>7</sub>NO<sub>4</sub>: C, 55.96; H, 3.65; N, 7.25; Found: C, 56.00; H, 3.67; N, 7.23.

#### **2-(6-Chloro-2-oxobenzo[*d*]oxazol-3(2*H*)-yl)acetic acid (BX\_03b)**

The compound was synthesized according to the general procedure using *tert*-butyl 2-(6-chloro-2-oxobenzo[*d*]oxazol-3(2*H*)-yl)acetate (BX\_02b) (1.35 g, 4.75 mmol), and TFA (1.08 g, 9.51 mmol) to afford BX\_03b (0.91 g, 87.7 %) as white solid. M.p: 268-270 °C. <sup>1</sup>H NMR (DMSO-*d*<sub>6</sub>):  $\delta_H$  11.20 (s, 1H), 8.14 – 7.31 (m, 3H), 4.14 (s, 2H). <sup>13</sup>C NMR (DMSO-*d*<sub>6</sub>):  $\delta_C$  176.2, 154.8, 140.1, 131.6, 130.4, 126.0, 123.6, 122.7, 56.3. ESI-MS  $m/z$  226 (M-H)<sup>-</sup>. Anal. Calcd. for C<sub>9</sub>H<sub>6</sub>ClNO<sub>4</sub>: C, 47.49; H, 2.66; N, 6.15; Found: C, 47.52; H, 2.65; N, 6.13.

#### **2-(6-Nitro-2-oxobenzo[*d*]oxazol-3(2*H*)-yl)acetic acid (BX\_03c)**

The compound was synthesized according to the general procedure using *tert*-butyl 2-(6-nitro-2-oxobenzo[*d*]oxazol-3(2*H*)-yl)acetate (BX\_02c) (1.5 g, 5.09 mmol), and TFA (1.16 g, 10.19 mmol) to afford BX\_03c (0.95 g, 78.7 %) as white solid. M.p: 261-263 °C. <sup>1</sup>H NMR

(DMSO- $d_6$ ):  $\delta_H$  11.22 (s, 1H), 8.31 – 7.98 (m, 3H), 4.17 (s, 2H).  $^{13}C$  NMR (DMSO- $d_6$ ):  $\delta_C$  176.3, 154.6, 144.2, 140.0, 138.5, 123.2, 121.1, 117.7, 55.4. ESI-MS  $m/z$  237 (M-H) $^-$ . Anal. Calcd. for  $C_9H_6N_2O_6$ : C, 45.39; H, 2.54; N, 11.76; Found: C, 45.42; H, 2.52; N, 11.78.

#### **2-(2-Oxobenzo[*d*]oxazol-3(2*H*)-yl)-*N*-phenylacetamide (BX\_04)**

The compound was synthesized according to the general procedure using 2-(2-oxobenzo[*d*]oxazol-3(2*H*)-yl)acetic acid (**BX\_03a**) (0.1 g, 0.51 mmol), aniline (0.057 g, 0.62 mmol), EDC (0.12 g, 0.62 mmol) and HOBT (0.083 g, 0.62 mmol) to afford **BX\_04** (0.092 g, 66.6 %) as white solid. M.p: 190-191 °C.  $^1H$  NMR (DMSO- $d_6$ ):  $\delta_H$  10.25 (s, 1H), 8.16 – 7.04 (m, 9H), 4.76 (s, 2H).  $^{13}C$  NMR (DMSO- $d_6$ ):  $\delta_C$  169.5, 155.6, 139.0, 138.7, 132.1, 128.3, 128.0, 125.7, 124.6, 121.2, 116.4, 115.9, 54.1. ESI-MS  $m/z$  269 (M+H) $^+$ . Anal. Calcd. for  $C_{15}H_{12}N_2O_3$ : C, 67.16; H, 4.51; N, 10.44; Found: C, 67.12; H, 4.52; N, 10.42.

#### **2-(6-Chloro-2-oxobenzo[*d*]oxazol-3(2*H*)-yl)-*N*-phenylacetamide (BX\_05)**

The compound was synthesized according to the general procedure using 2-(6-chloro-2-oxobenzo[*d*]oxazol-3(2*H*)-yl)acetic acid (**BX\_03b**) (0.1 g, 0.43 mmol), aniline (0.049 g, 0.52 mmol), EDC (0.10 g, 0.52 mmol) and HOBT (0.070 g, 0.52 mmol) to afford **BX\_05** (0.097 g, 73.2 %) as white solid. M.p: 181-183 °C.  $^1H$  NMR (DMSO- $d_6$ ):  $\delta_H$  10.26 (s, 1H), 8.22 - 7.05 (m, 8H), 4.77 (s, 2H).  $^{13}C$  NMR (DMSO- $d_6$ ):  $\delta_C$  169.6, 154.8, 140.1, 138.7, 131.3, 130.6, 128.7, 128.3, 125.4, 123.5, 122.7, 121.6, 54.2. ESI-MS  $m/z$  301 (M-H) $^-$ . Anal. Calcd. for  $C_{15}H_{11}ClN_2O_3$ : C, 59.52; H, 3.66; N, 9.25; Found: C, 59.55; H, 3.64; N, 9.28.

#### **2-(6-Nitro-2-oxobenzo[*d*]oxazol-3(2*H*)-yl)-*N*-phenylacetamide (BX\_06)**

The compound was synthesized according to the general procedure using 2-(6-nitro-2-oxobenzo[*d*]oxazol-3(2*H*)-yl)acetic acid (**BX\_03c**) (0.1 g, 0.41 mmol), aniline (0.046 g, 0.50 mmol), EDC (0.098 g, 0.50 mmol) and HOBT (0.067 g, 0.50 mmol) to afford **BX\_06** (0.096 g, 73.3 %) as pale yellow solid. M.p: 222-223 °C.  $^1H$  NMR (DMSO- $d_6$ ):  $\delta_H$  10.28 (s, 1H), 7.92 – 7.06 (m, 8H), 4.83 (s, 2H).  $^{13}C$  NMR (DMSO- $d_6$ ):  $\delta_C$  169.6, 154.9, 143.9, 140.2, 138.6, 138.4, 129.0, 128.2, 122.8, 121.7, 120.9, 117.7, 54.4. ESI-MS  $m/z$  312 (M-H) $^-$ . Anal. Calcd. for  $C_{15}H_{11}N_3O_5$ : C, 57.51; H, 3.54; N, 13.41; Found: C, 57.55; H, 3.52; N, 13.44.



***N*-(2-Chloro-5-(trifluoromethyl)phenyl)-2-(2-oxobenzo[*d*]oxazol-3(2*H*)-yl)acetamide (BX\_07)**

The compound was synthesized according to the general procedure using 2-(2-oxobenzo[*d*]oxazol-3(2*H*)-yl)acetic acid (**BX\_03a**) (0.1 g, 0.51 mmol), 2-chloro-5-(trifluoromethyl)aniline (0.12 g, 0.62 mmol), EDC (0.12 g, 0.62 mmol) and HOBT (0.083 g, 0.62 mmol) to afford **BX\_07** (0.13 g, 69.6 %) as pale yellow solid. M.p: 157-159 °C. <sup>1</sup>H NMR (DMSO-*d*<sub>6</sub>): δ<sub>H</sub> 9.97 (s, 1H), 8.10 – 7.19 (m, 7H), 4.82 (s, 2H). <sup>13</sup>C NMR (DMSO-*d*<sub>6</sub>): δ<sub>C</sub> 169.7, 168.6, 139.1, 137.9, 132.2, 129.5, 129.3, 125.9, 125.7, 124.8, 124.3, 122.2, 118.7, 116.6, 116.1, 54.2. ESI-MS *m/z* 369 (M-H)<sup>-</sup>. Anal. Calcd. for C<sub>16</sub>H<sub>10</sub>ClF<sub>3</sub>N<sub>2</sub>O<sub>3</sub>: C, 51.84; H, 2.72; N, 7.56; Found: C, 51.87; H, 2.70; N, 7.53.

***2*-(6-Chloro-2-oxobenzo[*d*]oxazol-3(2*H*)-yl)-*N*-(2-chloro-5-(trifluoromethyl)phenyl)acetamide (BX\_08)**

The compound was synthesized according to the general procedure using 2-(6-chloro-2-oxobenzo[*d*]oxazol-3(2*H*)-yl)acetic acid (**BX\_03b**) (0.1 g, 0.43 mmol), 2-chloro-5-(trifluoromethyl)aniline (0.10 g, 0.52 mmol), EDC (0.10 g, 0.52 mmol) and HOBT (0.070 g, 0.52 mmol) to afford **BX\_08** (0.13 g, 74.3 %) as white solid. M.p: 139-140 °C. <sup>1</sup>H NMR (DMSO-*d*<sub>6</sub>): δ<sub>H</sub> 9.98 (s, 1H), 8.11 – 7.19 (m, 6H), 4.82 (s, 2H). <sup>13</sup>C NMR (DMSO-*d*<sub>6</sub>): δ<sub>C</sub> 169.5, 154.0, 140.8, 137.3, 131.7, 130.5, 129.6, 129.4, 125.9, 125.6, 124.4, 123.7, 122.8, 122.2, 118.9, 54.5. ESI-MS *m/z* 404 (M-H)<sup>-</sup>. Anal. Calcd. for C<sub>16</sub>H<sub>9</sub>Cl<sub>2</sub>F<sub>3</sub>N<sub>2</sub>O<sub>3</sub>: C, 47.43; H, 2.24; N, 6.91; Found: C, 47.45; H, 2.25; N, 6.94.

***N*-(2-Chloro-5-(trifluoromethyl)phenyl)-2-(6-nitro-2-oxobenzo[*d*]oxazol-3(2*H*)-yl)acetamide (BX\_09)**

The compound was synthesized according to the general procedure using 2-(6-nitro-2-oxobenzo[*d*]oxazol-3(2*H*)-yl)acetic acid (**BX\_03c**) (0.1 g, 0.41 mmol), 2-chloro-5-(trifluoromethyl)aniline (0.097 g, 0.50 mmol), EDC (0.098 g, 0.50 mmol) and HOBT (0.067 g, 0.50 mmol) to afford **BX\_09** (0.13 g, 78.5 %) as pale yellow solid. M.p: 127-129 °C. <sup>1</sup>H NMR (DMSO-*d*<sub>6</sub>): δ<sub>H</sub> 9.98 (s, 1H), 8.12 – 7.19 (m, 6H), 4.83 (s, 2H). <sup>13</sup>C NMR (DMSO-*d*<sub>6</sub>): δ<sub>C</sub> 169.4, 154.6, 143.9, 140.1, 138.5, 137.7, 129.5, 129.3, 126.1, 124.3, 122.9, 122.4, 121.0, 118.8, 117.7, 54.2. ESI-MS *m/z* 414 (M-H)<sup>-</sup>. Anal. Calcd. for C<sub>16</sub>H<sub>9</sub>ClF<sub>3</sub>N<sub>3</sub>O<sub>5</sub>: C, 46.23; H, 2.18; N, 10.11; Found: C, 46.19; H, 2.16; N, 10.14.

### 2-(2-Oxobenzo[*d*]oxazol-3(2*H*)-yl)-*N*-(pyridin-2-yl)acetamide (**BX\_10**)

The compound was synthesized according to the general procedure using 2-(2-oxobenzo[*d*]oxazol-3(2*H*)-yl)acetic acid (**BX\_03a**) (0.1 g, 0.51 mmol), pyridin-2-amine (0.058 g, 0.62 mmol), EDC (0.12 g, 0.62 mmol) and HOBT (0.083 g, 0.62 mmol) to afford **BX\_10** (0.094 g, 68.2 %) as white solid. M.p: 221-223 °C. <sup>1</sup>H NMR (DMSO-*d*<sub>6</sub>): δ<sub>H</sub> 10.42 (s, 1H), 8.67 – 7.02 (m, 8H), 4.87 (s, 2H). <sup>13</sup>C NMR (DMSO-*d*<sub>6</sub>): δ<sub>C</sub> 169.5, 154.7, 151.8, 146.7, 139.1, 138.5, 132.1, 127.6, 124.8, 124.3, 116.5, 116.1, 115.8, 52.4. ESI-MS *m/z* 270 (M+H)<sup>+</sup>. Anal. Calcd. for C<sub>14</sub>H<sub>11</sub>N<sub>3</sub>O<sub>3</sub>: C, 62.45; H, 4.12; N, 15.61; Found: C, 62.42; H, 4.10; N, 15.59.

### 2-(6-Chloro-2-oxobenzo[*d*]oxazol-3(2*H*)-yl)-*N*-(pyridin-2-yl)acetamide (**BX\_11**)

The compound was synthesized according to the general procedure using 2-(6-chloro-2-oxobenzo[*d*]oxazol-3(2*H*)-yl)acetic acid (**BX\_03b**) (0.1 g, 0.43 mmol), pyridin-2-amine (0.048 g, 0.52 mmol), EDC (0.10 g, 0.52 mmol) and HOBT (0.070 g, 0.52 mmol) to afford **BX\_11** (0.086 g, 65.3 %) as white solid. M.p: 243-245 °C. <sup>1</sup>H NMR (DMSO-*d*<sub>6</sub>): δ<sub>H</sub> 10.44 (s, 1H), 8.67 – 7.10 (m, 7H), 4.88 (s, 2H). <sup>13</sup>C NMR (DMSO-*d*<sub>6</sub>): δ<sub>C</sub> 169.6, 154.8, 151.6, 146.6, 140.2, 138.5, 131.4, 130.4, 125.7, 124.3, 123.6, 122.7, 116.6, 52.3. ESI-MS *m/z* 302 (M-H)<sup>-</sup>. Anal. Calcd. for C<sub>14</sub>H<sub>10</sub>ClN<sub>3</sub>O<sub>3</sub>: C, 55.37; H, 3.32; N, 13.84; Found: C, 55.34; H, 3.35; N, 13.87.

### 2-(6-Nitro-2-oxobenzo[*d*]oxazol-3(2*H*)-yl)-*N*-(pyridin-2-yl)acetamide (**BX\_12**)

The compound was synthesized according to the general procedure using 2-(6-nitro-2-oxobenzo[*d*]oxazol-3(2*H*)-yl)acetic acid (**BX\_03c**) (0.1 g, 0.41 mmol), pyridin-2-amine (0.047 g, 0.50 mmol), EDC (0.098 g, 0.50 mmol) and HOBT (0.067 g, 0.50 mmol) to afford **BX\_12** (0.088 g, 67.1 %) as pale yellow solid. M.p: 253-255 °C. <sup>1</sup>H NMR (DMSO-*d*<sub>6</sub>): δ<sub>H</sub> 10.51 (s, 1H), 8.68 – 7.11 (m, 7H), 4.89 (s, 2H). <sup>13</sup>C NMR (DMSO-*d*<sub>6</sub>): δ<sub>C</sub> 168.9, 154.9, 151.8, 146.7, 144.0, 139.9, 138.8, 138.4, 124.6, 122.9, 121.2, 117.2, 115.9, 52.6. ESI-MS *m/z* 313 (M-H)<sup>-</sup>. Anal. Calcd. for C<sub>14</sub>H<sub>10</sub>N<sub>4</sub>O<sub>5</sub>: C, 53.51; H, 3.21; N, 17.83; Found: C, 53.48; H, 3.18; N, 17.86.

### **2-(2-Oxobenzo[*d*]oxazol-3(2*H*)-yl)-*N*-(pyridin-2-ylmethyl)acetamide (BX\_13)**

The compound was synthesized according to the general procedure using 2-(2-oxobenzo[*d*]oxazol-3(2*H*)-yl)acetic acid (**BX\_03a**) (0.1 g, 0.51 mmol), pyridin-2-ylmethanamine (0.067 g, 0.62 mmol), EDC (0.12 g, 0.62 mmol) and HOBT (0.083 g, 0.62 mmol) to afford **BX\_13** (0.095 g, 65.2 %) as white solid. M.p: 162-164 °C. <sup>1</sup>H NMR (DMSO-*d*<sub>6</sub>): δ<sub>H</sub> 9.921 (s, 1H), 8.37 – 7.01 (m, 8H), 4.75 (s, 2H), 4.54 (s, 2H). <sup>13</sup>C NMR (DMSO-*d*<sub>6</sub>): δ<sub>C</sub> 169.6, 155.8, 154.2, 148.5, 139.5, 139.2, 132.0, 125.9, 124.8, 124.2, 121.1, 116.4, 116.1, 54.3, 45.2. ESI-MS *m/z* 284 (M+H)<sup>+</sup>. Anal. Calcd. for C<sub>15</sub>H<sub>13</sub>N<sub>3</sub>O<sub>3</sub>: C, 63.60; H, 4.63; N, 14.83; Found: C, 63.57; H, 4.60; N, 14.81.

### **2-(6-Chloro-2-oxobenzo[*d*]oxazol-3(2*H*)-yl)-*N*-(pyridin-2-ylmethyl)acetamide (BX\_14)**

The compound was synthesized according to the general procedure using 2-(6-chloro-2-oxobenzo[*d*]oxazol-3(2*H*)-yl)acetic acid (**BX\_03b**) (0.1 g, 0.43 mmol), pyridin-2-ylmethanamine (0.056 g, 0.52 mmol), EDC (0.10 g, 0.52 mmol) and HOBT (0.070 g, 0.52 mmol) to afford **BX\_14** (0.089 g, 64.4 %) as white solid. M.p: 182-184 °C. <sup>1</sup>H NMR (DMSO-*d*<sub>6</sub>): δ<sub>H</sub> 9.92 (s, 1H), 8.41 – 7.01 (m, 7H), 4.81 (s, 2H), 4.55 (s, 2H). <sup>13</sup>C NMR (DMSO-*d*<sub>6</sub>): δ<sub>C</sub> 169.7, 156.2, 154.3, 148.8, 140.7, 139.9, 131.8, 130.1, 125.7, 124.3, 126.3, 122.2, 121.1, 54.4, 45.5. ESI-MS *m/z* 316 (M-H)<sup>-</sup>. Anal. Calcd. for C<sub>15</sub>H<sub>12</sub>ClN<sub>3</sub>O<sub>3</sub>: C, 56.70; H, 3.81; N, 13.23; Found: C, 56.66; H, 3.78; N, 13.20.

### **2-(6-Nitro-2-oxobenzo[*d*]oxazol-3(2*H*)-yl)-*N*-(pyridin-2-ylmethyl)acetamide (BX\_15)**

The compound was synthesized according to the general procedure using 2-(6-nitro-2-oxobenzo[*d*]oxazol-3(2*H*)-yl)acetic acid (**BX\_03c**) (0.1 g, 0.41 mmol), pyridin-2-ylmethanamine (0.054 g, 0.50 mmol), EDC (0.098 g, 0.50 mmol) and HOBT (0.067 g, 0.50 mmol) to afford **BX\_15** (0.092 g, 66.7 %) as white solid. M.p: 187-189 °C. <sup>1</sup>H NMR (DMSO-*d*<sub>6</sub>): δ<sub>H</sub> 9.92 (s, 1H), 8.42 – 7.02 (m, 7H), 4.83 (s, 2H), 4.55 (s, 2H). <sup>13</sup>C NMR (DMSO-*d*<sub>6</sub>): δ<sub>C</sub> 169.5, 156.3, 154.9, 148.3, 144.2, 139.9, 139.6, 138.4, 124.5, 123.1, 121.1, 120.8, 117.7, 54.4, 45.4. ESI-MS *m/z* 327 (M-H)<sup>-</sup>. Anal. Calcd. for C<sub>15</sub>H<sub>12</sub>N<sub>4</sub>O<sub>5</sub>: C, 54.88; H, 3.68; N, 17.07; Found: C, 54.87; H, 3.70; N, 17.10.

### ***N*-(Furan-2-ylmethyl)-2-(2-oxobenzo[*d*]oxazol-3(2*H*)-yl)acetamide (BX\_16)**

The compound was synthesized according to the general procedure using 2-(2-oxobenzo[*d*]oxazol-3(2*H*)-yl)acetic acid (**BX\_03a**) (0.1 g, 0.51 mmol), furan-2-ylmethanamine (0.060 g, 0.62 mmol), EDC (0.12 g, 0.62 mmol) and HOBT (0.083 g, 0.62 mmol) to afford **BX\_16** (0.101 g, 72.2 %) as white solid. M.p: 110-112 °C. <sup>1</sup>H NMR (DMSO-*d*<sub>6</sub>): δ<sub>H</sub> 9.76 (s, 1H), 7.45 – 6.79 (m, 7H), 4.79 (s, 2H), 4.33 (s, 2H). <sup>13</sup>C NMR (DMSO-*d*<sub>6</sub>): δ<sub>C</sub> 169.3, 154.2, 149.3, 142.5, 132.1, 130.3, 124.5, 122.6, 119.2, 116.1, 110.4, 108.6, 51.3, 35.0. ESI-MS *m/z* 273 (M+H)<sup>+</sup>. Anal. Calcd. for C<sub>14</sub>H<sub>12</sub>N<sub>2</sub>O<sub>4</sub>: C, 61.76; H, 4.44; N, 10.29; Found: C, 61.73; H, 4.42; N, 10.26.

### **2-(6-Chloro-2-oxobenzo[*d*]oxazol-3(2*H*)-yl)-*N*-(furan-2-ylmethyl)acetamide (BX\_17)**

The compound was synthesized according to the general procedure using 2-(6-chloro-2-oxobenzo[*d*]oxazol-3(2*H*)-yl)acetic acid (**BX\_03b**) (0.1 g, 0.43 mmol), furan-2-ylmethanamine (0.050 g, 0.52 mmol), EDC (0.10 g, 0.52 mmol) and HOBT (0.070 g, 0.52 mmol) to afford **BX\_17** (0.098 g, 73.4 %) as white solid. M.p: 142-144 °C. <sup>1</sup>H NMR (DMSO-*d*<sub>6</sub>): δ<sub>H</sub> 10.42 (s, 1H), 7.60 – 6.36 (m, 6H), 4.62 (s, 2H), 4.33 (s, 2H). <sup>13</sup>C NMR (DMSO-*d*<sub>6</sub>): δ<sub>C</sub> 169.5, 154.6, 154.1, 149.2, 142.6, 132.3, 130.0, 122.7, 119.0, 116.3, 110.6, 108.3, 51.5, 34.9. ESI-MS *m/z* 305 (M-H)<sup>-</sup>. Anal. Calcd. for C<sub>14</sub>H<sub>11</sub>ClN<sub>2</sub>O<sub>4</sub>: C, 54.83; H, 3.62; N, 9.13; Found: C, 54.79; H, 3.60; N, 9.15.

### ***N*-(Furan-2-ylmethyl)-2-(6-nitro-2-oxobenzo[*d*]oxazol-3(2*H*)-yl)acetamide (BX\_18)**

The compound was synthesized according to the general procedure using 2-(6-nitro-2-oxobenzo[*d*]oxazol-3(2*H*)-yl)acetic acid (**BX\_03c**) (0.1 g, 0.41 mmol), furan-2-ylmethanamine (0.048 g, 0.50 mmol), EDC (0.098 g, 0.50 mmol) and HOBT (0.067 g, 0.50 mmol) to afford **BX\_18** (0.097 g, 73.2 %) as pale yellow solid. M.p: 165-167 °C. <sup>1</sup>H NMR (DMSO-*d*<sub>6</sub>): δ<sub>H</sub> 11.04 (s, 1H), 7.75 – 6.80 (m, 6H), 4.81 (s, 2H), 4.33 (s, 2H). <sup>13</sup>C NMR (DMSO-*d*<sub>6</sub>): δ<sub>C</sub> 169.7, 154.5, 144.2, 149.2, 142.4, 132.2, 130.0, 122.5, 119.2, 116.4, 110.7, 108.5, 51.2, 34.9. ESI-MS *m/z* 316 (M-H)<sup>-</sup>. Anal. Calcd. for C<sub>14</sub>H<sub>11</sub>N<sub>3</sub>O<sub>6</sub>: C, 53.00; H, 3.49; N, 13.24; Found: C, 52.97; H, 3.46; N, 13.22.

### **2-(2-Oxobenzo[*d*]oxazol-3(2*H*)-yl)-*N*-(thiophen-2-ylmethyl)acetamide (BX\_19)**

The compound was synthesized according to the general procedure using 2-(2-oxobenzo[*d*]oxazol-3(2*H*)-yl)acetic acid (**BX\_03a**) (0.1 g, 0.51 mmol), thiophen-2-ylmethanamine (0.070 g, 0.62 mmol), EDC (0.12 g, 0.62 mmol) and HOBT (0.083 g, 0.62 mmol) to afford **BX\_19** (0.111 g, 74.4 %) as white solid. M.p: 128-130 °C. <sup>1</sup>H NMR (DMSO-*d*<sub>6</sub>): δ<sub>H</sub> 9.87 (s, 1H), 7.47 – 6.81 (m, 7H), 4.79 (s, 2H), 4.34 (s, 2H). <sup>13</sup>C NMR (DMSO-*d*<sub>6</sub>): δ<sub>C</sub> 169.6, 154.7, 153.2, 138.2, 128.8, 128.7, 127.2, 126.8, 126.3, 123.3, 119.1, 116.6, 51.6, 36.3. ESI-MS *m/z* 287 (M-H)<sup>-</sup>. Anal. Calcd. for C<sub>14</sub>H<sub>12</sub>N<sub>2</sub>O<sub>3</sub>S: C, 58.32; H, 4.20; N, 9.72; Found: C, 58.35; H, 4.18; N, 9.73.

### **2-(6-Chloro-2-oxobenzo[*d*]oxazol-3(2*H*)-yl)-*N*-(thiophen-2-ylmethyl)acetamide (BX\_20)**

The compound was synthesized according to the general procedure using 2-(6-chloro-2-oxobenzo[*d*]oxazol-3(2*H*)-yl)acetic acid (**BX\_03b**) (0.1 g, 0.43 mmol), thiophen-2-ylmethanamine (0.058 g, 0.52 mmol), EDC (0.10 g, 0.52 mmol) and HOBT (0.070 g, 0.52 mmol) to afford **BX\_20** (0.102 g, 72.3 %) as white solid. M.p: 166-168 °C. <sup>1</sup>H NMR (DMSO-*d*<sub>6</sub>): δ<sub>H</sub> 10.32 (s, 1H), 7.52 – 6.24 (m, 6H), 4.79 (s, 2H), 4.35 (s, 2H). <sup>13</sup>C NMR (DMSO-*d*<sub>6</sub>): δ<sub>C</sub> 169.4, 154.6, 153.0, 139.6, 139.4, 129.5, 128.3, 126.7, 126.0, 124.5, 120.4, 115.6, 51.4, 36.3. ESI-MS *m/z* 321 (M-H)<sup>-</sup>. Anal. Calcd. for C<sub>14</sub>H<sub>11</sub>ClN<sub>2</sub>O<sub>3</sub>S: C, 52.10; H, 3.44; N, 8.68; Found: C, 52.13; H, 3.42; N, 8.66.

### **2-(6-Nitro-2-oxobenzo[*d*]oxazol-3(2*H*)-yl)-*N*-(thiophen-2-ylmethyl)acetamide (BX\_21)**

The compound was synthesized according to the general procedure using 2-(6-nitro-2-oxobenzo[*d*]oxazol-3(2*H*)-yl)acetic acid (**BX\_03c**) (0.1 g, 0.41 mmol), thiophen-2-ylmethanamine (0.056 g, 0.50 mmol), EDC (0.098 g, 0.50 mmol) and HOBT (0.067 g, 0.50 mmol) to afford **BX\_21** (0.104 g, 74.7 %) as white solid. M.p: 220-222 °C. <sup>1</sup>H NMR (DMSO-*d*<sub>6</sub>): δ<sub>H</sub> 11.06 (s, 1H), 7.76 – 6.97 (m, 6H), 4.81 (s, 2H), 4.50 (s, 2H). <sup>13</sup>C NMR (DMSO-*d*<sub>6</sub>): δ<sub>C</sub> 169.2, 154.4, 152.5, 146.1, 137.9, 130.2, 128.0, 127.4, 126.8, 126.2, 114.2, 111.1, 51.2, 36.4. ESI-MS *m/z* 332 (M-H)<sup>-</sup>. Anal. Calcd. for C<sub>14</sub>H<sub>11</sub>N<sub>3</sub>O<sub>5</sub>S: C, 50.45; H, 3.33; N, 12.61; Found: C, 50.42; H, 3.35; N, 12.64.

### **2-Chloro-*N*-(5-nitrothiazol-2-yl)acetamide (BX\_22a)**

The compound was synthesized according to the general procedure using chloroacetyl chloride (1.55 g, 13.77 mmol) and 5-nitrothiazol-2-amine (1.0 g, 6.88 mmol) to afford **BX\_22a** (1.03 g, 67.7 %) as pale yellow solid. M.p: 252-254 °C. <sup>1</sup>H NMR (DMSO-d<sub>6</sub>): δ<sub>H</sub> 9.94 (s, 1H), 8.34 (s, 1H), 4.45 (s, 2H). <sup>13</sup>C NMR (DMSO-d<sub>6</sub>): δ<sub>C</sub> 169.4, 166.3, 148.1, 138.6, 43.1. ESI-MS *m/z* 220 (M-H)<sup>-</sup>. Anal. Calcd. for C<sub>5</sub>H<sub>4</sub>ClN<sub>3</sub>O<sub>3</sub>S: C, 27.10; H, 1.82; N, 18.96; Found: C, 27.13; H, 1.79; N, 18.99.

### ***N*-(Benzo[*d*]thiazol-2-yl)-2-chloroacetamide (BX\_22b)**

The compound was synthesized according to the general procedure using chloroacetyl chloride (1.50 g, 13.31 mmol) and benzo[*d*]thiazol-2-amine (1.0 g, 6.65 mmol) to afford **BX\_22b** (0.92 g, 66.2 %) as pale yellow solid. M.p: 276-278 °C. <sup>1</sup>H NMR (DMSO-d<sub>6</sub>): δ<sub>H</sub> 11.78 (s, 1H), 8.21 – 7.63 (m, 4H), 4.39 (s, 2H). <sup>13</sup>C NMR (DMSO-d<sub>6</sub>): δ<sub>C</sub> 173.7, 168.8, 153.4, 130.9, 125.5, 124.7, 121.5, 118.4, 42.9. ESI-MS *m/z* 225 (M-H)<sup>-</sup>. Anal. Calcd. for C<sub>9</sub>H<sub>7</sub>ClN<sub>2</sub>OS: C, 47.69; H, 3.11; N, 12.36; Found: C, 47.72; H, 3.13; N, 12.39.

### **2-Chloro-*N*-(6-nitrobenzo[*d*]thiazol-2-yl)acetamide (BX\_22c)**

The compound was synthesized according to the general procedure using chloroacetyl chloride (1.15 g, 10.24 mmol) and 6-nitrobenzo[*d*]thiazol-2-amine (1.0 g, 5.12 mmol) to afford **BX\_22c** (0.92 g, 66.2 %) as pale yellow solid. M.p: 273-275 °C. <sup>1</sup>H NMR (DMSO-d<sub>6</sub>): δ<sub>H</sub> 12.62 (s 1H), 9.11 (s, 1H), 8.34 – 7.97 (m, 2H), 4.55 (s, 2H). <sup>13</sup>C NMR (DMSO-d<sub>6</sub>): δ<sub>C</sub> 173.9, 168.5, 159.6, 144.8, 131.6, 121.5, 119.2, 117.1, 43.0. ESI-MS *m/z* 270 (M-H)<sup>-</sup>. Anal. Calcd. for C<sub>9</sub>H<sub>6</sub>ClN<sub>3</sub>O<sub>3</sub>S: C, 39.79; H, 2.23; N, 15.47; Found: C, 39.76; H, 2.22; N, 15.50.

### ***N*-(5-Nitrothiazol-2-yl)-2-(2-oxobenzo[*d*]oxazol-3(2*H*)-yl)acetamide (BX\_23)**

The compound was synthesized according to the general procedure using 2-chloro-*N*-(5-nitrothiazol-2-yl)acetamide (**BX\_22a**) (0.137 g, 0.62 mmol) and benzo[*d*]oxazol-2(3*H*)-one (**BX\_01a**) (0.1g, 0.51 mmol) to afford **BX\_23** (0.11 g, 72.2 %) as pale yellow solid. M.p: 193-195 °C. <sup>1</sup>H NMR (DMSO-d<sub>6</sub>): δ<sub>H</sub> 13.60 (s, 1H), 8.67 (s, 1H), 7.41 – 7.15 (m, 4H), 4.95 (s, 2H). <sup>13</sup>C NMR (DMSO-d<sub>6</sub>): δ<sub>C</sub> 169.5, 162.8, 154.4, 145.7, 138.8, 135.5, 132.5, 125.8, 124.7, 116.6, 116.1, 53.2. ESI-MS *m/z* 319 (M-H)<sup>-</sup>. Anal. Calcd. for C<sub>12</sub>H<sub>8</sub>N<sub>4</sub>O<sub>5</sub>S: C, 45.00; H, 2.52; N, 17.49; Found: C, 45.04; H, 2.49; N, 17.46.

### **2-(6-Chloro-2-oxobenzo[*d*]oxazol-3(2*H*)-yl)-*N*-(5-nitrothiazol-2-yl)acetamide (BX\_24)**

The compound was synthesized according to the general procedure using 2-chloro-*N*-(5-nitrothiazol-2-yl)acetamide (**BX\_22a**) (0.156 g, 0.70 mmol) and 6-chlorobenzo[*d*]oxazol-2(3*H*)-one (**BX\_01b**) (0.1g, 0.58 mmol) to afford **BX\_24** (0.148 g, 70.9 %) as pale yellow solid. M.p: 268-270 °C. <sup>1</sup>H NMR (DMSO-*d*<sub>6</sub>): δ<sub>H</sub> 13.51 (s, 1H), 8.65 (s, 1H), 7.89 – 7.12 (m, 3H), 4.81 (s, 2H). <sup>13</sup>C NMR (DMSO-*d*<sub>6</sub>): δ<sub>C</sub> 169.6, 162.6, 154.7, 147.1, 140.0, 135.6, 131.5, 130.4, 125.9, 123.5, 122.8, 53.4. ESI-MS *m/z* 353 (M-H)<sup>-</sup>. Anal. Calcd. for C<sub>12</sub>H<sub>7</sub>ClN<sub>4</sub>O<sub>5</sub>S: C, 40.63; H, 1.99; N, 15.79; Found: C, 40.60; H, 2.01; N, 15.81.

### **2-(6-Nitro-2-oxobenzo[*d*]oxazol-3(2*H*)-yl)-*N*-(5-nitrothiazol-2-yl)acetamide (BX\_25)**

The compound was synthesized according to the general procedure using 2-chloro-*N*-(5-nitrothiazol-2-yl)acetamide (**BX\_22a**) (0.147 g, 0.66 mmol) and 6-nitrobenzo[*d*]oxazol-2(3*H*)-one (**BX\_01c**) (0.1g, 0.55 mmol) to afford **BX\_25** (0.149 g, 73.6 %) as pale yellow solid. M.p: 273-275 °C. <sup>1</sup>H NMR (DMSO-*d*<sub>6</sub>): δ<sub>H</sub> 13.50 (s, 1H), 8.55 (s, 1H), 7.89 – 7.19 (m, 3H), 4.83 (s, 2H). <sup>13</sup>C NMR (DMSO-*d*<sub>6</sub>): δ<sub>C</sub> 169.6, 162.8, 154.2, 147.1, 143.3, 140.2, 138.5, 135.6, 123.2, 121.3, 117.7, 53.2. ESI-MS *m/z* 364 (M-H)<sup>-</sup>. Anal. Calcd. for C<sub>12</sub>H<sub>7</sub>N<sub>5</sub>O<sub>7</sub>S: C, 39.46; H, 1.93; N, 19.17; Found: C, 39.49; H, 1.94; N, 19.20.

### ***N*-(Benzo[*d*]thiazol-2-yl)-2-(2-oxobenzo[*d*]oxazol-3(2*H*)-yl)acetamide (BX\_26)**

The compound was synthesized according to the general procedure using *N*-(benzo[*d*]thiazol-2-yl)-2-chloroacetamide (**BX\_22b**) (0.140 g, 0.62 mmol) and benzo[*d*]oxazol-2(3*H*)-one (**BX\_01a**) (0.1g, 0.51 mmol) to afford **BX\_26** (0.11 g, 67.9 %) as white solid. M.p: 250-252 °C. <sup>1</sup>H NMR (DMSO-*d*<sub>6</sub>): δ<sub>H</sub> 10.68 (s, 1H), 7.85 – 7.37 (m, 8H), 4.79 (s, 2H). <sup>13</sup>C NMR (DMSO-*d*<sub>6</sub>): δ<sub>C</sub> 173.5, 168.6, 154.7, 153.3, 139.2, 132.4, 130.9, 125.8, 125.5, 124.7, 124.5, 121.9, 118.7, 116.6, 116.0, 54.2. ESI-MS *m/z* 326 (M+H)<sup>+</sup>. Anal. Calcd. for C<sub>16</sub>H<sub>11</sub>N<sub>3</sub>O<sub>3</sub>S: C, 59.07; H, 3.41; N, 12.92; Found: C, 59.04; H, 3.38; N, 12.89.

### ***N*-(Benzo[*d*]thiazol-2-yl)-2-(6-chloro-2-oxobenzo[*d*]oxazol-3(2*H*)-yl)acetamide (BX\_27)**

The compound was synthesized according to the general procedure using *N*-(benzo[*d*]thiazol-2-yl)-2-chloroacetamide (**BX\_22b**) (0.158 g, 0.70 mmol) and 6-chlorobenzo[*d*]oxazol-2(3*H*)-one (**BX\_01b**) (0.1g, 0.58 mmol) to afford **BX\_27** (0.108 g, 68.4 %) as white solid. M.p: 267-269 °C. <sup>1</sup>H NMR (DMSO-*d*<sub>6</sub>): δ<sub>H</sub> 10.73 (s, 1H), 8.02 – 7.34 (m, 7H), 4.81 (s, 2H). <sup>13</sup>C

NMR (DMSO- $d_6$ ):  $\delta_C$  173.4, 168.5, 154.2, 153.5, 140.8, 131.7, 130.8, 130.5, 125.9, 125.5, 124.3, 123.5, 122.8, 121.9, 118.8, 54.4. ESI-MS  $m/z$  358 (M-H) $^-$ . Anal. Calcd. for  $C_{16}H_{10}ClN_3O_3S$ : C, 53.41; H, 2.80; N, 11.68; Found: C, 53.39; H, 2.78; N, 11.71.

#### ***N*-(Benzo[*d*]thiazol-2-yl)-2-(6-nitro-2-oxobenzo[*d*]oxazol-3(2*H*)-yl)acetamide (BX\_28)**

The compound was synthesized according to the general procedure using *N*-(benzo[*d*]thiazol-2-yl)-2-chloroacetamide (**BX\_22b**) (0.135 g, 0.66 mmol) and 6-nitrobenzo[*d*]oxazol-2(3*H*)-one (**BX\_01c**) (0.1g, 0.55 mmol) to afford **BX\_28** (0.105 g, 67.6 %) as pale yellow solid. M.p: 256-258 °C.  $^1H$  NMR (DMSO- $d_6$ ):  $\delta_H$  10.75 (s, 1H), 8.12 – 7.41 (m, 7H), 4.81 (s, 2H).  $^{13}C$  NMR (DMSO- $d_6$ ):  $\delta_C$  173.7, 168.7, 154.8, 153.1, 144.2, 139.8, 138.6, 130.9, 125.5, 124.9, 123.3, 121.9, 121.0, 118.4, 117.7, 54.2. ESI-MS  $m/z$  369 (M-H) $^-$ . Anal. Calcd. for  $C_{16}H_{10}N_4O_5S$ : C, 51.89; H, 2.72; N, 15.13; Found: C, 51.86; H, 2.70; N, 15.16.

#### ***N*-(6-Nitrobenzo[*d*]thiazol-2-yl)-2-(2-oxobenzo[*d*]oxazol-3(2*H*)-yl)acetamide (BX\_29)**

The compound was synthesized according to the general procedure using 2-chloro-*N*-(6-nitrobenzo[*d*]thiazol-2-yl)acetamide (**BX\_22c**) (0.168 g, 0.62 mmol) and benzo[*d*]oxazol-2(3*H*)-one (**BX\_01a**) (0.1g, 0.51 mmol) to afford **BX\_29** (0.124 g, 64.8 %) as pale yellow solid. M.p: >280 °C.  $^1H$  NMR (DMSO- $d_6$ ):  $\delta_H$  13.08 (s, 1H), 8.46 (s, 1H), 8.23 – 6.99 (m, 6H), 4.78 (s, 2H).  $^{13}C$  NMR (DMSO- $d_6$ ):  $\delta_C$  173.5, 168.6, 159.5, 154.7, 144.5, 139.2, 132.5, 131.5, 125.8, 124.4, 121.1, 119.6, 117.4, 116.4, 116.1, 54.4. ESI-MS  $m/z$  369 (M-H) $^-$ . Anal. Calcd. for  $C_{16}H_{10}N_4O_5S$ : C, 51.89; H, 2.72; N, 15.13; Found: C, 51.86; H, 2.74; N, 15.10.

#### **2-(6-Chloro-2-oxobenzo[*d*]oxazol-3(2*H*)-yl)-*N*-(6-nitrobenzo[*d*]thiazol-2-yl)acetamide (BX\_30)**

The compound was synthesized according to the general procedure using 2-chloro-*N*-(6-nitrobenzo[*d*]thiazol-2-yl)acetamide (**BX\_22c**) (0.190 g, 0.70 mmol) and 6-chlorobenzo[*d*]oxazol-2(3*H*)-one (**BX\_01b**) (0.1g, 0.58 mmol) to afford **BX\_30** (0.156 g, 65.7 %) as pale yellow solid. M.p: 269-271 °C.  $^1H$  NMR (DMSO- $d_6$ ):  $\delta_H$  13.00 (s, 1H), 8.46 (s, 1H), 8.24 – 7.11 (m, 5H), 4.89 (s, 2H).  $^{13}C$  NMR (DMSO- $d_6$ ):  $\delta_C$  173.3, 168.7, 160.1, 154.6, 144.7, 140.4, 131.7, 131.5, 130.6, 125.7, 123.3, 122.5, 121.7, 119.4, 117.7, 54.5. ESI-MS  $m/z$  403 (M-H) $^-$ . Anal. Calcd. for  $C_{16}H_9ClN_4O_5S$ : C, 47.47; H, 2.24; N, 13.84; Found: C, 47.44; H, 2.22; N, 13.82.



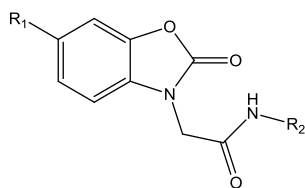
**2-(6-Nitro-2-oxobenzo[d]oxazol-3(2H)-yl)-N-(6-nitrobenzo[d]thiazol-2-yl)acetamide (BX\_31)**

The compound was synthesized according to the general procedure using 2-chloro-*N*-(6-nitrobenzo[d]thiazol-2-yl)acetamide (**BX\_22c**) (0.179 g, 0.66 mmol) and 6-nitrobenzo[d]oxazol-2(3H)-one (**BX\_01c**) (0.1g, 0.55 mmol) to afford **BX\_31** (0.157 g, 68.1 %) as pale yellow solid. M.p: 265-267 °C. <sup>1</sup>H NMR (DMSO-d<sub>6</sub>): δ<sub>H</sub> 13.02 (s, 1H), 8.46 (s, 1H), 8.24 – 7.82 (m, 5H), 4.89 (s, 2H). <sup>13</sup>C NMR (DMSO-d<sub>6</sub>): δ<sub>C</sub> 174.0, 168.8, 160.0, 154.9, 144.9, 144.3, 140.2, 138.6, 131.7, 123.1, 121.4, 121.2, 119.4, 117.7, 117.5, 54.6. ESI-MS *m/z* 414 (M-H)<sup>-</sup>. Anal. Calcd. for C<sub>16</sub>H<sub>9</sub>N<sub>5</sub>O<sub>7</sub>S: C, 46.27; H, 2.18; N, 16.86; Found: C, 46.24; H, 2.17; N, 16.84.

**5.1.4 *In vitro* Mycobacterium tuberculosis InhA inhibition assay, antimycobacterial potency and cytotoxicity studies of the synthesised molecules**

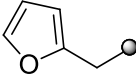
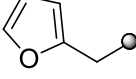
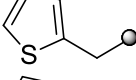
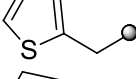
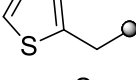
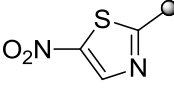
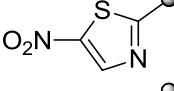
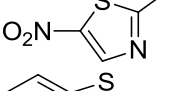
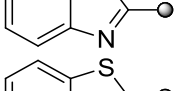
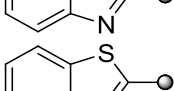
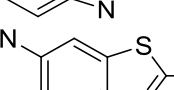
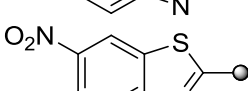
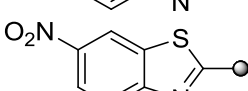

All the synthesized derivatives were first evaluated for their *in vitro* *Mycobacterium tuberculosis* InhA inhibitory potency as steps towards the derivation of structure-activity relationship (SAR) and hit optimization. The compounds were further subjected to a whole cell screening against *Mycobacterium tuberculosis* H37Rv strain to understand their bactericidal potency using the agar dilution method and later the safety profile of these molecules were evaluated by checking the *in vitro* cytotoxicity against RAW 264.7 cell line (mouse macrophage) at 100 and 50 μM concentration by MTT assay, and the results are tabulated in **Table 5.2**.

**Table 5.2:** *In vitro* biological evaluation of the synthesized derivatives **BX\_04** – **BX\_21** and **BX\_23** – **BX\_31**.



| Comp         | R <sub>1</sub>  | R <sub>2</sub> | % of InhA inhibition at 10 $\mu$ M (IC <sub>50</sub> in $\mu$ M) <sup>a</sup> | MIC ( $\mu$ M) <sup>b</sup> |                 |                | Cytotoxicity <sup>c</sup> (% inhib) |               |
|--------------|-----------------|----------------|---|-----------------------------|-----------------|----------------|-------------------------------------|---------------|
|              |                 |                |   | MTB                         | MTB (Verapamil) | MTB (Piperine) | at 100 $\mu$ M                      | at 50 $\mu$ M |
| <b>BX_04</b> | H               |                | 32.41±0.23  | 46.59                       | 23.29           | 23.29          | 39.82                               | 35.10         |
| <b>BX_05</b> | Cl              |                | 28.16±0.31  | 82.58                       | 20.64           | 41.29          | 20.23                               | 15.79         |
| <b>BX_06</b> | NO <sub>2</sub> |                | 46.12±1.34  | 79.80                       | 19.95           | 9.97           | 26.35                               | 18.04         |
| <b>BX_07</b> | H               |                | 26.80±0.95  | 67.43                       | 33.71           | 16.86          | 15.36                               | 12.30         |
| <b>BX_08</b> | Cl              |                | 40.12±1.52  | 61.70                       | 15.42           | 15.42          | 12.08                               | 1.61          |
| <b>BX_09</b> | NO <sub>2</sub> |                | 32.16±0.63  | 60.13                       | 15.03           | 30.06          | 31.59                               | 12.80         |
| <b>BX_10</b> | H               |                | 26.12±0.55  | 46.42                       | 4.64            | 9.28           | 28.42                               | 20.16         |
| <b>BX_11</b> | Cl              |                | 51.60±0.44  | 82.31                       | 10.29           | 10.29          | 43.68                               | 33.02         |
| <b>BX_12</b> | NO <sub>2</sub> |                | 15.63±0.79  | 39.77                       | 19.88           | 9.94           | 47.28                               | 38.61         |
| <b>BX_13</b> | H               |                | 42.18±1.63  | 88.25                       | 22.06           | 44.12          | 38.68                               | 37.26         |
| <b>BX_14</b> | Cl              |                | 43.12±1.79  | 39.34                       | 4.91            | 4.91           | 40.03                               | 36.15         |
| <b>BX_15</b> | NO <sub>2</sub> |                | 68.12±0.92 (8.23±0.65)  | 76.15                       | 38.07           | 9.51           | 33.35                               | 21.81         |
| <b>BX_16</b> | H               |                | 30.12±0.85  | 22.95                       | 22.95           | 22.95          | 33.83                               | 32.82         |

Contd...

| Comp  | R <sub>1</sub>  | R <sub>2</sub>  | % of InhA inhibition at 10 μM (IC <sub>50</sub> in μM) <sup>a</sup> | MIC (μM) <sup>b</sup> |                 |                | Cytotoxicity <sup>c</sup> (% inhib) |          |
|-------|-----------------|---|---|-----------------------|-----------------|----------------|-------------------------------------|----------|
|       |                 |   |   | MTB                   | MTB (Verapamil) | MTB (Piperine) | at 100 μM                           | at 50 μM |
| BX_17 | Cl              |    | 47.48±0.66  | 40.75                 | 20.37           | 10.18          | 50.32                               | 27.75    |
| BX_18 | NO <sub>2</sub> |    | 36.86±0.54  | 78.80                 | 39.40           | 39.40          | 60.10                               | 26.78    |
| BX_19 | H               |    | 26.12±0.84  | 21.66                 | 10.83           | 5.41           | 49.13                               | 23.39    |
| BX_20 | Cl              |    | 45.62±2.93  | 38.72                 | 9.64            | 9.64           | 53.60                               | 20.31    |
| BX_21 | NO <sub>2</sub> |    | 35.71±0.86  | 18.75                 | 18.75           | 18.75          | 40.95                               | 36.55    |
| BX_23 | H               |    | 48.15±1.34  | 78.05                 | 39.02           | 19.51          | 44.62                               | 24.98    |
| BX_24 | Cl              |   | 72.60±2.73<br>(6.82±0.53)   | 17.61                 | 8.81            | 17.61          | 50.64                               | 14.26    |
| BX_25 | NO <sub>2</sub> |  | 82.43±0.83<br>(5.12±0.44)   | 17.11                 | 8.55            | 8.55           | 43.79                               | 20.24    |
| BX_26 | H               |  | 42.10±0.63  | 19.21                 | 9.60            | 9.60           | 59.64                               | 43.54    |
| BX_27 | Cl              |  | 58.16±0.72<br>(8.90±0.38)   | 17.37                 | 8.68            | 17.37          | 52.52                               | 38.68    |
| BX_28 | NO <sub>2</sub> |  | 60.80±0.88<br>(7.62±0.59)   | 33.75                 | 33.75           | 33.75          | 56.07                               | 22.69    |
| BX_29 | H               |  | 45.12±1.72  | 33.75                 | 8.43            | 4.21           | 19.19                               | 12.41    |
| BX_30 | Cl              |  | 48.60±0.82  | 30.88                 | 7.72            | 7.72           | 14.23                               | 12.49    |
| BX_31 | NO <sub>2</sub> |  | 51.70±0.84  | 15.04                 | 3.75            | 3.75           | 38.97                               | 14.77    |
|       |                 | <b>Isoniazid</b>  |   | 0.72                  | NT              | NT             | NT                                  | NT       |
|       |                 | <b>Ethambutol</b>   |   | 7.64                  | NT              | NT             | NT                                  | NT       |
|       |                 | <b>Rifampicin</b>   |   | 0.15                  | NT              | NT             | NT                                  | NT       |
|       |                 | <b>Ofloxacin</b>  |   | 2.16                  | NT              | NT             | NT                                  | NT       |

IC<sub>50</sub>, 50% inhibitory concentration; MTB, *Mycobacterium tuberculosis*; MIC, minimum inhibitory concentration; NT, not tested

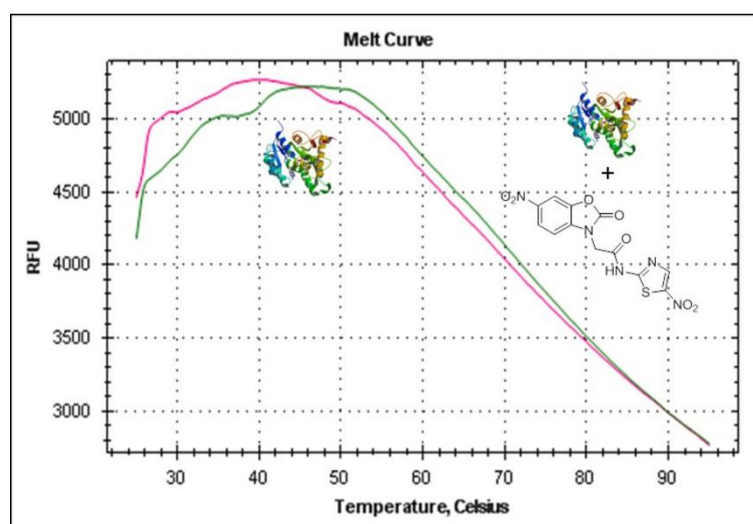
<sup>a</sup>MTB InhA enzyme inhibition activity

<sup>b</sup>*In vitro* activity against MTB H37Rv

<sup>c</sup>Against RAW 264.7 cells

### 5.1.5 Evaluation of protein interaction and stability using biophysical characterization experiment

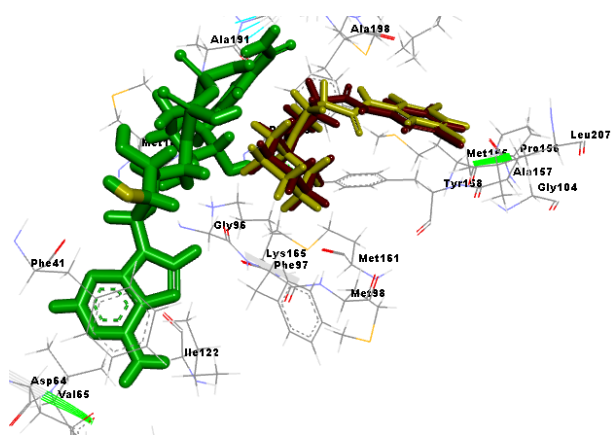
The most potent compound from this series of chemical class of molecules was further investigated using a biophysical technique, differential scanning fluorimetry (DSF). The ability of the compounds to stabilize the catalytic domain of the InhA protein was assessed utilizing the DSF technique by which the thermal stability of the catalytic domain of InhA native protein and of the protein bound with the ligand was measured. Complex with compound **BX\_25** was heated stepwise from 25 to 95 °C in steps of 0.1 °C rise in the presence of a fluorescent dye (sypro orange), whose fluorescence increased as it interacted with hydrophobic residues of the InhA protein. As the protein was denatured, the amino acid residues became exposed to the dye. A right side positive shift of  $T_m$  in comparison to native protein meant higher stabilization of the protein-ligand complex, which was a consequence of the inhibitor binding. In our study, compound **BX\_25** showed significant positive  $T_m$  shift of 1.9 °C confirming the stability of the protein-ligand complex as shown in **Figure 5.4** which depicts the curves obtained in the DSF experiment for the *Mycobacterium tuberculosis* InhA protein (pink) and protein-compound **BX\_25** complex (green).



**Figure 5.4:** DSF experiment for compound **BX\_25** showing an increase in thermal stability between the native InhA protein (pink) and InhA protein-compound **BX\_25** complex (green). Protein  $T_m$  39.90 °C and protein with ligand  $T_m$  41.80 °C.

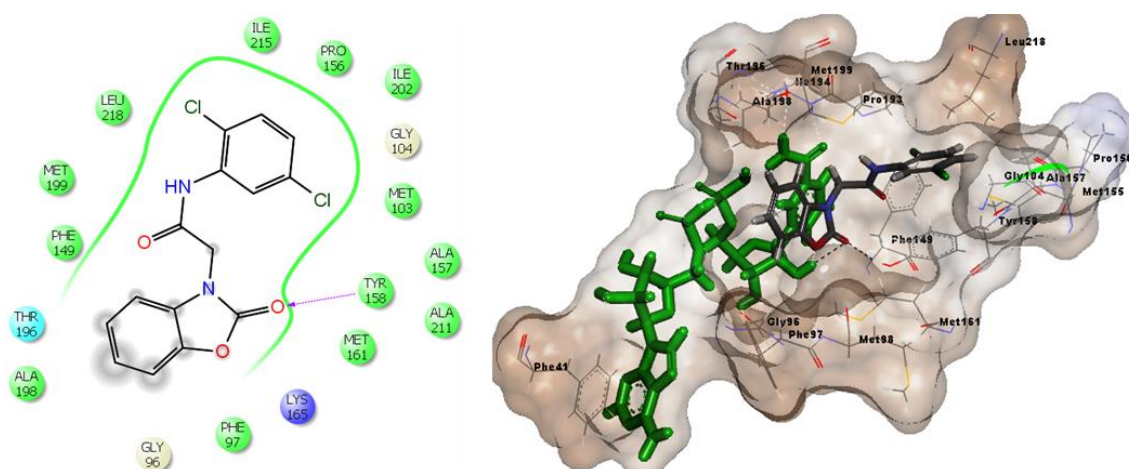
### 5.1.6 Discussion

To study the SAR, we carried out docking studies of all the synthesized compounds together with lead compound **UPS 14** for comparison. The crystal structure of *Mycobacterium tuberculosis* InhA complexed with reference inhibitor 1-cyclohexyl-*N*-(3,5-dichlorophenyl)-5-oxopyrrolidine-3-carboxamide (PDB ID:2H7M) having resolution of 1.62 Å was selected and docking results obtained with Glide, version 5.7, Schrodinger, LLC, New York, NY, 2012. Analysis of the crystal structure of 2H7M revealed that the reference inhibitor in the InhA active site formed hydrogen-bonding network between Tyr158, enzyme active site residues, and the NAD<sup>+</sup> cofactor that probably served as the key feature that governed the orientation of the compound within the active site. Dual hydrogen bonding network was involved with the oxygen atom on the pyrrolidine carbonyl group, InhA catalytic residue Tyr158, and the NAD<sup>+</sup>. This hydrogen bonding network seemed to be a conserved feature among all the InhA-inhibitor complexes identified so far. The reference 1-cyclohexyl-*N*-(3,5-dichlorophenyl)-5-oxopyrrolidine-3-carboxamide was re-docked with the active site residues of the *Mycobacterium tuberculosis* InhA to validate the active site cavity. The ligand exhibited highest Glide score of -8.02 kcal/mol and was found in the vicinity of amino acids Tyr158, Phe149, Met199, Ile215, Pro156, Leu218, Met155, Ala211, Ile202, Met103, Leu207, Ala157, Met161, Phe97, Met98, Gly96, Gly104 and Lys165 residues. Re-docking results showed that the compound exhibited similar interactions as that of the original crystal structure with RMSD of 0.87 Å suggesting reliability of the docking method in terms of. The superimposition of Glide docked conformation of co-crystal with co-crystal of 2H7M is shown in **Figure 5.5**.



**Figure 5.5:** Superimposition of docked pose of the reported reference inhibitor (Yellow) to the original pose of the reference inhibitor (Red).

The binding mode of lead compound **UPS 14** with InhA enzyme was analysed in more detail. The binding orientation of lead compound *N*-(2,5-dichlorophenyl)-2-(2-oxobenzo[*d*]oxazol-3(2*H*)-yl)acetamide (**UPS 14**) within the InhA binding pocket is represented in **Figure 5.6**. The predicted bound conformation of the lead compound **UPS 14** showed that the carbonyl oxygen atom of benzo[*d*]oxazol-2(3*H*)-one ring formed hydrogen bond with the side chain of the Tyr158. The 2,5-dichlorophenyl ring attached to benzo[*d*]oxazol-2(3*H*)-one ring through an acetamide linker was surrounded by hydrophobic amino acids such as Phe149, Met199, Leu218, Ile215, Pro156, Ile202, Met103 and Ala157. The compound was very well fit into the active site cavity of the protein with a docking score of -7.52 kcal/mol.

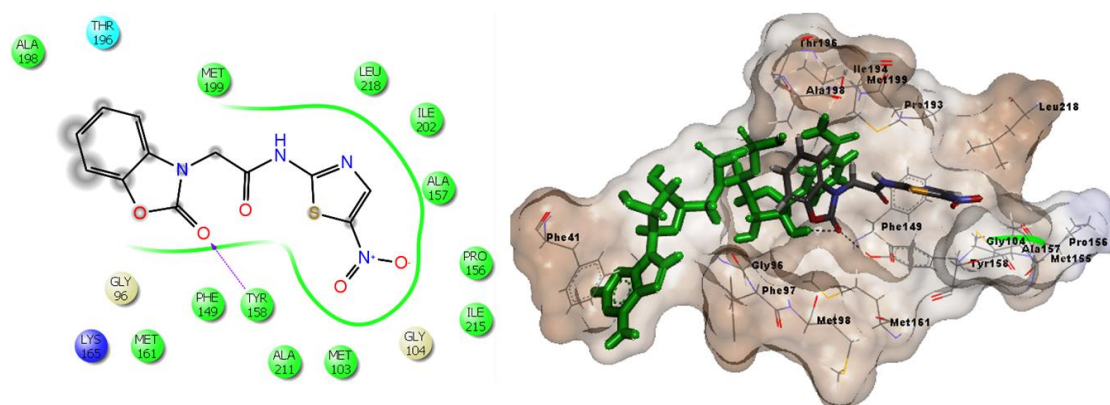


**Figure 5.6:** Binding pose and interaction pattern of lead molecule **UPS 14**.

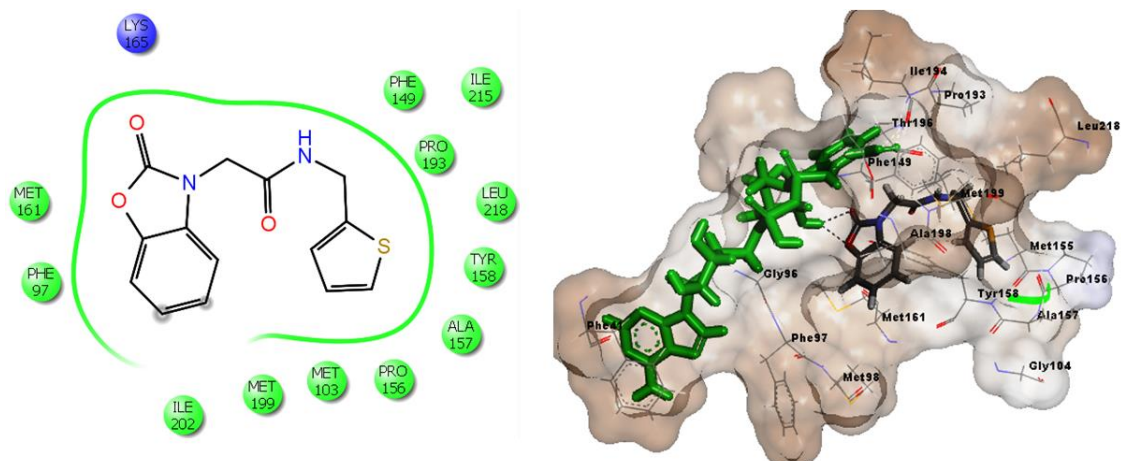
Our SAR studies started from various substituted aryl/heteroaryl ring systems attached to benzo[*d*]oxazol-2(3*H*)-one ring through an acetamide linker. The effect of various aryl/heteroaryl substitutions at the R<sub>2</sub> position was explored. As shown in **Table 5.2**, the activity of most of the compounds exhibited % inhibition in the range of 26.12 to 82.43 % at 10 μM against InhA which was better than the lead compound **UPS 14** (19.5 % at 10 μM).

The first subset of compounds (**BX\_04**, **BX\_07**, **BX\_10**, **BX\_13**, **BX\_16**, **BX\_19**, **BX\_23**, **BX\_26** and **BX\_29**), contained H atom as R<sub>1</sub> substituent while various substituted aryl/heteroaryl groups were at R<sub>2</sub> position as shown in **Table 5.2**. The phenyl group substituent at the R<sub>2</sub> position (compound **BX\_04**) displayed good InhA inhibitory activity. Compound with substitution at 2<sup>nd</sup> and 5<sup>th</sup> position of the phenyl ring (2-chloro-5-(trifluoromethyl)-2-phenyl group) (compound **BX\_07**) displayed moderate InhA inhibitory activity, similar was the introduction of 2-pyridyl group at R<sub>2</sub> position (compound **BX\_10**).

The compounds substituted with 2-pyridylmethyl, 2-benzothiazolyl, 6-nitro-2-benzothiazolyl and 5-nitro-2-thiazolyl group (respective compounds **BX\_13**, **BX\_26**, **BX\_29** and **BX\_23**) at R<sub>2</sub> position resulted in satisfactory *in vitro* InhA inhibitory activity in the range of 42.15 to 48.15 % inhibition at 10  $\mu$ M, whereas substitution with 2-thiophenylmethyl ring (compound **BX\_19**) led to less potency compared to other compounds from this subset. This was well supported by the interaction profile of all the molecules in the docking studies. The docking score of all the compounds from this subset was found to be in the range of -6.87 to -7.59 kcal/mol. All compounds, except compound **BX\_10**, were found to be associated with hydrogen bonding interactions with side chain of Tyr158 and NAD<sup>+</sup>. In most of the compounds the carbonyl oxygen atom on benzo[*d*]oxazol-2(3*H*)-one ring interacted with the side chain of Tyr158. Eventually, SAR from this subset of compounds revealed compound **BX\_23** as most selective inhibitor of InhA and compound **BX\_19** to be comparatively least active. The bound conformation of compound **BX\_23** showed carbonyl oxygen atom of benzo[*d*]oxazol-2(3*H*)-one ring forming hydrogen bond with the side chain of Tyr158 and ribose hydroxyl group of NAD<sup>+</sup>, which was also observed in the crystal ligand and also well correlated with the *in vitro* InhA inhibitory activity. 5-Nitro-2-thiazolyl ring was buried in the hydrophobic cavity surrounded by Met199, Leu218, Ile202, Ala157, Pro156, Ile215, Met103, Ile215, Met103, Ala211 and Phe149 (**Figure 5.7**). The binding analysis of compound **BX\_19** in the active site of protein revealed that the compound failed to produce any hydrogen bonding interaction with the side chain of Tyr158 residue of the protein and thus the inactivity of the compound could be related (**Figure 5.8**).



**Figure 5.7:** Binding pose and its interaction pattern of the compound **BX\_23**.

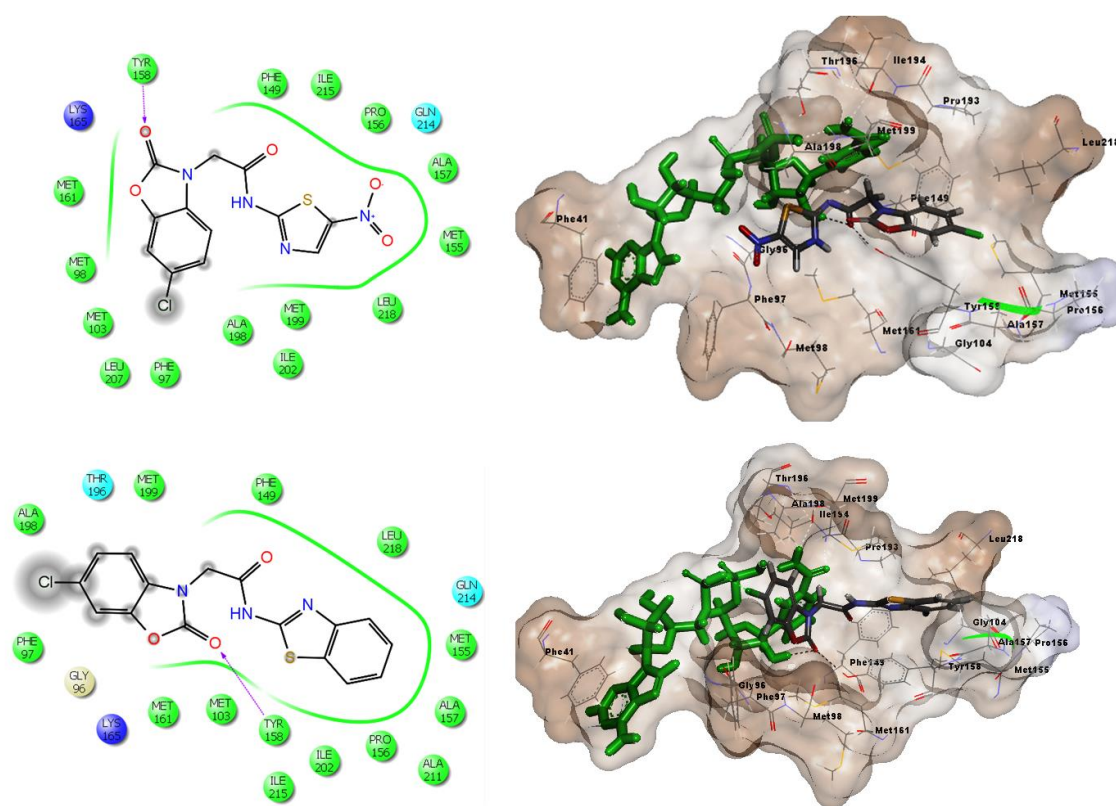


**Figure 5.8:** Binding pose and its interaction pattern of the compound **BX\_19**.

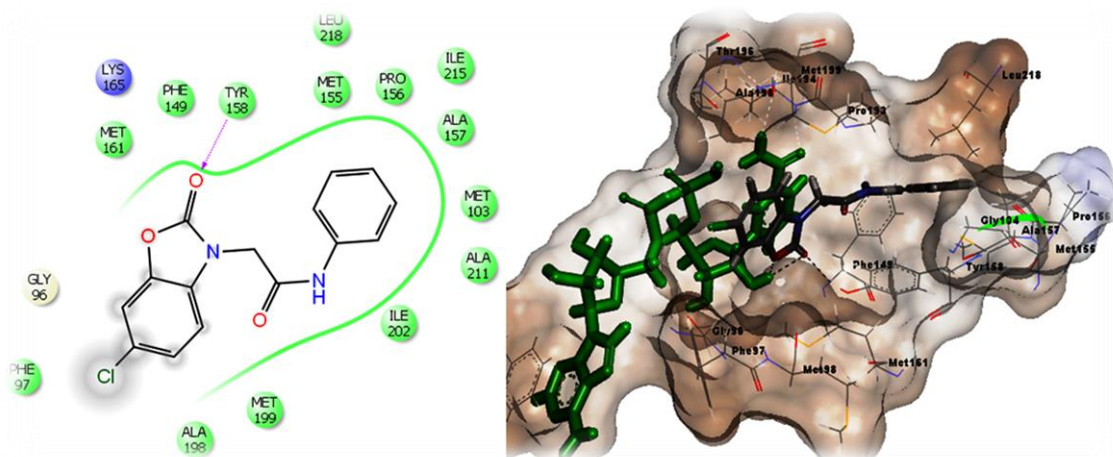
In the second subset of compounds (**BX\_05**, **BX\_08**, **BX\_11**, **BX\_14**, **BX\_17**, **BX\_20**, **BX\_24**, **BX\_27** and **BX\_30**), the effect of chloro substitution on the benzo[*d*]oxazol-2(3*H*)-one ring at R<sub>1</sub> position was investigated to understand the effect of same aryl/heteroaryl substituent's at R<sub>2</sub> position. SAR study revealed that, hydrophobic chloro group at R<sub>1</sub> position increased hydrophobicity of the compounds due to hydrophobic interactions with the active site which was crucial for inhibition. This subset of compounds displayed more inhibitory potency than the previous subset. Here, all the compounds showed satisfactory *in vitro* InhA inhibitory activity in the range of 28.16 to 72.60 % inhibition at 10  $\mu$ M concentrations. The compounds **BX\_08**, **BX\_11** and **BX\_30** with 2-chloro-5-(trifluoromethyl)-2-phenyl, 2-pyridyl and 6-nitro-2-benzothiazoyl groups respectively as R<sub>2</sub> substituents, showed good InhA inhibitory activity, whereas compound **BX\_24** with 5-nitro-2-thiazolyl group as R<sub>2</sub> substituent was more active than compound **BX\_27** with 2-benzothiazolyl group as R<sub>2</sub> substituent. It was observed that phenyl substitution at R<sub>2</sub> (**BX\_05**) was somewhat less favoured than the other substitutions at the R<sub>2</sub> position. Additionally, 2-furylmethyl ring, 2-pyridylmethyl and 2-thiophenylmethyl ring substitutions at R<sub>2</sub> position (respective compounds **BX\_17**, **BX\_14** and **BX\_20**) also showed good activity in InhA enzyme inhibition studies. In this subset, compounds **BX\_24** and **BX\_27** were demonstrated to be effective InhA inhibitors with good activity. Both the compounds displayed docking scores of -7.12 and -7.073 kcal/mol respectively. The predicted binding pose of the most active compounds (**BX\_24** and **BX\_27**) suggested that the observed potency may be due to the extensive hydrophobic interactions predicted to be formed with the side chains of Met199, Leu218, Met155, Pro156, Ala157, Ile202, Met103, Phe149 and Met161 along with hydrogen bonding interactions with side chain of Tyr158 as well as with the



ribose hydroxyl group of NAD<sup>+</sup> correlating with the protein-inhibitor complex interactions outlined in InhA crystal structure (**Figure 5.9**). Ligand binding analysis of one of the less active derivative from this subset (**BX\_05**) showed hydrophobic interactions between the phenyl ring and amino acid residues Met199, Leu218, Met155, Pro156, Ala157, Ile202, Met103, Phe149 and Met161. It also displayed hydrogen bonding interaction between carbonyl oxygen atom of 6-chlorobenzo[*d*]oxazol-2(3*H*)-one ring and side chain of Tyr158 amino acid residue. However, the orientation in the active site cavity of InhA pushed the chloro group away from the cavity, which could explain its less enzyme inhibition activity (**Figure 5.10**).

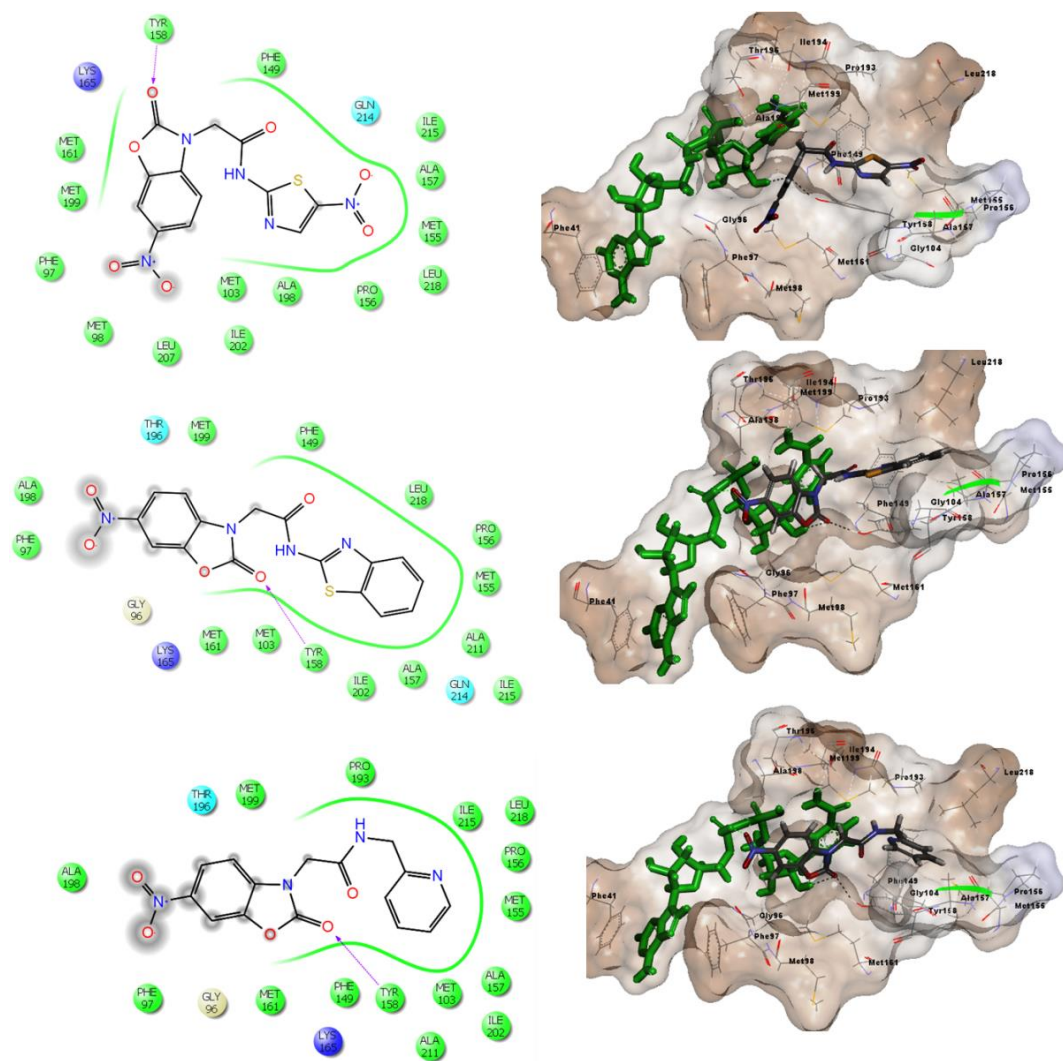


**Figure 5.9:** Binding pose and its interaction pattern of the compound **BX\_24** and **BX\_27**.

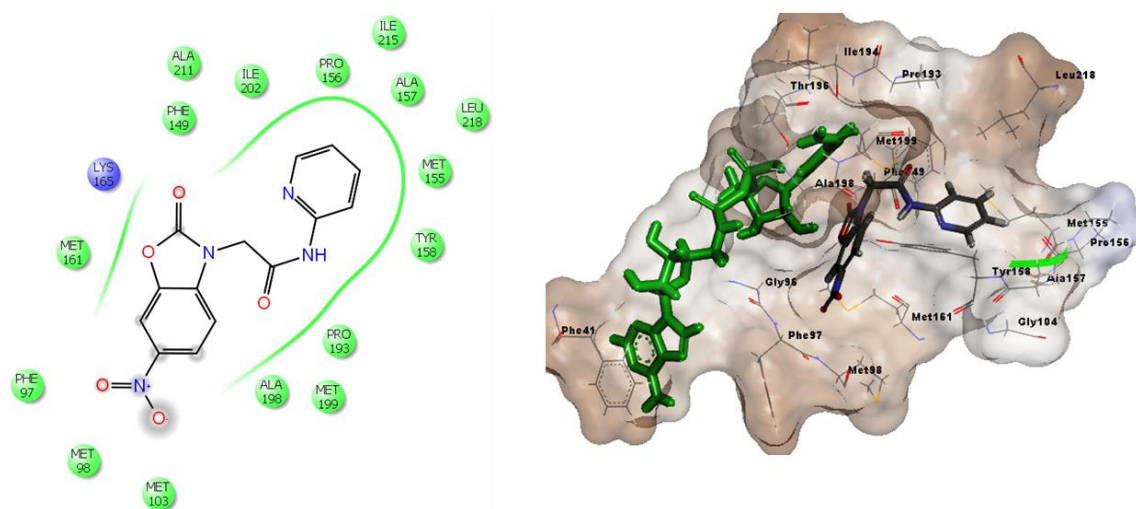


**Figure 5.10:** Binding pose and its interaction pattern of the compound **BX\_05**.

In the third subset of compounds (**BX\_06**, **BX\_09**, **BX\_12**, **BX\_15**, **BX\_18**, **BX\_21**, **BX\_25**, **BX\_28** and **BX\_31**), R<sub>1</sub> consisted of nitro group and R<sub>2</sub> was substituted with various aryl/heteroaryl groups same as previous two subsets as shown in **Table 5.2**. The compounds **BX\_25**, **BX\_28** and **BX\_15** with 5-nitro-2-thiazolyl, 2-benzothiazolyl and 2-pyridylmethyl substitution at R<sub>2</sub> respectively, emerged as most active compounds from this subset showing satisfactory *in vitro* InhA inhibitory activity in the range of 60.80 to 82.43 % inhibition at 10  $\mu$ M with IC<sub>50</sub> of 5.12 to 8.23  $\mu$ M. This was well supported by their interaction profile in docking studies where docking score of these compounds were found in the range of -7.11 to -7.48 kcal/mol. Closer analysis of compounds **BX\_25**, **BX\_28** and **BX\_15** in the binding site revealed that the carbonyl oxygen atom on 6-nitrobenzo[*d*]oxazol-2(3*H*)-one ring was involved in hydrogen bonding interactions with side chain of Tyr158 residue as well as with ribose hydroxyl group of NAD<sup>+</sup>. All these three compounds were buried in the well-defined hydrophobic pocket and made extensive hydrophobic interactions with the Phe149, Leu218, Met155, Pro156, Ala157, Ile215, Met199 and Met103 (**Figure 5.11**). In this subset of compounds, 2-pyridyl at R<sub>2</sub> position (**BX\_12**) showed least activity in the whole series with 15.63 % inhibition at 10  $\mu$ M concentration. *In silico* analysis of this compound indicated that the molecule was oriented in a different manner than that of other active derivatives and failed to demonstrate any interaction with Tyr158 residue as well as with NAD<sup>+</sup> resulting in less enzyme inhibition potency (**Figure 5.12**).



**Figure 5.11:** Binding pose and its interaction pattern of the compound **BX\_25**, **BX\_28** and **BX\_15**.



**Figure 5.12:** Binding pose and its interaction pattern of the compound **BX\_12**.

From the docking results, it was evident that the formation of hydrogen bonds with side chain of Tyr158 and hydroxyl group of NAD<sup>+</sup> along with hydrophobic interactions with the active site were predicted to be the most crucial factors affecting the inhibitory potency of these compounds. The overall trend in enzyme inhibition activity showed that substitution at R<sub>1</sub> position with nitro group was more favoured than chloro group whereas H substitution was least favoured. In case of R<sub>2</sub> position, substitutions with heteroaryl groups such as 5-nitro-2-thiazolyl, 2-benzothiazolyl, 6-nitro-2-benzothiazolyl, 2-methylpyridyl, 2-furylmethyl and 2-thiophenylmethyl group were more favoured than with 2-chloro-5-(trifluoromethyl)-2-phenyl, phenyl and 2-pyridyl group.

In case of antimycobacterial activity, all the synthesized compounds exhibited MIC ranging from 15.04 to 82.58  $\mu$ M. Six compounds (**BX\_21**, **BX\_24** - **BX\_27** and **BX\_31**) inhibited *Mycobacterium tuberculosis* with MIC of <20  $\mu$ M. Compound **BX\_25** which showed IC<sub>50</sub> of 5.12 $\pm$ 0.44  $\mu$ M in the *Mycobacterium tuberculosis* InhA enzyme also exhibited *Mycobacterium tuberculosis* MIC of 17.11  $\mu$ M. In general, compounds which possessed (sub)-thiazolyl and -benzothiazolyl showed good MICs. Some of the molecules showed good potency in the enzyme inhibition study but failed to exhibit equally potent inhibition of *Mycobacterium tuberculosis*, and this seem to be a major challenge in the arena of TB drug discovery. Among other parameters, efflux mechanism contributes in a major way to intrinsic resistance to drugs. In the current work, we also carried out *Mycobacterium tuberculosis* screening of the synthesized compounds in the presence of reported efflux pump inhibitors verapamil (50  $\mu$ g/mL) and piperine (8  $\mu$ g/mL). In most of the cases MIC decreased 2 to 10 fold when compared to the absence of an efflux pump inhibitor. Compound **BX\_25** showed *Mycobacterium tuberculosis* MIC of 8.55  $\mu$ M in the presence of verapamil and piperine, and its *Mycobacterium tuberculosis* InhA IC<sub>50</sub> was very well correlated as shown in **Table 5.2**.

The safety profile of all of the compounds was also assessed by testing their *in vitro* cytotoxicity against RAW 264.7 cells at 100 and 50  $\mu$ M concentrations using the MTT assay as described in the materials and methods section. Most of the tested compounds were not cytotoxic (less than 50% inhibition at 50  $\mu$ M) to RAW 264.7 cells and their percentage growth inhibitions are reported in **Table 5.2**. The most active *Mycobacterium tuberculosis* InhA inhibitor (**BX\_25**) showed lesser toxicity of 20.24 and 43.79 % inhibition at 50 and 100  $\mu$ M drug concentrations respectively.

All the synthesized derivatives were further evaluated for their predicted ADMET properties using the QikProp3.5 module of Schrodinger software. Although most of the compounds from this series showed drug-like characteristics (as shown in **Table 5.3**), the most active compound **BX\_25** showed poor membrane permeability with QPPCaco and QPPMDCK value of 9.36 and 4.83 respectively. All compounds were predicted to adhere to Lipinski rule of five presenting their candidature for further optimization against *Mycobacterium tuberculosis* InhA from pharmaceutical point of view.

**Table 5.3:** QikProp analysis of the ADMET properties of the synthesized derivatives **BX\_04** – **BX\_21** and **BX\_23** – **BX\_31**.

| Comp         | QLogPo/w <sup>a</sup> | QLogHERG <sup>b</sup> | QPPCaco <sup>c</sup> | QLogBB <sup>d</sup> | QPPMDCK <sup>e</sup> | Percent Human Oral Absorption <sup>f</sup> | Rule of Five <sup>g</sup> |
|--------------|-----------------------|-----------------------|----------------------|---------------------|----------------------|--|---------------------------|
| <b>BX_04</b> | -1.09                 | -2.15                 | 6726.93              | 0.44                | 3882.59              | 89.05                                      | 0                         |
| <b>BX_05</b> | 2.71                  | -5.69                 | 1196.47              | -0.35               | 1480.53              | 100  | 0                         |
| <b>BX_06</b> | 1.62                  | -5.69                 | 142.97               | -1.52               | 60.43                | 74.98                                      | 0                         |
| <b>BX_07</b> | 0.74                  | -5.13                 | 3750.16              | 0.55                | 10000                | 95.27                                      | 0                         |
| <b>BX_08</b> | 4.07                  | -5.43                 | 1309.56              | 0.07                | 10000                | 100  | 0                         |
| <b>BX_09</b> | 2.86                  | -5.42                 | 156.6                | -1.13               | 570.49               | 82.98                                      | 0                         |
| <b>BX_10</b> | 1.49                  | -5.43                 | 681.1                | -0.72               | 326.64               | 86.39                                      | 0                         |
| <b>BX_11</b> | -1.09                 | -1.89                 | 6726.74              | 0.58                | 8021.68              | 89.09                                      | 0                         |
| <b>BX_12</b> | -3.91                 | -2.03                 | 1223.49              | -0.12               | 615.23               | 59.29                                      | 0                         |
| <b>BX_13</b> | 1.3                   | -4.26                 | 678.18               | -0.71               | 431.53               | 85.24                                      | 0                         |
| <b>BX_14</b> | -0.92                 | -3.02                 | 2994.76              | 0.26                | 3344.93              | 83.77                                      | 0                         |
| <b>BX_15</b> | -3.75                 | -3.12                 | 544.71               | -0.53               | 256.55               | 53.97                                      | 0                         |
| <b>BX_16</b> | -2.09                 | -2.69                 | 3828.07              | 0.23                | 2110.97              | 78.82                                      | 0                         |
| <b>BX_17</b> | 1.73                  | -4.13                 | 656                  | -0.49               | 1250.86              | 87.51                                      | 0                         |
| <b>BX_18</b> | 0.54                  | -3.89                 | 91.99                | -1.57               | 56.63                | 65.25                                      | 0                         |
| <b>BX_19</b> | -0.95                 | -2.78                 | 3787.22              | 0.29                | 3042.9               | 85.4                                       | 0                         |
| <b>BX_20</b> | 2.36                  | -4.08                 | 728.04               | -0.33               | 2585.9               | 91.96                                      | 0                         |
| <b>BX_21</b> | 1.05                  | -3.74                 | 95.06                | -1.45               | 106.12               | 68.49                                      | 0                         |
| <b>BX_23</b> | -3.91                 | -1.41                 | 2612.75              | 0.22                | 1896.68              | 65.19                                      | 0                         |
| <b>BX_24</b> | 1.53                  | -4.97                 | 78.3                 | -1.57               | 118.2                | 69.79                                      | 0                         |
| <b>BX_25</b> | 0.27                  | -4.99                 | 9.36                 | -2.75               | 4.83                 | 32.93                                      | 0                         |
| <b>BX_26</b> | 2.14                  | -5.94                 | 676.81               | -0.7                | 519.64               | 90.16                                      | 0                         |
| <b>BX_27</b> | -0.77                 | -2.04                 | 6692.35              | 0.6                 | 8955.81              | 90.93                                      | 0                         |
| <b>BX_28</b> | -3.59                 | -2.18                 | 1217.2               | -0.11               | 686.85               | 61.13                                      | 0                         |
| <b>BX_29</b> | -3.61                 | -2.24                 | 1241.36              | -0.11               | 701.59               | 61.19                                      | 0                         |

Contd...

| Comp         | QLogPo/w <sup>a</sup> | QLogHERG <sup>b</sup> | QPPCaco <sup>c</sup> | QLogBB <sup>d</sup> | QPPMDCK <sup>e</sup> | Percent Human Oral Absorption <sup>f</sup> | Rule of Five <sup>g</sup> |
|--------------|-----------------------|-----------------------|----------------------|---------------------|----------------------|--|---------------------------|
| <b>BX_30</b> | 1.91                  | -5.8                  | 80.94                | -1.63               | 128.88               | 72.3                                       | 0                         |
| <b>BX_31</b> | 0.7                   | -5.8                  | 9.67                 | -2.87               | 5.26                 | 35.73                                      | 0                         |

<sup>a</sup>Predicted octanol/water partition coefficient logP (acceptable range: -2.0 to 6.5)

<sup>b</sup>Predicted IC<sub>50</sub> value for blockage of hERG K<sup>+</sup> channels.(below -5)

<sup>c</sup>Predicted apparent Caco-2 cell permeability in nm/sec (<25 poor; >500 great)

<sup>d</sup>Predicted brain/blood partition coefficient (-3.0 to 1.2)

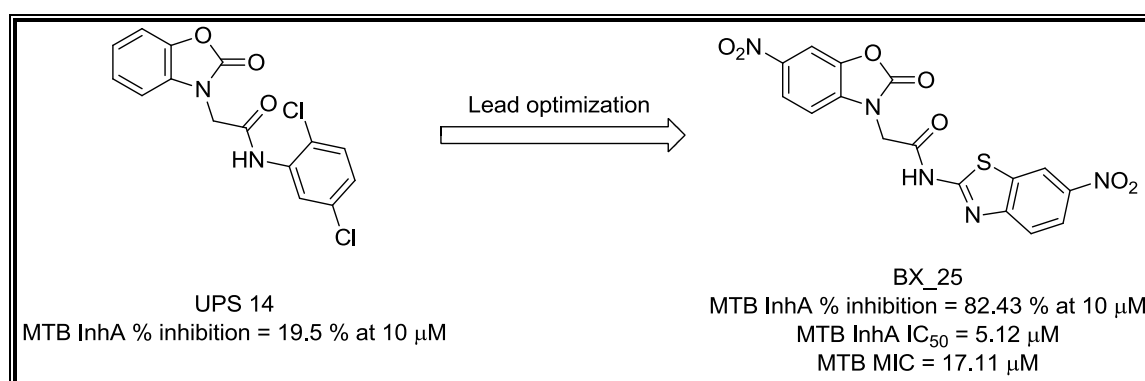
<sup>e</sup>Predicted apparent MDCK cell (model for blood-brain barrier) permeability in nm/s. (< 25 poor, > 500 great)

<sup>f</sup>Percent human oral absorption (< 25% is poor and > 80% is high)

<sup>g</sup>Rule of 5 violation (mol\_MW < 500, QLogPo/w < 5, donorHB ≤ 5, acptHB ≤ 10) (concern above 1)

### 5.1.7 Highlights of the study

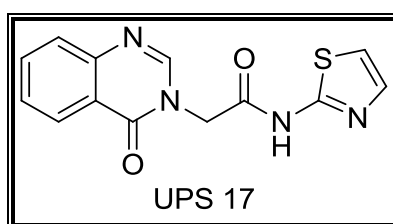
In present work, we report synthesis and screening results of twenty seven substituted 2-(2-oxobenzodioxazol-3(2H)-yl)acetamide derivatives against *Mycobacterium tuberculosis* InhA as well as drug sensitive *Mycobacterium tuberculosis* strains. Most of the synthesized compounds showed better InhA inhibition as compared to lead molecules, and **BX\_25** (2-(6-nitro-2-oxobenzodioxazol-3(2H)-yl)-N-(5-nitrothiazol-2-yl)acetamide) was found to be the most active compound with IC<sub>50</sub> of 5.12 μM against *Mycobacterium tuberculosis* InhA, inhibited drug sensitive *Mycobacterium tuberculosis* with MIC of 17.11 μM and was non-cytotoxic at 100 μM (**Figure 5.13**). The interaction with protein and enhancement of protein stability in complex with most active compound **BX\_25** was further confirmed biophysically using DSF.



**Figure 5.13:** Chemical structure and biological activity of the most active compound **BX\_25**.

## 5.2 Development of 2-(4-oxoquinazolin-3(4H)-yl)acetamide derivatives as potential *Mycobacterium tuberculosis* InhA inhibitors

The quest for more potent molecules encouraged us to utilize lead molecule 2-(4-oxoquinazolin-3(4H)-yl)-*N*-(thiazol-2-yl)acetamide (**UPS 17**) (**Figure 5.14**) as a structural framework to construct a library for developing a strong structure-activity relationship (SAR) profile and also to understand the ideal site for introducing chemical diversity. Thus, a library of 28 molecules utilizing this lead as a template were designed using a combination of molecular docking and medicinal chemistry strategies, and is depicted in **Table 5.4**. Based on the input from protein-ligand interactions observed on docking of lead molecule **UPS 17**, the quinazolin-4(3H)-one core was decided to be retained in the initial SAR explorations. However, the introduction of chloro group at 6<sup>th</sup> position and a methyl tail at 2<sup>nd</sup> position of the quinazolin-4(3H)-one core, were found to be favourable in improving the interaction with the active site residues, and hence were attempted in synthesis. Various aryl and heteroaryl substituents (as shown in **Table 5.4**) were also attempted as the right hand core in the hit expansion step to introduce structural diversification.



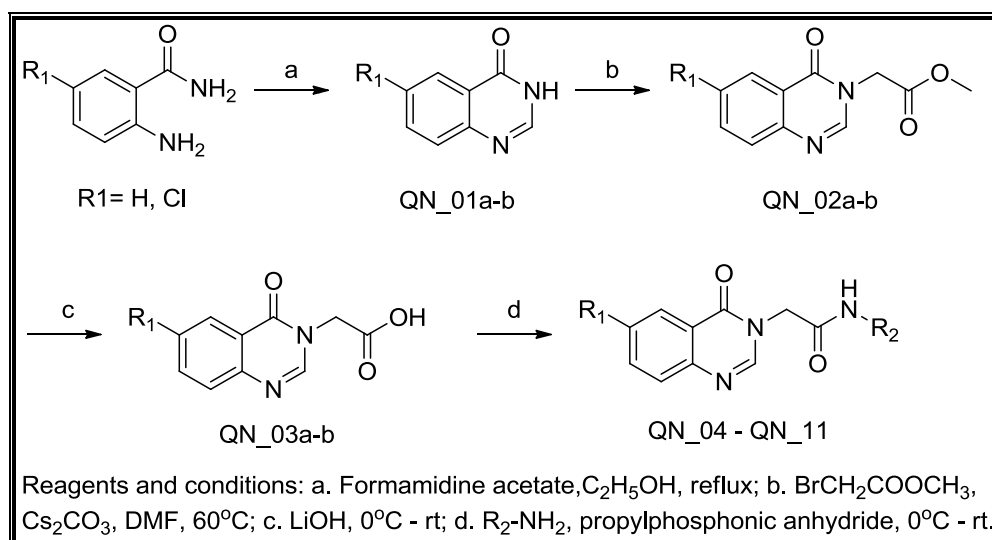
**Figure 5.14:** Chemical structure of lead molecule **UPS 17**.

### 5.2.1 Chemical synthesis and characterization

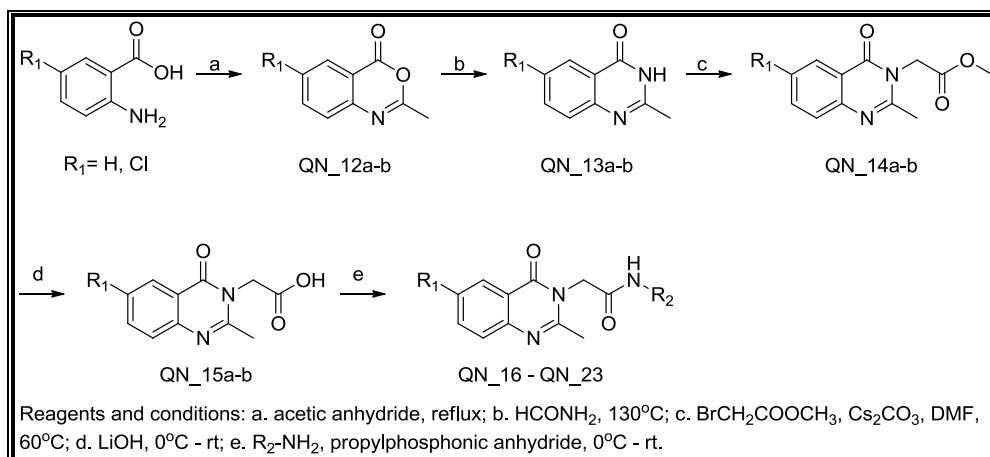
The target molecules were achieved by using a simple and straight forward strategy as depicted in **Figure 5.15** and **5.16**. Construction of the target molecule began by condensing commercially available and relatively cheap anthranilamide with formamidine acetate in refluxing ethanol as similarly reported by Li F. *et al.* [Li F. *et al.*, 2007]. Though the condensation reaction of unsubstituted and 5-chloro-substituted anthranilamide with formamidine acetate went smoothly yielding the desired quinazolin-4(3H)-one in very good yield, our initial effort to introduce a methyl tail at the 2<sup>nd</sup> position of the quinazolin-4(3H)-one core by condensing the appropriate anthranilamide with acetamidine hydrochloride gave the required product in very low yield. Hence, an alternate strategy by condensing



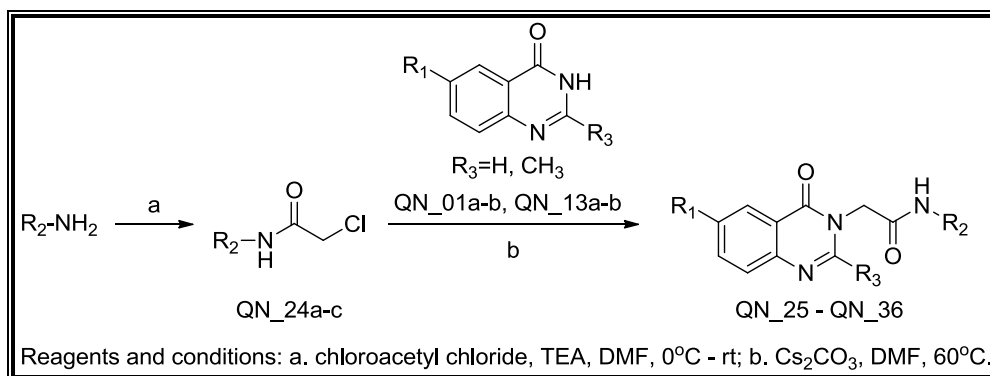
corresponding anthranilic acid with acetic anhydride followed by dehydration with formamide as previously demonstrated by Ning *et al.* [Ning W. *et al.*, 2013] was followed to achieve the desired 2-methylquinazolin-4(3*H*)-one in very good yield. Acetic acid linker was then introduced to the quinazolin-4(3*H*)-one core by alkylation with methyl bromoacetate followed by subsequent hydrolysis with lithium hydroxide. The final library was then assembled by coupling the so formed acid with various substituted amines to give the target compounds. Though the reaction progressed smoothly for aromatic amines in good yield, a similar conversion was not observed in the case of heterocyclic amines especially with 2-amino-5-nitrothiazole, 2-aminobenzothiazole and 2-amino-6-nitrobenzothiazole, probably due to their low nucleophilicity and solubility issues. Hence, an alternative strategy was designed as depicted in **Figure 5.17**, wherein the corresponding amine was first treated with chloroacetyl chloride in presence of TEA as base to give the corresponding 2-chloro-*N*-(aryl/heteroaryl)acetamide. The so formed 2-chloro-*N*-(aryl/heteroaryl)acetamide was then introduced into the desired quinazolin-4(3*H*)-one unit by alkylation using cesium carbonate ( $\text{Cs}_2\text{CO}_3$ ) as base at 60 °C.



**Figure 5.15:** Synthetic protocol utilized for synthesis of compounds **QN\_04 – QN\_11**.



**Figure 5.16:** Synthetic protocol utilized for synthesis of compounds **QN\_16 – QN\_23**.



**Figure 5.17:** Synthetic protocol utilized for synthesis of compounds **QN\_25 – QN\_36**.

## 5.2.2 Experimental protocol utilised for synthesis

### Procedure for the synthesis of quinazolin-4(3*H*)-ones (**QN\_01a-b**)

To a refluxing solution of corresponding anthranilamide (1 mmol) in ethanol (30 mL) was added formamidine acetate (2 mmol). The solution was refluxed for about 6 h (monitored by TLC & LCMS for completion), and solvent evaporated under reduced pressure. The residue was further diluted with water (30 mL) and ethyl acetate (50 mL) and the layers separated. The organic layer was dried over anhydrous sodium sulphate and evaporated under reduced pressure. The residue was purified by silica gel column chromatography using hexane: ethyl acetate as eluent to give the corresponding quinazolin-4(3*H*)-one (**QN\_01a-b**) in good yield.

### **Procedure for the synthesis of methyl 2-(4-oxoquinazolin-3(4*H*)-yl)acetates (QN\_02a-b)**

To a stirred mixture of corresponding quinazolin-4(3*H*)-one (QN\_01a-b) (1 mmol) and methyl bromoacetate (1.2 mmol) in DMF (15 mL) was added anhydrous cesium carbonate (1.5 mmol) at rt. The mixture was heated at 60 °C for about 3 h (monitored by TLC & LCMS for completion). The reaction mixture was filtered through celite and concentrated under reduced pressure. The residue was partitioned between ethyl acetate (20 mL) and water (15 mL), and the organic layer dried over anhydrous sodium sulphate, and concentrated under reduced pressure. The crude product was purified by silica gel column chromatography using hexane: ethyl acetate as eluent to give the corresponding methyl 2-(4-oxoquinazolin-3(4*H*)-yl)acetate (QN\_02a-b).

### **Procedure for the synthesis of 2-(4-oxoquinazolin-3(4*H*)-yl)acetic acids (QN\_03a-b)**

To a stirred mixture of corresponding methyl 2-(4-oxoquinazolin-3(4*H*)-yl)acetate (QN\_02a-b) (1 mmol) in THF (6 mL) at rt was added dropwise lithium hydroxide (2 mmol) dissolved in water (2 mL). The reaction mixture was slowly warmed to rt and stirred for 3 h (monitored by TLC & LCMS for completion), and solvent evaporated under reduced pressure. The residue was diluted with water (10 mL) and ethyl acetate (10 mL), and the layers separated. The aqueous layer was acidified with 2 N hydrochloric acid and further extracted with DCM (10 mL). The organic layer was dried over anhydrous sodium sulphate and evaporated under reduced pressure. The crude product was further purified by silica gel column chromatography using hexane: ethyl acetate as eluent to give the corresponding 2-(4-oxoquinazolin-3(4*H*)-yl)acetic acid (QN\_03a-b).

### **Procedure for the synthesis of substituted 2-(4-oxoquinazolin-3(4*H*)-yl)acetamides (QN\_04 – QN\_11)**

To a solution of corresponding amine (1.1 mmol) in dry DCM (4 mL) was added TEA (2 mmol) and corresponding 2-(4-oxoquinazolin-3(4*H*)-yl)acetic acid (QN\_03a-b) (1 mmol) at 0 °C. Propylphosphonic anhydride solution (T3P) (≥50 wt. % in ethyl acetate; 2 mmol) was then added dropwise to the reaction mixture and was stirred at rt for 6 h (monitored by TLC & LCMS for completion). The reaction mixture was then washed with water (4 mL), brine (4 mL). The organic layer was dried over anhydrous sodium sulphate and evaporated under reduced pressure. The crude product was further purified by silica gel column

chromatography using hexane: ethyl acetate as eluent to give the corresponding 2-(4-oxoquinazolin-3(4*H*)-yl)acetamides (QN\_04 – QN\_11).

**Procedure for the synthesis of 2-methyl-4*H*-benzo[*d*][1,3]oxazin-4-ones (QN\_12a-b)**

A solution of corresponding anthranilic acid (1 mmol) in acetic anhydride (15 mL) was heated to reflux for 1 h (monitored by TLC & LCMS for completion), quenched with ice and concentrated under reduced pressure. The residue was partitioned between ethyl acetate (20 mL) and water (20 mL), and organic layer was dried over anhydrous sodium sulphate, filtered, and concentrated under reduced pressure. The crude product was purified by silica gel column chromatography using hexane: ethyl acetate as eluent to give the corresponding 2-methyl-4*H*-benzo[*d*][1,3]oxazin-4-one (QN\_12a-b).

**Procedure for the synthesis of 2-methylquinazolin-4(3*H*)-ones (QN\_13a-b)**

A solution of corresponding 2-methyl-4*H*-benzo[*d*][1,3]oxazin-4-one (QN\_12a-b) (1 mmol) in formamide (15 mL) was heated to 130 °C for 7 h (monitored by TLC & LCMS for completion). Upon cooling, the mixture got solidified, which was further washed with water, and recrystallized from ethanol to give 2-methylquinazolin-4(3*H*)-one (QN\_13a-b).

**Procedure for the synthesis of methyl 2-(2-methyl-4-oxoquinazolin-3(4*H*)-yl)acetates (QN\_14a-b)**

To a stirred mixture of corresponding 2-methylquinazolin-4(3*H*)-ones (QN\_13a-b) (1 mmol) and methyl bromoacetate (1.2 mmol) in DMF (15 mL) at rt was added cesium carbonate (1.5 mmol). The mixture was heated to 60 °C for about 3h (monitored by TLC & LCMS for completion). The reaction mixture was filtered through celite and concentrated under reduced pressure. The residue was partitioned between ethyl acetate (20 mL) and water (15 mL) and the organic layer dried over anhydrous sodium sulphate, filtered, and concentrated under reduced pressure. The crude product was purified by silica gel column chromatography using hexane: ethyl acetate as eluent to give the corresponding methyl 2-(2-methyl-4-oxoquinazolin-3(4*H*)-yl)acetate (QN\_14a-b).

**Procedure for the synthesis of 2-(2-methyl-4-oxoquinazolin-3(4*H*)-yl)acetic acids (QN\_15a-b)**

To a stirred solution of corresponding methyl 2-(2-methyl-4-oxoquinazolin-3(4*H*)-yl)acetate (QN\_14a-b) (1 mmol) in THF (6 mL) at rt was added dropwise lithium hydroxide (2 mmol) dissolved in water (2 mL). The reaction mixture was stirred at rt for 3 h (monitored by TLC & LCMS for completion), and solvent evaporated under reduced pressure. The residue was diluted with water (10 mL) and ethyl acetate (10 mL) and the layers separated. The aqueous layer was acidified with 2 N hydrochloric acid and further extracted with DCM (10 mL). The organic layer was dried over anhydrous sodium sulphate and evaporated under reduced pressure. The crude product was further purified by silica gel column chromatography using hexane: ethyl acetate as eluent to give the corresponding 2-(2-methyl-4-oxoquinazolin-3(4*H*)-yl)acetic acid (QN\_15a-b).

**Procedure for the synthesis of substituted 2-(2-methyl-4-oxoquinazolin-3(4*H*)-yl)acetamides (QN\_16 – QN\_23)**

To a solution of corresponding amine (1.1 mmol) in dry DCM (4 mL) was added TEA (2 mmol) and corresponding 2-(2-methyl-4-oxoquinazolin-3(4*H*)-yl)acetic acid (QN\_15a-b) (1 mmol) at 0 °C. Propylphosphonic anhydride solution (T3P) ( $\geq 50$  wt. % in ethyl acetate; 2 mmol) was then added dropwise at 0 °C, and the reaction mixture was slowly warmed to rt and stirred for 6 h (monitored by TLC & LCMS for completion). The reaction mixture was then washed with water (4 mL) and brine (4 mL). The organic layer was dried over anhydrous sodium sulphate and evaporated under reduced pressure. The crude product was further purified by silica gel column chromatography using hexane: ethyl acetate as eluent to give the corresponding 2-(2-methyl-4-oxoquinazolin-3(4*H*)-yl)acetamides (QN\_16 - QN\_23).

**Procedure for the synthesis of 2-chloro-*N*-(aryl/heteroaryl)acetamides (QN\_24a-c)**

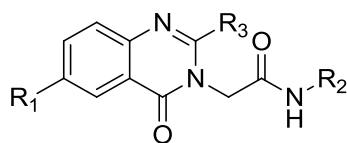
Chloroacetyl chloride (2 mmol) was added dropwise to a well stirred suspension of corresponding amine (1 mmol) and TEA (3 mmol) in DMF (15 mL) at 0 °C. The reaction mixture was then stirred at rt for about 3 h (monitored by TLC & LCMS for completion), and the solvent evaporated under reduced pressure. The residue was further diluted with water (20 mL) and ethyl acetate (30 mL), and the layers separated. The aqueous layer was re-extracted with ethyl acetate (2×30 mL) and the combined organic layer was washed with brine (20

mL), dried over anhydrous sodium sulphate and evaporated under reduced pressure. The residue was purified by silica column chromatography using hexane: ethyl acetate as eluent to give corresponding 2-chloro-*N*-(aryl/heteroaryl)acetamides (**QN\_24a-c**).

**Procedure for the synthesis of substituted 2-(4-oxoquinazolin-3(4*H*)-yl)acetamides (QN\_25 – QN\_36)**

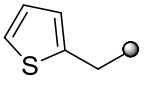
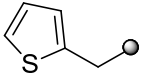
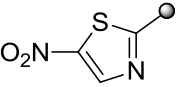
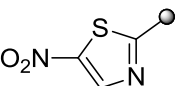
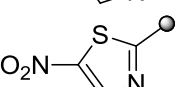
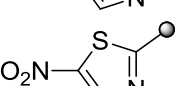
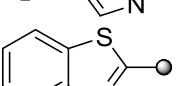
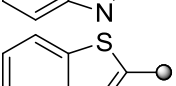
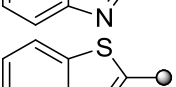
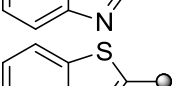
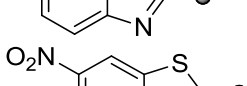
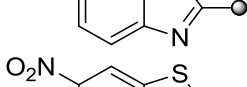
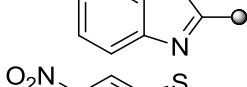
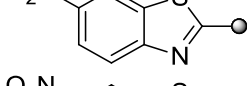
To a solution of corresponding 2-chloro-*N*-(aryl/heteroaryl)acetamides (**28a-c**) (1.2 mmol) in DMF (3 mL) was added anhydrous cesium carbonate (2 mmol) and corresponding quinazolin-4(3*H*)-one (**QN\_01a-b**, **QN\_13a-b**) (1 mmol). The reaction mixture was heated at 60 °C for 3 h (monitored by TLC & LCMS for completion). The residue was further diluted with water (10 mL) and ethyl acetate (20 mL) and the layers separated. The aqueous layer was re-extracted with ethyl acetate (2 x 15 mL) and the combined organic layer was washed with brine (15 mL), dried over anhydrous sodium sulphate and evaporated under reduced pressure and the residue was purified by silica column chromatography using hexane: ethyl acetate as eluent to give the desired substituted 2-(4-oxoquinazolin-3(4*H*)-yl)acetamides (**QN\_25 – QN\_36**). The physicochemical properties of synthesized derivatives are shown in **Table 5.4**.

**Table 5.4:** Physicochemical properties of synthesized compounds **QN\_04 – QN\_11, QN\_16 – QN\_23** and **QN\_25 – QN\_36**.



| Comp  | R <sub>1</sub> | R <sub>2</sub> | R <sub>3</sub>  | Yield (%) | Melting point (°C) | Molecular formula  | Molecular weight |
|-------|----------------|----------------|-----------------|-----------|--------------------|--|------------------|
| QN_04 | H              |                | H               | 72.2      | 241-243            | C <sub>16</sub> H <sub>13</sub> N <sub>3</sub> O <sub>2</sub>                                | 279.29           |
| QN_05 | Cl             |                | H               | 73.1      | 258-260            | C <sub>16</sub> H <sub>12</sub> ClN <sub>3</sub> O <sub>2</sub>                              | 313.74           |
| QN_06 | H              |                | H               | 70.6      | 260-262            | C <sub>17</sub> H <sub>11</sub> ClF <sub>3</sub> N <sub>3</sub> O <sub>2</sub>               | 381.74           |
| QN_07 | Cl             |                | H               | 74.5      | 218-220            | C <sub>17</sub> H <sub>10</sub> Cl <sub>2</sub> F <sub>3</sub> N <sub>3</sub> O <sub>2</sub> | 416.18           |
| QN_08 | H              |                | H               | 70.6      | 187-189            | C <sub>15</sub> H <sub>13</sub> N <sub>3</sub> O <sub>3</sub>                                | 283.28           |
| QN_09 | Cl             |                | H               | 76.2      | 223-225            | C <sub>15</sub> H <sub>12</sub> ClN <sub>3</sub> O <sub>3</sub>                              | 317.73           |
| QN_10 | H              |                | H               | 71.4      | 234-236            | C <sub>15</sub> H <sub>13</sub> N <sub>3</sub> O <sub>2</sub> S                              | 299.35           |
| QN_11 | Cl             |                | H               | 78.6      | 212-214            | C <sub>15</sub> H <sub>12</sub> ClN <sub>3</sub> O <sub>2</sub> S                            | 333.79           |
| QN_16 | H              |                | CH <sub>3</sub> | 72.4      | 261-263            | C <sub>17</sub> H <sub>15</sub> N <sub>3</sub> O <sub>2</sub>                                | 293.32           |
| QN_17 | Cl             |                | CH <sub>3</sub> | 71.2      | 260-262            | C <sub>17</sub> H <sub>14</sub> ClN <sub>3</sub> O <sub>2</sub>                              | 327.76           |
| QN_18 | H              |                | CH <sub>3</sub> | 74.5      | 219-221            | C <sub>18</sub> H <sub>13</sub> ClF <sub>3</sub> N <sub>3</sub> O <sub>2</sub>               | 395.76           |
| QN_19 | Cl             |                | CH <sub>3</sub> | 70.3      | 237-239            | C <sub>18</sub> H <sub>12</sub> Cl <sub>2</sub> F <sub>3</sub> N <sub>3</sub> O <sub>2</sub> | 430.21           |
| QN_20 | H              |                | CH <sub>3</sub> | 71.2      | 216-218            | C <sub>16</sub> H <sub>15</sub> N <sub>3</sub> O <sub>3</sub>                                | 297.31           |
| QN_21 | Cl             |                | CH <sub>3</sub> | 69.8      | 234-236            | C <sub>16</sub> H <sub>14</sub> ClN <sub>3</sub> O <sub>3</sub>                              | 331.75           |

Contd...

| Comp  | R <sub>1</sub> | R <sub>2</sub>  | R <sub>3</sub>  | Yield (%) | Melting point (°C) | Molecular formula   | Molecular weight |
|-------|----------------|---|-----------------|-----------|--------------------|---|------------------|
| QN_22 | H              |    | CH <sub>3</sub> | 70.6      | 243-245            | C <sub>16</sub> H <sub>15</sub> N <sub>3</sub> O <sub>2</sub> S   | 313.37           |
| QN_23 | Cl             |    | CH <sub>3</sub> | 69.3      | 222-224            | C <sub>16</sub> H <sub>14</sub> ClN <sub>3</sub> O <sub>2</sub> S | 347.82           |
| QN_25 | H              |    | H               | 68.6      | 223-225            | C <sub>13</sub> H <sub>9</sub> N <sub>5</sub> O <sub>4</sub> S    | 331.31           |
| QN_26 | Cl             |    | H               | 70.1      | 198-200            | C <sub>13</sub> H <sub>8</sub> ClN <sub>5</sub> O <sub>4</sub> S  | 365.75           |
| QN_27 | H              |    | CH <sub>3</sub> | 73.4      | 226-228            | C <sub>14</sub> H <sub>11</sub> N <sub>5</sub> O <sub>4</sub> S   | 345.33           |
| QN_28 | Cl             |    | CH <sub>3</sub> | 72.7      | 217-219            | C <sub>14</sub> H <sub>10</sub> ClN <sub>5</sub> O <sub>4</sub> S | 379.78           |
| QN_29 | H              |    | H               | 67.8      | 196-198            | C <sub>17</sub> H <sub>12</sub> N <sub>4</sub> O <sub>2</sub> S   | 336.37           |
| QN_30 | Cl             |    | H               | 73.5      | 209-211            | C <sub>17</sub> H <sub>11</sub> ClN <sub>4</sub> O <sub>2</sub> S | 370.81           |
| QN_31 | H              |   | CH <sub>3</sub> | 68.7      | 206-208            | C <sub>18</sub> H <sub>14</sub> N <sub>4</sub> O <sub>2</sub> S   | 350.39           |
| QN_32 | Cl             |  | CH <sub>3</sub> | 69.7      | 237-239            | C <sub>18</sub> H <sub>13</sub> ClN <sub>4</sub> O <sub>2</sub> S | 384.84           |
| QN_33 | H              |  | H               | 71.6      | 237-239            | C <sub>17</sub> H <sub>11</sub> N <sub>5</sub> O <sub>4</sub> S   | 381.87           |
| QN_34 | Cl             |  | H               | 69.5      | >280               | C <sub>17</sub> H <sub>10</sub> ClN <sub>5</sub> O <sub>4</sub> S | 415.81           |
| QN_35 | H              |  | CH <sub>3</sub> | 71.9      | 196-198            | C <sub>18</sub> H <sub>13</sub> N <sub>5</sub> O <sub>4</sub> S   | 395.39           |
| QN_36 | Cl             |  | CH <sub>3</sub> | 71.6      | 234-236            | C <sub>18</sub> H <sub>12</sub> ClN <sub>5</sub> O <sub>4</sub> S | 429.84           |

### 5.2.3 Characterization of synthesized compounds

Both analytical and spectral data (<sup>1</sup>H NMR, <sup>13</sup>C NMR and mass spectra) of all the synthesized compounds were in full agreement with the proposed structures.



### **Quinazolin-4(3H)-one (QN\_01a)**

The compound was synthesized according to the general procedure using anthranilamide (2.0 g, 14.68 mmol) and formamidine acetate (3.05 g, 29.37 mmol) to afford **QN\_01a** (1.95 g, 90.7 %) as white solid. M.p: 152-154 °C. <sup>1</sup>H NMR (DMSO-d<sub>6</sub>): δ<sub>H</sub> 10.34 (s, 1H), 8.13 – 7.72 (m, 5H). <sup>13</sup>C NMR (DMSO-d<sub>6</sub>): δ<sub>C</sub> 161.1, 148.4, 146.0, 134.1, 128.2, 125.5, 125.2, 120.9. ESI-MS m/z 147 (M+H)<sup>+</sup>. Anal. Calcd. for C<sub>8</sub>H<sub>6</sub>N<sub>2</sub>O: C, 65.75; H, 4.14; N, 19.17; Found: C, 65.71; H, 4.12; N, 19.19.

### **6-Chloroquinazolin-4(3H)-one (QN\_01b)**

The compound was synthesized according to the general procedure using 2-amino-5-chlorobenzamide (2.0 g, 11.72 mmol) and formamidine acetate (2.44 g, 23.44 mmol) to afford **QN\_01b** (1.87 g, 88.6 %) as off white solid. M.p: 192-194 °C. <sup>1</sup>H NMR (DMSO-d<sub>6</sub>): δ<sub>H</sub> 10.41 (s, 1H), 8.34 – 7.48 (m, 4H). <sup>13</sup>C NMR (DMSO-d<sub>6</sub>): δ<sub>C</sub> 161.3, 146.6, 144.5, 135.1, 134.7, 129.1, 128.8, 122.5. ESI-MS m/z 179 (M-H)<sup>-</sup>. Anal. Calcd. for C<sub>8</sub>H<sub>5</sub>ClN<sub>2</sub>O: C, 53.21; H, 2.79; N, 15.51; Found: C, 53.25; H, 2.77; N, 15.49.

### **Methyl 2-(4-oxoquinazolin-3(4H)-yl)acetate (QN\_02a)**

The compound was synthesized according to the general procedure using quinazolin-4(3H)-one (**QN\_01a**) (1.5 g, 10.26 mmol) and methyl bromoacetate (1.88 g, 12.31 mmol) to afford **QN\_02a** (1.84 g, 82.4 %) as white solid. M.p: 222-224 °C. <sup>1</sup>H NMR (DMSO-d<sub>6</sub>): δ<sub>H</sub> 8.27 – 7.61 (m, 5H), 4.42 (s, 2H), 3.58 (s, 3H). <sup>13</sup>C NMR (DMSO-d<sub>6</sub>): δ<sub>C</sub> 168.2, 161.4, 148.0, 147.3, 133.1, 127.5, 126.8, 126.5, 120.9, 56.3, 46.2. ESI-MS m/z 219 (M+H)<sup>+</sup>. Anal. Calcd. for C<sub>11</sub>H<sub>10</sub>N<sub>2</sub>O<sub>3</sub>: C, 60.55; H, 4.62; N, 12.84; Found: C, 60.51; H, 4.64; N, 12.82.

### **Methyl 2-(6-chloro-4-oxoquinazolin-3(4H)-yl)acetate (QN\_02b)**

The compound was synthesized according to the general procedure using 6-chloroquinazolin-4(3H)-one (**QN\_01b**) (1.5 g, 8.30 mmol) and methyl bromoacetate (1.52 g, 9.96 mmol) to afford **QN\_02b** (1.68 g, 80.1 %) as white solid. M.p: 263-265 °C. <sup>1</sup>H NMR (DMSO-d<sub>6</sub>): δ<sub>H</sub> 8.28 (s, 1H), 7.96 – 7.46 (m, 3H), 4.49 (s, 2H), 3.60 (s, 3H). <sup>13</sup>C NMR (DMSO-d<sub>6</sub>): δ<sub>C</sub> 168.1, 161.5, 147.4, 146.5, 133.6, 133.1, 127.9, 127.6, 122.1, 51.5, 46.2. ESI-MS m/z 251 (M-H)<sup>-</sup>. Anal. Calcd. for C<sub>11</sub>H<sub>9</sub>ClN<sub>2</sub>O<sub>3</sub>: C, 52.29; H, 3.59; N, 11.09; Found: C, 52.31; H, 3.61; N, 11.06.

### **2-(4-Oxoquinazolin-3(4*H*)-yl)acetic acid (QN\_03a)**

The compound was synthesized according to the general procedure using methyl 2-(4-oxoquinazolin-3(4*H*)-yl)acetate (**QN\_02a**) (1.5 g, 6.87 mmol) to afford **QN\_03a** (1.1 g, 78.7 %) as white solid. M.p: 261-263 °C. <sup>1</sup>H NMR (DMSO-*d*<sub>6</sub>): δ<sub>H</sub> 11.23 (s, 1H), 8.67 – 7.51 (m, 5H), 4.64 (s, 2H). <sup>13</sup>C NMR (DMSO-*d*<sub>6</sub>): δ<sub>C</sub> 169.4, 161.7, 148.4, 147.6, 133.5, 127.4, 126.9, 126.7, 120.3, 49.9. ESI-MS *m/z* 203 (M-H)<sup>-</sup>. Anal. Calcd. for C<sub>10</sub>H<sub>8</sub>N<sub>2</sub>O<sub>3</sub>: C, 58.82; H, 3.95; N, 13.72; Found: C, 58.79; H, 3.94; N, 13.69.

### **2-(6-Chloro-4-oxoquinazolin-3(4*H*)-yl)acetic acid (QN\_03b)**

The compound was synthesized according to the general procedure using methyl 2-(6-chloro-4-oxoquinazolin-3(4*H*)-yl)acetate (**QN\_02b**) (1.5 g, 5.93 mmol) to afford **QN\_03b** (1.1 g, 78.1 %) as white solid. M.p: 249-251 °C. <sup>1</sup>H NMR (DMSO-*d*<sub>6</sub>): δ<sub>H</sub> 11.17 (s, 1H), 8.61 – 7.41 (m, 4H), 4.58 (s, 2H). <sup>13</sup>C NMR (DMSO-*d*<sub>6</sub>): δ<sub>C</sub> 169.2, 161.4, 147.7, 146.1, 133.3, 133.0, 127.7, 127.5, 122.5, 49.7. ESI-MS *m/z* 237 (M-H)<sup>-</sup>. Anal. Calcd. for C<sub>10</sub>H<sub>7</sub>ClN<sub>2</sub>O<sub>3</sub>: C, 50.33; H, 2.96; N, 11.74; Found: C, 50.29; H, 2.95; N, 11.72.

### **2-(4-Oxoquinazolin-3(4*H*)-yl)-*N*-phenylacetamide (QN\_04)**

The compound was synthesized according to the general procedure using aniline (0.05 g, 0.53 mmol) and 2-(4-oxoquinazolin-3(4*H*)-yl)acetic acid (**QN\_03a**) (0.1 g, 0.48 mmol) to afford **QN\_04** (0.098 g, 72.2 %) as pale yellow solid. M.p: 241-243 °C. <sup>1</sup>H NMR (DMSO-*d*<sub>6</sub>): δ<sub>H</sub> 10.45 (s, 1H), 8.37 – 7.04 (m, 10H), 4.86 (s, 2H). <sup>13</sup>C NMR (DMSO-*d*<sub>6</sub>): δ<sub>C</sub> 161.3, 161.7, 148.5, 147.6, 138.7, 133.6, 128.8, 128.2, 127.5, 126.9, 126.4, 121.7, 121.0, 50.2. ESI-MS *m/z* 280 (M+H)<sup>+</sup>. Anal. Calcd. for C<sub>16</sub>H<sub>13</sub>N<sub>3</sub>O<sub>2</sub>: C, 68.81; H, 4.69; N, 15.05; Found: C, 68.78; H, 4.67; N, 15.02.

### **2-(6-Chloro-4-oxoquinazolin-3(4*H*)-yl)-*N*-phenylacetamide (QN\_05)**

The compound was synthesized according to the general procedure using aniline (0.042 g, 0.46 mmol) and 2-(6-chloro-4-oxoquinazolin-3(4*H*)-yl)acetic acid (**QN\_03b**) (0.1 g, 0.41 mmol) to afford **QN\_05** (0.096 g, 73.1 %) as off white solid. M.p: 258-260 °C. <sup>1</sup>H NMR (DMSO-*d*<sub>6</sub>): δ<sub>H</sub> 10.32 (s, 1H), 8.57 – 7.15 (m, 9H), 5.01 (s, 2H). <sup>13</sup>C NMR (DMSO-*d*<sub>6</sub>): δ<sub>C</sub> 168.6, 161.8, 147.7, 146.5, 138.7, 135.4, 133.0, 129.0, 128.1, 127.8, 127.6, 122.4, 121.7,

50.3. ESI-MS  $m/z$  314 (M+H)<sup>+</sup>. Anal. Calcd. for C<sub>16</sub>H<sub>12</sub>ClN<sub>3</sub>O<sub>2</sub>: C, 61.25; H, 3.86; N, 13.39; Found: C, 61.21; H, 3.88; N, 13.42.

***N*-(2-Chloro-5-(trifluoromethyl)phenyl)-2-(4-oxoquinazolin-3(4*H*)-yl)acetamide (QN\_06)**

The compound was synthesized according to the general procedure using 2-chloro-5-trifluoromethylaniline (0.1 g, 0.53 mmol) and 2-(4-oxoquinazolin-3(4*H*)-yl)acetic acid (QN\_03a) (0.1 g, 0.48 mmol) to afford QN\_06 (0.13 g, 70.6 %) as white solid. M.p: 260-262 °C. <sup>1</sup>H NMR (DMSO-*d*<sub>6</sub>): δ<sub>H</sub> 10.24 (s, 1H), 8.61 – 7.27 (m, 8H), 5.04 (s, 2H). <sup>13</sup>C NMR (DMSO-*d*<sub>6</sub>): δ<sub>C</sub> 168.7, 161.8, 148.4, 147.7, 137.7, 133.5, 129.5, 129.3, 127.6, 126.8, 126.6, 126.1, 124.2, 122.2, 120.0, 118.9, 50.7. ESI-MS  $m/z$  380 (M-H)<sup>-</sup>. Anal. Calcd. for C<sub>17</sub>H<sub>11</sub>ClF<sub>3</sub>N<sub>3</sub>O<sub>2</sub>: C, 53.49; H, 2.90; N, 11.01; Found: C, 53.52; H, 2.92; N, 11.02.

**2-(6-Chloro-4-oxoquinazolin-3(4*H*)-yl)-*N*-(2-chloro-5-(trifluoromethyl)phenyl)acetamide (QN\_07)**

The compound was synthesized according to the general procedure using 2-chloro-5-trifluoromethylaniline (0.089 g, 0.46 mmol) and 2-(6-chloro-4-oxoquinazolin-3(4*H*)-yl)acetic acid (QN\_03b) (0.1 g, 0.41 mmol) to afford QN\_07 (0.13 g, 74.5 %) as white solid. M.p: 218-220 °C. <sup>1</sup>H NMR (DMSO-*d*<sub>6</sub>): δ<sub>H</sub> 10.34 (s, 1H), 8.43 – 7.55 (m, 7H), 5.06 (s, 2H). <sup>13</sup>C NMR (DMSO-*d*<sub>6</sub>): δ<sub>C</sub> 168.8, 161.6, 147.8, 146.4, 137.7, 133.6, 133.0, 129.5, 129.3, 127.8, 127.6, 126.1, 124.2, 122.3, 122.0, 118.9, 50.6. ESI-MS  $m/z$  415 (M-H)<sup>-</sup>. Anal. Calcd. for C<sub>17</sub>H<sub>10</sub>Cl<sub>2</sub>F<sub>3</sub>N<sub>3</sub>O<sub>2</sub>: C, 49.06; H, 2.42; N, 10.10; Found: C, 49.09; H, 2.43; N, 10.12.

***N*-(Furan-2-yl-methyl)-2-(4-oxoquinazolin-3(4*H*)-yl)acetamide (QN\_08)**

The compound was synthesized according to the general procedure using furfurylamine (0.051 g, 0.53 mmol) and 2-(4-oxoquinazolin-3(4*H*)-yl)acetic acid (QN\_03a) (0.1 g, 0.48 mmol) to afford QN\_08 (0.097 g, 70.6 %) as pale yellow solid. M.p: 187-189 °C. <sup>1</sup>H NMR (DMSO-*d*<sub>6</sub>): δ<sub>H</sub> 8.83 (s, 1H), 8.42 – 6.27 (m, 8H), 4.35 (s, 2H), 4.29 (s, 2H). <sup>13</sup>C NMR (DMSO-*d*<sub>6</sub>): δ<sub>C</sub> 171.2, 161.4, 148.4, 147.7, 145.9, 142.3, 133.5, 127.6, 126.8, 126.5, 120.9, 110.7, 110.5, 50.4, 37.3. ESI-MS  $m/z$  284 (M+H)<sup>+</sup>. Anal. Calcd. for C<sub>15</sub>H<sub>13</sub>N<sub>3</sub>O<sub>3</sub>: C, 63.60; H, 4.63; N, 14.83; Found: C, 63.57; H, 4.65; N, 14.81.

### **2-(6-Chloro-4-oxoquinazolin-3(4*H*)-yl)-*N*-(furan-2-ylmethyl)acetamide (QN\_09)**

The compound was synthesized according to the general procedure using furfurylamine (0.044 g, 0.46 mmol) and 2-(6-chloro-4-oxoquinazolin-3(4*H*)-yl)acetic acid (**QN\_03b**) (0.1 g, 0.41 mmol) to afford **QN\_09** (0.10 g, 76.2 %) as white solid. M.p: 223-225 °C. <sup>1</sup>H NMR (DMSO-*d*<sub>6</sub>): δ<sub>H</sub> 8.86 (s, 1H), 8.48 – 6.31 (m, 7H), 4.87 (s, 2H), 4.32 (s, 2H). <sup>13</sup>C NMR (DMSO-*d*<sub>6</sub>): δ<sub>C</sub> 171.2, 161.7, 147.7, 146.2, 145.9, 142.2, 133.6, 133.0, 127.6, 127.4, 122.3, 110.5, 110.3, 50.1, 36.9. ESI-MS *m/z* 318 (M+H)<sup>+</sup>. Anal. Calcd. for C<sub>15</sub>H<sub>12</sub>ClN<sub>3</sub>O<sub>3</sub>: C, 56.70; H, 3.81; N, 13.23; Found: C, 56.74; H, 3.83; N, 13.20.

### **2-(4-Oxoquinazolin-3(4*H*)-yl)-*N*-(thiophen-2-ylmethyl)acetamide (QN\_10)**

The compound was synthesized according to the general procedure using 2-thiophenemethylamine (0.059 g, 0.53 mmol) and 2-(4-oxoquinazolin-3(4*H*)-yl)acetic acid (**QN\_03a**) (0.1 g, 0.48 mmol) to afford **QN\_10** (0.10 g, 71.4 %) as white solid. M.p: 234-236 °C. <sup>1</sup>H NMR (DMSO-*d*<sub>6</sub>): δ<sub>H</sub> 8.97 (s, 1H), 8.52 – 6.98 (m, 8H), 4.74 (s, 2H), 4.40 (s, 2H). <sup>13</sup>C NMR (DMSO-*d*<sub>6</sub>): δ<sub>C</sub> 171.2, 161.4, 148.3, 147.7, 140.5, 133.6, 127.4, 127.1, 126.8, 126.5, 126.3, 125.4, 121.0, 51.1, 43.2. ESI-MS *m/z* 300 (M+H)<sup>+</sup>. Anal. Calcd. for C<sub>15</sub>H<sub>13</sub>N<sub>3</sub>O<sub>2</sub>S: C, 60.18; H, 4.38; N, 14.04; Found: C, 60.21; H, 4.37; N, 14.06.

### **2-(6-Chloro-4-oxoquinazolin-3(4*H*)-yl)-*N*-(thiophen-2-ylmethyl)acetamide (QN\_11)**

The compound was synthesized according to the general procedure using 2-thiophenemethylamine (0.052 g, 0.46 mmol) and 2-(6-chloro-4-oxoquinazolin-3(4*H*)-yl)acetic acid (**QN\_03b**) (0.1 g, 0.41 mmol) to afford **QN\_11** (0.11 g, 78.6 %) as white solid. M.p: 212-214 °C. <sup>1</sup>H NMR (DMSO-*d*<sub>6</sub>): δ<sub>H</sub> 8.95 (s, 1H), 8.54 – 6.95 (m, 7H), 4.89 (s, 2H), 4.42 (s, 2H). <sup>13</sup>C NMR (DMSO-*d*<sub>6</sub>): δ<sub>C</sub> 171.2, 161.5, 147.7, 146.2, 140.8, 133.6, 133.1, 127.6, 127.4, 127.1, 126.8, 125.3, 122.1, 51.2, 42.9. ESI-MS *m/z* 334 (M+H)<sup>+</sup>. Anal. Calcd. for C<sub>15</sub>H<sub>12</sub>ClN<sub>3</sub>O<sub>2</sub>S: C, 53.97; H, 3.62; N, 12.59; Found: C, 54.00; H, 3.64; N, 12.62.

### **2-Methyl-4*H*-benzo[*d*][1,3]oxazin-4-one (QN\_12a)**

The compound was synthesized according to the general procedure using anthranilic acid (2.0 g, 14.58 mmol) to afford **QN\_12a** (1.84 g, 78.4 %) as white solid. M.p: 117-119 °C. <sup>1</sup>H NMR (DMSO-*d*<sub>6</sub>): δ<sub>H</sub> 8.19 – 7.58 (m, 4H), 1.21 (s, 3H). <sup>13</sup>C NMR (DMSO-*d*<sub>6</sub>): δ<sub>C</sub> 163.9, 160.1,

144.6, 135.4, 128.3, 126.7, 124.3, 114.2, 25.5. ESI-MS  $m/z$  162 (M+H)<sup>+</sup>. Anal. Calcd. for C<sub>9</sub>H<sub>7</sub>NO<sub>2</sub>: C, 67.07; H, 4.38; N, 8.69; Found: C, 67.10; H, 4.40; N, 8.66.

### **6-Chloro-2-methyl-4H-benzo[d][1,3]oxazin-4-one (QN\_12b)**

The compound was synthesized according to the general procedure using 2-amino-5-chlorobenzoic acid (2.0 g, 11.65 mmol) to afford **QN\_12b** (1.74 g, 76.7 %) as white solid. M.p: 158-160 °C. <sup>1</sup>H NMR (DMSO-d<sub>6</sub>): δ<sub>H</sub> 8.07 – 7.52 (m, 3H), 1.19 (s, 3H). <sup>13</sup>C NMR (DMSO-d<sub>6</sub>): δ<sub>C</sub> 173.1, 161.8, 154.2, 131.1, 128.0, 121.2, 39.6, 16.6, 8.8. ESI-MS  $m/z$  194 (M-H)<sup>-</sup>. Anal. Calcd. for C<sub>9</sub>H<sub>6</sub>ClNO<sub>2</sub>: C, 55.26; H, 3.09; N, 7.16; Found: C, 55.30; H, 3.07; N, 7.13.

### **2-Methylquinazolin-4(3H)-one (QN\_13a)**

The compound was synthesized according to the general procedure using 2-methyl-4H-benzo[d][1,3]oxazin-4-one (**QN\_12a**) (1.6 g, 9.98 mmol) to afford **QN\_13a** (1.31 g, 82.8 %) as white solid. M.p: 247-249 °C. <sup>1</sup>H NMR (DMSO-d<sub>6</sub>): δ<sub>H</sub> 12.19 (s, 1H), 8.08 – 7.42 (m, 4H), 2.34 (s, 3H). <sup>13</sup>C NMR (DMSO-d<sub>6</sub>): δ<sub>C</sub> 161.4, 155.0, 147.2, 134.2, 127.9, 125.7, 125.3, 120.6, 21.2. ESI-MS  $m/z$  161 (M+H)<sup>+</sup>. Anal. Calcd. for C<sub>9</sub>H<sub>8</sub>N<sub>2</sub>O: C, 67.49; H, 5.03; N, 17.49; Found: C, 67.52; H, 5.01; N, 17.47.

### **6-Chloro-2-methylquinazolin-4(3H)-one (QN\_13b)**

The compound was synthesized according to the general procedure using 6-chloro-2-methyl-4H-benzo[d][1,3]oxazin-4-one (**QN\_12b**) (1.6 g, 8.22 mmol) to afford **QN\_13b** (1.31 g, 82.7 %) as white solid. M.p: 251-253 °C. <sup>1</sup>H NMR (DMSO-d<sub>6</sub>): δ<sub>H</sub> 10.07 (s, 1H), 8.01 – 7.39 (m, 3H), 2.45 (s, 3H). <sup>13</sup>C NMR (DMSO-d<sub>6</sub>): δ<sub>C</sub> 161.1, 155.0, 145.7, 134.2, 130.8, 128.3, 126.9, 121.2, 22.4. ESI-MS  $m/z$  193 (M-H)<sup>-</sup>. Anal. Calcd. for C<sub>9</sub>H<sub>7</sub>ClN<sub>2</sub>O: C, 55.54; H, 3.63; N, 14.39; Found: C, 55.51; H, 3.64; N, 14.36.

### **Methyl 2-(2-methyl-4-oxoquinazolin-3(4H)-yl)acetate (QN\_14a)**

The compound was synthesized according to the general procedure using 2-methylquinazolin-4(3H)-ones (**QN\_13a**) (1.3 g, 8.11 mmol) and methyl bromoacetate (1.48 g, 9.73 mmol) to afford **QN\_14a** (1.47 g, 78.4 %) as white solid. M.p: 235-237 °C. <sup>1</sup>H NMR (DMSO-d<sub>6</sub>): δ<sub>H</sub> 8.01 – 7.59 (m, 4H), 4.47 (s, 2H), 3.63 (s, 3H), 2.52 (s, 3H). <sup>13</sup>C NMR (DMSO-d<sub>6</sub>): δ<sub>C</sub> 168.1, 161.4, 154.7, 147.1, 133.5, 127.5, 126.6, 126.3, 120.9, 51.8, 43.4,

22.2. ESI-MS  $m/z$  233 ( $M+H$ )<sup>+</sup>. Anal. Calcd. for C<sub>12</sub>H<sub>12</sub>N<sub>2</sub>O<sub>3</sub>: C, 62.06; H, 5.21; N, 12.06; Found: C, 62.09; H, 5.19; N, 12.09.

#### **Methyl 2-(6-chloro-2-methyl-4-oxoquinazolin-3(4*H*)-yl)acetate (QN\_14b)**

The compound was synthesized according to the general procedure using 6-chloro-2-methylquinazolin-4(3*H*)-one (**QN\_13b**) (1.3 g, 6.67 mmol) and methyl bromoacetate (1.22 g, 8.01 mmol) to afford **QN\_14b** (1.36 g, 76.8 %) as white solid. M.p: 267-269 °C. <sup>1</sup>H NMR (DMSO-*d*<sub>6</sub>): δ<sub>H</sub> 7.89 – 7.41 (m, 3H), 4.49 (s, 2H), 3.62 (s, 3H), 2.53 (s, 3H). <sup>13</sup>C NMR (DMSO-*d*<sub>6</sub>): δ<sub>C</sub> 168.3, 161.4, 154.5, 145.2, 133.4, 133.1, 127.7, 127.4, 122.3, 51.3, 43.2, 22.4. ESI-MS  $m/z$  265 ( $M-H$ )<sup>-</sup>. Anal. Calcd. for C<sub>12</sub>H<sub>11</sub>ClN<sub>2</sub>O<sub>3</sub>: C, 54.05; H, 4.16; N, 10.50; Found: C, 54.08; H, 4.15; N, 10.53.

#### **2-(2-Methyl-4-oxoquinazolin-3(4*H*)-yl)acetic acid (QN\_15a)**

The compound was synthesized according to the general procedure using methyl 2-(2-methyl-4-oxoquinazolin-3(4*H*)-yl)acetate (**QN\_14a**) (1.3 g, 5.59 mmol) and lithium hydroxide (0.26 g, 11.18 mmol) to afford **QN\_15a** (0.95 g, 78.6 %) as white solid. M.p: 244-246 °C. <sup>1</sup>H NMR (DMSO-*d*<sub>6</sub>): δ<sub>H</sub> 10.96 (s, 1H), 8.06 – 7.38 (m, 4H), 4.49 (s, 2H), 2.52 (s, 3H). <sup>13</sup>C NMR (DMSO-*d*<sub>6</sub>): δ<sub>C</sub> 168.9, 161.7, 154.6, 147.1, 133.6, 127.6, 126.8, 126.6, 121.0, 47.9, 22.4. ESI-MS  $m/z$  217 ( $M-H$ )<sup>-</sup>. Anal. Calcd. for C<sub>11</sub>H<sub>10</sub>N<sub>2</sub>O<sub>3</sub>: C, 60.55; H, 4.62; N, 12.84; Found: C, 60.58; H, 4.60; N, 12.87.

#### **2-(6-Chloro-2-methyl-4-oxoquinazolin-3(4*H*)-yl)acetic acid (QN\_15b)**

The compound was synthesized according to the general procedure using methyl 2-(6-chloro-2-methyl-4-oxoquinazolin-3(4*H*)-yl)acetate (**QN\_14b**) (1.3 g, 4.87 mmol) and lithium hydroxide (0.23 g, 9.74 mmol) to afford **QN\_15b** (0.91 g, 74.5 %) as white solid. M.p: 261-263 °C. <sup>1</sup>H NMR (DMSO-*d*<sub>6</sub>): δ<sub>H</sub> 11.02 (s, 1H), 8.03 – 7.52 (m, 3H), 4.47 (s, 2H), 2.47 (s, 3H). <sup>13</sup>C NMR (DMSO-*d*<sub>6</sub>): δ<sub>C</sub> 169.1, 161.8, 154.8, 145.3, 133.8, 133.1, 127.8, 127.5, 122.5, 48.4, 22.3. ESI-MS  $m/z$  251 ( $M-H$ )<sup>-</sup>. Anal. Calcd. for C<sub>11</sub>H<sub>9</sub>ClN<sub>2</sub>O<sub>3</sub>: C, 52.29; H, 3.59; N, 11.09; Found: C, 52.32; H, 3.61; N, 11.12.

#### **2-(2-Methyl-4-oxoquinazolin-3(4*H*)-yl)-*N*-phenylacetamide (QN\_16)**

The compound was synthesized according to the general procedure using aniline (0.046 g, 0.50 mmol) and 2-(2-methyl-4-oxoquinazolin-3(4*H*)-yl)acetic acid (**QN\_15a**) (0.1 g, 0.45

mmol) to afford **QN\_16** (0.11 g, 72.4 %) as white solid. M.p: 261-263 °C. <sup>1</sup>H NMR (DMSO-d<sub>6</sub>): δ<sub>H</sub> 10.41 (s, 1H), 8.35 – 7.11 (m, 9H), 4.72 (s, 2H), 2.49 (s, 3H). <sup>13</sup>C NMR (DMSO-d<sub>6</sub>): δ<sub>C</sub> 168.8, 161.6, 154.8, 147.1, 138.5, 133.6, 129.1, 128.1, 127.5, 126.8, 126.6, 121.8, 120.7, 49.1, 22.3. ESI-MS m/z 294 (M+H)<sup>+</sup>. Anal. Calcd. for C<sub>17</sub>H<sub>15</sub>N<sub>3</sub>O<sub>2</sub>: C, 69.61; H, 5.15; N, 14.33; Found: C, 69.64; H, 5.13; N, 14.30.

### **2-(6-Chloro-2-methyl-4-oxoquinazolin-3(4H)-yl)-N-phenylacetamide (QN\_17)**

The compound was synthesized according to the general procedure using aniline (0.040 g, 0.43 mmol) and 2-(6-chloro-2-methyl-4-oxoquinazolin-3(4H)-yl)acetic acid (**QN\_15b**) (0.1 g, 0.39 mmol) to afford **QN\_17** (0.09 g, 71.2 %) as off white solid. M.p: 260-262 °C. <sup>1</sup>H NMR (DMSO-d<sub>6</sub>): δ<sub>H</sub> 10.38 (s, 1H), 8.33 – 7.13 (m, 8H), 4.75 (s, 2H), 2.58 (s, 3H). <sup>13</sup>C NMR (DMSO-d<sub>6</sub>): δ<sub>C</sub> 168.7, 161.9, 154.7, 145.2, 138.7, 133.6, 133.1, 129.1, 128.2, 127.8, 127.6, 122.0, 121.5, 49.0, 22.0. ESI-MS m/z 328 (M+H)<sup>+</sup>. Anal. Calcd. for C<sub>17</sub>H<sub>14</sub>ClN<sub>3</sub>O<sub>2</sub>: C, 62.30; H, 4.31; N, 12.82; Found: C, 62.34; H, 4.29; N, 12.84.

### **N-(2-Chloro-5-(trifluoromethyl)phenyl)-2-(2-methyl-4-oxoquinazolin-3(4H)-yl)acetamide (QN\_18)**

The compound was synthesized according to the general procedure using 2-chloro-5-trifluoromethylaniline (0.097 g, 0.50 mmol) and 2-(2-methyl-4-oxoquinazolin-3(4H)-yl)acetic acid (**QN\_15a**) (0.1 g, 0.45 mmol) to afford **QN\_18** (0.13 g, 74.5 %) as white solid. M.p: 219-221 °C. <sup>1</sup>H NMR (DMSO-d<sub>6</sub>): δ<sub>H</sub> 10.26 (s, 1H), 8.60 – 7.22 (m, 7H), 5.03 (s, 2H), 2.50 (s, 3H). <sup>13</sup>C NMR (DMSO-d<sub>6</sub>): δ<sub>C</sub> 168.6, 161.5, 154.6, 147.2, 137.7, 133.6, 129.4, 129.2, 127.4, 126.8, 126.5, 126.1, 124.3, 122.2, 120.9, 118.9, 48.3, 22.4. ESI-MS m/z 394 (M-H)<sup>-</sup>. Anal. Calcd. for C<sub>18</sub>H<sub>13</sub>ClF<sub>3</sub>N<sub>3</sub>O<sub>2</sub>: C, 54.63; H, 3.31; N, 10.62; Found: C, 54.66; H, 3.29; N, 10.59.

### **2-(6-Chloro-2-methyl-4-oxoquinazolin-3(4H)-yl)-N-(2-chloro-5-(trifluoromethyl)phenyl)acetamide (QN\_19)**

The compound was synthesized according to the general procedure using 2-chloro-5-trifluoromethylaniline (0.084 g, 0.43 mmol) and 2-(6-chloro-2-methyl-4-oxoquinazolin-3(4H)-yl)acetic acid (**QN\_15b**) (0.1 g, 0.39 mmol) to afford **QN\_19** (0.11 g, 70.3 %) as white solid. M.p: 237-239 °C. <sup>1</sup>H NMR (DMSO-d<sub>6</sub>): δ<sub>H</sub> 10.35 (s, 1H), 8.64 – 7.19 (m, 6H), 5.01 (s, 2H), 2.52 (s, 3H). <sup>13</sup>C NMR (DMSO-d<sub>6</sub>): δ<sub>C</sub> 168.7, 161.7, 154.7, 145.2, 137.8, 133.6, 133.1,

129.4, 129.1, 127.7, 127.4, 126.0, 124.3, 122.3, 122.1, 118.9, 48.2, 21.9. ESI-MS  $m/z$  429 (M-H). Anal. Calcd. for  $C_{18}H_{12}Cl_2F_3N_3O_2$ : C, 50.25; H, 2.81; N, 9.77; Found: C, 50.28; H, 2.84; N, 9.75.

#### ***N*-(Furan-2-ylmethyl)-2-(2-methyl-4-oxoquinazolin-3(4*H*)-yl)acetamide (QN\_20)**

The compound was synthesized according to the general procedure using furfurylamine (0.048 g, 0.50 mmol) and 2-(2-methyl-4-oxoquinazolin-3(4*H*)-yl)acetic acid (**QN\_15a**) (0.1 g, 0.45 mmol) to afford **QN\_20** (0.097 g, 71.2 %) as white solid. M.p: 216-218 °C.  $^1H$  NMR (DMSO- $d_6$ ):  $\delta_H$  8.81 (s, 1H), 8.09 – 6.27 (m, 7H), 4.79 (s, 2H), 4.31 (s, 2H), 2.47 (s, 3H).  $^{13}C$  NMR (DMSO- $d_6$ ):  $\delta_C$  171.6, 163.8, 154.7, 146.3, 144.9, 141.5, 133.6, 127.5, 126.9, 126.7, 121.0, 110.9, 110.5, 47.1, 37.1, 22.5. ESI-MS  $m/z$  298 (M+H) $^+$ . Anal. Calcd. for  $C_{16}H_{15}N_3O_3$ : C, 64.64; H, 5.09; N, 14.13; Found: C, 64.68; H, 5.06; N, 14.16.

#### **2-(6-Chloro-2-methyl-4-oxoquinazolin-3(4*H*)-yl)-*N*-(furan-2-ylmethyl)acetamide (QN\_21)**

The compound was synthesized according to the general procedure using furfurylamine (0.041 g, 0.43 mmol) and 2-(6-chloro-2-methyl-4-oxoquinazolin-3(4*H*)-yl)acetic acid (**QN\_15b**) (0.1 g, 0.39 mmol) to afford **QN\_21** (0.091 g, 69.8 %) as white solid. M.p: 234-236 °C.  $^1H$  NMR (DMSO- $d_6$ ):  $\delta_H$  8.85 (s, 1H), 8.01 – 6.21 (m, 6H), 4.92 (s, 2H), 4.34 (s, 2H), 2.51 (s, 3H).  $^{13}C$  NMR (DMSO- $d_6$ ):  $\delta_C$  171.1, 161.6, 154.3, 145.7, 145.1, 142.3, 133.6, 133.0, 127.9, 127.6, 122.3, 110.7, 110.4, 48.1, 37.4, 22.3. ESI-MS  $m/z$  332 (M+H) $^+$ . Anal. Calcd. for  $C_{16}H_{14}ClN_3O_3$ : C, 57.93; H, 4.25; N, 12.67; Found: C, 57.97; H, 4.22; N, 12.64.

#### **2-(2-Methyl-4-oxoquinazolin-3(4*H*)-yl)-*N*-(thiophen-2-ylmethyl)acetamide (QN\_22)**

The compound was synthesized according to the general procedure using 2-thiophenemethylamine (0.056 g, 0.50 mmol) and 2-(2-methyl-4-oxoquinazolin-3(4*H*)-yl)acetic acid (**QN\_15a**) (0.1 g, 0.45 mmol) to afford **QN\_22** (0.10 g, 70.6 %) as white solid. M.p: 243-245 °C.  $^1H$  NMR (DMSO- $d_6$ ):  $\delta_H$  8.34 (s, 1H), 8.05 – 6.94 (m, 7H), 4.83 (s, 2H), 4.33 (s, 2H), 2.49 (s, 3H).  $^{13}C$  NMR (DMSO- $d_6$ ):  $\delta_C$  171.1, 161.5, 154.5, 147.1, 140.8, 133.5, 127.4, 127.1, 126.8, 126.6, 126.3, 125.4, 121.0, 48.6, 43.1, 22.3. ESI-MS  $m/z$  314 (M+H) $^+$ . Anal. Calcd. for  $C_{16}H_{15}N_3O_2S$ : C, 61.32; H, 4.82; N, 13.41; Found: C, 61.36; H, 4.84; N, 13.39.



**2-(6-Chloro-2-methyl-4-oxoquinazolin-3(4H)-yl)-N-(thiophen-2-ylmethyl)acetamide (QN\_23)**

The compound was synthesized according to the general procedure using 2-thiophenemethylamine (0.048 g, 0.43 mmol) and 2-(6-chloro-2-methyl-4-oxoquinazolin-3(4H)-yl)acetic acid (**QN\_15b**) (0.1 g, 0.39 mmol) to afford **QN\_23** (0.095 g, 69.3 %) as white solid. M.p: 222-224 °C. <sup>1</sup>H NMR (DMSO-d<sub>6</sub>): δ<sub>H</sub> 8.95 (s, 1H), 8.03 – 6.95 (m, 6H), 4.79 (s, 2H), 4.48 (s, 2H), 2.48 (s, 3H). <sup>13</sup>C NMR (DMSO-d<sub>6</sub>): δ<sub>C</sub> 166.3, 160.2, 155.9, 145.8, 141.8, 134.5, 130.4, 128.8, 126.6, 125.5, 125.19, 125.11, 120.9, 46.1, 37.3, 22.7. ESI-MS m/z 348 (M+H)<sup>+</sup>. Anal. Calcd. for C<sub>16</sub>H<sub>14</sub>ClN<sub>3</sub>O<sub>2</sub>S: C, 55.25; H, 4.06; N, 12.08; Found: C, 55.28; H, 4.04; N, 12.11.

**2-Chloro-N-(5-nitrothiazol-2-yl)acetamide (QN\_24a)**

The compound was synthesized according to the general procedure using chloroacetyl chloride (1.55 g, 13.77 mmol) and 5-nitrothiazol-2-amine (1.0 g, 6.88 mmol) to afford **QN\_24a** (1.03 g, 67.7 %) as pale yellow solid. M.p: 252-254 °C. <sup>1</sup>H NMR (DMSO-d<sub>6</sub>): δ<sub>H</sub> 9.94 (s, 1H), 8.34 (s, 1H), 4.45 (s, 2H). <sup>13</sup>C NMR (DMSO-d<sub>6</sub>): δ<sub>C</sub> 169.4, 166.3, 148.1, 138.6, 43.1. ESI-MS m/z 220 (M-H)<sup>-</sup>. Anal. Calcd. for C<sub>5</sub>H<sub>4</sub>ClN<sub>3</sub>O<sub>3</sub>S: C, 27.10; H, 1.82; N, 18.96; Found: C, 27.14; H, 1.79; N, 18.99.

**N-(Benzo[d]thiazol-2-yl)-2-chloroacetamide (QN\_24b)**

The compound was synthesized according to the general procedure using chloroacetyl chloride (1.50 g, 13.31 mmol) and benzo[d]thiazol-2-amine (1.0 g, 6.65 mmol) to afford **QN\_24b** (0.92 g, 66.2 %) as pale yellow solid. M.p: 276-278 °C. <sup>1</sup>H NMR (DMSO-d<sub>6</sub>): δ<sub>H</sub> 11.78 (s, 1H), 8.21 – 7.63 (m, 4H), 4.39 (s, 2H). <sup>13</sup>C NMR (DMSO-d<sub>6</sub>): δ<sub>C</sub> 173.7, 168.8, 153.4, 130.9, 125.5, 124.7, 121.5, 118.4, 42.9. ESI-MS m/z 225 (M-H)<sup>-</sup>. Anal. Calcd. for C<sub>9</sub>H<sub>7</sub>ClN<sub>2</sub>OS: C, 47.69; H, 3.11; N, 12.36; Found: C, 47.72; H, 3.13; N, 12.39.

**2-Chloro-N-(6-nitrobenzo[d]thiazol-2-yl)acetamide (QN\_24c)**

The compound was synthesized according to the general procedure using chloroacetyl chloride (1.15 g, 10.24 mmol) and 6-nitrobenzo[d]thiazol-2-amine (1.0 g, 5.12 mmol) to afford **QN\_24c** (0.92 g, 66.2 %) as pale yellow solid. M.p: 273-275 °C. <sup>1</sup>H NMR (DMSO-d<sub>6</sub>): δ<sub>H</sub> 12.62 (s 1H), 9.11 (s, 1H), 8.34 – 7.97 (m, 2H), 4.55 (s, 2H). <sup>13</sup>C NMR (DMSO-d<sub>6</sub>):

$\delta_C$  173.9, 168.5, 159.6, 144.8, 131.6, 121.5, 119.2, 117.1, 43.0. ESI-MS  $m/z$  270 (M-H)<sup>-</sup>. Anal. Calcd. for C<sub>9</sub>H<sub>6</sub>ClN<sub>3</sub>O<sub>3</sub>S: C, 39.79; H, 2.23; N, 15.47; Found: C, 39.76; H, 2.25; N, 15.50.

#### ***N*-(5-Nitrothiazol-2-yl)-2-(4-oxoquinazolin-3(4*H*)-yl)acetamide (QN\_25)**

The compound was synthesized according to the general procedure using 2-chloro-*N*-(5-nitrothiazol-2-yl)acetamide (**QN\_24a**) (0.16 g, 0.75 mmol) and quinazolin-4(3*H*)-one (**QN\_01a**) (0.1 g, 0.68 mmol) to afford **QN\_25** (0.15 g, 68.6 %) as pale yellow solid. M.p: 223-225 °C. <sup>1</sup>H NMR (DMSO-*d*<sub>6</sub>):  $\delta_H$  12.15 (s, 1H), 8.61 – 7.57 (m, 6H), 4.51 (s, 2H). <sup>13</sup>C NMR (DMSO-*d*<sub>6</sub>):  $\delta_C$  168.6, 162.8, 161.5, 148.1, 147.6, 147.4, 135.4, 133.2, 127.4, 126.8, 126.5, 120.9, 50.8. ESI-MS  $m/z$  332 (M-H)<sup>-</sup>. Anal. Calcd. for C<sub>13</sub>H<sub>9</sub>N<sub>5</sub>O<sub>4</sub>S: C, 47.13; H, 2.74; N, 21.14; Found: C, 47.17; H, 2.72; N, 21.16.

#### **2-(6-Chloro-4-oxoquinazolin-3(4*H*)-yl)-*N*-(5-nitrothiazol-2-yl)acetamide (QN\_26)**

The compound was synthesized according to the general procedure using 2-chloro-*N*-(5-nitrothiazol-2-yl)acetamide (**QN\_24a**) (0.134 g, 0.60 mmol) and 6-chloroquinazolin-4(3*H*)-one (**QN\_01b**) (0.1 g, 0.55 mmol) to afford **QN\_26** (0.14 g, 70.1 %) as pale yellow solid. M.p: 198-200 °C. <sup>1</sup>H NMR (DMSO-*d*<sub>6</sub>):  $\delta_H$  12.17 (s, 1H), 8.64 – 7.49 (m, 5H), 4.48 (s, 2H). <sup>13</sup>C NMR (DMSO-*d*<sub>6</sub>):  $\delta_C$  168.6, 162.8, 161.5, 147.7, 147.4, 146.4, 135.4, 133.7, 133.1, 127.8, 127.5, 122.3, 51.0. ESI-MS  $m/z$  364 (M-H)<sup>-</sup>. Anal. Calcd. for C<sub>13</sub>H<sub>8</sub>ClN<sub>5</sub>O<sub>4</sub>S: C, 42.69; H, 2.20; N, 19.15; Found: C, 42.65; H, 2.22; N, 19.17.

#### **2-(2-Methyl-4-oxoquinazolin-3(4*H*)-yl)-*N*-(5-nitrothiazol-2-yl)acetamide (QN\_27)**

The compound was synthesized according to the general procedure using 2-chloro-*N*-(5-nitrothiazol-2-yl)acetamide (**QN\_24a**) (0.152 g, 0.68 mmol) and 2-methylquinazolin-4(3*H*)-one (**QN\_13a**) (0.1 g, 0.62 mmol) to afford **QN\_27** (0.15 g, 73.4 %) as pale yellow solid. M.p: 226-228 °C. <sup>1</sup>H NMR (DMSO-*d*<sub>6</sub>):  $\delta_H$  12.21 (s, 1H), 8.60 – 7.61 (m, 5H), 4.47 (s, 2H), 2.49 (s, 3H). <sup>13</sup>C NMR (DMSO-*d*<sub>6</sub>):  $\delta_C$  168.7, 162.9, 161.7, 154.6, 147.4, 147.1, 135.4, 133.2, 127.5, 126.7, 126.5, 120.9, 48.2, 22.2. ESI-MS  $m/z$  344 (M-H)<sup>-</sup>. Anal. Calcd. for C<sub>14</sub>H<sub>11</sub>N<sub>5</sub>O<sub>4</sub>S: C, 48.69; H, 3.21; N, 20.28; Found: C, 48.70; H, 3.23; N, 20.25.

**2-(6-Chloro-2-methyl-4-oxoquinazolin-3(4H)-yl)-N-(5-nitrothiazol-2-yl)acetamide (QN\_28)**

The compound was synthesized according to the general procedure using 2-chloro-*N*-(5-nitrothiazol-2-yl)acetamide (**QN\_24a**) (0.125 g, 0.56 mmol) and 6-chloro-2-methylquinazolin-4(3*H*)-one (**QN\_13b**) (0.1 g, 0.51 mmol) to afford **QN\_28** (0.14 g, 72.7 %) as pale yellow solid. M.p: 217-219 °C. <sup>1</sup>H NMR (DMSO-*d*<sub>6</sub>): δ<sub>H</sub> 12.23 (s, 1H), 8.62 – 7.43 (m, 4H), 4.46 (s, 2H), 2.52 (s, 3H). <sup>13</sup>C NMR (DMSO-*d*<sub>6</sub>): δ<sub>C</sub> 168.6, 162.7, 161.4, 154.5, 147.3, 144.8, 135.2, 133.7 133.1, 127.7, 127.4, 122.0, 48.2, 22.3. ESI-MS *m/z* 378 (M-H)<sup>-</sup>. Anal. Calcd. for C<sub>14</sub>H<sub>10</sub>ClN<sub>5</sub>O<sub>4</sub>S: C, 44.28; H, 2.65; N, 18.44; Found: C, 44.31; H, 2.67; N, 18.42.

**N-(Benzo[*d*]thiazol-2-yl)-2-(4-oxoquinazolin-3(4H)-yl)acetamide (QN\_29)**

The compound was synthesized according to the general procedure using *N*-(benzo[*d*]thiazol-2-yl)-2-chloroacetamide (**QN\_24b**) (0.17 g, 0.75 mmol) and quinazolin-4(3*H*)-one (**QN\_01a**) (0.1 g, 0.68 mmol) to afford **QN\_29** (0.15 g, 67.8 %) as pale yellow solid. M.p: 196-198 °C. <sup>1</sup>H NMR (DMSO-*d*<sub>6</sub>): δ<sub>H</sub> 10.67 (s, 1H), 8.63 (s, 1H), 8.21 – 7.56 (m, 8H), 4.74 (s, 2H). <sup>13</sup>C NMR (DMSO-*d*<sub>6</sub>): δ<sub>C</sub> 174.6, 168.7, 161.5, 153.4, 148.5, 147.7, 133.6, 131.0, 127.4, 126.7, 126.4, 125.2, 124.6, 122.0, 120.9, 118.4, 50.7. ESI-MS *m/z* 337 (M+H)<sup>+</sup>. Anal. Calcd. for C<sub>17</sub>H<sub>12</sub>N<sub>4</sub>O<sub>2</sub>S: C, 60.70; H, 3.60; N, 16.66; Found: C, 60.73; H, 3.61; N, 16.64.

**N-(Benzo[*d*]thiazol-2-yl)-2-(6-chloro-4-oxoquinazolin-3(4H)-yl)acetamide (QN\_30)**

The compound was synthesized according to the general procedure using *N*-(benzo[*d*]thiazol-2-yl)-2-chloroacetamide (**QN\_24b**) (0.136 g, 0.60 mmol) and 6-chloroquinazolin-4(3*H*)-one (**QN\_01b**) (0.1 g, 0.55 mmol) to afford **QN\_30** (0.15 g, 73.5 %) as pale yellow solid. M.p: 209-211 °C. <sup>1</sup>H NMR (DMSO-*d*<sub>6</sub>): δ<sub>H</sub> 10.68 (s, 1H), 8.61 (s, 1H), 8.19 – 7.41 (m, 7H), 4.71 (s, 2H). <sup>13</sup>C NMR (DMSO-*d*<sub>6</sub>): δ<sub>C</sub> 174.4, 168.6, 161.6, 153.1, 147.7, 146.5, 133.4, 133.1, 130.9, 127.7, 127.5, 125.4, 124.6, 122.3, 121.9, 118.6, 50.4. ESI-MS *m/z* 371 (M+H)<sup>+</sup>. Anal. Calcd. for C<sub>17</sub>H<sub>11</sub>ClN<sub>4</sub>O<sub>2</sub>S: C, 55.06; H, 2.99; N, 15.11; Found: C, 55.10; H, 3.00; N, 15.13.

**N-(Benzo[*d*]thiazol-2-yl)-2-(2-methyl-4-oxoquinazolin-3(4H)-yl)acetamide (QN\_31)**

The compound was synthesized according to the general procedure using *N*-(benzo[*d*]thiazol-2-yl)-2-chloroacetamide (**QN\_24b**) (0.154 g, 0.68 mmol) and 2-methylquinazolin-4(3*H*)-one

(**QN\_13a**) (0.1 g, 0.62 mmol) to afford **QN\_31** (0.14 g, 68.7 %) as pale yellow solid. M.p: 206-208 °C. <sup>1</sup>H NMR (DMSO-d<sub>6</sub>): δ<sub>H</sub> 10.61 (s, 1H), 8.22 – 7.49 (m, 8H), 4.41 (s, 2H), 2.53 (s, 3H). <sup>13</sup>C NMR (DMSO-d<sub>6</sub>): δ<sub>C</sub> 174.7, 168.7, 161.4, 154.5, 153.3, 147.2, 133.6, 131.0, 127.3, 126.7, 126.4, 125.1, 124.8, 121.9, 121.0, 118.5, 48.2, 22.1. ESI-MS m/z 351 (M+H)<sup>+</sup>. Anal. Calcd. for C<sub>18</sub>H<sub>14</sub>N<sub>4</sub>O<sub>2</sub>S: C, 61.70; H, 4.03; N, 15.99; Found: C, 61.73; H, 4.01; N, 15.97.

***N*-(Benzo[*d*]thiazol-2-yl)-2-(6-chloro-2-methyl-4-oxoquinazolin-3(4*H*)-yl)acetamide**  
(**QN\_32**)

The compound was synthesized according to the general procedure using *N*-(benzo[*d*]thiazol-2-yl)-2-chloroacetamide (**QN\_24b**) (0.126 g, 0.56 mmol) and 6-chloro-2-methylquinazolin-4(3*H*)-one (**QN\_13b**) (0.1 g, 0.51 mmol) to afford **QN\_32** (0.13 g, 69.7 %) as pale yellow solid. M.p: 237-239 °C. <sup>1</sup>H NMR (DMSO-d<sub>6</sub>): δ<sub>H</sub> 10.62 (s, 1H), 8.19 – 7.54 (m, 7H), 4.47 (s, 2H), 2.57 (s, 3H). <sup>13</sup>C NMR (DMSO-d<sub>6</sub>): δ<sub>C</sub> 174.5, 168.5, 161.3, 154.7, 153.3, 145.2, 133.6, 133.1, 130.9, 127.6, 127.4, 125.3, 124.4, 122.6, 122.0, 118.6, 48.3, 22.4. ESI-MS m/z 385 (M+H)<sup>+</sup>. Anal. Calcd. for C<sub>18</sub>H<sub>13</sub>ClN<sub>4</sub>O<sub>2</sub>S: C, 56.18; H, 3.40; N, 14.56; Found: C, 56.22; H, 3.42; N, 14.54.

***N*-(6-Nitrobenzo[*d*]thiazol-2-yl)-2-(4-oxoquinazolin-3(4*H*)-yl)acetamide** (**QN\_33**)

The compound was synthesized according to the general procedure using 2-chloro-*N*-(6-nitrobenzo[*d*]thiazol-2-yl)acetamide (**QN\_24c**) (0.20 g, 0.75 mmol) and quinazolin-4(3*H*)-one (**QN\_01a**) (0.1 g, 0.68 mmol) to afford **QN\_33** (0.18 g, 71.6 %) as pale yellow solid. M.p: 237-239 °C. <sup>1</sup>H NMR (DMSO-d<sub>6</sub>): δ<sub>H</sub> 9.33 (s, 1H), 8.64 – 7.58 (m, 8H), 4.56 (s, 2H). <sup>13</sup>C NMR (DMSO-d<sub>6</sub>): δ<sub>C</sub> 174.6, 168.5, 161.7, 159.4, 148.4, 147.7, 144.5, 133.8, 131.6, 127.4, 126.8, 126.5, 121.4, 120.9, 119.2, 117.3, 50.8. ESI-MS m/z 380 (M-H)<sup>-</sup>. Anal. Calcd. for C<sub>17</sub>H<sub>11</sub>N<sub>5</sub>O<sub>4</sub>S: C, 53.54; H, 2.91; N, 18.36; Found: C, 53.52; H, 2.93; N, 18.39.

**2-(6-Chloro-4-oxoquinazolin-3(4*H*)-yl)-*N*-(6-nitrobenzo[*d*]thiazol-2-yl)acetamide**  
(**QN\_34**)

The compound was synthesized according to the general procedure using 2-chloro-*N*-(6-nitrobenzo[*d*]thiazol-2-yl)acetamide (**QN\_24c**) (0.163 g, 0.60 mmol) and 6-chloroquinazolin-4(3*H*)-one (**QN\_01b**) (0.1 g, 0.55 mmol) to afford **QN\_34** (0.15 g, 69.5 %) as pale yellow solid. M.p: >280 °C. <sup>1</sup>H NMR (DMSO-d<sub>6</sub>): δ<sub>H</sub> 9.37 (s, 1H), 8.63 – 7.41 (m, 7H), 4.61 (s, 2H).

$^{13}\text{C}$  NMR (DMSO- $d_6$ ):  $\delta_{\text{C}}$  174.4, 168.6, 161.5, 159.4, 147.7, 146.6, 144.5, 133.5, 133.0, 131.4, 127.6, 127.3, 122.3, 121.5, 119.1, 117.4, 50.3. ESI-MS  $m/z$  414 (M-H) $^-$ . Anal. Calcd. for  $\text{C}_{17}\text{H}_{10}\text{ClN}_5\text{O}_4\text{S}$ : C, 49.10; H, 2.42; N, 16.84; Found: C, 49.13; H, 2.40; N, 16.86.

**2-(2-Methyl-4-oxoquinazolin-3(4H)-yl)-N-(6-nitrobenzo[d]thiazol-2-yl)acetamide (QN\_35)**

The compound was synthesized according to the general procedure using 2-chloro-*N*-(6-nitrobenzo[d]thiazol-2-yl)acetamide (**QN\_24c**) (0.184 g, 0.68 mmol) and 2-methylquinazolin-4(3H)-one (**QN\_13a**) (0.1 g, 0.62 mmol) to afford **QN\_35** (0.17 g, 71.9 %) as pale yellow solid. M.p: 196-198 °C.  $^1\text{H}$  NMR (DMSO- $d_6$ ):  $\delta_{\text{H}}$  9.36 (s, 1H), 8.65 – 7.68 (m, 7H), 4.59 (s, 2H), 2.49 (s, 3H).  $^{13}\text{C}$  NMR (DMSO- $d_6$ ):  $\delta_{\text{C}}$  174.6, 168.7, 161.4, 159.4, 154.5, 147.0, 144.2, 133.5, 131.4, 127.4, 126.5, 126.3, 121.3, 120.9, 119.4, 117.6, 48.4, 22.3. ESI-MS  $m/z$  394 (M-H) $^-$ . Anal. Calcd. for  $\text{C}_{18}\text{H}_{13}\text{N}_5\text{O}_4\text{S}$ : C, 54.68; H, 3.31; N, 17.71; Found: C, 54.71; H, 3.33; N, 17.74.

**2-(6-Chloro-2-methyl-4-oxoquinazolin-3(4H)-yl)-N-(6-nitrobenzo[d]thiazol-2-yl)acetamide (QN\_36)**

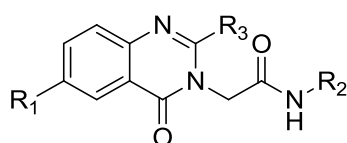
The compound was synthesized according to the general procedure using 2-chloro-*N*-(6-nitrobenzo[d]thiazol-2-yl)acetamide (**QN\_24c**) (0.152 g, 0.56 mmol) and 6-chloro-2-methylquinazolin-4(3H)-one (**QN\_13b**) (0.1 g, 0.51 mmol) to afford **QN\_36** (0.15 g, 71.6 %) as pale yellow solid. M.p: 234-236 °C.  $^1\text{H}$  NMR (DMSO- $d_6$ ):  $\delta_{\text{H}}$  9.39 (s, 1H), 8.67 – 7.39 (m, 6H), 4.57 (s, 2H), 2.44 (s, 3H).  $^{13}\text{C}$  NMR (DMSO- $d_6$ ):  $\delta_{\text{C}}$  174.5, 168.6, 161.7, 159.1, 154.5, 145.1, 144.4, 133.6, 133.1, 131.5, 127.6, 127.4, 122.3, 121.5, 119.3, 117.2, 48.2, 22.4. ESI-MS  $m/z$  428 (M-H) $^-$ . Anal. Calcd. for  $\text{C}_{18}\text{H}_{12}\text{ClN}_5\text{O}_4\text{S}$ : C, 50.30; H, 2.81; N, 16.29; Found: C, 50.33; H, 2.83; N, 16.32.

**5.2.4 *In vitro* Mycobacterium tuberculosis InhA inhibition assay, antimycobacterial potency and cytotoxicity studies of the synthesised molecules**

All the synthesized derivatives were first evaluated for their *in vitro* *Mycobacterium tuberculosis* InhA inhibitory potency as steps towards the derivation of structure-activity relationships and hit optimization. The compounds were further subjected to a whole cell screening against *Mycobacterium tuberculosis* H37Rv strain to understand their bactericidal potency using the agar dilution method and later the safety profile of these molecules were

evaluated by checking the *in vitro* cytotoxicity against RAW 264.7 cell line (mouse macrophage) at 100 and 50  $\mu\text{M}$  concentration by MTT assay, and the results are tabulated in **Table 5.5**.

**Table 5.5:** *In vitro* biological evaluation of the synthesized derivatives **QN\_04** – **QN\_11**, **QN\_16** – **QN\_23** and **QN\_25** – **QN\_36**.



| Comp  | R <sub>1</sub> | R <sub>2</sub> | R <sub>3</sub>  | % of InhA inhibition at 10 $\mu\text{M}$ <sup>a</sup> (IC <sub>50</sub> in $\mu\text{M}$ ) | MIC ( $\mu\text{M}$ ) <sup>b</sup> |                | Cytotoxicity <sup>c</sup> (% inhibition) |                     |
|-------|----------------|----------------|-----------------|--|------------------------------------|----------------|--|---------------------|
|       |                |                |                 |  | MTB                                | MTB (Piperine) | at 100 $\mu\text{M}$                     | at 50 $\mu\text{M}$ |
| QN_04 | H              |                | H               | 52.10±1.33   | 11.18                              | 5.58           | 31.10                                    | 21.20               |
| QN_05 | Cl             |                | H               | 58.34±2.64 (7.78±0.42)   | 4.97                               | 1.24           | 53.02                                    | 3.51                |
| QN_06 | H              |                | H               | 58.12±1.87 (8.16±0.34)   | 8.18                               | 2.04           | 35.63                                    | 10.12               |
| QN_07 | Cl             |                | H               | 80.12±2.75 (4.56±0.55)   | 3.74                               | 1.87           | 53.62                                    | 48.88               |
| QN_08 | H              |                | H               | 46.12±1.22   | 5.50                               | 2.75           | 13.74                                    | 1.96                |
| QN_09 | Cl             |                | H               | 82.43±2.67 (3.12±0.24)   | 4.91                               | 4.91           | 42.50                                    | 30.69               |
| QN_10 | H              |                | H               | 33.70±0.83   | 5.21                               | 1.30           | 41.36                                    | 4.38                |
| QN_11 | Cl             |                | H               | 68.90±0.77 (7.12±0.38)   | 9.36                               | 2.33           | 45.19                                    | 32.43               |
| QN_16 | H              |                | CH <sub>3</sub> | 60.12±0.54 (8.92±0.31)   | 10.65                              | 5.31           | 29.74                                    | 11.19               |
| QN_17 | Cl             |                | CH <sub>3</sub> | 88.12±1.74 (3.12±0.46)   | 4.76                               | 2.38           | 28.68                                    | 19.85               |
| QN_18 | H              |                | CH <sub>3</sub> | 56.12±1.22 (9.06±0.52)   | 15.79                              | 3.94           | 33.65                                    | 25.46               |

Contd...

| Comp  | R <sub>1</sub> | R <sub>2</sub> | R <sub>3</sub>  | % of InhA inhibition at 10 μM <sup>a</sup> (IC <sub>50</sub> in μM) | MIC (μM) <sup>b</sup> |                | Cytotoxicity <sup>c</sup> (% inhibition) |          |
|-------|----------------|----------------|-----------------|---|-----------------------|----------------|--|----------|
|       |                |                |                 |   | MTB                   | MTB (Piperine) | at 100 μM                                | at 50 μM |
| QN_19 | Cl             |                | CH <sub>3</sub> | 62.12±1.65 (7.16±0.33)  | 7.26                  | 3.62           | 25.76                                    | 17.23    |
| QN_20 | H              |                | CH <sub>3</sub> | 70.12±2.25 (6.86±0.31)  | 84.08                 | 42.04          | 41.46                                    | 25.52    |
| QN_21 | Cl             |                | CH <sub>3</sub> | 78.12±2.71 (4.52±0.38)  | 4.70                  | 1.17           | 5.37                                     | 3.36     |
| QN_22 | H              |                | CH <sub>3</sub> | 68.16±0.89 (6.01±0.66)  | 9.97                  | 4.97           | 38.65                                    | 35.57    |
| QN_23 | Cl             |                | CH <sub>3</sub> | 70.16±0.88 (6.76±0.57)  | 17.96                 | 4.48           | 51.67                                    | 47.51    |
| QN_25 | H              |                | H               | 41.23±0.38  | 37.72                 | 9.43           | 40.38                                    | 14.62    |
| QN_26 | Cl             |                | H               | 48.90±0.88  | 34.17                 | 17.08          | 39.96                                    | 39.56    |
| QN_27 | H              |                | CH <sub>3</sub> | 34.12±0.42  | 72.39                 | NT             | 21.31                                    | 4.78     |
| QN_28 | Cl             |                | CH <sub>3</sub> | 45.68±0.79  | 32.91                 | NT             | 39.54                                    | 31.23    |
| QN_29 | H              |                | H               | 40.44±0.66  | 37.16                 | NT             | 50.61                                    | 5.36     |
| QN_30 | Cl             |                | H               | 54.56±1.45  | 33.70                 | NT             | 46.34                                    | 38.42    |
| QN_31 | H              |                | CH <sub>3</sub> | 52.12±0.95  | >71.34                | NT             | 47.76                                    | 22.69    |
| QN_32 | Cl             |                | CH <sub>3</sub> | 60.32±1.62 (8.36±0.42)  | 16.24                 | NT             | 6.43                                     | 1.11     |
| QN_33 | H              |                | H               | 72.18±1.75 (5.12±0.46)  | 4.09                  | 1.02           | 50.54                                    | 13.08    |
| QN_34 | Cl             |                | H               | 45.62±0.97  | 30.06                 | 30.06          | 62.84                                    | 15.83    |
| QN_35 | H              |                | CH <sub>3</sub> | 64.02±1.55 (6.16±0.37)  | >63.22                | NT             | 37.43                                    | 33.98    |
| QN_36 | Cl             |                | CH <sub>3</sub> | 54.12±0.63  | 58.16                 | NT             | 33.67                                    | 28.39    |

Contd...

| Comp | R <sub>1</sub> | R <sub>2</sub>    | R <sub>3</sub> | % of InhA inhibition at 10 $\mu$ M <sup>a</sup> (IC <sub>50</sub> in $\mu$ M) | MIC ( $\mu$ M) <sup>b</sup> |                | Cytotoxicity <sup>c</sup> (% inhibition) |               |
|------|----------------|-------------------|----------------|---|-----------------------------|----------------|--|---------------|
|      |                |                   |                |   | MTB                         | MTB (Piperine) | at 100 $\mu$ M                           | at 50 $\mu$ M |
|      |                | <b>Isoniazid</b>  |                |   | 0.72                        | NT             | NT                                       | NT            |
|      |                | <b>Ethambutol</b> |                |   | 7.64                        | NT             | NT                                       | NT            |
|      |                | <b>Rifampicin</b> |                |   | 0.15                        | NT             | NT                                       | NT            |
|      |                | <b>Ofloxacin</b>  |                |   | 2.16                        | NT             | NT                                       | NT            |

IC<sub>50</sub>, 50% inhibitory concentration; MTB, *Mycobacterium tuberculosis*; MIC, minimum inhibitory concentration; NT, not tested

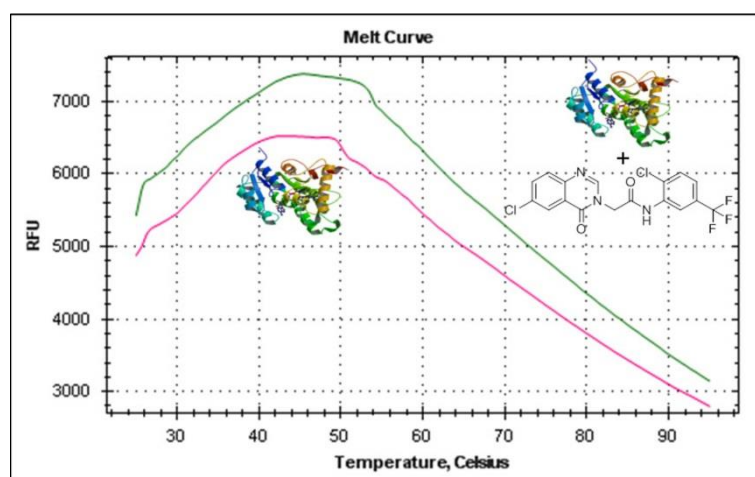
<sup>a</sup>MTB InhA enzyme inhibition activity

<sup>b</sup>*In vitro* activity against MTB H37Rv

<sup>c</sup>Against RAW 264.7 cells

### 5.2.5 Evaluation of protein interaction and stability using biophysical characterization experiment

One of the active compounds from this series was further investigated using a DSF. In our study, compound **QN\_07** showed significant positive T<sub>m</sub> shift of 2.2 °C confirming the stability of the protein-ligand complex as shown in **Figure 5.18**.

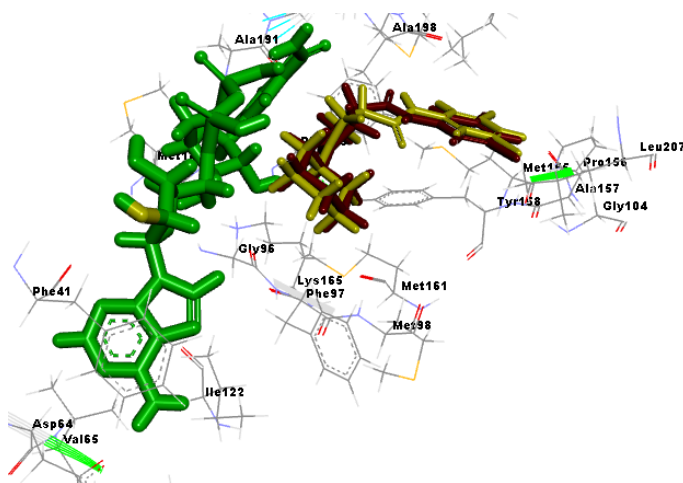


**Figure 5.18:** DSF experiment for compound **QN\_07** (protein-ligand complex, green) showing an increase in the thermal shift of 2.2 °C compared with the native InhA protein (pink). Protein T<sub>m</sub> 38.40 °C and protein with ligand T<sub>m</sub> 40.60 °C.



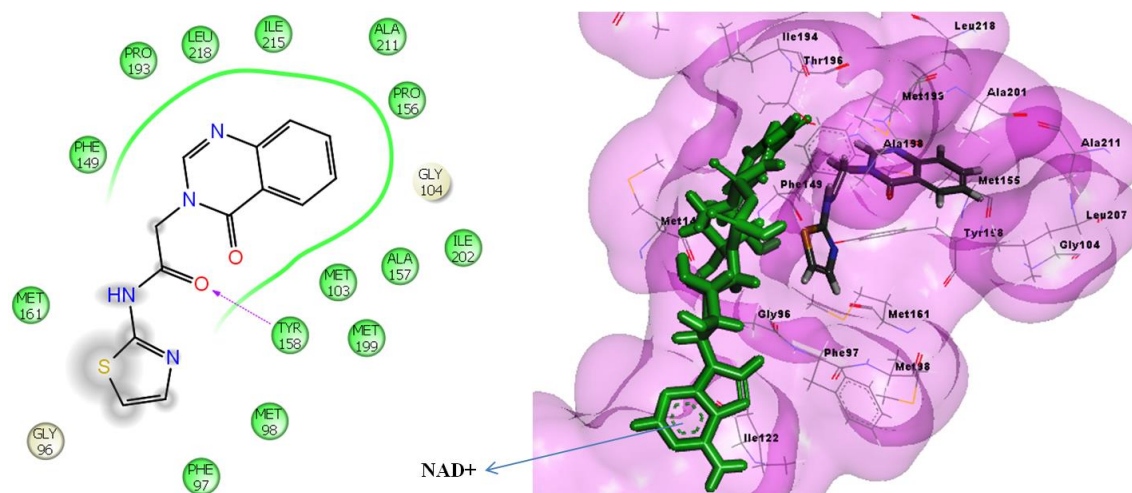
### 5.2.6 Discussion

To support the SAR, we carried out docking studies for all the synthesized compounds and compared with lead compound **UPS 17** (**Figure 5.14**). The crystal structure of *Mycobacterium tuberculosis* InhA complexed with reference inhibitor 1-cyclohexyl-*N*-(3,5-dichlorophenyl)-5-oxopyrrolidine-3-carboxamide (PDB ID: 2H7M with a resolution of 1.62Å) was downloaded and docking was carried out using Glide, version 5.7, Schrodinger, LLC (New York, NY, 2012). Analysis of the crystal structure of 2H7M revealed that the reference inhibitor in the InhA active site formed hydrogen bonding network with Tyr158, and the NAD<sup>+</sup> cofactor that probably served as the key feature to govern the orientation of the compound within the active site. Dual hydrogen bonding network involved the oxygen atom on the pyrrolidine carbonyl group, InhA catalytic residue Tyr158, and the NAD<sup>+</sup>. This hydrogen bonding network seemed to be conserved among all the InhA-inhibitor complexes identified so far. We also analysed the pi-stacking interactions at the active site cavity where some pi-stacking interactions were observed between the quinazoline nucleus and, Phe97 and Phe149 amino acid residues. All compounds showed pi-stacking interactions but were weak as compared to observed hydrogen bonding interactions. The reference inhibitor was re-docked with the active site residues of the InhA to validate the active site cavity. The ligand exhibited good Glide score of -8.02 kcal/mol and was found in the vicinity of amino acids Tyr158, Phe149, Met199, Ile215, Pro156, Leu218, Met155, Ala211, Ile202, Met103, Leu207, Ala157, Met161, Phe97, Met98, Gly96, Gly104 and Lys165. Re-docking results showed that the compound exhibited similar interactions as that of the original crystal structure and showed RMSD of 0.87 Å suggesting a high docking reliability of the docking method in terms of reproducing the experimentally observed binding mode. The superimposition of Glide docked conformation of co-crystal with the original crystal pose of 2H7M is shown in **Figure 5.19**.



**Figure 5.19:** Superimposition of docked pose of the reference inhibitor (Yellow) to the original pose of the reference inhibitor (Red).

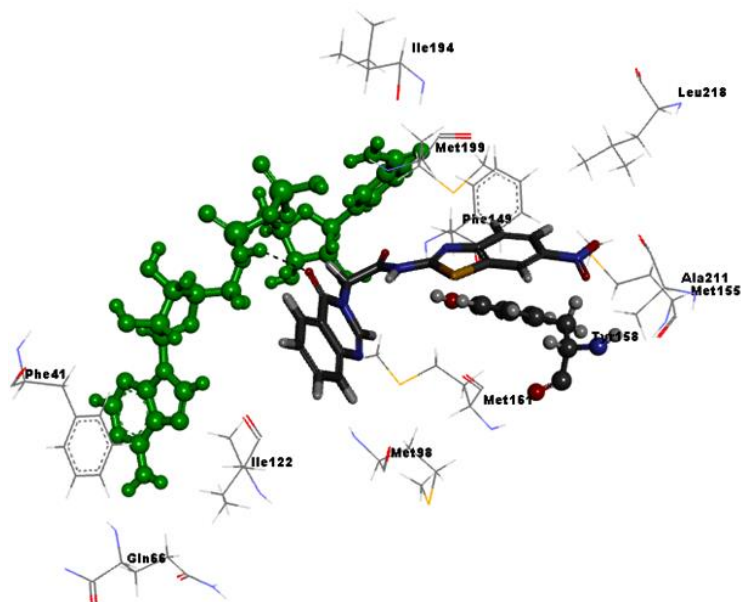
With the aim of getting insights into the structural basis of activity, lead compound **UPS 17** was analysed in more detail. Docking of the lead compound 2-(4-oxo-3,4-dihydroquinazolin-3-yl)-*N*-(1,3-thiazol-2-yl)acetamide (**UPS 17**) within the active site of the InhA protein is illustrated in **Figure 5.20**. The predicted bound conformation of the lead compound **UPS 17** showed that the oxygen atom of carbonyl group of the acetamide linker formed a hydrogen bonding network with the side chain of the Tyr158. The quinazolin-4(3*H*)-one ring was surrounded by hydrophobic amino acids such as Phe149, Pro193, Leu218, Ile215, Ala211, Pro156, Ala157, Met103 and Met199. The thiazole ring was enclosed by hydrophobic amino acids such as Met98, Phe97 and Met161. The compound was very well fit in the active site cavity with docking score of -6.75 kcal/mol. The effect of various aryl/heteroaryl substitutions at the R<sub>2</sub> position was explored. As shown in **Table 5.5**, all the compounds showed % inhibition in the range of 88.12 to 33.70% at 10  $\mu$ M concentration against *Mycobacterium tuberculosis* InhA which was better than the lead compound **UPS 17** (31% at 10  $\mu$ M).



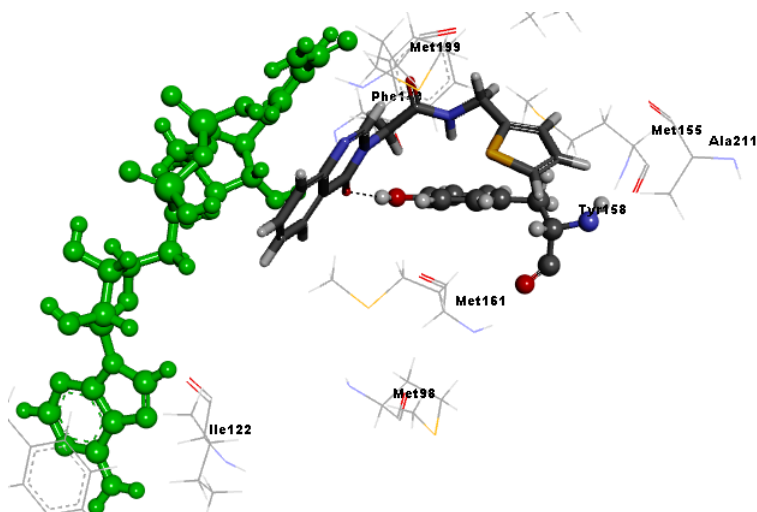
**Figure 5.20:** Binding pose and its interaction pattern of lead molecule **UPS 17**.

The first subset of compounds (**QN\_04**, **QN\_06**, **QN\_08**, **QN\_10**, **QN\_25**, **QN\_29** and **QN\_33**), with various aryl/heteroaryl groups at R<sub>2</sub> position through an acetamide linker is shown in **Table 5.5**. The phenyl group substituent at the R<sub>2</sub> position (compound **QN\_04**) displayed good InhA inhibitory activity. Compound containing substitution at 2<sup>nd</sup> and 5<sup>th</sup> position of the phenyl ring (2-chloro-5-(trifluoromethyl)-2-phenyl group) (compound **QN\_06**) provided moderate InhA inhibitory activity, whereas introduction of 2-furylmethyl group at R<sub>2</sub> position (compound **QN\_08**) slightly reduced InhA inhibitory activity. The compounds substituted with heteroaryl groups such as 2-benzothiazoyl and 5-nitro-2-thiazolyl group (compound **QN\_29** and **QN\_25** respectively) at R<sub>2</sub> position resulted in satisfactory *in vitro* InhA inhibitory activity. The 6-nitro-2-benzothiazolyl group substituent at the R<sub>2</sub> position (compound **QN\_33**) displayed highest activity with IC<sub>50</sub> of 5.12 μM whereas 2-thiophenylmethyl ring at the R<sub>2</sub> position (compound **QN\_10**) led to less potency compared to other compounds from this subset. The *in vitro* InhA inhibitory activity of compounds from this subset was in the range of 72.18 to 33.70% at 10 μM concentrations and the docking score was found in the range of -7.61 to -7.27 kcal/mol suggesting that these compounds were well fit in the active site of the InhA enzyme. Docking analysis of compound **QN\_33** at the active site revealed hydrogen bonding interaction with the hydroxyl ribose group of the NAD<sup>+</sup> whereas interaction with Tyr158 was found missing (**Figure 5.21**). The 6-nitro-2-benzothiazolyl ring was buried into the hydrophobic pocket and was found to make contacts with Tyr158, Ile215, Met155, Leu218, Pro156, Ala157, Met103 and. Apart from hydrophobic interactions the nitro group present at 6<sup>th</sup> position on benzothiazole ring made polar contact with Gln214. On the other hand, compound **QN\_10** was found to be

oriented in a similar manner to that of lead **UPS 17** retaining hydrogen bonding with Tyr158, but failed to demonstrate any interaction with hydroxyl ribose group of the NAD<sup>+</sup> which was earlier demonstrated to be crucial for activity and specificity observed at the enzyme level and thus may have resulted in reduced activity (**Figure 5.22**).



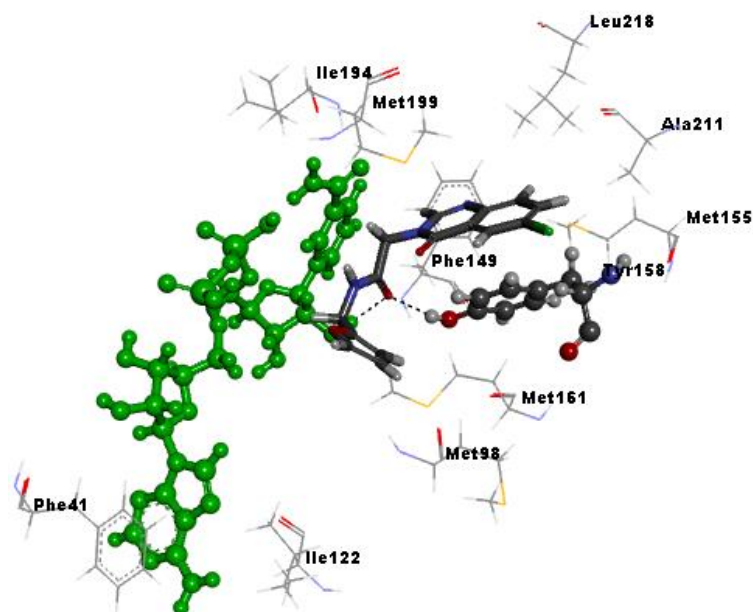
**Figure 5.21:** Binding pose and its interaction pattern of the compound **QN\_33** in the active site of the InhA protein.



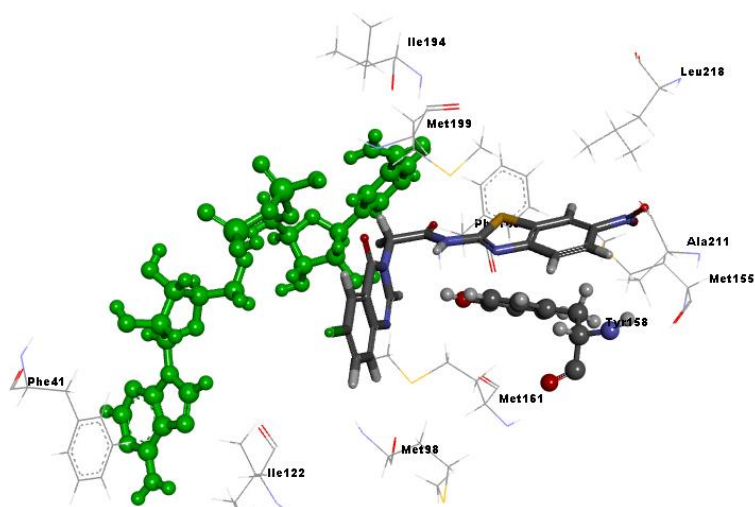
**Figure 5.22:** Interacting pattern of the compound **QN\_10** in the active site of the InhA protein.

In the second subset of compounds (**QN\_05**, **QN\_07**, **QN\_09**, **QN\_11**, **QN\_26**, **QN\_30** and **QN\_34**), effect of chloro group substituent at R<sub>1</sub> position on the quinazolin-4(3*H*)-one ring

was investigated to understand the effect of similar aryl/heteroaryl substituents at R<sub>2</sub> position. The SAR study revealed that, hydrophobic chloro group at R<sub>1</sub> position increased hydrophobicity of the compounds and hydrophobic interactions with the active site which was crucial for inhibition of the enzyme. This subset of compounds displayed better potency than the previous subset. Here, all the compounds showed satisfactory *in vitro* InhA inhibitory activity in the range of 82.43 to 45.62 % at 10 μM concentration. The compounds **QN\_07**, **QN\_11** and **QN\_05** with 2-chloro-5-(trifluoromethyl)-2-phenyl, 2-thiophenylmethyl and phenyl groups respectively as R<sub>2</sub> substituents showed good InhA enzyme inhibition activity (IC<sub>50</sub> of 4.56, 7.12, and 7.78 μM respectively). It was observed that substitution with heteroaryl groups such as 2-benzothiazolyl, 6-nitro-2-benzothiazolyl and 5-nitro-2-thiozolyl group at R<sub>2</sub> position (respectively **QN\_30**, **QN\_34** and **QN\_26**) was somewhat less favoured than the other substitutions at the R<sub>2</sub> position. Compound **QN\_09** with 2-furylmethyl ring as R<sub>2</sub> substituent exhibited the most promising inhibitory potency with IC<sub>50</sub> of 3.12 μM whereas compound **QN\_34** with 6-nitro-2-benzothiazolyl group at R<sub>2</sub> position showed lesser potency compared to other compounds from this subset. The ligand binding analysis of compound **QN\_09** revealed two hydrogen bonding interactions by oxygen atom of carbonyl group of the acetamide linker with the enzyme, first with side chain of Tyr158 and another with the ribose hydroxyl group of the NAD<sup>+</sup>, correlating with the protein–inhibitor complex interactions outlined in InhA crystal structure. The compound was very well fit in to the active site cavity of the protein with docking score of -7.86 kcal/mol and the 6-chloroquinazolin-4(3*H*)-one ring was surrounded by hydrophobic amino acids residues such as Phe149, Leu218, Ile215, Pro156, Met103, Ala211, Ala157, Ile202 and Leu207. The 2-furylmethyl ring was enclosed by hydrophobic amino acids like Met161, Phe97 and Met98 (**Figure 5.23**). Also, the orientation of compound **QN\_09** was found to be similar to that of crystal ligand exhibiting a very good fitness in the active site pocket making this compound more potent. The ligand binding analysis of one of the less active derivative from this subset (compound **QN\_34**) demonstrated that it was well inserted into the hydrophobic cavity but failed to produce any hydrogen bonding interactions with the protein which explained its reduced activity (**Figure 5.24**).



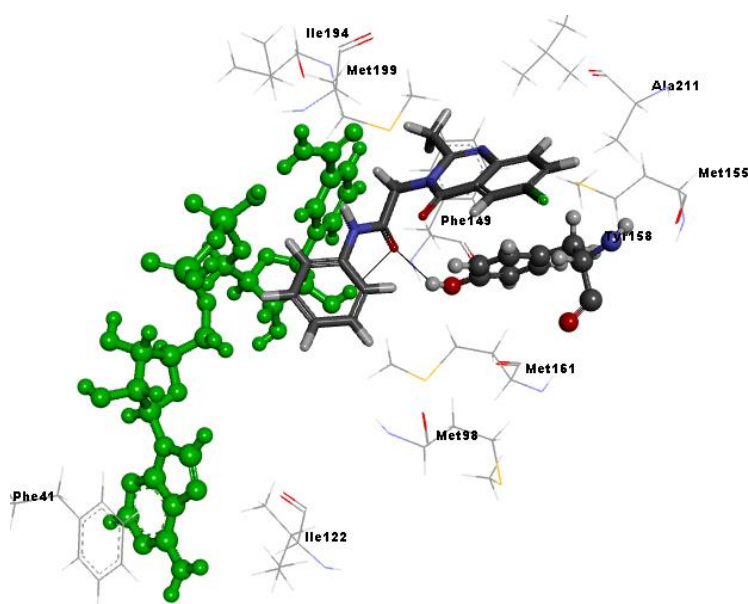
**Figure 5.23:** Binding pose and its interaction pattern of the compound **QN\_09** in the active site of the InhA protein.



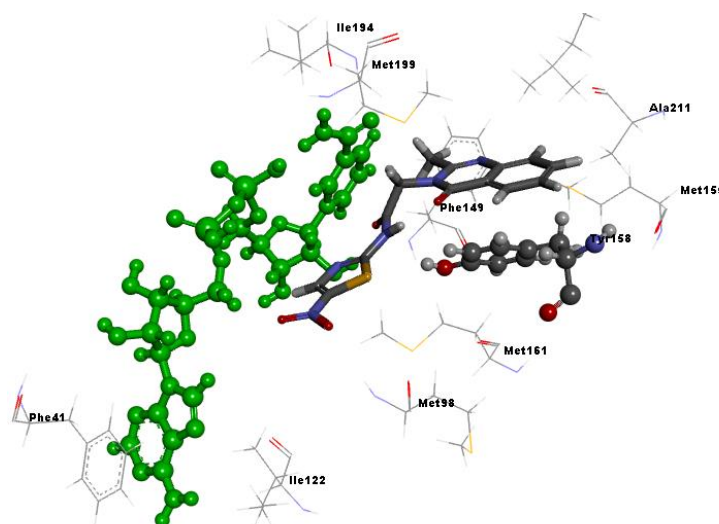
**Figure 5.24:** Interacting pattern of the compound **QN\_34** in the active site of the InhA protein.

The third subset of compounds (**QN\_16**, **QN\_18**, **QN\_20**, **QN\_22**, **QN\_27**, **QN\_31** and **QN\_35**) consisted of methyl substituent at  $R_3$  position on the quinazolin-4(3*H*)-one ring and  $R_2$  was substituted with various aryl/heteroaryl groups same as that of the above two subsets as shown in **Table 5.5**. Here, all the 7 compounds exhibited inhibitory potency in the range of 70.12 to 34.12 %. Compounds **QN\_20** and **QN\_35** with 2-furylmethyl and 6-nitro-2-

benzothiazolyl groups respectively at R<sub>2</sub> position, showed good InhA inhibition potency with IC<sub>50</sub> of 6.86 and 6.16 μM respectively, whereas compounds with phenyl and 2-chloro-5-(trifluoromethyl)-2-phenyl groups at R<sub>2</sub> position (compounds **QN\_16** and **QN\_18** respectively), showed moderate IC<sub>50</sub> of 8.92 and 9.06 μM. It was interesting to note that compound substituted with 2-thiophenemethyl ring as R<sub>2</sub> substituent (compound **QN\_22**) exhibited the most promising inhibitory potency (IC<sub>50</sub> of 6.01 μM) whereas compound **QN\_27** substituted with 5-nitro-2-thiozoly group at R<sub>2</sub> position showed less potency compared to other compounds from this subset. Closer analysis of compound **QN\_22** in the binding site revealed hydrogen bonding interactions with side chain of Tyr158 as well as ribose hydroxyl group of the NAD<sup>+</sup> similar to other active compounds. The compound was well placed in the active site of the protein and further stabilized by the hydrophobic interaction with Phe149, Leu218, Met155, Pro156, Ala157, Ile215, Met199 and Met103 (**Figure 5.25**). One of the less active derivatives from this subset, compound **QN\_27** showed low docking score of -5.46 kcal/mol as compared to other active compounds and though the compound was well inserted into the active site pocket of the protein, it was not involved in any hydrogen bonding interactions resulting in reduced activity (**Figure 5.26**).



**Figure 5.25:** Interacting pattern of the compound **QN\_22** in the active site of the InhA protein.

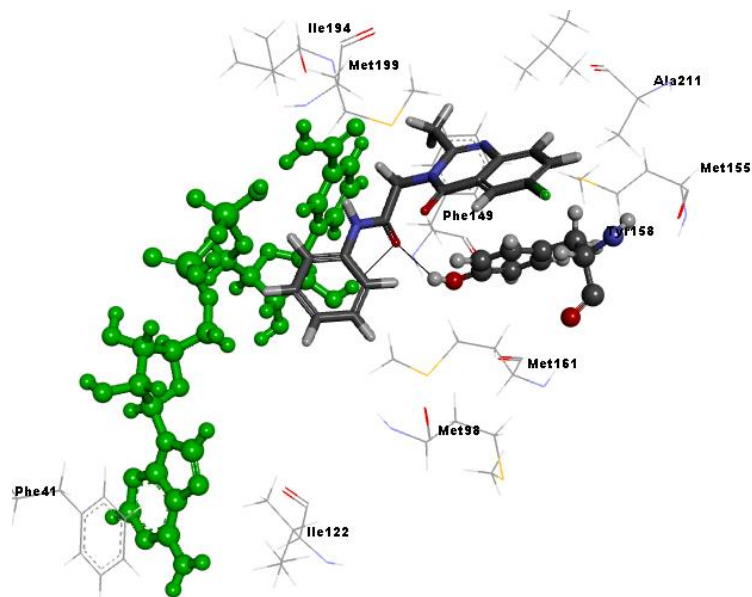


**Figure 5.26:** Interacting pattern of the compound **QN\_27** in the active site of the InhA protein.

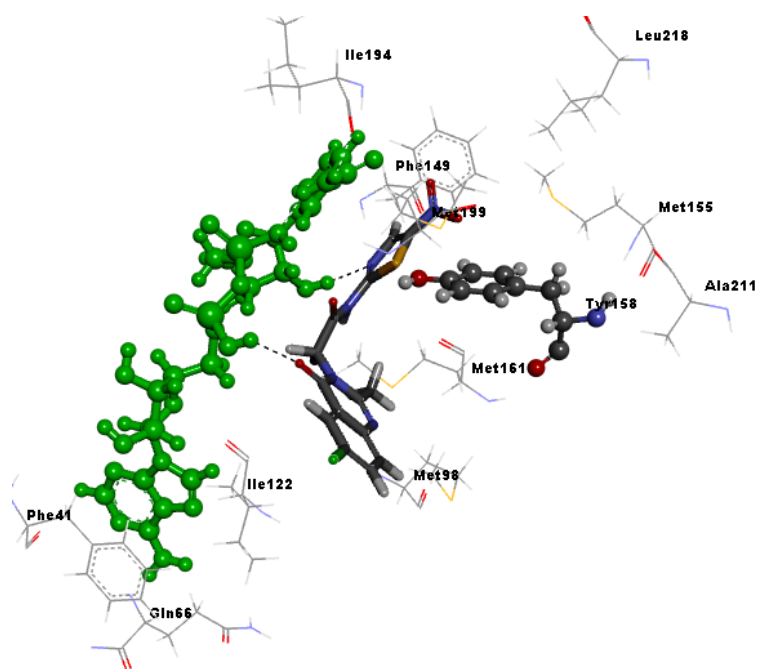
In the fourth subset of compounds (**QN\_17**, **QN\_19**, **QN\_21**, **QN\_23**, **QN\_28**, **QN\_32** and **QN\_36**) effect of chloro group at  $R_1$  position and methyl group at  $R_3$  position on the quinazolin-4(3*H*)-one ring was investigated to understand the effect of same aryl/heteroaryl substituent's at  $R_2$  position. In this subset, all the compounds exhibited good inhibitory potency in the range of 88.12 to 45.68 %. Compounds substituted with 2-furylmethyl and 2-thiophenylmethyl group at  $R_3$  position (**QN\_21** and **QN\_23**) displayed good inhibitory potency ( $IC_{50}$  of 4.52 and 6.76  $\mu$ M respectively). It was noted that heteroaryl 5-nitro-2-thiazolyl, 6-nitro-2-benzothiazolyl and 2-benzothiazolyl group substitutions (compounds **QN\_28**, **QN\_36** and **QN\_32**) were less favoured than other substituents at  $R_2$  position. Compound **QN\_17** where the phenyl ring was substituted at  $R_2$  position emerged as most active compound among the entire series with InhA inhibitory  $IC_{50}$  of 3.12  $\mu$ M which was well supported by a very good interaction profile in docking study as well with a glide docking score of -8.06 kcal/mol. The *in silico* analysis of the most active compound **QN\_17** displayed two hydrogen bonding interactions, one with the side chain of Tyr158 and another with ribose hydroxyl group of the NAD<sup>+</sup> with similar orientation to that of crystal ligand which was considered to be crucial for bioactivity making this compound more potent (**Figure 5.27**). Further the 6-chloro-2-methylquinazolin-4(3*H*)-one ring was oriented deeply into the hydrophobic pocket and found to be stabilized by hydrophobic interactions with the Pro193, Ile215, Leu218, Pro156, Ala211, Ile202, Met103, Leu207, Ala157, and Met199. The ligand binding analysis of one of the less active compound **QN\_28** showed its association



with two hydrogen bonding interactions with  $\text{NAD}^+$ , but it was disorientated in the active site of protein along with low docking energy of  $-6.05$  kcal/mol (**Figure 5.28**).



**Figure 5.27:** Interacting pattern of the compound QN\_17 at the active site of the InhA protein.



**Figure 5.28:** Binding pose and its interaction pattern of the compound QN\_28 in the active site of the InhA protein.

From the docking results, presence of hydrogen bonds with side chain of Tyr158 and hydroxyl group of NAD<sup>+</sup> along with hydrophobic interactions with the active site were predicted to be the most crucial factors affecting the inhibitory potency of these compounds. An analysis of enzyme inhibition activity revealed the following trend at R<sub>1</sub> and R<sub>3</sub> positions. (R<sub>1</sub> = chloro group, R<sub>3</sub> = methyl group) > (R<sub>1</sub> = chloro group, R<sub>3</sub> = H atom) > (R<sub>1</sub> = H atom, R<sub>3</sub> = methyl group) > (R<sub>1</sub> = R<sub>3</sub> = H atom). In case of substitution at R<sub>2</sub> position, substitution with 2-furylmethyl and 2-thiophenylmethyl group was more favoured than aryl/heteroaryl groups such as 6-nitro-2-benzothiazolyl, 2-chloro-5-(trifluoromethyl)-2-phenyl, phenyl, 2-benzothiazolyl and 5-nitro-2-thiazolyl group.

In case of antimycobacterial activity, all synthesized compounds showed activity against *Mycobacterium tuberculosis* with MIC ranging from 3.74 to 84.08 μM. Six compounds (QN\_05, QN\_07, QN\_09, QN\_17, QN\_21 and QN\_33) inhibited *Mycobacterium tuberculosis* with MIC of <5 μM. Compound QN\_17 which showed IC<sub>50</sub> of 3.12±0.46 μM in the *Mycobacterium tuberculosis* InhA enzyme inhibition activity, showed *Mycobacterium tuberculosis* MIC of 4.76 μM. In general compounds which contained (sub)-nitrothiazolyl, -benzothiazolyl and -nitrobenzothiazolyl showed higher MIC as compared to other compounds in this series. Some of the compounds failed to exhibit inhibition of *Mycobacterium tuberculosis* despite good potency in the enzyme inhibition study, and this could be a major challenge in TB drug discovery. Among other causes, efflux mechanisms contribute in a major way to intrinsic resistance to drugs. In the current work, we repeated the *Mycobacterium tuberculosis* screening of the synthesized compounds in presence of reported efflux pump inhibitor piperine (8 μg/mL). In most of the cases MIC decreased 2 to 4 fold when compared to absence of an efflux pump inhibitor. Compound QN\_17 showed *Mycobacterium tuberculosis* MIC of 2.38 μM in the presence of piperine and the *Mycobacterium tuberculosis* InhA IC<sub>50</sub> was well correlated as shown in **Table 5.5**.

The safety profile of all of the compounds was also assessed by testing their *in vitro* cytotoxicity against RAW 264.7 cells at 100 and 50 μM concentrations using the MTT assay as described in the materials and methods section. Most of the tested compounds were not cytotoxic (less than 50% inhibition at 50 μM) to RAW 264.7 cells and their percentage growth inhibitions are reported in **Table 5.5**. The most active *Mycobacterium tuberculosis* InhA inhibitor (compound QN\_17) showed no cytotoxicity (19.85 and 28.68 % inhibition at 50 and 100 μM drug concentrations respectively).

All the synthesized derivatives were further evaluated for their predicted ADMET properties using the QikProp3.5 module of Schrodinger software. A preliminary view of pharmacokinetic parameters depicted that many hits preserved the basic criterion of drug-likeness showing characteristics (as shown in **Table 5.6**) of a promising drug candidate, but some compounds were predicted to be associated with hERG cardiotoxicity. The most active compound from this series **QN\_17** was predicted to have excellent membrane permeability albeit its predicted hERG cardiotoxicity may impede its further development as a promising drug-candidate. All compounds were predicted to obey Lipinski rule of five which is considered crucial from pharmaceutical point of view.

**Table 5.6:** QikProp analysis of the ADMET properties of the synthesized derivatives **QN\_04** – **QN\_11**, **QN\_16** – **QN\_23** and **QN\_25** – **QN\_36**.

| Comp  | QPlogPo/w <sup>a</sup> | QPlogHERG <sup>b</sup> | QPPCaco <sup>c</sup> | QPlogBB <sup>d</sup> | QPPMDCK <sup>e</sup> | Percent Human Oral Absorption <sup>f</sup> | Rule of Five <sup>g</sup> |
|-------|------------------------|------------------------|----------------------|----------------------|----------------------|--|---------------------------|
| QN_04 | 2.16                   | -6.25                  | 1146.60              | -0.57                | 573.54               | 94.40                                      | 0                         |
| QN_05 | 2.56                   | -6.18                  | 1146.99              | -0.41                | 1415.36              | 96.75                                      | 0                         |
| QN_06 | 3.60                   | -5.84                  | 1499.21              | -0.05                | 6113.82              | 100  | 0                         |
| QN_07 | 4.04                   | -5.77                  | 1499.66              | 0.09                 | 10000                | 100  | 0                         |
| QN_08 | 1.21                   | -4.68                  | 599.92               | -0.70                | 484.81               | 83.79                                      | 0                         |
| QN_09 | 1.69                   | -4.60                  | 600.39               | -0.55                | 1196.62              | 86.62                                      | 0                         |
| QN_10 | 1.78                   | -4.43                  | 798.88               | -0.49                | 1098.57              | 89.37                                      | 0                         |
| QN_11 | 2.29                   | -4.44                  | 776.11               | -0.35                | 2583.63              | 92.10                                      | 0                         |
| QN_16 | 2.47                   | -6.19                  | 1553.69              | -0.44                | 796.51               | 100  | 0                         |
| QN_17 | 2.83                   | -6.12                  | 1553.34              | -0.29                | 1964.37              | 100  | 0                         |
| QN_18 | 3.91                   | -5.89                  | 1889.35              | 0.03                 | 8019.62              | 100  | 0                         |
| QN_19 | 4.39                   | -5.79                  | 1891.13              | 0.18                 | 10000                | 100  | 0                         |
| QN_20 | 1.57                   | -4.62                  | 852.81               | -0.58                | 672.89               | 88.59                                      | 0                         |
| QN_21 | 2.05                   | -4.54                  | 852.33               | -0.42                | 1659.69              | 91.42                                      | 0                         |
| QN_22 | 2.19                   | -4.56                  | 953.25               | -0.42                | 1397.01              | 93.12                                      | 0                         |
| QN_23 | 2.68                   | -4.49                  | 950.68               | -0.26                | 3441.07              | 95.95                                      | 0                         |
| QN_25 | 1.49                   | -3.70                  | 16.76                | -1.87                | 11.39                | 57.62                                      | 0                         |
| QN_26 | 2.07                   | -3.63                  | 16.77                | -1.75                | 28.10                | 61.03                                      | 0                         |
| QN_27 | 1.86                   | -3.52                  | 23.12                | -1.71                | 15.77                | 62.26                                      | 0                         |
| QN_28 | 2.57                   | -3.45                  | 23.14                | -1.58                | 38.94                | 66.41                                      | 0                         |
| QN_29 | 2.09                   | -6.39                  | 649.10               | -0.77                | 496.68               | 89.52                                      | 0                         |
| QN_30 | 2.58                   | -6.31                  | 649.46               | -0.62                | 1225.96              | 92.42                                      | 0                         |
| QN_31 | 2.45                   | -6.33                  | 878.36               | -0.64                | 688.74               | 94.01                                      | 0                         |
| QN_32 | 2.94                   | -6.25                  | 878.25               | -0.49                | 1698.77              | 96.84                                      | 0                         |
| QN_33 | 1.39                   | -6.34                  | 77.64                | -1.87                | 49.98                | 68.91                                      | 0                         |

Contd...

| Comp  | QPlogPo/w <sup>a</sup> | QPlogHERG <sup>b</sup> | QPPCaco <sup>c</sup> | QPlogBB <sup>d</sup> | QPPMDCK <sup>e</sup> | Percent Human Oral Absorption <sup>f</sup> | Rule of Five <sup>g</sup> |
|-------|------------------------|------------------------|----------------------|----------------------|----------------------|--|---------------------------|
| QN_34 | 1.87                   | -6.25                  | 77.66                | -1.75                | 123.33               | 71.74                                      | 0                         |
| QN_35 | 1.74                   | -6.28                  | 105.06               | -1.76                | 69.30                | 73.33                                      | 0                         |
| QN_36 | 2.22                   | -6.19                  | 105.03               | -1.63                | 170.91               | 76.16                                      | 0                         |

<sup>a</sup>Predicted octanol/water partition coefficient logP (acceptable range: -2.0 to 6.5)

<sup>b</sup>Predicted IC<sub>50</sub> value for blockage of hERG K<sup>+</sup> channels.(below -5)

<sup>c</sup>Predicted apparent Caco-2 cell permeability in nm/sec (<25 poor; >500 great)

<sup>d</sup>Predicted brain/blood partition coefficient (-3.0 to 1.2)

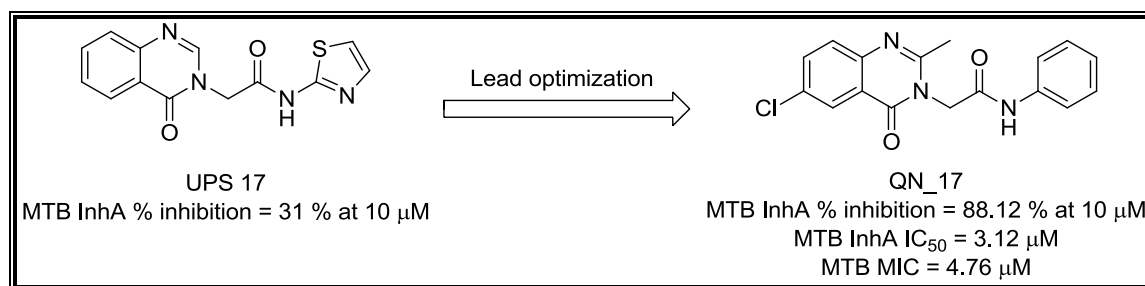
<sup>e</sup>Predicted apparent MDCK cell (model for blood-brain barrier) permeability in nm/s. (< 25 poor, > 500 great)

<sup>f</sup>Percent human oral absorption (< 25% is poor and > 80% is high)

<sup>g</sup>Rule of 5 violation (mol\_MW < 500, QPlogPo/w < 5, donorHB ≤ 5, acptHB ≤ 10) (concern above 1)

### 5.2.7 Highlights of the study

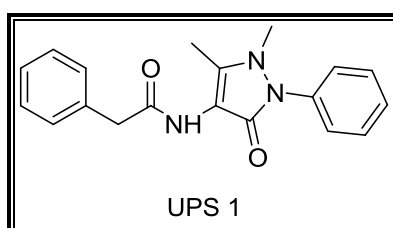
In present work, we report the synthesis and screening results of twenty eight substituted 2-(4-oxoquinazolin-3(4*H*)-yl)acetamide derivatives against *Mycobacterium tuberculosis* InhA as well as drug sensitive *Mycobacterium tuberculosis* strain. All the synthesized compounds showed better InhA inhibition as compared to lead molecule, and compound **QN\_17** emerged as the most active compound exhibiting 88.12 % inhibition of InhA at 10 μM with an IC<sub>50</sub> of 3.12 μM. It inhibited drug sensitive *Mycobacterium tuberculosis* with MIC of 4.76 μM and was non-cytotoxic at 100 μM (**Figure 5.29**).



**Figure 5.29:** Chemical structure and biological activity of the most active compound **QN\_17**.

### 5.3 Development of 4-amino-1,5-dimethyl-2-phenyl-1*H*-pyrazol-3(2*H*)-one derivatives as potential *Mycobacterium tuberculosis* InhA inhibitors

In continuation to our efforts to increase the molecular diversity in the series of antimicrobial InhA inhibitors, we envisaged that re-engineering the previously reported lead *N*-(1,5-dimethyl-3-oxo-2-phenyl-2,3-dihydro-1*H*-pyrazol-4-yl)-2-phenylacetamide (**UPS 1** shown in **Figure 5.30** identified by our research group earlier) with *Mycobacterium tuberculosis* InhA IC<sub>50</sub> 16.01±0.79 μM could deliver more potent hits with better antimycobacterial activities [Kumar U.C. *et al.*, 2013]. A thorough investigation into the interaction profile of the lead molecule enlightened us the importance of retaining the pyrazolone core in activity determination. Hence it was decided to retain the 4-amino-1,5-dimethyl-2-phenyl-1*H*-pyrazol-3(2*H*)-one core in the initial SAR studies and introduce structural diversity by exploring various substitutions of amino group at the 4<sup>th</sup> position of the pyrazolone nucleus. Further analysis of the lead molecules enabled us to design the reaction sequence as depicted in **Figure 5.31** for achieving the desired scaffold 4-amino-1,5-dimethyl-2-phenyl-1*H*-pyrazol-3(2*H*)-one (**PR\_03**) for further optimization in the hit expansion step.

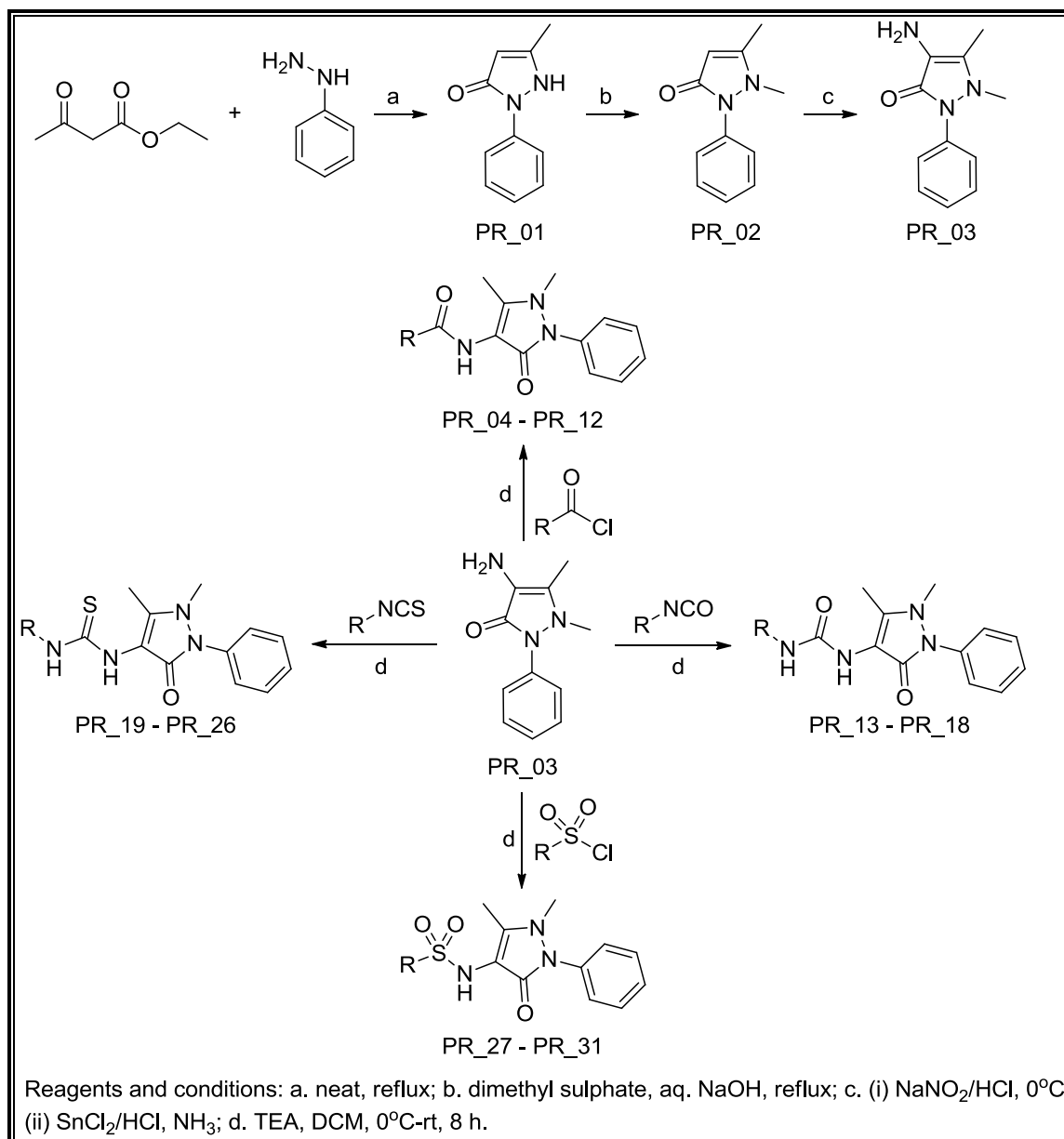


**Figure 5.30:** Chemical structure of lead molecule **UPS 1**.

#### 5.3.1 Chemical synthesis and characterization

The synthesis started with commercially available and relatively cheap starting materials, ethyl acetoacetate and phenyl hydrazine, which were fused together at 180-185 °C to give 5-methyl-2-phenyl-1*H*-pyrazol-3(2*H*)-one (**PR\_01**) in 78 % yield. This on subsequent methylation at the N-1 position with dimethyl sulphate under refluxing condition gave 1,5-dimethyl-2-phenyl-1*H*-pyrazol-3(2*H*)-one (**PR\_02**) in desired yield and purity. The amino group at the 4<sup>th</sup> position of the pyrazolone nucleus was achieved by nitrosation followed by reduction to give 4-amino-1,5-dimethyl-2-phenyl-1*H*-pyrazol-3(2*H*)-one (**PR\_03**) in good yield [Lattmann E. *et al.*, 2007]. The final library was then assembled by treating the so obtained 4-amino-1,5-dimethyl-2-phenyl-1*H*-pyrazol-3(2*H*)-one (**PR\_03**) with respective

substituted acid chlorides, substituted phenyl/benzyl isocyanates and isothiocyanates, and substituted sulfonyl chlorides to give the corresponding amides (**PR\_04 – PR\_12**), ureas (**PR\_13 – PR\_18**), thioureas (**PR\_19 – PR\_26**), and sulphonamides (**PR\_27 – PR\_31**), as depicted in **Figure 5.31** and **Table 5.7**.



**Figure 5.31:** Synthetic protocol utilized for synthesis of compounds **PR\_04 – PR\_31**.

### 5.3.2 Experimental protocol utilised for synthesis

#### Procedure for the synthesis of 5-methyl-2-phenyl-1*H*-pyrazol-3(2*H*)-one (PR\_01)

A mixture of ethyl acetoacetate (5.0 g, 38.42 mmol) and phenylhydrazine (4.0 g, 36.98 mmol) was refluxed for about 2 h (monitored by TLC & LCMS for completion). The heavy reddish syrup formed during reflux, which solidified upon cooling to rt was stirred with diethyl ether (10 mL). The residue was filtered and then washed with diethyl ether (2 × 5 mL), and further upon recrystallization from hot water gave desired product **PR\_01** in pure form (5.2 g, 78.2 %).

#### Procedure for the synthesis of 1,5-dimethyl-2-phenyl-1*H*-pyrazol-3(2*H*)-one (PR\_02)

Dimethyl sulphate (3.6 g, 28.54 mmol) was added dropwise to a warm mixture of 5-methyl-2-phenyl-1*H*-pyrazol-3(2*H*)-one (**PR\_01**) (5.0 g, 28.72 mmol) in methanol (3 mL) and 1 N sodium hydroxide (20 mL). The mixture was refluxed for 1 h (monitored by TLC & LCMS for completion), and allowed to cool to rt with stirring. The solvent was then removed under reduced pressure and the residue further diluted with water (15 mL). The aqueous layer was extracted with DCM (20 mL), and the organic layer dried over anhydrous sodium sulphate and evaporated under reduced pressure. The residue was further purified by silica gel column chromatography using hexane: ethyl acetate as eluent to give the 1,5-dimethyl-2-phenyl-1*H*-pyrazol-3(2*H*)-one (**PR\_02**) (3.92 g, 72.6 %).

#### Procedure for the synthesis of 4-amino-1,5-dimethyl-2-phenyl-1*H*-pyrazol-3(2*H*)-one (PR\_03)

A solution of 1,5-dimethyl-2-phenyl-1*H*-pyrazol-3(2*H*)-one (**PR\_02**) (3.5 g, 18.59 mmol) in concentrated hydrochloric acid (20 mL) was warmed and carefully diluted with water (upto 100 mL) followed by dropwise addition of solution of sodium nitrite (1.3 g, 18.59 mmol) in water (20 mL) at 0 °C with stirring. The solution was allowed to stand for about 1 h and the precipitate formed was filtered and washed with ice-cold water. The residue was further dissolved in ethanol (85 mL) and to this solution was added dropwise a hot mixture of stannous chloride (7.2 g, 29.14 mmol) in 20 % hydrochloric acid (40 mL). The mixture was allowed to cool slowly to rt, and allowed to stand overnight. To this mixture was then added concentrated ammonia solution dropwise until no further precipitation occurred. The precipitate was filtered, washed with ethanol (5 mL) and purified by silica gel column



chromatography using hexane: ethyl acetate as eluent to give 4-amino-1,5-dimethyl-2-phenyl-1*H*-pyrazol-3(2*H*)-one (**PR\_03**) (1.34 g, 42.3 %).

**Procedure for the synthesis of substituted *N*-(1,5-dimethyl-3-oxo-2-phenyl-2,3-dihydro-1*H*-pyrazol-4-yl)acetamides (**PR\_04 – PR\_12**)**

To a solution of 4-amino-1,5-dimethyl-2-phenyl-1*H*-pyrazol-3(2*H*)-one (**PR\_03**) in DCM (4 mL) was added TEA (3 mmol) and corresponding acid chloride (1.2 mmol) dropwise at 0 °C, and the reaction mixture and was stirred at rt for 8 h (monitored by TLC & LCMS for completion). The reaction mixture was then washed with water (4 mL), and the organic layer dried over anhydrous sodium sulphate and evaporated under reduced pressure. The crude product was further purified by silica gel column chromatography using hexane: ethyl acetate as eluent to give the corresponding substituted *N*-(1,5-dimethyl-3-oxo-2-phenyl-2,3-dihydro-1*H*-pyrazol-4-yl)acetamides (**PR\_04 – PR\_12**).

**Procedure for the synthesis of substituted 1-(1,5-dimethyl-3-oxo-2-phenyl-2,3-dihydro-1*H*-pyrazol-4-yl)ureas (**PR\_13 - PR\_18**)**

To a solution of 4-amino-1,5-dimethyl-2-phenyl-1*H*-pyrazol-3(2*H*)-one (**PR\_03**) (1 mmol) in dry DCM (4 mL) was added TEA (3 mmol) and corresponding substituted phenyl/benzyl isocyanate (1.2 mmol) dropwise at 0 °C, and the reaction mixture was stirred at rt for 8 h (monitored by TLC & LCMS for completion). The reaction mixture was then washed with water (4 mL), and the organic layer dried over anhydrous sodium sulphate and evaporated under reduced pressure. The crude product was further purified by silica gel column chromatography using hexane: ethyl acetate as eluent to give the corresponding substituted 1-(1,5-dimethyl-3-oxo-2-phenyl-2,3-dihydro-1*H*-pyrazol-4-yl)urea (**PR\_13 - PR\_18**).

**Procedure for the synthesis of substituted 1-(1,5-dimethyl-3-oxo-2-phenyl-2,3-dihydro-1*H*-pyrazol-4-yl)thioureas (**PR\_19 - PR\_26**)**

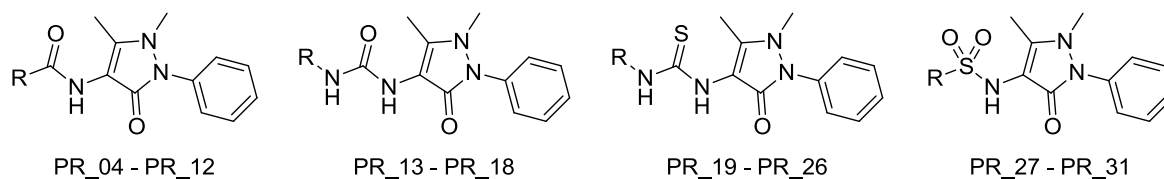
To a solution of 4-amino-1,5-dimethyl-2-phenyl-1*H*-pyrazol-3(2*H*)-one (**PR\_03**) (1 mmol) in dry DCM (4 mL) was added TEA (3 mmol) and corresponding substituted phenyl/benzyl isothiocyanate (1.2 mmol) dropwise at 0 °C, and the reaction mixture was stirred at rt for 8 h (monitored by TLC & LCMS for completion). The reaction mixture was then washed with water (4 mL), and the organic layer dried over anhydrous sodium sulphate and evaporated under reduced pressure. The crude product was further purified by silica gel column


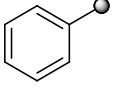
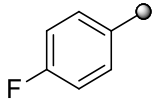
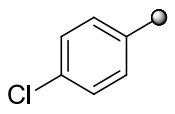
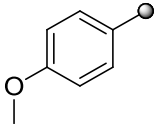
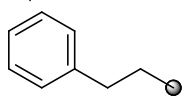
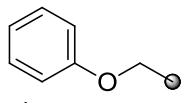
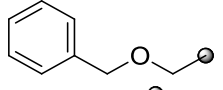
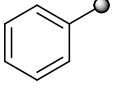
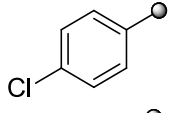
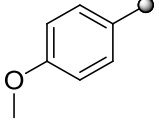
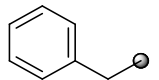
chromatography using hexane: ethyl acetate as eluent to give the corresponding substituted 1-(1,5-dimethyl-3-oxo-2-phenyl-2,3-dihydro-1*H*-pyrazol-4-yl)thiourea (**PR\_19 - PR\_26**).

**Procedure for the synthesis of substituted *N*-(1,5-dimethyl-3-oxo-2-phenyl-2,3-dihydro-1*H*-pyrazol-4-yl)benzene/phenylmethanesulfonamides (**PR\_27 - PR\_31**)**

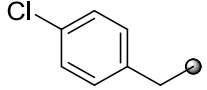
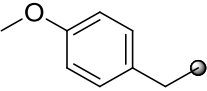
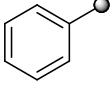
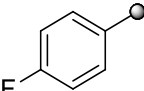
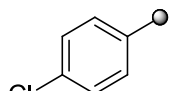
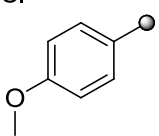
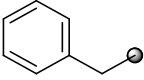
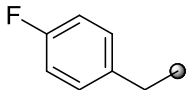
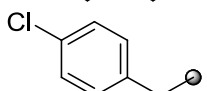
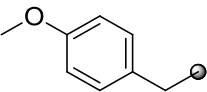
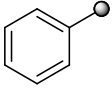
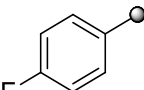
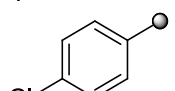
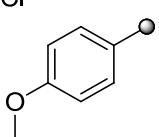
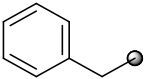
To a solution of 4-amino-1,5-dimethyl-2-phenyl-1*H*-pyrazol-3(2*H*)-one (**PR\_03**) (1 mmol) in dry DCM (4 mL) was added TEA (3 mmol) and corresponding substituted benzene/phenylmethanesulfonyl chloride (1.2 mmol) dropwise at 0 °C, and the reaction mixture was stirred at rt for 8 h (monitored by TLC & LCMS for completion). The reaction mixture was then washed with water (4 mL), and the organic layer was dried over anhydrous sodium sulphate and evaporated under reduced pressure. The crude product was further purified by silica gel column chromatography using hexane: ethyl acetate as eluent to give the corresponding substituted *N*-(1,5-dimethyl-3-oxo-2-phenyl-2,3-dihydro-1*H*-pyrazol-4-yl)benzene/phenylmethanesulfonamides (**PR\_27 - PR\_31**). The physicochemical properties of synthesized derivatives are shown in **Table 5.7**.

**Table 5.7:** Physicochemical properties of synthesized compounds **PR\_04 – PR\_31**.



| Comp  | R   | Yield (%) | Melting Point (°C) | Molecular formula   | Molecular weight |
|-------|---|-----------|--------------------|---|------------------|
| PR_04 | CH <sub>3</sub>   | 78.3      | 198-200            | C <sub>13</sub> H <sub>15</sub> N <sub>3</sub> O <sub>2</sub>   | 245.28           |
| PR_05 |    | 74.2      | 226-228            | C <sub>16</sub> H <sub>21</sub> N <sub>3</sub> O <sub>2</sub>   | 287.36           |
| PR_06 |    | 69.7      | 144-146            | C <sub>18</sub> H <sub>17</sub> N <sub>3</sub> O <sub>2</sub>   | 307.37           |
| PR_07 |    | 72.7      | 174-176            | C <sub>18</sub> H <sub>16</sub> FN <sub>3</sub> O <sub>2</sub>  | 325.34           |
| PR_08 |   | 67.6      | 192-194            | C <sub>18</sub> H <sub>16</sub> ClN <sub>3</sub> O <sub>2</sub> | 341.79           |
| PR_09 |  | 68.4      | 158-160            | C <sub>19</sub> H <sub>19</sub> N <sub>3</sub> O <sub>3</sub>   | 337.37           |
| PR_10 |  | 69.1      | 174-176            | C <sub>20</sub> H <sub>21</sub> N <sub>3</sub> O <sub>2</sub>   | 335.40           |
| PR_11 |  | 68.8      | 145-147            | C <sub>19</sub> H <sub>19</sub> N <sub>3</sub> O <sub>3</sub>   | 337.37           |
| PR_12 |  | 67.3      | 126-128            | C <sub>20</sub> H <sub>21</sub> N <sub>3</sub> O <sub>3</sub>   | 351.40           |
| PR_13 |  | 72.5      | 135-137            | C <sub>18</sub> H <sub>18</sub> N <sub>4</sub> O <sub>2</sub>   | 322.36           |
| PR_14 |  | 66.3      | 198-200            | C <sub>18</sub> H <sub>17</sub> ClN <sub>4</sub> O <sub>2</sub> | 356.81           |
| PR_15 |  | 68.1      | 193-195            | C <sub>19</sub> H <sub>20</sub> N <sub>4</sub> O <sub>3</sub>   | 352.39           |
| PR_16 |  | 68.4      | 160-162            | C <sub>19</sub> H <sub>20</sub> N <sub>4</sub> O <sub>2</sub>   | 336.39           |

Contd...

| Comp  | R   | Yield (%) | Melting Point (°C) | Molecular formula   | Molecular weight |
|-------|---|-----------|--------------------|---|------------------|
| PR_17 |    | 71.2      | 226-228            | C <sub>19</sub> H <sub>19</sub> ClN <sub>4</sub> O <sub>2</sub>   | 370.83           |
| PR_18 |    | 70.6      | 184-186            | C <sub>20</sub> H <sub>22</sub> N <sub>4</sub> O <sub>3</sub>     | 366.41           |
| PR_19 |    | 72.8      | 179-181            | C <sub>18</sub> H <sub>18</sub> N <sub>4</sub> OS                 | 338.41           |
| PR_20 |    | 73.1      | 193-195            | C <sub>18</sub> H <sub>17</sub> FN <sub>4</sub> OS                | 356.42           |
| PR_21 |    | 68.8      | 182-184            | C <sub>18</sub> H <sub>17</sub> ClN <sub>4</sub> OS               | 372.87           |
| PR_22 |    | 66.9      | 184-186            | C <sub>19</sub> H <sub>20</sub> N <sub>4</sub> O <sub>2</sub> S   | 368.45           |
| PR_23 |   | 67.4      | 172-174            | C <sub>19</sub> H <sub>20</sub> N <sub>4</sub> OS                 | 352.45           |
| PR_24 |  | 66.3      | 183-185            | C <sub>19</sub> H <sub>19</sub> FN <sub>4</sub> OS                | 370.44           |
| PR_25 |  | 70.0      | 192-194            | C <sub>19</sub> H <sub>19</sub> ClN <sub>4</sub> OS               | 386.90           |
| PR_26 |  | 68.6      | 183-185            | C <sub>20</sub> H <sub>22</sub> N <sub>4</sub> O <sub>2</sub> S   | 383.48           |
| PR_27 |  | 69.4      | 171-173            | C <sub>17</sub> H <sub>17</sub> N <sub>3</sub> O <sub>3</sub> S   | 343.40           |
| PR_28 |  | 67.7      | 170-172            | C <sub>17</sub> H <sub>16</sub> FN <sub>3</sub> O <sub>3</sub> S  | 361.39           |
| PR_29 |  | 70.8      | 199-201            | C <sub>17</sub> H <sub>16</sub> ClN <sub>3</sub> O <sub>3</sub> S | 377.85           |
| PR_30 |  | 71.4      | 160-162            | C <sub>18</sub> H <sub>19</sub> N <sub>3</sub> O <sub>4</sub> S   | 373.43           |
| PR_31 |  | 66.8      | 163-165            | C <sub>18</sub> H <sub>19</sub> N <sub>3</sub> O <sub>3</sub> S   | 357.43           |

### 5.3.3 Characterization of synthesized compounds

Both analytical and spectral data ( $^1\text{H}$  NMR,  $^{13}\text{C}$  NMR and mass spectra) of all the synthesized compounds were in full agreement with the proposed structures.

#### 5-Methyl-2-phenyl-1*H*-pyrazol-3(2*H*)-one (PR\_01)

M.p: 128-130 °C.  $^1\text{H}$  NMR (DMSO- $d_6$ ):  $\delta_{\text{H}}$  6.97 – 7.71 (m, 5H), 5.60 (s, 1H), 4.71 (s, 1H), 2.11 (s, 3H).  $^{13}\text{C}$  NMR (DMSO- $d_6$ ):  $\delta_{\text{C}}$  165.2, 152.3, 137.1, 129.0, 122.9, 120.5, 94.8, 14.2. ESI-MS  $m/z$  175 (M+H) $^+$ . Anal. Calcd. for  $\text{C}_{10}\text{H}_{10}\text{N}_2\text{O}$ : C, 68.95; H, 5.79; N, 16.08; Found: C, 68.98; H, 5.77; N, 16.10.

#### 1,5-Dimethyl-2-phenyl-1*H*-pyrazol-3(2*H*)-one (PR\_02)

M.p: 114-116 °C.  $^1\text{H}$  NMR (DMSO- $d_6$ ):  $\delta_{\text{H}}$  6.97 – 7.42 (m, 5H), 5.01 (s, 1H), 3.10 (s, 3H), 2.13 (s, 3H).  $^{13}\text{C}$  NMR (DMSO- $d_6$ ):  $\delta_{\text{C}}$  165.6, 157.1, 134.2, 129.0, 124.1, 123.2, 97.6, 35.3, 14.6. ESI-MS  $m/z$  189 (M+H) $^+$ . Anal. Calcd. for  $\text{C}_{11}\text{H}_{12}\text{N}_2\text{O}$ : C, 70.19; H, 6.43; N, 14.88; Found: C, 70.22; H, 6.41; N, 14.86.

#### 4-Amino-1,5-dimethyl-2-phenyl-1*H*-pyrazol-3(2*H*)-one (PR\_03)

M.p: 109-111 °C.  $^1\text{H}$  NMR (DMSO- $d_6$ ):  $\delta_{\text{H}}$  8.43 (s, 2H), 6.99 – 7.42 (m, 5H), 3.21 (s, 3H), 2.11 (s, 3H).  $^{13}\text{C}$  NMR (DMSO- $d_6$ ):  $\delta_{\text{C}}$  160.9, 134.2, 131.7, 129.5, 124.0, 123.3, 116.8, 35.3, 12.3. ESI-MS  $m/z$  204 (M+H) $^+$ . Anal. Calcd. for  $\text{C}_{11}\text{H}_{13}\text{N}_3\text{O}$ : C, 65.01; H, 6.45; N, 20.68; Found: C, 65.04; H, 6.47; N, 20.70.

#### *N*-(1,5-Dimethyl-3-oxo-2-phenyl-2,3-dihydro-1*H*-pyrazol-4-yl)acetamide (PR\_04)

The compound was synthesized according to the general procedure using 4-amino-1,5-dimethyl-2-phenyl-1*H*-pyrazol-3(2*H*)-one (PR\_03) (0.1 g, 0.49 mmol) and acetyl chloride (0.046 g, 0.59 mmol) to afford PR\_04 (0.094 g, 78.3 %) as pale yellow solid. M.p: 198-200 °C.  $^1\text{H}$  NMR (DMSO- $d_6$ ):  $\delta_{\text{H}}$  8.13 (s, 1H), 6.92 – 7.49 (m, 5H), 3.14 (s, 3H), 2.22 (s, 3H), 1.89 (s, 3H).  $^{13}\text{C}$  NMR (DMSO- $d_6$ ):  $\delta_{\text{C}}$  171.1, 161.4, 134.0, 133.6, 129.3, 124.0, 122.9, 103.7, 35.8, 23.6, 11.5. ESI-MS  $m/z$  246 (M+H) $^+$ . Anal. Calcd. for  $\text{C}_{13}\text{H}_{15}\text{N}_3\text{O}_2$ : C, 63.66; H, 6.16; N, 17.13; Found: C, 63.69; H, 6.14; N, 17.16.

#### ***N*-(1,5-Dimethyl-3-oxo-2-phenyl-2,3-dihydro-1*H*-pyrazol-4-yl)pivalamide (PR\_05)**

The compound was synthesized according to the general procedure using 4-amino-1,5-dimethyl-2-phenyl-1*H*-pyrazol-3(2*H*)-one (**PR\_03**) (0.1 g, 0.49 mmol) and pivaloyl chloride (0.071 g, 0.59 mmol) to afford **PR\_05** (0.104 g, 74.2 %) as pale yellow solid. M.p: 226-228 °C. <sup>1</sup>H NMR (DMSO-*d*<sub>6</sub>): δ<sub>H</sub> 8.19 (s, 1H), 6.96 – 7.41 (m, 5H), 3.15 (s, 3H), 2.23 (s, 3H), 1.31 (s, 9H). <sup>13</sup>C NMR (DMSO-*d*<sub>6</sub>): δ<sub>C</sub> 172.7, 161.2, 133.9, 133.6, 129.1, 123.9, 122.8, 103.3, 39.9, 35.1, 28.2, 11.6. ESI-MS *m/z* 288 (M+H)<sup>+</sup>. Anal. Calcd. for C<sub>16</sub>H<sub>21</sub>N<sub>3</sub>O<sub>2</sub>: C, 66.88; H, 7.37; N, 14.62; Found: C, 66.92; H, 7.35; N, 14.65.

#### ***N*-(1,5-Dimethyl-3-oxo-2-phenyl-2,3-dihydro-1*H*-pyrazol-4-yl)benzamide (PR\_06)**

The compound was synthesized according to the general procedure using 4-amino-1,5-dimethyl-2-phenyl-1*H*-pyrazol-3(2*H*)-one (**PR\_03**) (0.1 g, 0.49 mmol) and benzoyl chloride (0.082 g, 0.59 mmol) to afford **PR\_06** (0.105 g, 69.7 %) as pale yellow solid. M.p: 144-146 °C. <sup>1</sup>H NMR (DMSO-*d*<sub>6</sub>): δ<sub>H</sub> 8.63 (s, 1H), 7.01 – 8.12 (m, 10H), 3.16 (s, 3H), 2.21 (s, 3H). <sup>13</sup>C NMR (DMSO-*d*<sub>6</sub>): δ<sub>C</sub> 166.3, 161.4, 134.1, 133.6, 133.4, 132.2, 129.4, 128.9, 127.4, 124.1, 122.7, 103.6, 35.2, 11.7. ESI-MS *m/z* 308 (M+H)<sup>+</sup>. Anal. Calcd. for C<sub>18</sub>H<sub>17</sub>N<sub>3</sub>O<sub>2</sub>: C, 70.34; H, 5.58; N, 13.67; Found: C, 70.38; H, 5.56; N, 13.69.

#### ***N*-(1,5-Dimethyl-3-oxo-2-phenyl-2,3-dihydro-1*H*-pyrazol-4-yl)-4-fluorobenzamide (PR\_07)**

The compound was synthesized according to the general procedure using 4-amino-1,5-dimethyl-2-phenyl-1*H*-pyrazol-3(2*H*)-one (**PR\_03**) (0.1 g, 0.49 mmol) and 4-fluorobenzoyl chloride (0.093 g, 0.59 mmol) to afford **PR\_07** (0.116 g, 72.7 %) as pale yellow solid. M.p: 174-176 °C. <sup>1</sup>H NMR (DMSO-*d*<sub>6</sub>): δ<sub>H</sub> 8.62 (s, 1H), 7.02 – 8.21 (m, 9H), 3.08 (s, 3H), 2.16 (s, 3H). <sup>13</sup>C NMR (DMSO-*d*<sub>6</sub>): δ<sub>C</sub> 166.5, 166.2, 161.1, 134.0, 133.7, 129.3, 129.0, 128.7, 124.1, 122.8, 115.7, 103.5, 35.2, 12.1. ESI-MS *m/z* 326 (M+H)<sup>+</sup>. Anal. Calcd. for C<sub>18</sub>H<sub>16</sub>FN<sub>3</sub>O<sub>2</sub>: C, 66.45; H, 4.96; N, 12.92; Found: C, 66.41; H, 4.97; N, 12.90.

#### **4-Chloro-*N*-(1,5-dimethyl-3-oxo-2-phenyl-2,3-dihydro-1*H*-pyrazol-4-yl)benzamide (PR\_08)**

The compound was synthesized according to the general procedure using 4-amino-1,5-dimethyl-2-phenyl-1*H*-pyrazol-3(2*H*)-one (**PR\_03**) (0.1 g, 0.49 mmol) and 4-chlorobenzoyl

chloride (0.103 g, 0.59 mmol) to afford **PR\_08** (0.113 g, 67.6 %) as pale yellow solid. M.p: 192-194 °C. <sup>1</sup>H NMR (DMSO-d<sub>6</sub>): δ<sub>H</sub> 8.86 (s, 1H), 7.06 – 8.05 (m, 9H), 3.13 (s, 3H), 2.12 (s, 3H). <sup>13</sup>C NMR (DMSO-d<sub>6</sub>): δ<sub>C</sub> 166.4, 161.3, 137.8, 134.2, 133.6, 131.4, 130.0, 129.3, 1291.1, 124.1, 122.6, 103.3, 35.3, 11.5. ESI-MS *m/z* 342 (M+H)<sup>+</sup>. Anal. Calcd. for C<sub>18</sub>H<sub>16</sub>ClN<sub>3</sub>O<sub>2</sub>: C, 63.25; H, 4.72; N, 12.29; Found: C, 63.29; H, 4.70; N, 12.32.

***N*-(1,5-Dimethyl-3-oxo-2-phenyl-2,3-dihydro-1*H*-pyrazol-4-yl)-4-methoxybenzamide (PR\_09)**

The compound was synthesized according to the general procedure using 4-amino-1,5-dimethyl-2-phenyl-1*H*-pyrazol-3(2*H*)-one (**PR\_03**) (0.1 g, 0.49 mmol) and 4-methoxybenzoyl chloride (0.100 g, 0.59 mmol) to afford **PR\_09** (0.012 g, 68.4 %) as pale yellow solid. M.p: 158-160 °C. <sup>1</sup>H NMR (DMSO-d<sub>6</sub>): δ<sub>H</sub> 8.62 (s, 1H), 7.98 – 8.02 (m, 9H), 3.91 (s, 3H), 3.09 (s, 3H), 2.12 (s, 3H). <sup>13</sup>C NMR (DMSO-d<sub>6</sub>): δ<sub>C</sub> 166.4, 164.9, 164.1, 134.1, 133.8, 129.4, 125.6, 124.5, 124.1, 122.8, 114.6, 103.4, 56.1, 35.2, 12.2. ESI-MS *m/z* 338 (M+H)<sup>+</sup>. Anal. Calcd. for C<sub>19</sub>H<sub>19</sub>N<sub>3</sub>O<sub>3</sub>: C, 67.64; H, 5.68; N, 12.46; Found: C, 67.60; H, 5.70; N, 12.49.

***N*-(1,5-Dimethyl-3-oxo-2-phenyl-2,3-dihydro-1*H*-pyrazol-4-yl)-3-phenylpropanamide (PR\_10)**

The compound was synthesized according to the general procedure using 4-amino-1,5-dimethyl-2-phenyl-1*H*-pyrazol-3(2*H*)-one (**PR\_03**) (0.1 g, 0.49 mmol) and hydrocinnamoyl chloride (0.099 g, 0.59 mmol) to afford **PR\_10** (0.114 g, 69.1 %) as pale yellow solid. M.p: 174-176 °C. <sup>1</sup>H NMR (DMSO-d<sub>6</sub>): δ<sub>H</sub> 8.86 (s, 1H), 6.99 – 7.47 (m, 10H), 3.09 (s, 3H), 2.82 – 2.84 (t, *J* = 7.1, 2H), 2.61 -2.63 (t, *J* = 7.1, 2H), 2.11 (s, 3H). <sup>13</sup>C NMR (DMSO-d<sub>6</sub>): δ<sub>C</sub> 170.7, 161.3, 141.2, 134.1, 133.6, 129.3, 128.8, 127.9, 126.2, 124.1, 123.0, 103.6, 35.8, 35.1, 31.0, 11.8. ESI-MS *m/z* 336 (M+H)<sup>+</sup>. Anal. Calcd. for C<sub>20</sub>H<sub>21</sub>N<sub>3</sub>O<sub>2</sub>: C, 71.62; H, 6.31; N, 12.53; Found: C, 71.65; H, 6.29; N, 12.56.

***N*-(1,5-Dimethyl-3-oxo-2-phenyl-2,3-dihydro-1*H*-pyrazol-4-yl)-2-phenoxyacetamide (PR\_11)**

The compound was synthesized according to the general procedure using 4-amino-1,5-dimethyl-2-phenyl-1*H*-pyrazol-3(2*H*)-one (**PR\_03**) (0.1 g, 0.49 mmol) and phenoxyacetyl chloride (0.100 g, 0.59 mmol) to afford **PR\_11** (0.114 g, 68.8 %) as pale yellow solid. M.p:

145-147 °C. <sup>1</sup>H NMR (DMSO-d<sub>6</sub>): δ<sub>H</sub> 8.94 (s, 1H), 6.97 – 7.46 (m, 10H), 4.69 (s, 2H), 3.10 (s, 3H), 2.11 (s, 3H). <sup>13</sup>C NMR (DMSO-d<sub>6</sub>): δ<sub>C</sub> 167.1, 161.3, 158.3, 134.2, 133.6, 129.7, 129.1, 124.1, 122.7, 120.8, 115.1, 103.1, 66.8, 35.3, 11.8. ESI-MS *m/z* 338 (M+H)<sup>+</sup>. Anal. Calcd. for C<sub>19</sub>H<sub>19</sub>N<sub>3</sub>O<sub>3</sub>: C, 67.64; H, 5.68; N, 12.46; Found: C, 67.70; H, 5.70; N, 12.43.

**2-(Benzyloxy)-*N*-(1,5-dimethyl-3-oxo-2-phenyl-2,3-dihydro-1*H*-pyrazol-4-yl)acetamide (PR\_12)**

The compound was synthesized according to the general procedure using 4-amino-1,5-dimethyl-2-phenyl-1*H*-pyrazol-3(2*H*)-one (**PR\_03**) (0.1 g, 0.49 mmol) and benzyloxyacetyl chloride (0.108 g, 0.59 mmol) to afford **PR\_12** (0.116 g, 67.3 %) as pale yellow solid. M.p: 126-128 °C. <sup>1</sup>H NMR (DMSO-d<sub>6</sub>): δ<sub>H</sub> 8.93 (s, 1H), 7.29 – 7.52 (m, 10H), 4.60 (s, 2H), 4.08 (s, 2H), 3.05 (s, 3H), 2.13 (s, 3H). <sup>13</sup>C NMR (DMSO-d<sub>6</sub>): δ<sub>C</sub> 167.6, 161.9, 137.7, 134.2, 133.6, 129.0, 128.7, 127.7, 127.3, 123.8, 122.7, 103.6, 71.8, 69.8, 35.2, 10.72. ESI-MS *m/z* 352 (M+H)<sup>+</sup>. Anal. Calcd. for C<sub>20</sub>H<sub>21</sub>N<sub>3</sub>O<sub>3</sub>: C, 68.36; H, 6.02; N, 11.96; Found: C, 68.40; H, 6.05; N, 11.99.

**1-(1,5-Dimethyl-3-oxo-2-phenyl-2,3-dihydro-1*H*-pyrazol-4-yl)-3-phenylurea (PR\_13)**

The compound was synthesized according to the general procedure using 4-amino-1,5-dimethyl-2-phenyl-1*H*-pyrazol-3(2*H*)-one (**PR\_03**) (0.1 g, 0.49 mmol) and phenyl isocyanate (0.070 g, 0.59 mmol) to afford **PR\_13** (0.114 g, 72.5 %) as pale yellow solid. M.p: 135-137 °C. <sup>1</sup>H NMR (DMSO-d<sub>6</sub>): δ<sub>H</sub> 8.68 (s, 1H), 8.15 (s, 1H), 7.02 – 7.72 (m, 10H), 3.10 (s, 3H), 2.12 (s, 3H). <sup>13</sup>C NMR (DMSO-d<sub>6</sub>): δ<sub>C</sub> 162.0, 145.7, 140.2, 134.1, 133.6, 129.5, 129.2, 127.8, 124.2, 122.9, 121.8, 103.8, 35.4, 11.6. ESI-MS *m/z* 323 (M+H)<sup>+</sup>. Anal. Calcd. for C<sub>18</sub>H<sub>18</sub>N<sub>4</sub>O<sub>2</sub>: C, 67.07; H, 5.63; N, 17.38; Found: C, 67.04; H, 5.65; N, 17.35.

**1-(4-Chlorophenyl)-3-(1,5-dimethyl-3-oxo-2-phenyl-2,3-dihydro-1*H*-pyrazol-4-yl)urea (PR\_14)**

The compound was synthesized according to the general procedure using 4-amino-1,5-dimethyl-2-phenyl-1*H*-pyrazol-3(2*H*)-one (**PR\_03**) (0.1 g, 0.49 mmol) and 4-chlorophenyl isocyanate (0.090 g, 0.59 mmol) to afford **PR\_14** (0.116 g, 66.3 %) as pale yellow solid. M.p: 198-200 °C. <sup>1</sup>H NMR (DMSO-d<sub>6</sub>): δ<sub>H</sub> 8.72 (s, 1H), 8.06 (s, 1H), 7.02 – 7.81 (m, 9H), 3.14 (s, 3H), 2.13 (s, 3H). <sup>13</sup>C NMR (DMSO-d<sub>6</sub>): δ<sub>C</sub> 161.5, 145.7, 137.3, 134.1, 133.8, 133.2, 129.3,



129.0, 124.1, 123.0, 120.9, 103.7, 35.2, 11.8. ESI-MS  $m/z$  357 (M+H)<sup>+</sup>. Anal. Calcd. for C<sub>18</sub>H<sub>17</sub>ClN<sub>4</sub>O<sub>2</sub>: C, 60.59; H, 4.80; N, 15.70; Found: C, 60.62; H, 4.82; N, 15.72.

**1-(1,5-Dimethyl-3-oxo-2-phenyl-2,3-dihydro-1H-pyrazol-4-yl)-3-(4-methoxyphenyl)urea (PR\_15)**

The compound was synthesized according to the general procedure using 4-amino-1,5-dimethyl-2-phenyl-1H-pyrazol-3(2H)-one (**PR\_03**) (0.1 g, 0.49 mmol) and 4-methoxyphenyl isocyanate (0.087 g, 0.59 mmol) to afford **PR\_15** (0.118 g, 68.1 %) as pale yellow solid. M.p: 193-195 °C. <sup>1</sup>H NMR (DMSO-d<sub>6</sub>): δ<sub>H</sub> 8.70 (s, 1H), 7.96 (s, 1H), 6.82 – 7.53 (m, 9H), 3.70 (s, 3H), 3.03 (s, 3H), 2.19 (s, 3H). <sup>13</sup>C NMR (DMSO-d<sub>6</sub>): δ<sub>C</sub> 161.3, 159.2, 145.6, 134.1, 133.8, 131.6, 129.4, 124.2, 123.0, 120.1, 114.7, 103.6, 56.2, 35.3, 10.7. ESI-MS  $m/z$  353 (M+H)<sup>+</sup>. Anal. Calcd. for C<sub>19</sub>H<sub>20</sub>N<sub>4</sub>O<sub>3</sub>: C, 64.76; H, 5.72; N, 15.90; Found: C, 64.79; H, 5.74; N, 15.92.

**1-Benzyl-3-(1,5-dimethyl-3-oxo-2-phenyl-2,3-dihydro-1H-pyrazol-4-yl)urea (PR\_16)**

The compound was synthesized according to the general procedure using 4-amino-1,5-dimethyl-2-phenyl-1H-pyrazol-3(2H)-one (**PR\_03**) (0.1 g, 0.49 mmol) and 4-benzyl isocyanate (0.078 g, 0.59 mmol) to afford **PR\_16** (0.113 g, 68.4 %) as pale yellow solid. M.p: 160-162 °C. <sup>1</sup>H NMR (DMSO-d<sub>6</sub>): δ<sub>H</sub> 8.72 (s, 1H), 8.06 (s, 1H), 7.02 – 7.46 (m, 10H), 4.37 – 4.39 (d, *J* = 6.3, 2H), 3.16 (s, 3H), 2.19 (s, 3H). <sup>13</sup>C NMR (DMSO-d<sub>6</sub>): δ<sub>C</sub> 162.3, 156.4, 151.8, 140.5, 135.1, 128.9, 128.1, 126.9, 126.5, 125.9, 123.1, 108.9, 42.9, 36.1, 11.1. ESI-MS  $m/z$  337 (M+H)<sup>+</sup>. Anal. Calcd. for C<sub>19</sub>H<sub>20</sub>N<sub>4</sub>O<sub>2</sub>: C, 67.84; H, 5.99; N, 16.66; Found: C, 67.81; H, 6.01; N, 16.68.

**1-(4-Chlorobenzyl)-3-(1,5-dimethyl-3-oxo-2-phenyl-2,3-dihydro-1H-pyrazol-4-yl)urea (PR\_17)**

The compound was synthesized according to the general procedure using 4-amino-1,5-dimethyl-2-phenyl-1H-pyrazol-3(2H)-one (**PR\_03**) (0.1 g, 0.49 mmol) and 4-chlorobenzyl isocyanate (0.098 g, 0.59 mmol) to afford **PR\_17** (0.129 g, 71.2 %) as pale yellow solid. M.p: 226-228 °C. <sup>1</sup>H NMR (DMSO-d<sub>6</sub>): δ<sub>H</sub> 8.72 (s, 1H), 8.17 (s, 1H), 7.11 – 7.53 (m, 9H), 4.71 – 4.72 (d, *J* = 5.7, 2H), 3.10 (s, 3H), 2.16 (s, 3H). <sup>13</sup>C NMR (DMSO-d<sub>6</sub>): δ<sub>C</sub> 161.9, 151.3, 136.2, 134.7, 134.1, 133.6, 132.4, 129.3, 128.8, 124.2, 122.9, 104.1, 44.7, 35.4, 11.7. ESI-MS

$m/z$  371 (M+H)<sup>+</sup>. Anal. Calcd. for C<sub>19</sub>H<sub>19</sub>ClN<sub>4</sub>O<sub>2</sub>: C, 61.54; H, 5.16; N, 15.11; Found: C, 61.50; H, 5.18; N, 15.13.

**1-(1,5-Dimethyl-3-oxo-2-phenyl-2,3-dihydro-1H-pyrazol-4-yl)-3-(4-methoxybenzyl)urea (PR\_18)**

The compound was synthesized according to the general procedure using 4-amino-1,5-dimethyl-2-phenyl-1H-pyrazol-3(2H)-one (PR\_03) (0.1 g, 0.49 mmol) and 4-methoxybenzyl isocyanate (0.096 g, 0.59 mmol) to afford PR\_18 (0.127 g, 70.6 %) as pale yellow solid. M.p: 184-186 °C. <sup>1</sup>H NMR (DMSO-d<sub>6</sub>): δ<sub>H</sub> 8.71 (s, 1H), 8.09 (s, 1H), 6.91 – 7.48 (m, 9H), 4.29 – 4.30 (d, *J* = 5.7, 2H), 3.87 (s, 3H), 3.12 (s, 3H), 2.11 (s, 3H). <sup>13</sup>C NMR (DMSO-d<sub>6</sub>): δ<sub>C</sub> 161.7, 158.8, 151.4, 134.2, 133.8, 130.7, 130.0, 124.5, 124.2, 122.9, 114.3, 103.7, 56.1, 44.8, 35.3, 11.6. ESI-MS  $m/z$  367 (M+H)<sup>+</sup>. Anal. Calcd. for C<sub>20</sub>H<sub>22</sub>N<sub>4</sub>O<sub>3</sub>: C, 65.56; H, 6.05; N, 15.29; Found: C, 65.52; H, 6.03; N, 15.31.

**1-(1,5-Dimethyl-3-oxo-2-phenyl-2,3-dihydro-1H-pyrazol-4-yl)-3-phenylthiourea (PR\_19)**

The compound was synthesized according to the general procedure using 4-amino-1,5-dimethyl-2-phenyl-1H-pyrazol-3(2H)-one (PR\_03) (0.1 g, 0.49 mmol) and phenyl isothiocyanate (0.079 g, 0.59 mmol) to afford PR\_19 (0.121 g, 72.8 %) as pale yellow solid. M.p: 179-181 °C. <sup>1</sup>H NMR (DMSO-d<sub>6</sub>): δ<sub>H</sub> 8.67 (s, 1H), 8.20 (s, 1H), 6.92 – 7.82 (m, 10H), 3.14 (s, 3H), 2.20 (s, 3H). <sup>13</sup>C NMR (DMSO-d<sub>6</sub>): δ<sub>C</sub> 176.0, 161.1, 138.7, 134.1, 131.6, 129.4, 129.1, 128.5, 126.6, 124.0, 122.9, 116.7, 35.2, 12.6. ESI-MS  $m/z$  339 (M+H)<sup>+</sup>. Anal. Calcd. for C<sub>18</sub>H<sub>18</sub>N<sub>4</sub>OS: C, 63.88; H, 5.36; N, 16.56; Found: C, 63.92; H, 5.34; N, 16.59.

**1-(1,5-Dimethyl-3-oxo-2-phenyl-2,3-dihydro-1H-pyrazol-4-yl)-3-(4-fluorophenyl)thiourea (PR\_20)**

The compound was synthesized according to the general procedure using 4-amino-1,5-dimethyl-2-phenyl-1H-pyrazol-3(2H)-one (PR\_03) (0.1 g, 0.49 mmol) and 4-fluorophenyl isothiocyanate (0.090 g, 0.59 mmol) to afford PR\_20 (0.128 g, 73.1 %) as pale yellow solid. M.p: 193-195 °C. <sup>1</sup>H NMR (DMSO-d<sub>6</sub>): δ<sub>H</sub> 8.71 (s, 1H), 8.21 (s, 1H), 6.57 – 7.42 (m, 9H), 3.12 (s, 3H), 2.21 (s, 3H). <sup>13</sup>C NMR (DMSO-d<sub>6</sub>): δ<sub>C</sub> 178.2, 164.2, 160.9, 134.3, 134.0, 131.7, 131.1, 129.3, 123.9, 122.8, 116.7, 115.9, 35.4, 11.8. ESI-MS  $m/z$  357 (M+H)<sup>+</sup>. Anal. Calcd. for C<sub>18</sub>H<sub>17</sub>FN<sub>4</sub>OS: C, 60.66; H, 4.81; N, 15.72; Found: C, 60.62; H, 4.83; N, 15.74.

**1-(4-Chlorophenyl)-3-(1,5-dimethyl-3-oxo-2-phenyl-2,3-dihydro-1H-pyrazol-4-yl)thiourea (PR\_21)**

The compound was synthesized according to the general procedure using 4-amino-1,5-dimethyl-2-phenyl-1H-pyrazol-3(2H)-one (**PR\_03**) (0.1 g, 0.49 mmol) and 4-chlorophenyl isothiocyanate (0.100 g, 0.59 mmol) to afford **PR\_21** (0.126 g, 68.8 %) as pale yellow solid. M.p: 182-184 °C. <sup>1</sup>H NMR (DMSO-d<sub>6</sub>): δ<sub>H</sub> 8.68 (s, 1H), 8.18 (s, 1H), 6.63 – 7.47 (m, 9H), 3.14 (s, 3H), 2.23 (s, 3H). <sup>13</sup>C NMR (DMSO-d<sub>6</sub>): δ<sub>C</sub> 177.9, 160.8, 136.8, 134.2, 133.7, 131.6, 131.2, 129.5, 129.1, 124.1, 123.0, 116.8, 34.9, 12.0. ESI-MS *m/z* 373 (M+H)<sup>+</sup>. Anal. Calcd. for C<sub>18</sub>H<sub>17</sub>ClN<sub>4</sub>OS: C, 57.98; H, 4.60; N, 15.03; Found: C, 58.02; H, 4.61; N, 15.00.

**1-(1,5-Dimethyl-3-oxo-2-phenyl-2,3-dihydro-1H-pyrazol-4-yl)-3-(4-methoxyphenyl)thiourea (PR\_22)**

The compound was synthesized according to the general procedure using 4-amino-1,5-dimethyl-2-phenyl-1H-pyrazol-3(2H)-one (**PR\_03**) (0.1 g, 0.49 mmol) and 4-methoxyphenyl isothiocyanate (0.097 g, 0.59 mmol) to afford **PR\_22** (0.121 g, 66.9 %) as pale yellow solid. M.p: 184-186 °C. <sup>1</sup>H NMR (DMSO-d<sub>6</sub>): δ<sub>H</sub> 8.73 (s, 1H), 8.12 (s, 1H), 6.42 – 7.44 (m, 9H), 3.91 (s, 3H), 3.15 (s, 3H), 2.17 (s, 3H). <sup>13</sup>C NMR (DMSO-d<sub>6</sub>): δ<sub>C</sub> 176.4, 160.8, 159.5, 134.1, 131.6, 130.9, 129.4, 127.7, 124.1, 123.1, 116.8, 114.7, 56.2, 35.4, 12.8. ESI-MS *m/z* 369 (M+H)<sup>+</sup>. Anal. Calcd. for C<sub>19</sub>H<sub>20</sub>N<sub>4</sub>O<sub>2</sub>S: C, 61.94; H, 5.47; N, 15.21; Found: C, 61.99; H, 5.45; N, 15.24.

**1-Benzyl-3-(1,5-dimethyl-3-oxo-2-phenyl-2,3-dihydro-1H-pyrazol-4-yl)thiourea (PR\_23)**

The compound was synthesized according to the general procedure using 4-amino-1,5-dimethyl-2-phenyl-1H-pyrazol-3(2H)-one (**PR\_03**) (0.1 g, 0.49 mmol) and benzyl isothiocyanate (0.088 g, 0.59 mmol) to afford **PR\_23** (0.116 g, 67.4 %) as pale yellow solid. M.p: 172-174 °C. <sup>1</sup>H NMR (DMSO-d<sub>6</sub>): δ<sub>H</sub> 8.62 (s, 1H), 8.18 (s, 1H), 7.01 – 7.48 (m, 10H), 4.74 – 4.76 (d, *J* = 6.0, 2H), 3.09 (s, 3H), 2.13 (s, 3H). <sup>13</sup>C NMR (DMSO-d<sub>6</sub>): δ<sub>C</sub> 182.2, 160.9, 137.8, 134.2, 131.6, 129.3, 128.7, 127.0, 126.6, 124.1, 122.9, 116.7, 51.1, 35.3, 11.6. ESI-MS *m/z* 353 (M+H)<sup>+</sup>. Anal. Calcd. for C<sub>19</sub>H<sub>20</sub>N<sub>4</sub>OS: C, 64.75; H, 5.72; N, 15.90; Found: C, 64.71; H, 5.70; N, 15.93.

**1-(1,5-Dimethyl-3-oxo-2-phenyl-2,3-dihydro-1H-pyrazol-4-yl)-3-(4-fluorobenzyl) thiourea (PR\_24)**

The compound was synthesized according to the general procedure using 4-amino-1,5-dimethyl-2-phenyl-1H-pyrazol-3(2H)-one (**PR\_03**) (0.1 g, 0.49 mmol) and 4-fluorobenzyl isothiocyanate (0.098 g, 0.59 mmol) to afford **PR\_24** (0.120 g, 66.3 %) as pale yellow solid. M.p: 183-185 °C. <sup>1</sup>H NMR (DMSO-d<sub>6</sub>): δ<sub>H</sub> 8.70 (s, 1H), 8.19 (s, 1H), 7.10 – 7.52 (m, 9H), 4.70 – 4.72 (d, *J* = 5.7, 2H), 3.09 (s, 3H), 2.10 (s, 3H). <sup>13</sup>C NMR (DMSO-d<sub>6</sub>): δ<sub>C</sub> 182.6, 162.6, 161.7, 153.5, 135.5, 135.0, 129.0, 128.8, 126.2, 123.6, 114.8, 114.6, 46.6, 35.5, 10.6. ESI-MS *m/z* 371 (M+H)<sup>+</sup>. Anal. Calcd. for C<sub>19</sub>H<sub>19</sub>FN<sub>4</sub>OS: C, 61.60; H, 5.17; N, 15.12; Found: C, 61.64; H, 5.18; N, 15.13.

**1-(4-Chlorobenzyl)-3-(1,5-dimethyl-3-oxo-2-phenyl-2,3-dihydro-1H-pyrazol-4-yl) thiourea (PR\_25)**

The compound was synthesized according to the general procedure using 4-amino-1,5-dimethyl-2-phenyl-1H-pyrazol-3(2H)-one (**PR\_03**) (0.1 g, 0.49 mmol) and 4-chlorobenzyl isothiocyanate (0.108 g, 0.59 mmol) to afford **PR\_25** (0.133 g, 70.0 %) as pale yellow solid. M.p: 192-194 °C. <sup>1</sup>H NMR (DMSO-d<sub>6</sub>): δ<sub>H</sub> 8.68 (s, 1H), 8.22 (s, 1H), 7.03 – 7.49 (m, 9H), 4.71 – 4.72 (d, *J* = 5.7, 2H), 3.06 (s, 3H), 2.11 (s, 3H). <sup>13</sup>C NMR (DMSO-d<sub>6</sub>): δ<sub>C</sub> 182.5, 161.3, 136.2, 134.4, 134.1, 132.5, 131.3, 129.4, 128.8, 124.0, 123.0, 116.7, 51.1, 35.3, 10.9. ESI-MS *m/z* 387 (M+H)<sup>+</sup>. Anal. Calcd. for C<sub>19</sub>H<sub>19</sub>ClN<sub>4</sub>OS: C, 58.98; H, 4.95; N, 14.48; Found: C, 59.02; H, 4.93; N, 14.51.

**1-(1,5-Dimethyl-3-oxo-2-phenyl-2,3-dihydro-1H-pyrazol-4-yl)-3-(4-methoxybenzyl) thiourea (PR\_26)**

The compound was synthesized according to the general procedure using 4-amino-1,5-dimethyl-2-phenyl-1H-pyrazol-3(2H)-one (**PR\_03**) (0.1 g, 0.49 mmol) and 4-methoxybenzyl isothiocyanate (0.105 g, 0.59 mmol) to afford **PR\_26** (0.129 g, 68.6 %) as pale yellow solid. M.p: 183-185 °C. <sup>1</sup>H NMR (DMSO-d<sub>6</sub>): δ<sub>H</sub> 8.67 (s, 1H), 8.14 (s, 1H), 6.93 – 7.34 (m, 9H), 4.73 – 4.75 (d, *J* = 6.3, 2H), 3.85 (s, 3H), 3.08 (s, 3H), 2.14 (s, 3H). <sup>13</sup>C NMR (DMSO-d<sub>6</sub>): δ<sub>C</sub> 182.7, 161.2, 159.2, 134.1, 131.7, 130.7, 130.0, 129.4, 124.1, 122.7, 116.5, 114.3, 57.1, 51.2, 35.4, 11.3. ESI-MS *m/z* 383 (M+H)<sup>+</sup>. Anal. Calcd. for C<sub>20</sub>H<sub>22</sub>N<sub>4</sub>O<sub>2</sub>S: C, 62.80; H, 5.80; N, 14.65; Found: C, 62.84; H, 5.82; N, 14.62.

***N*-(1,5-Dimethyl-3-oxo-2-phenyl-2,3-dihydro-1*H*-pyrazol-4-yl)benzenesulfonamide (PR\_27)**

The compound was synthesized according to the general procedure using 4-amino-1,5-dimethyl-2-phenyl-1*H*-pyrazol-3(2*H*)-one (PR\_03) (0.1 g, 0.49 mmol) and benzenesulfonyl chloride (0.104 g, 0.59 mmol) to afford PR\_27 (0.117 g, 69.4 %) as pale yellow solid. M.p: 171-173 °C. <sup>1</sup>H NMR (DMSO-*d*<sub>6</sub>): δ<sub>H</sub> 8.78 (s, 1H), 7.02 – 7.98 (m, 10H), 3.10 (s, 3H), 2.23 (s, 3H). <sup>13</sup>C NMR (DMSO-*d*<sub>6</sub>): δ<sub>C</sub> 161.3, 141.2, 134.0, 132.1, 131.7, 129.4, 129.1, 127.3, 124.0, 122.9, 116.5, 35.1, 12.4. ESI-MS *m/z* 342 (M-H)<sup>+</sup>. Anal. Calcd. for C<sub>17</sub>H<sub>17</sub>N<sub>3</sub>O<sub>3</sub>S: C, 59.46; H, 4.99; N, 12.24; Found: C, 59.42; H, 4.97; N, 12.22.

***N*-(1,5-Dimethyl-3-oxo-2-phenyl-2,3-dihydro-1*H*-pyrazol-4-yl)-4-fluorobenzene sulfonamide (PR\_28)**

The compound was synthesized according to the general procedure using 4-amino-1,5-dimethyl-2-phenyl-1*H*-pyrazol-3(2*H*)-one (PR\_03) (0.1 g, 0.49 mmol) and 4-fluorobenzenesulfonyl chloride (0.114 g, 0.59 mmol) to afford PR\_28 (0.120 g, 67.7 %) as pale yellow solid. M.p: 170-172 °C. <sup>1</sup>H NMR (DMSO-*d*<sub>6</sub>): δ<sub>H</sub> 8.84 (s, 1H), 7.27 – 7.99 (m, 9H), 3.26 (s, 3H), 2.01 (s, 3H). <sup>13</sup>C NMR (DMSO-*d*<sub>6</sub>): δ<sub>C</sub> 165.8, 161.4, 136.5, 134.1, 131.3, 130.8, 129.4, 124.1, 122.7, 116.3, 116.1, 35.4, 10.6. ESI-MS *m/z* 360 (M-H)<sup>+</sup>. Anal. Calcd. for C<sub>17</sub>H<sub>16</sub>FN<sub>3</sub>O<sub>3</sub>S: C, 56.50; H, 4.46; N, 11.63; Found: C, 56.54; H, 4.44; N, 11.66.

**4-Chloro-*N*-(1,5-dimethyl-3-oxo-2-phenyl-2,3-dihydro-1*H*-pyrazol-4-yl)benzene sulfonamide (PR\_29)**

The compound was synthesized according to the general procedure using 4-amino-1,5-dimethyl-2-phenyl-1*H*-pyrazol-3(2*H*)-one (PR\_03) (0.1 g, 0.49 mmol) and 4-chlorobenzenesulfonyl chloride (0.124 g, 0.59 mmol) to afford PR\_29 (0.131 g, 70.8 %) as pale yellow solid. M.p: 199-201 °C. <sup>1</sup>H NMR (DMSO-*d*<sub>6</sub>): δ<sub>H</sub> 8.80 (s, 1H), 6.93 – 7.92 (m, 9H), 3.17 (s, 3H), 2.21 (s, 3H). <sup>13</sup>C NMR (DMSO-*d*<sub>6</sub>): δ<sub>C</sub> 161.5, 139.2, 137.6, 134.2, 131.5, 129.3, 129.1, 128.4, 124.0, 122.9, 116.7, 35.6, 11.9. ESI-MS *m/z* 376 (M-H)<sup>+</sup>. Anal. Calcd. for C<sub>17</sub>H<sub>16</sub>ClN<sub>3</sub>O<sub>3</sub>S: C, 54.04; H, 4.27; N, 11.12; Found: C, 54.01; H, 4.29; N, 11.15.

***N*-(1,5-Dimethyl-3-oxo-2-phenyl-2,3-dihydro-1*H*-pyrazol-4-yl)-4-methoxybenzene sulfonamide (PR\_30)**

The compound was synthesized according to the general procedure using 4-amino-1,5-dimethyl-2-phenyl-1*H*-pyrazol-3(2*H*)-one (PR\_03) (0.1 g, 0.49 mmol) and 4-methoxybenzenesulfonyl chloride (0.121 g, 0.59 mmol) to afford PR\_30 (0.130 g, 71.4 %) as pale yellow solid. M.p: 160-162 °C. <sup>1</sup>H NMR (DMSO-*d*<sub>6</sub>): δ<sub>H</sub> 8.76 (s, 1H), 6.90 – 7.72 (m, 9H), 3.86 (s, 3H), 3.13 (s, 3H), 2.24 (s, 3H). <sup>13</sup>C NMR (DMSO-*d*<sub>6</sub>): δ<sub>C</sub> 164.3, 161.1, 134.1, 133.3, 131.7, 129.4, 126.3, 124.0, 122.9, 116.6, 114.7, 56.2, 35.3, 12.2. ESI-MS *m/z* 372 (M-H)<sup>+</sup>. Anal. Calcd. for C<sub>18</sub>H<sub>19</sub>N<sub>3</sub>O<sub>4</sub>S: C, 57.89; H, 5.13; N, 11.25; Found: C, 57.86; H, 5.11; N, 11.27.

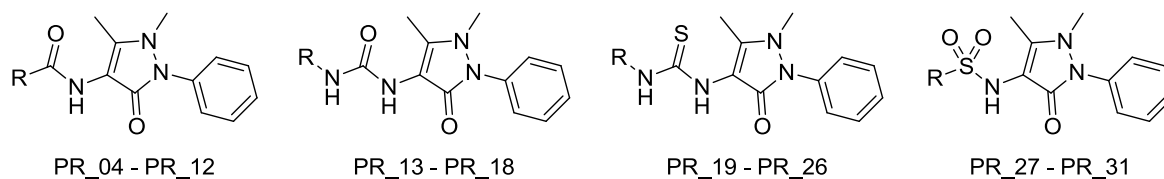
***N*-(1,5-Dimethyl-3-oxo-2-phenyl-2,3-dihydro-1*H*-pyrazol-4-yl)-1-phenylmethane sulfonamide (PR\_31)**

The compound was synthesized according to the general procedure using 4-amino-1,5-dimethyl-2-phenyl-1*H*-pyrazol-3(2*H*)-one (PR\_03) (0.1 g, 0.49 mmol) and phenylmethanesulfonyl chloride (0.112 g, 0.59 mmol) to afford PR\_31 (0.117 g, 66.8 %) as pale yellow solid. M.p: 163-165 °C. <sup>1</sup>H NMR (DMSO-*d*<sub>6</sub>): δ<sub>H</sub> 8.81 (s, 1H), 7.04 – 7.51 (m, 10H), 4.41 (s, 2H), 3.20 (s, 3H), 2.19 (s, 3H). <sup>13</sup>C NMR (DMSO-*d*<sub>6</sub>): δ<sub>C</sub> 161.2, 134.1, 133.4, 131.7, 130.9, 129.4, 128.7, 125.8, 124.1, 123.0, 116.6, 66.5, 35.2, 11.8. ESI-MS *m/z* 356 (M-H)<sup>+</sup>. Anal. Calcd. for C<sub>18</sub>H<sub>19</sub>N<sub>3</sub>O<sub>3</sub>S: C, 60.49; H, 5.36; N, 11.76; Found: C, 60.53; H, 5.34; N, 11.79.

**5.3.4 *In vitro* Mycobacterium tuberculosis InhA inhibition assay, antimycobacterial potency and cytotoxicity studies of the synthesised molecules**

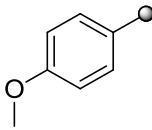
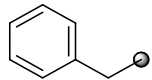
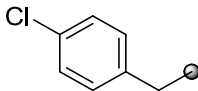
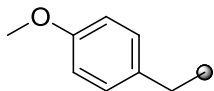
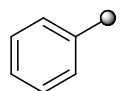
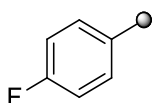
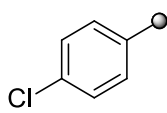
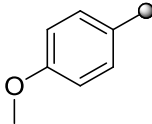
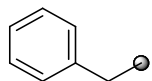
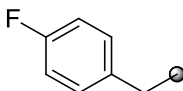
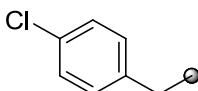
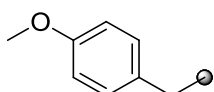
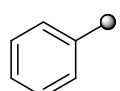
All the synthesized derivatives were first evaluated for their *in vitro* *Mycobacterium tuberculosis* InhA inhibitory potency as steps towards the derivation of structure-activity relationships and hit optimization. The compounds were further subjected to a whole cell screening against *Mycobacterium tuberculosis* H37Rv strain to understand their bactericidal potency using the agar dilution method and later the safety profile of these molecules were evaluated by checking the *in vitro* cytotoxicity against RAW 264.7 cell line (mouse macrophage) at 50 μM concentration by MTT assay, and the results are tabulated in **Table 5.8**.

**Table 5.8:** *In vitro* biological evaluation of the synthesized derivatives **PR\_04 – PR\_31**.



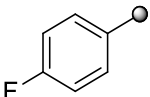
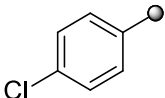
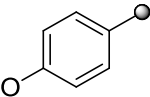
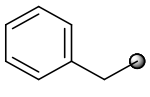
| Comp  | R               | % inhib of InhA<br>at 10 $\mu$ M<br>(IC <sub>50</sub> in $\mu$ M) <sup>a</sup> | MIC ( $\mu$ M) <sup>b</sup> |                   | Cytotoxicity <sup>c</sup><br>at 50 $\mu$ M<br>(% inhib) |
|-------|-----------------|--|-----------------------------|-------------------|---|
|       |                 |  | MTB                         | MTB<br>(Piperine) |   |
| PR_04 | CH <sub>3</sub> | 52.10±0.34   | 1.59                        | 1.59              | 15.56   |
| PR_05 |                 | 48.16±0.58   | 5.42                        | 2.71              | 23.65   |
| PR_06 |                 | 42.56±1.27   | 81.34                       | 40.67             | 31.71   |
| PR_07 |                 | 38.60±0.97   | 9.60                        | 4.79              | 27.81   |
| PR_08 |                 | 82.08±2.27<br>(5.52±0.31)  | 2.28                        | 1.14              | 32.33   |
| PR_09 |                 | 30.12±1.31   | 9.26                        | 4.62              | 31.42   |
| PR_10 |                 | 72.12±2.66<br>(6.12±0.42)  | 1.16                        | 0.58              | 17.84   |
| PR_11 |                 | 50.23±0.52   | 9.26                        | 4.62              | 34.67   |
| PR_12 |                 | 60.12±0.86<br>(8.92±0.71)  | 4.43                        | 2.22              | 36.23   |
| PR_13 |                 | 68.98±0.27<br>(7.32±0.47)  | 19.38                       | 19.38             | 22.28   |
| PR_14 |                 | 63.23±0.73<br>(7.12±0.42)  | 8.75                        | 4.37              | 19.26   |

Contd...

| Comp  | R   | % inhib of InhA<br>at 10 $\mu$ M<br>(IC <sub>50</sub> in $\mu$ M) <sup>a</sup> | MIC ( $\mu$ M) <sup>b</sup> |                   | Cytotoxicity <sup>c</sup><br>at 50 $\mu$ M<br>(% inhib) |
|-------|---|--|-----------------------------|-------------------|---|
|       |   |  | MTB                         | MTB<br>(Piperine) |   |
| PR_15 |    | 93.12±1.88<br>(2.96±0.21)  | 8.86                        | 4.42              | 24.34   |
| PR_16 |    | 34.23±0.82   | 2.31                        | 0.58              | 35.56   |
| PR_17 |    | 67.80±0.78<br>(7.18±0.46)  | 4.20                        | 1.05              | 34.91   |
| PR_18 |    | 45.78±0.56   | 2.12                        | 1.06              | 16.72   |
| PR_19 |    | 50.25±0.92   | 18.46                       | 9.23              | 23.66   |
| PR_20 |   | 41.08±1.28   | 4.37                        | 2.18              | 30.31   |
| PR_21 |  | 43.23±0.87   | 8.38                        | 4.18              | 34.45   |
| PR_22 |  | 42.12±0.36   | 16.96                       | 8.48              | 22.95   |
| PR_23 |  | 30.12±0.47   | 2.21                        | 1.10              | 31.61   |
| PR_24 |  | 28.15±0.65   | 16.87                       | 16.87             | 28.55   |
| PR_25 |  | 30.12±0.33   | 16.15                       | 8.07              | 23.56   |
| PR_26 |  | 34.17±0.38   | 65.36                       | 32.68             | 20.21   |
| PR_27 |  | 18.12±0.77   | 36.40                       | 9.10              | 30.33   |

Contd...



| Comp  | R   | % inhib of InhA<br>at 10 $\mu$ M<br>(IC <sub>50</sub> in $\mu$ M) <sup>a</sup> | MIC ( $\mu$ M) <sup>b</sup> |                   | Cytotoxicity <sup>c</sup><br>at 50 $\mu$ M<br>(% inhib) |
|-------|---|--|-----------------------------|-------------------|---|
|       |   |  | MTB                         | MTB<br>(Piperine) |   |
| PR_28 |  | 30.12 $\pm$ 1.34   | 34.58                       | 17.29             | 23.56   |
| PR_29 |  | 26.12 $\pm$ 0.92   | 33.08                       | 16.54             | 21.28   |
| PR_30 |  | 46.89 $\pm$ 1.22   | 8.35                        | 4.17              | 24.45   |
| PR_31 |  | 31.16 $\pm$ 0.86   | 17.48                       | 4.36              | 34.67   |
|       | <b>Isoniazid</b>  |  | 0.72                        | NT                | NT  |
|       | <b>Ethambutol</b>   |  | 7.64                        | NT                | NT  |
|       | <b>Rifampicin</b>   |  | 0.15                        | NT                | NT  |
|       | <b>Ofloxacin</b>  |  | 2.16                        | NT                | NT  |

IC<sub>50</sub>, 50% inhibitory concentration; MTB, *Mycobacterium tuberculosis*; MIC, minimum inhibitory concentration; NT, not tested

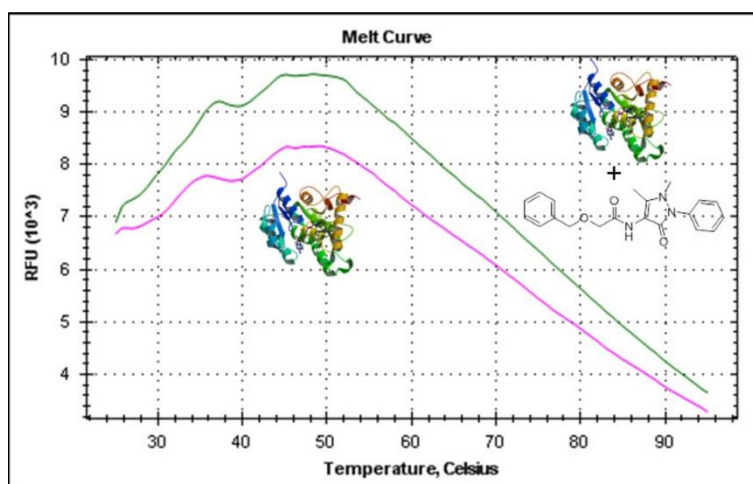
<sup>a</sup>MTB InhA enzyme inhibition activity

<sup>b</sup>*In vitro* activity against MTB H37Rv

<sup>c</sup>Against RAW 264.7 cells

### 5.3.5 Evaluation of protein interaction and stability using biophysical characterization experiment

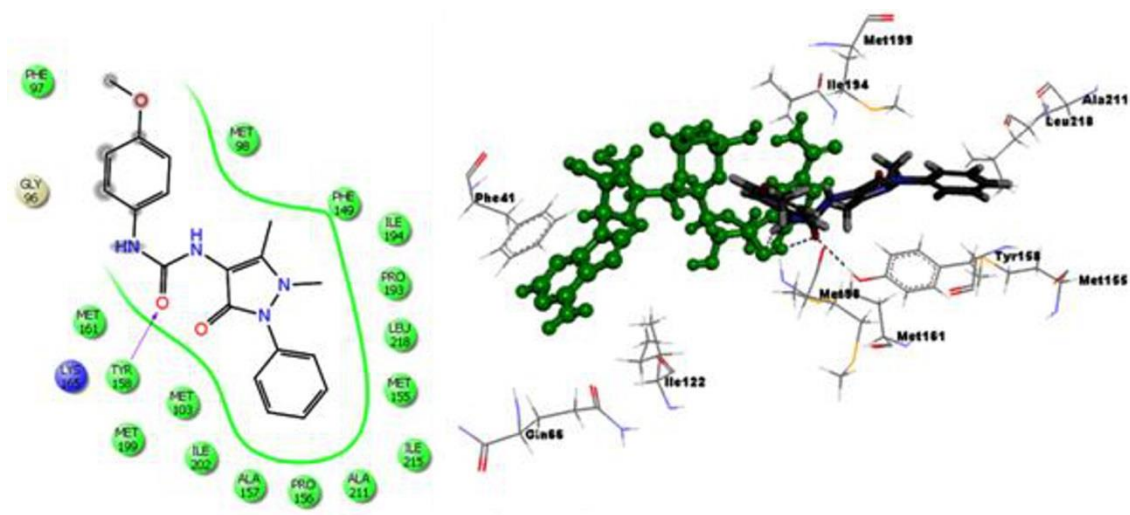
One of the active compounds from this series was further investigated using DSF. In our study, compound **PR\_12** showed significant positive  $T_m$  shift of 0.9 °C confirming the stability of the protein-ligand complex as shown in **Figure 5.32**.



**Figure 5.32:** DSF experiment for compound **PR\_12** (protein-ligand complex, green) showing an increase in the thermal shift of 0.9 °C compared with the native InhA protein (pink). Protein T<sub>m</sub> 39.90 °C and protein with ligand T<sub>m</sub> 40.80 °C.

### 5.3.6 Discussion

All synthesized compounds (except compound **PR\_27**) showed the percentage InhA inhibition in the range of 93.12 to 26.12 % at 10 μM concentration where eighteen compounds displayed better percentage inhibition compared to lead molecule (**UPS 1**). Seven compounds (**PR\_08**, **PR\_10**, **PR\_12 - PR\_15** and **PR\_17**) displayed more than 60 % enzyme inhibition and were subsequently tested for their IC<sub>50</sub> values. Compound **PR\_15** (1-(1,5-dimethyl-3-oxo-2-phenyl-2,3-dihydro-1H-pyrazol-4-yl)-3-(4-methoxyphenyl)urea) emerged as the most active compound *in vitro* with IC<sub>50</sub> of 2.96±0.21 μM. With the aim of getting insights into the structural basis for its activity, compound **PR\_15** was docked into the active site of the InhA protein (PDB ID:2H7M), where it displayed docking score of -8.06 kcal/mol and was involved in three hydrogen bonding interactions, one with Tyr158 and two with NAD<sup>+</sup>. This hydrogen bonding network is observed as a conserved feature among all potent InhA-inhibitor complexes identified so far. The pyrazolone core was involved in hydrophobic interactions with Phe149, Ile194, Pro193, Leu218, Met155, Ile215, Ala211, Pro156, Ala157, Ile202 and Met103 amino acid residues (**Figure 5.33**).



**Figure 5.33:** Binding pose and its interaction pattern of compound **PR\_15**.

Ureas (**PR\_13 - PR\_18**) displayed good InhA inhibition in the range of 93.12 – 34.23 % whereas amides (**PR\_04 - PR\_12**) showed moderate inhibition potency in the range of 82.08 to 30.12 %. In general, thioureas (**PR\_19 - PR\_26**) were less active compared to corresponding urea derivatives (**PR\_13 - PR\_18**) and similarly InhA inhibitory potency of sulphonamide derivatives (**PR\_27 - PR\_31**) was less in comparison with corresponding amides (**PR\_04 - PR\_12**). This highlights the importance of oxygen atom in formation of hydrogen bonds and hydrophobic interactions with the active site which are considered to be the most crucial factors affecting the inhibitory potency of these compounds.

The synthesized compounds were further evaluated for their *in vitro* anti-tubercular activity against *Mycobacterium tuberculosis* H37Rv (ATCC27294) using an agar dilution method with drug concentrations ranging from 50 to 0.78 µg/mL in duplicates. The minimum inhibitory concentration (MIC) was determined for each compound which was measured as the minimum concentration of compound required to completely inhibit the bacterial growth. Isoniazid, ethambutol, rifampicin and ofloxacin were used as reference compounds for comparison. The MIC values of the synthesized compounds along with the standard drugs for comparison are presented in **Table 5.8**. All the 4-amino-1,5-dimethyl-2-phenyl-1*H*-pyrazol-3(2*H*)-one derivatives showed *in vitro* activity against *Mycobacterium tuberculosis* with MIC ranging from 1.16 to 81.34 µM. Seventeen compounds (**PR\_04 - PR\_05, PR\_07 - PR\_12, PR\_14 - PR\_18, PR\_20 - PR\_21, PR\_23** and **PR\_30**) inhibited *Mycobacterium tuberculosis* with MIC of less than 10 µM and compound **PR\_10** (*N*-(1,5-dimethyl-3-oxo-2-phenyl-2,3-dihydro-1*H*-pyrazol-4-yl)-3-phenylpropanamide) emerged as the most potent

antimycobacterial molecule among the synthesized derivatives with a MIC of 1.16  $\mu\text{M}$ . Ten compounds (**PR\_04** - **PR\_05**, **PR\_08**, **PR\_10**, **PR\_12**, **PR\_16** - **PR\_18**, **PR\_20** and **PR\_23**) exhibited better *Mycobacterium tuberculosis* MIC values than the standard drug Ethambutol. As in certain cases, the efflux mechanisms are also reported to contribute in a major way to intrinsic resistance to drugs, the *in vitro* *Mycobacterium tuberculosis* potency of the synthesized derivatives were also evaluated in presence of reported efflux pump inhibitor piperine (8  $\mu\text{g/mL}$ ). It was observed that in most cases, *Mycobacterium tuberculosis* MIC decreased by 2 to 4 fold when tested in presence of piperine as shown in **Table 5.8**. Also, two compounds (**PR\_10** and **PR\_16**) exhibited submicromolar *Mycobacterium tuberculosis* MIC of 0.58  $\mu\text{M}$  in this study.

The synthesized compounds were further tested for cytotoxicity in a RAW 264.7 cell line (mouse leukemic monocyte macrophage) at 50  $\mu\text{M}$ . After 72 h of exposure, viability of the cells was assessed on the basis of cellular conversion of MTT into a formazan product using the Promega Cell Titer 96 non-radioactive cell proliferation assay. All tested compounds were not cytotoxic (less than 50% inhibition at 50  $\mu\text{M}$ ) to RAW 264.7 cells and their percentage growth inhibitions were reported in **Table 5.8**. The most active *Mycobacterium tuberculosis* InhA inhibitor (compound **PR\_15**) has shown toxicity of 24.34 % inhibition at 50  $\mu\text{M}$ .

All the synthesized derivatives were also evaluated for their predicted ADMET properties using the QikProp3.5 module of Schrodinger software. Almost all compounds exhibited excellent predicted pharmacokinetic parameters including Lipinski rule of five evaluated for drug-likeness showing characteristics (as shown in **Table 5.9**), but the predicted hERG cardiotoxicity associated with most of compounds may restrict their further development as promising drug candidate. The most active compound **PR\_15** was predicted to have moderately lipophilic nature required for ideal drug candidate but its predicted hERG toxicity may impede its further optimization and development.

**Table 5.9:** QikProp analysis of the ADMET properties of the synthesized derivatives **PR\_04** – **PR\_31**.

| Comp         | QPlogPo/w <sup>a</sup> | QPlogHERG <sup>b</sup> | QPPCaco <sup>c</sup> | QPlogBB <sup>d</sup> | QPPMDCK <sup>e</sup> | Percent Human Oral Absorption <sup>f</sup> | Rule of Five <sup>g</sup> |
|--------------|------------------------|------------------------|----------------------|----------------------|----------------------|--|---------------------------|
| <b>PR_04</b> | 1.84                   | -4.88                  | 1450.72              | -0.31                | 739.61               | 94.35                                      | 0                         |
| <b>PR_05</b> | 3.01                   | -4.98                  | 2714.32              | -0.11                | 1455.75              | 100  | 0                         |
| <b>PR_06</b> | 3.29                   | -6.24                  | 2043.26              | -0.26                | 1070.96              | 100  | 0                         |
| <b>PR_07</b> | 3.45                   | -6.03                  | 1816.99              | -0.20                | 1707.17              | 100  | 0                         |
| <b>PR_08</b> | 3.79                   | -6.17                  | 2044.20              | -0.10                | 2645.49              | 100  | 0                         |
| <b>PR_09</b> | 3.25                   | -6.15                  | 2043.26              | -0.34                | 1070.96              | 100  | 0                         |
| <b>PR_10</b> | 3.91                   | -6.68                  | 1904.90              | -0.47                | 992.79               | 100  | 0                         |
| <b>PR_11</b> | 3.40                   | -6.59                  | 1672.87              | -0.51                | 862.75               | 100  | 0                         |
| <b>PR_12</b> | 3.36                   | -6.46                  | 1555.15              | -0.60                | 797.32               | 100  | 0                         |
| <b>PR_13</b> | 2.95                   | -5.24                  | 976.54               | -0.49                | 690.87               | 100  | 0                         |
| <b>PR_14</b> | 3.46                   | -5.15                  | 973.37               | -0.34                | 1706.49              | 100  | 0                         |
| <b>PR_15</b> | 3.04                   | -5.14                  | 972.61               | -0.58                | 690.59               | 100  | 0                         |
| <b>PR_16</b> | 3.25                   | -5.37                  | 896.02               | -0.56                | 710.45               | 100  | 0                         |
| <b>PR_17</b> | 3.84                   | -5.27                  | 881.61               | -0.41                | 1723.41              | 100  | 0                         |
| <b>PR_18</b> | 3.44                   | -5.25                  | 882.32               | -0.65                | 698.79               | 100  | 0                         |
| <b>PR_19</b> | 3.79                   | -6.55                  | 2625.64              | -0.05                | 2666.64              | 100  | 0                         |
| <b>PR_20</b> | 4.21                   | -6.42                  | 2625.41              | 0.05                 | 4824.59              | 100  | 0                         |
| <b>PR_21</b> | 4.47                   | -6.46                  | 2625.44              | 0.10                 | 6582.26              | 100  | 0                         |
| <b>PR_22</b> | 4.06                   | -6.43                  | 2623.57              | -0.13                | 2664.26              | 100  | 0                         |
| <b>PR_23</b> | 4.30                   | -6.82                  | 2821.44              | -0.10                | 3003.86              | 100  | 0                         |
| <b>PR_24</b> | 4.65                   | -6.69                  | 2821.43              | 0.01                 | 5435.26              | 100  | 0                         |
| <b>PR_25</b> | 4.91                   | -6.72                  | 2820.98              | 0.06                 | 7414.34              | 100  | 0                         |
| <b>PR_26</b> | 4.51                   | -6.70                  | 2716.71              | -0.19                | 2878.63              | 100  | 0                         |
| <b>PR_27</b> | 2.01                   | -5.31                  | 771.77               | -0.64                | 382.51               | 90.41                                      | 0                         |
| <b>PR_28</b> | 2.42                   | -5.38                  | 1091.21              | -0.42                | 995.19               | 95.50                                      | 0                         |

Contd...

| Comp  | QLogPo/w <sup>a</sup> | QLogHERG <sup>b</sup> | QPPCaco <sup>c</sup> | QLogBB <sup>d</sup> | QPPMDCK <sup>e</sup> | Percent Human Oral Absorption <sup>f</sup> | Rule of Five <sup>g</sup> |
|-------|-----------------------|-----------------------|----------------------|---------------------|----------------------|--|---------------------------|
| PR_29 | 2.59                  | -5.07                 | 1061.73              | -0.35               | 1292.31              | 96.27                                      | 0                         |
| PR_30 | 2.17                  | -5.08                 | 1055.08              | -0.59               | 531.05               | 93.77                                      | 0                         |
| PR_31 | 2.20                  | -4.69                 | 1080.46              | -0.53               | 547.06               | 94.17                                      | 0                         |

<sup>a</sup>Predicted octanol/water partition coefficient logP (acceptable range: -2.0 to 6.5)

<sup>b</sup>Predicted IC<sub>50</sub> value for blockage of hERG K<sup>+</sup> channels.(below -5)

<sup>c</sup>Predicted apparent Caco-2 cell permeability in nm/sec (<25 poor; >500 great)

<sup>d</sup>Predicted brain/blood partition coefficient (-3.0 to 1.2)

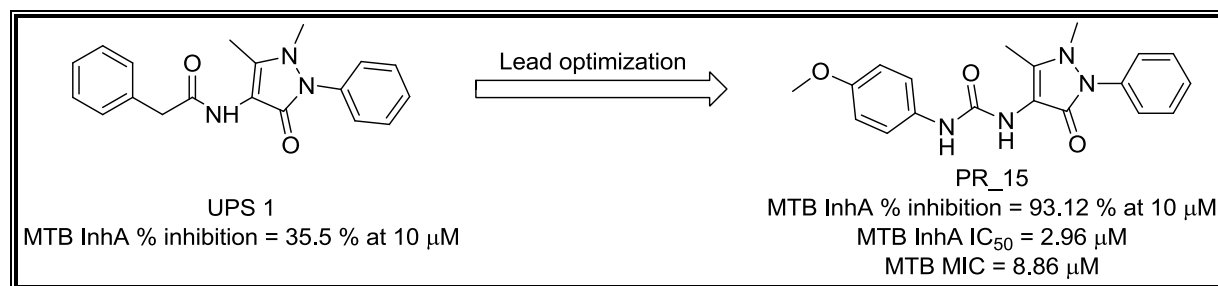
<sup>e</sup>Predicted apparent MDCK cell (model for blood-brain barrier) permeability in nm/s. (< 25 poor, > 500 great)

<sup>f</sup>Percent human oral absorption (< 25% is poor and > 80% is high)

<sup>g</sup>Rule of 5 violation (mol\_MW < 500, QLogPo/w < 5, donorHB ≤ 5, acqptHB ≤ 10) (concern above 1)

### 5.3.7 Highlights of the study

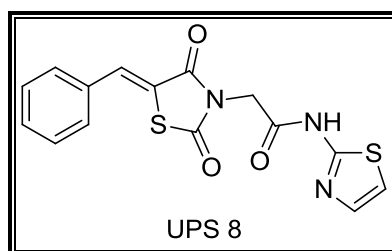
A series of twenty eight novel 4-amino-1,5-dimethyl-2-phenyl-1*H*-pyrazol-3(2*H*)-one derivatives was synthesised and screened against *Mycobacterium tuberculosis* InhA as well as drug sensitive *Mycobacterium tuberculosis* strains. Eighteen synthesized compounds showed better InhA inhibition as compared to lead molecules, and compound **PR\_15** (1-(1,5-dimethyl-3-oxo-2-phenyl-2,3-dihydro-1*H*-pyrazol-4-yl)-3-(4-methoxyphenyl)urea) emerged as the most potent molecule with IC<sub>50</sub> of 2.96 μM against *Mycobacterium tuberculosis* InhA, inhibited drug sensitive *Mycobacterium tuberculosis* with MIC of 8.86 μM and was non-cytotoxic at 50 μM (**Figure 5.34**).



**Figure 5.34:** Chemical structure and biological activity of the most active compound **PR\_15**.

#### 5.4 Development of 5-arylalkylidene-2-(4-oxo-2-thioxothiazolidin-3-yl)acetamide/propanamide derivatives as potential *Mycobacterium tuberculosis* InhA inhibitors

One of the lead 2-(5-benzylidene-2,4-dioxothiazolidin-3-yl)-*N*-(thiazol-2-yl)acetamide (**UPS 8**) from our previous study with thiazolidine-2,4-diones core displayed 27.2 % *Mycobacterium tuberculosis* InhA inhibition at 10  $\mu$ M (**Figure 5.35**) [Kumar U.C. *et al.*, 2013]. Our quest for more potent molecules encouraged us to utilize this lead molecule as a structural framework to construct a library to improve InhA inhibition potency. However, our initial efforts to improve potency of thiazolidine-2,4-diones resulted in less active compounds. Recently, Mendgen T. *et al.* [Mendgen T. *et al.*, 2012] compared the role of exocyclic, double-bonded sulphur present in rhodanine (2-thioxothiazolidin-4-one), whose tendency to form polar, intermolecular interactions was very prominent in comparison to the exocyclic, double-bonded oxygen atom at the same position in thiazolidine-2,4-dione. As a result, rhodanine possess greater potential for interactions with proteins than is the case for thiazolidine-2,4-diones. This prompted us to replace double-bonded oxygen at 2<sup>nd</sup> position to double-bonded sulphur atom in our lead molecule.

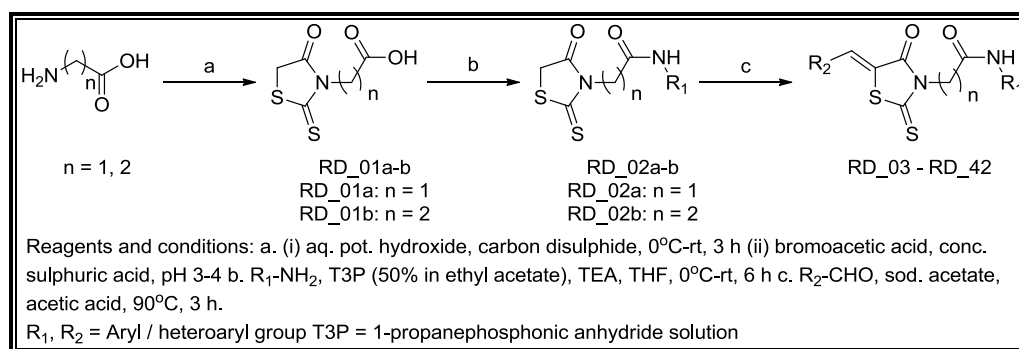


**Figure 5.35:** Chemical structure of lead molecule **UPS 8**.

##### 5.4.1 Chemical synthesis and characterization

An analysis of the lead molecule (**UPS 8**), keeping in mind replacement of double-bonded oxygen at 2<sup>nd</sup> position to double-bonded sulphur atom, led to reaction sequence delineated in **Figure 5.36**, which was utilised for lead expansion step to generate the library molecules **RD\_03 – RD\_42** (as shown in **Table 5.10**). As depicted, the synthesis was achieved by

adopting the classical approach for developing rhodanine derivatives starting from commercially available and relatively cheap amino acids glycine and  $\beta$ -alanine as precursors. The respective precursor on treatment with carbon disulphide in basic media followed by addition of bromoacetic acid on acid workup gave the rhodanine derivatives with one and two carbon carboxylic acid tail **RD\_01a** and **RD\_01b** respectively [McKee T. *et al.*, 2003]. These were later transformed into the corresponding carboxamide derivatives **RD\_02a-h** by coupling with the respective amines using propyl phosphonic anhydride solution (T3P) as the coupling agent. The final library was then constructed by Knoevenagel condensation of the so formed scaffolds **RD\_02a-h** with the desired aldehyde to give the final library **RD\_03 – RD\_42** as shown in **Table 5.10** in good yield and purity.



**Figure 5.36:** Synthetic protocol utilized for synthesis of compounds **RD\_03 – RD\_42**.

## 5.4.2 Experimental protocol utilised for synthesis

### Synthesis of 2-(4-oxo-2-thioxothiazolidin-3-yl)acetic acid (**RD\_01a**)

To a solution of glycine (6.8 g, 90.59 mmol) in 34 ml of 22 % aqueous potassium hydroxide (158.53 mmol), carbon disulphide (6.0 mL, 99.65 mmol) was added dropwise at 0 °C. The solution was allowed to mix at rt for 3 h during which time bromoacetic acid (12.8 g, 90.59 mmol) was added as solid in small portions over about 20 min. The reaction was allowed to mix for additional 3 h, at which time a precipitate formed. The pH of reaction mixture was adjusted to 3-4 using conc. sulphuric acid and it was allowed to stand overnight at rt. The solid was filtered off, washed with water and dried in vacuum oven to get desired 2-(4-oxo-2-thioxothiazolidin-3-yl)acetic acid (**RD\_01a**) as an off-white solid (5.41 g, 31.12 %). M.p: 146-148 °C. <sup>1</sup>H NMR (DMSO-d<sub>6</sub>):  $\delta_{\text{H}}$  12.23 (s, 1H), 4.53 (s, 2H), 4.33 (s, 2H). ESI-MS *m/z* 190 (M-H)<sup>-</sup>.



### Synthesis of 3-(4-oxo-2-thioxothiazolidin-3-yl)propionic acid (RD\_01b)

To a solution of  $\beta$ -alanine (6.8 g, 76.32 mmol) in 34 ml of 22 % aqueous potassium hydroxide (133.57 mmol), carbon disulphide (5.0 mL, 83.95 mmol) was added dropwise at 0 °C. The solution was allowed to mix at rt for 3 h during which time bromoacetic acid (10.7 g, 76.32 mmol) was added as a solid in small portions over about 20 min. The reaction was allowed to mix for additional 3 h, at which time a precipitate formed. The pH of reaction mixture was adjusted to 3-4 using conc. sulphuric acid and it was allowed to stand overnight at rt. The solid was filtered off, washed with water and dried in vacuum oven to get desired 2-(4-oxo-2-thioxothiazolidin-3-yl)propionic acid (RD\_01b) as an off-white solid (5.71 g, 36.39 %). M.p: 158-160 °C. <sup>1</sup>H NMR (DMSO-d<sub>6</sub>):  $\delta_{\text{H}}$  12.44 (s, 1H), 4.37 – 4.33 (t,  $J = 6.4$  Hz, 2H), 4.31 (s, 2H), 2.61 – 2.57 (t,  $J = 6.7$  Hz, 2H). ESI-MS  $m/z$  204 (M-H)<sup>-</sup>.

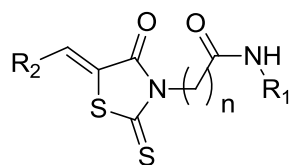
### Procedure for the synthesis of 2-(4-oxo-2-thioxothiazolidin-3-yl)-N-(aryl/heteroaryl)acetamide/propanamides (RD\_02a-h)

To a solution of corresponding amine (1.2 mmol) in THF (10 mL) was added TEA (2 mmol) and corresponding acid (RD\_01a-b) (1 mmol) at 0 °C. Propylphosphonic anhydride solution (T3P) ( $\geq 50$  wt. % in ethyl acetate; 2 mmol) was then added dropwise at 0 °C, and the reaction mixture was slowly warmed to rt and stirred for 6 h (monitored by TLC & LCMS for completion). The reaction mixture was then washed with water (4 mL), and the organic layer dried over anhydrous sodium sulphate and evaporated under reduced pressure. The crude product was further purified by silica gel column chromatography using hexane: ethyl acetate as eluent to give the corresponding product (RD\_02a-h).

### Procedure for the synthesis of 5-(aryl/heteroaryl)-4-oxo-2-thioxothiazolidin-3-yl-N-(aryl/heteroaryl)acetamide/propanamides (RD\_03 - RD\_42)

A mixture of corresponding RD\_02a-h (1 mmol) in glacial acetic acid (2 ml) and corresponding aldehyde (1.1 mmol) was heated at 90 °C for 3 h (monitored by TLC & LCMS for completion). The reaction mixture was concentrated under reduced pressure and the obtained solid was filtered off, washed with n-hexane to get corresponding 5-(aryl/heteroaryl)-4-oxo-2-thioxothiazolidin-3-yl-N-(aryl/heteroaryl)acetamide/propanamides (RD\_03 - RD\_42). The physicochemical properties of synthesized derivatives are shown in Table 5.10.

**Table 5.10:** Physicochemical properties of synthesized compounds **RD\_03 - RD\_42**.

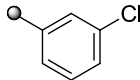
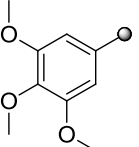
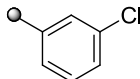
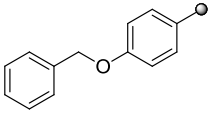
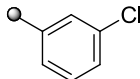
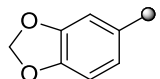
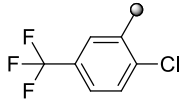
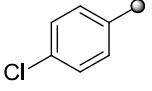
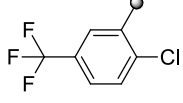
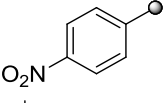
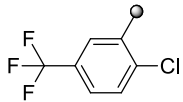
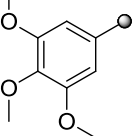
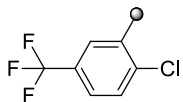
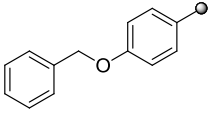
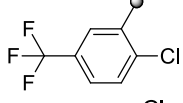
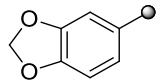
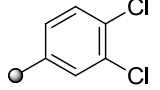
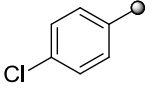
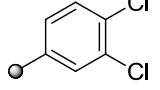
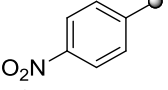
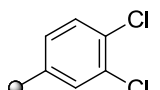
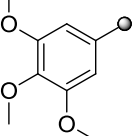
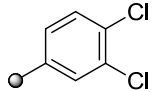
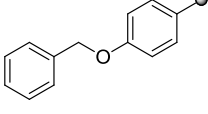
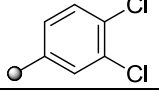
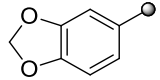


| Comp  | n | R <sub>1</sub> | R <sub>2</sub> | Yield (%) | Melting point (°C) | Molecular formula   | Molecular weight |
|-------|---|----------------|----------------|-----------|--------------------|---|------------------|
| RD_03 | 1 |                |                | 89.01     | 296-298            | C <sub>15</sub> H <sub>10</sub> ClN <sub>3</sub> O <sub>2</sub> S <sub>3</sub>                              | 395.91           |
| RD_04 | 1 |                |                | 87.13     | 284-286            | C <sub>15</sub> H <sub>10</sub> N <sub>4</sub> O <sub>4</sub> S <sub>3</sub>                                | 406.46           |
| RD_05 | 1 |                |                | 83.46     | 249-251            | C <sub>18</sub> H <sub>17</sub> N <sub>3</sub> O <sub>5</sub> S <sub>3</sub>                                | 451.54           |
| RD_06 | 1 |                |                | 81.29     | 271-273            | C <sub>22</sub> H <sub>17</sub> N <sub>3</sub> O <sub>3</sub> S <sub>3</sub>                                | 467.58           |
| RD_07 | 1 |                |                | 78.17     | 277-279            | C <sub>16</sub> H <sub>11</sub> N <sub>3</sub> O <sub>4</sub> S <sub>3</sub>                                | 405.47           |
| RD_08 | 1 |                |                | 69.59     | 286-288            | C <sub>18</sub> H <sub>12</sub> Cl <sub>2</sub> N <sub>2</sub> O <sub>2</sub> S <sub>2</sub>                | 423.34           |
| RD_09 | 1 |                |                | 72.36     | 260-262            | C <sub>18</sub> H <sub>12</sub> ClN <sub>3</sub> O <sub>4</sub> S <sub>2</sub>                              | 433.89           |
| RD_10 | 1 |                |                | 73.48     | 199-201            | C <sub>21</sub> H <sub>19</sub> ClN <sub>2</sub> O <sub>5</sub> S <sub>2</sub>                              | 478.97           |
| RD_11 | 1 |                |                | 69.14     | 224-228            | C <sub>25</sub> H <sub>19</sub> ClN <sub>2</sub> O <sub>3</sub> S <sub>2</sub>                              | 495.01           |
| RD_12 | 1 |                |                | 63.52     | 286-288            | C <sub>19</sub> H <sub>13</sub> ClN <sub>2</sub> O <sub>4</sub> S <sub>2</sub>                              | 432.90           |
| RD_13 | 1 |                |                | 88.23     | 276-278            | C <sub>19</sub> H <sub>11</sub> Cl <sub>2</sub> F <sub>3</sub> N <sub>2</sub> O <sub>2</sub> S <sub>2</sub> | 491.33           |
| RD_14 | 1 |                |                | 73.66     | 275-277            | C <sub>19</sub> H <sub>11</sub> ClF <sub>3</sub> N <sub>3</sub> O <sub>4</sub> S <sub>2</sub>               | 501.89           |

Contd...

| Comp  | n | R <sub>1</sub> | R <sub>2</sub> | Yield (%) | Melting point (°C) | Molecular formula   | Molecular weight |
|-------|---|----------------|----------------|-----------|--------------------|---|------------------|
| RD_15 | 1 |                |                | 68.72     | 232-234            | C <sub>22</sub> H <sub>18</sub> ClF <sub>3</sub> N <sub>2</sub> O <sub>5</sub> S <sub>2</sub> | 546.97           |
| RD_16 | 1 |                |                | 63.83     | 222-224            | C <sub>26</sub> H <sub>18</sub> ClF <sub>3</sub> N <sub>2</sub> O <sub>3</sub> S <sub>2</sub> | 563.01           |
| RD_17 | 1 |                |                | 65.43     | 236-238            | C <sub>20</sub> H <sub>12</sub> ClF <sub>3</sub> N <sub>2</sub> O <sub>4</sub> S <sub>2</sub> | 500.90           |
| RD_18 | 1 |                |                | 83.11     | 295-297            | C <sub>18</sub> H <sub>11</sub> Cl <sub>3</sub> N <sub>2</sub> O <sub>2</sub> S <sub>2</sub>  | 457.78           |
| RD_19 | 1 |                |                | 79.16     | 277-279            | C <sub>18</sub> H <sub>11</sub> Cl <sub>2</sub> N <sub>3</sub> O <sub>4</sub> S <sub>2</sub>  | 468.33           |
| RD_20 | 1 |                |                | 77.69     | 215-217            | C <sub>21</sub> H <sub>18</sub> Cl <sub>2</sub> N <sub>2</sub> O <sub>5</sub> S <sub>2</sub>  | 513.41           |
| RD_21 | 1 |                |                | 68.43     | 219-221            | C <sub>25</sub> H <sub>18</sub> Cl <sub>2</sub> N <sub>2</sub> O <sub>3</sub> S <sub>2</sub>  | 529.46           |
| RD_22 | 1 |                |                | 72.29     | 285-287            | C <sub>19</sub> H <sub>12</sub> Cl <sub>2</sub> N <sub>2</sub> O <sub>4</sub> S <sub>2</sub>  | 467.35           |
| RD_23 | 2 |                |                | 72.76     | 288-290            | C <sub>16</sub> H <sub>12</sub> ClN <sub>3</sub> O <sub>2</sub> S <sub>3</sub>                | 409.93           |
| RD_24 | 2 |                |                | 76.33     | 281-283            | C <sub>16</sub> H <sub>12</sub> N <sub>4</sub> O <sub>4</sub> S <sub>3</sub>                  | 420.49           |
| RD_25 | 2 |                |                | 63.72     | 265-267            | C <sub>19</sub> H <sub>19</sub> N <sub>3</sub> O <sub>5</sub> S <sub>3</sub>                  | 465.57           |
| RD_26 | 2 |                |                | 74.36     | 251-253            | C <sub>23</sub> H <sub>19</sub> N <sub>3</sub> O <sub>3</sub> S <sub>3</sub>                  | 481.61           |
| RD_27 | 2 |                |                | 67.31     | 269-271            | C <sub>17</sub> H <sub>13</sub> N <sub>3</sub> O <sub>4</sub> S <sub>3</sub>                  | 419.50           |
| RD_28 | 2 |                |                | 86.21     | 260-262            | C <sub>19</sub> H <sub>14</sub> Cl <sub>2</sub> N <sub>2</sub> O <sub>2</sub> S <sub>2</sub>  | 437.36           |
| RD_29 | 2 |                |                | 80.37     | 236-238            | C <sub>19</sub> H <sub>14</sub> ClN <sub>3</sub> O <sub>4</sub> S <sub>2</sub>                | 447.92           |

Contd...

| Comp  | n | R <sub>1</sub>  | R <sub>2</sub>  | Yield (%) | Melting point (°C) | Molecular formula   | Molecular weight |
|-------|---|---|---|-----------|--------------------|---|------------------|
| RD_30 | 2 |    |    | 73.28     | 201-203            | C <sub>22</sub> H <sub>21</sub> ClN <sub>2</sub> O <sub>5</sub> S <sub>2</sub>                              | 493.00           |
| RD_31 | 2 |    |    | 77.49     | 241-243            | C <sub>26</sub> H <sub>21</sub> ClN <sub>2</sub> O <sub>3</sub> S <sub>2</sub>                              | 509.04           |
| RD_32 | 2 |    |    | 81.52     | 231-233            | C <sub>20</sub> H <sub>15</sub> ClN <sub>2</sub> O <sub>4</sub> S <sub>2</sub>                              | 446.93           |
| RD_33 | 2 |    |    | 81.52     | 234-236            | C <sub>20</sub> H <sub>13</sub> Cl <sub>2</sub> F <sub>3</sub> N <sub>2</sub> O <sub>2</sub> S <sub>2</sub> | 505.36           |
| RD_34 | 2 |    |    | 76.63     | 247-249            | C <sub>20</sub> H <sub>13</sub> ClF <sub>3</sub> N <sub>3</sub> O <sub>4</sub> S <sub>2</sub>               | 515.91           |
| RD_35 | 2 |    |   | 81.33     | 221-223            | C <sub>23</sub> H <sub>20</sub> ClF <sub>3</sub> N <sub>2</sub> O <sub>5</sub> S <sub>2</sub>               | 560.99           |
| RD_36 | 2 |  |  | 79.11     | 211-213            | C <sub>27</sub> H <sub>20</sub> ClF <sub>3</sub> N <sub>2</sub> O <sub>3</sub> S <sub>2</sub>               | 577.04           |
| RD_37 | 2 |  |  | 82.73     | 213-215            | C <sub>21</sub> H <sub>14</sub> ClF <sub>3</sub> N <sub>2</sub> O <sub>4</sub> S <sub>2</sub>               | 514.93           |
| RD_38 | 2 |  |  | 78.18     | 253-255            | C <sub>19</sub> H <sub>13</sub> Cl <sub>3</sub> N <sub>2</sub> O <sub>2</sub> S <sub>2</sub>                | 471.81           |
| RD_39 | 2 |  |  | 75.44     | 226-228            | C <sub>19</sub> H <sub>13</sub> Cl <sub>2</sub> N <sub>3</sub> O <sub>4</sub> S <sub>2</sub>                | 482.36           |
| RD_40 | 2 |  |  | 78.14     | 239-241            | C <sub>22</sub> H <sub>20</sub> Cl <sub>2</sub> N <sub>2</sub> O <sub>5</sub> S <sub>2</sub>                | 527.44           |
| RD_41 | 2 |  |  | 81.38     | 254-256            | C <sub>26</sub> H <sub>20</sub> Cl <sub>2</sub> N <sub>2</sub> O <sub>3</sub> S <sub>2</sub>                | 543.48           |
| RD_42 | 2 |  |  | 72.61     | 251-253            | C <sub>20</sub> H <sub>14</sub> Cl <sub>2</sub> N <sub>2</sub> O <sub>4</sub> S <sub>2</sub>                | 481.37           |

### 5.4.3 Characterization of synthesized compounds

Both analytical and spectral data ( $^1\text{H}$  NMR,  $^{13}\text{C}$  NMR and mass spectra) of all the synthesized compounds were in full agreement with the proposed structures. Arylalkylidenerhodanines can form two isomers. According to references [Ohishi Y. *et al.*, 1990; Whittessit C.A. *et al.*, 1996; Khodair A.I., 2002], syntheses of these compounds result in the thermodynamically more stable *Z*-isomers.  $^1\text{H}$ -NMR signals of the methine-group hydrogens for *Z*-isomers are more downfield compared to *E*-isomers due to interaction with carbonyl group at 4<sup>th</sup> position. The experimental signals of methine-group hydrogens in the rhodanine derivatives studied in the present paper were in the range of 7.78-8.38 ppm and compared with the values reported previously. Thus, it can be concluded that all rhodanine derivatives reported in the present paper were obtained as single *Z*-isomers.

#### **2-(4-Oxo-2-thioxothiazolidin-3-yl)acetic acid (RD\_01a)**

M.p: 146-148 °C.  $^1\text{H}$  NMR (DMSO- $d_6$ ):  $\delta_{\text{H}}$  12.23 (s, 1H), 4.53 (s, 2H), 4.33 (s, 2H). ESI-MS  $m/z$  190 (M-H)<sup>-</sup>.

#### **3-(4-Oxo-2-thioxothiazolidin-3-yl)propionic acid (RD\_01b)**

M.p: 158-160 °C.  $^1\text{H}$  NMR (DMSO- $d_6$ ):  $\delta_{\text{H}}$  12.44 (s, 1H), 4.37 – 4.33 (t,  $J = 6.4$  Hz, 2H), 4.31 (s, 2H), 2.61 – 2.57 (t,  $J = 6.7$  Hz, 2H). ESI-MS  $m/z$  204 (M-H)<sup>-</sup>.

#### **2-(4-Oxo-2-thioxothiazolidin-3-yl)-*N*-(thiazol-2-yl)acetamide (RD\_02a)**

The compound was synthesized according to the general procedure using 2-aminothiazole (0.63 g, 6.27 mmol) and 2-(4-oxo-2-thioxothiazolidin-3-yl)acetic acid (**RD\_01a**) (1.0 g, 5.22 mmol) to afford **RD\_02a** (0.919 g, 64.78 %) as pale yellow solid. M.p: 231-235 °C.  $^1\text{H}$  NMR (DMSO- $d_6$ ):  $\delta_{\text{H}}$  12.12 (s, 1H), 7.49 – 7.46 (d,  $J = 7.2$  Hz, 1H), 7.24 – 7.22 (d,  $J = 7.2$  Hz, 1H), 4.87 (s, 2H), 4.36 (s, 2H). ESI-MS  $m/z$  272 (M-H)<sup>-</sup>.

#### ***N*-(3-Chlorophenyl)-2-(4-oxo-2-thioxothiazolidin-3-yl)acetamide (RD\_02b)**

The compound was synthesized according to the general procedure using 3-chloroaniline (0.78 g, 6.27 mmol) and 2-(4-oxo-2-thioxothiazolidin-3-yl)acetic acid (**RD\_01a**) (1.0 g, 5.22 mmol) to afford **RD\_02b** (1.026 g, 65.41 %) as pale yellow solid. M.p: 238-240 °C.  $^1\text{H}$  NMR

(DMSO- $d_6$ ):  $\delta_H$  10.58 (s, 1H), 7.92 (s, 1H), 7.52 – 7.20 (m, 3H), 4.73 (s, 2H), 4.32 (s, 2H). ESI-MS  $m/z$  299 (M-H) $^-$ .

***N*-(2-Chloro-5-(trifluoromethyl)phenyl)-2-(4-oxo-2-thioxothiazolidin-3-yl)acetamide (RD\_02c)**

The compound was synthesized according to the general procedure using 2-chloro-5-trifluoromethylaniline (1.22 g, 6.27 mmol) and 2-(4-oxo-2-thioxothiazolidin-3-yl)acetic acid (**RD\_01a**) (1.0 g, 5.22 mmol) to afford **RD\_02c** (2.235 g, 60.10 %) as pale yellow solid. M.p: 249-251 °C.  $^1H$  NMR (DMSO- $d_6$ ):  $\delta_H$  10.41 (s, 1H), 8.14 – 8.13 (d,  $J = 1.8$  Hz, 1H), 7.81 – 7.78 (d,  $J = 8.4$  Hz, 1H), 7.59 – 7.56 (dd,  $J = 6.3$  Hz,  $J = 1.8$  Hz, 1H), 4.93 (s, 2H), 4.37 (s, 2H). ESI-MS  $m/z$  367 (M-H) $^-$ .

***N*-(3,4-Dichlorophenyl)-2-(4-oxo-2-thioxothiazolidin-3-yl)acetamide (RD\_02d)**

The compound was synthesized according to the general procedure using 3,4-dichloroaniline (1.01 g, 6.27 mmol) and 2-(4-oxo-2-thioxothiazolidin-3-yl)acetic acid (**RD\_01a**) (1.0 g, 5.22 mmol) to afford **RD\_02d** (1.071 g, 61.23 %) as pale yellow solid. M.p: 259-262 °C.  $^1H$  NMR (DMSO- $d_6$ ):  $\delta_H$  10.32 (s, 1H), 8.38 (s, 1H), 7.56 – 7.53 (d,  $J = 8.7$  Hz, 1H), 7.44 – 7.40 (dd,  $J = 6.3$  Hz,  $J = 2.4$ , 1H), 5.01 (s, 2H), 4.34 (s, 2H). ESI-MS  $m/z$  334 (M-H) $^-$ .

**3-(4-Oxo-2-thioxothiazolidin-3-yl)-*N*-(thiazol-2-yl)propanamide (RD\_02e)**

The compound was synthesized according to the general procedure using 2-aminothiazole (0.58 g, 5.84 mmol) and 2-(4-oxo-2-thioxothiazolidin-3-yl)propionic acid (**RD\_01b**) (1.0 g, 4.87 mmol) to afford **RD\_02e** (0.889 g, 63.57 %) as pale yellow solid. M.p: 243-245 °C.  $^1H$  NMR (DMSO- $d_6$ ):  $\delta_H$  12.15 (s, 1H), 7.45 – 7.4 (d,  $J = 7.2$  Hz, 1H), 7.24 – 7.21 (d,  $J = 7.2$  Hz, 1H), 4.46 – 4.43 (d,  $J = 6.6$  Hz, 2H), 4.32 (s, 2H), 2.26 – 2.23 (d,  $J = 6.6$  Hz, 2H). ESI-MS  $m/z$  286 (M-H) $^-$ .

***N*-(3-Chlorophenyl)-3-(4-oxo-2-thioxothiazolidin-3-yl)propanamide (RD\_02f)**

The compound was synthesized according to the general procedure using 3-chloroaniline (0.74 g, 5.84 mmol) and 2-(4-oxo-2-thioxothiazolidin-3-yl)propionic acid (**RD\_01b**) (1.0 g, 4.87 mmol) to afford **RD\_02f** (0.988 g, 64.58 %) as pale yellow solid. M.p: 248-250 °C.  $^1H$  NMR (DMSO- $d_6$ ):  $\delta_H$  10.61 (s, 1H), 7.90 (s, 1H), 7.49 – 7.24 (m, 3H), 4.42 – 4.40 (d,  $J = 6.8$  Hz, 2H), 4.36 (s, 2H), 2.23 – 2.21 (d,  $J = 6.7$  Hz, 2H). ESI-MS  $m/z$  313 (M-H) $^-$ .

***N*-(2-Chloro-5-(trifluoromethyl)phenyl)-3-(4-oxo-2-thioxothiazolidin-3-yl)propanamide (RD\_02g)**

The compound was synthesized according to the general procedure using 2-chloro-5-trifluoromethylaniline (1.14 g, 5.84 mmol) and 2-(4-oxo-2-thioxothiazolidin-3-yl)propionic acid (**RD\_01b**) (1.0 g, 4.87 mmol) to afford **RD\_02g** (1.10 g, 59.17 %) as pale yellow solid. M.p: 261-263 °C. <sup>1</sup>H NMR (DMSO-d<sub>6</sub>): δ<sub>H</sub> 10.45 (s, 1H), 8.08 – 8.07 (d, *J* = 1.6 Hz, 1H), 7.82 – 7.79 (d, *J* = 8.2 Hz, 1H), 7.61 – 7.59 (dd, *J* = 6.2 Hz, *J* = 1.9 Hz, 1H), 4.43 – 4.41 (d, *J* = 6.9 Hz, 2H), 4.30 (s, 2H), 2.22 – 2.20 (d, *J* = 6.9 Hz, 2H). ESI-MS *m/z* 381 (M-H)<sup>-</sup>.

***N*-(3,4-Dichlorophenyl)-3-(4-oxo-2-thioxothiazolidin-3-yl)propanamide (RD\_02h)**

The compound was synthesized according to the general procedure using 3,4-dichloroaniline (0.94 g, 5.84 mmol) and 2-(4-oxo-2-thioxothiazolidin-3-yl)propionic acid (**RD\_01b**) (1.0 g, 4.87 mmol) to afford **RD\_02h** (1.005 g, 59.17 %) as pale yellow solid. M.p: 270-272 °C. <sup>1</sup>H NMR (DMSO-d<sub>6</sub>): δ<sub>H</sub> 10.27 (s, 1H), 8.34 (s, 1H), 7.54 – 7.51 (d, *J* = 8.2 Hz, 1H), 7.43 – 7.40 (dd, *J* = 6.9 Hz, *J* = 2.4 Hz, 1H), 4.41 – 4.39 (d, *J* = 7.2 Hz, 2H), 4.35 (s, 2H), 2.21 – 2.19 (d, *J* = 7.1 Hz, 2H). ESI-MS *m/z* 348 (M-H)<sup>-</sup>.

**2-(5-(4-Chlorobenzylidene)-4-oxo-2-thioxothiazolidin-3-yl)-*N*-(thiazol-2-yl)acetamide (RD\_03)**

The compound was synthesized according to the general procedure using 2-(4-oxo-2-thioxothiazolidin-3-yl)-*N*-(thiazol-2-yl)acetamide (**RD\_02a**) (0.1 g, 0.36 mmol) and 4-chlorobenzaldehyde (0.056 g, 0.40 mmol) to afford **RD\_03** (0.129 g, 89.01 %) as buff-coloured solid. M.p: 296-298 °C. <sup>1</sup>H NMR (DMSO-d<sub>6</sub>): δ<sub>H</sub> 12.13 (s, 1H), 7.84 (s, 1H), 7.71 – 7.31 (m, 6H), 4.33 (s, 2H). <sup>13</sup>C NMR (DMSO-d<sub>6</sub>): δ<sub>C</sub> 193.1, 168.5, 165.0, 160.7, 142.9, 133.7, 133.4, 131.9, 129.2 (2C), 128.8 (2C), 120.5, 113.3, 46.8. ESI-MS *m/z* 394 (M-H)<sup>-</sup>. Anal. Calcd. for C<sub>15</sub>H<sub>10</sub>ClN<sub>3</sub>O<sub>2</sub>S<sub>3</sub>: C, 45.51; H, 2.55; N, 10.61; Found: C, 45.58; H, 2.51; N, 10.57.

**2-(5-(4-Nitrobenzylidene)-4-oxo-2-thioxothiazolidin-3-yl)-*N*-(thiazol-2-yl)acetamide (RD\_04)**

The compound was synthesized according to the general procedure using 2-(4-oxo-2-thioxothiazolidin-3-yl)-*N*-(thiazol-2-yl)acetamide (**RD\_02a**) (0.1 g, 0.36 mmol) and 4-

nitrobenzaldehyde (0.060 g, 0.40 mmol) to afford **RD\_04** (0.130 g, 87.13 %) as pale yellow solid. M.p: 284-286 °C. <sup>1</sup>H NMR (DMSO-d<sub>6</sub>): δ<sub>H</sub> 12.03 (s, 1H), 8.36 – 7.52 (m, 7H), 4.31 (s, 2H). <sup>13</sup>C NMR (DMSO-d<sub>6</sub>): δ<sub>C</sub> 193.4, 168.2, 164.8, 161.0, 147.6, 143.1, 141.1, 132.4, 129.1 (2C), 124.1 (2C), 118.4, 113.0, 47.0. ESI-MS *m/z* 405 (M-H)<sup>-</sup>. Anal. Calcd. for C<sub>15</sub>H<sub>10</sub>N<sub>4</sub>O<sub>4</sub>S<sub>3</sub>: C, 44.32; H, 2.48; N, 13.78; Found: C, 44.37; H, 2.42; N, 13.72.

**2-(4-Oxo-2-thioxo-5-(3,4,5-trimethoxybenzylidene)thiazolidin-3-yl)-N-(thiazol-2-yl)acetamide (RD\_05)**

The compound was synthesized according to the general procedure using 2-(4-oxo-2-thioxothiazolidin-3-yl)-N-(thiazol-2-yl)acetamide (**RD\_02a**) (0.1 g, 0.36 mmol) and 3,4,5-trimethoxybenzaldehyde (0.078 g, 0.40 mmol) to afford **RD\_05** (0.137 g, 83.46 %) as pale yellow solid. M.p: 249-251 °C. <sup>1</sup>H NMR (DMSO-d<sub>6</sub>): δ<sub>H</sub> 12.10 (s, 1H), 8.03 (s, 1H), 7.61 – 6.79 (m, 4H), 4.32 (s, 2H), 3.84 (s, 6H), 3.76 (s, 3H). <sup>13</sup>C NMR (DMSO-d<sub>6</sub>): δ<sub>C</sub> 193.2, 168.1, 164.1, 158.2, 153.0 (2C), 143.1, 138.5, 132.2, 129.7, 116.0, 112.3, 104.1 (2C), 61.0, 56.2 (2C), 46.9. ESI-MS *m/z* 450 (M-H)<sup>-</sup>. Anal. Calcd. for C<sub>18</sub>H<sub>17</sub>N<sub>3</sub>O<sub>5</sub>S<sub>3</sub>: C, 47.88; H, 3.79; N, 9.31; Found: C, 47.96; H, 3.84; N, 9.26.

**2-(5-(4-(Benzyloxy)benzylidene)-4-oxo-2-thioxothiazolidin-3-yl)-N-(thiazol-2-yl)acetamide (RD\_06)**

The compound was synthesized according to the general procedure using 2-(4-oxo-2-thioxothiazolidin-3-yl)-N-(thiazol-2-yl)acetamide (**RD\_02a**) (0.1 g, 0.36 mmol) and 4-(benzyloxy)benzaldehyde (0.084 g, 0.40 mmol) to afford **RD\_06** (0.139 g, 81.29 %) as pale yellow solid. M.p: 271-273 °C. <sup>1</sup>H NMR (DMSO-d<sub>6</sub>): δ<sub>H</sub> 12.21 (s, 1H), 7.93 (s, 1H), 7.81 – 7.16 (m, 11H), 5.22 (s, 2H), 4.89 (s, 2H). <sup>13</sup>C NMR (DMSO-d<sub>6</sub>): δ<sub>C</sub> 193.3, 168.3, 165.1, 159.3, 157.3, 143.1, 136.3, 131.9, 130.4 (2C), 128.9 (2C), 127.7, 127.4, 127.3 (2C), 116.2, 114.3 (2C), 112.2, 71.2, 48.0. ESI-MS *m/z* 466 (M-H)<sup>-</sup>. Anal. Calcd. for C<sub>22</sub>H<sub>17</sub>N<sub>3</sub>O<sub>3</sub>S<sub>3</sub>: C, 56.51; H, 3.66; N, 8.99; Found: C, 56.57; H, 3.62; N, 9.06.

**2-(5-(Benzo[*d*][1,3]dioxol-5-ylmethylene)-4-oxo-2-thioxothiazolidin-3-yl)-N-(thiazol-2-yl)acetamide (RD\_07)**

The compound was synthesized according to the general procedure using 2-(4-oxo-2-thioxothiazolidin-3-yl)-N-(thiazol-2-yl)acetamide (**RD\_02a**) (0.1 g, 0.36 mmol) and piperonal (0.060 g, 0.40 mmol) to afford **RD\_07** (0.115 g, 78.17 %) as brown solid. M.p:



277-279 °C. <sup>1</sup>H NMR (DMSO-d<sub>6</sub>): δ<sub>H</sub> 12.13 (s, 1H), 7.82 (s, 1H), 7.71 – 7.01 (m, 5H), 6.09 (s, 2H), 4.77 (s, 2H). <sup>13</sup>C NMR (DMSO-d<sub>6</sub>): δ<sub>C</sub> 193.3, 168.6, 164.3, 159.3, 150.0, 148.5, 139.9, 132.9, 127.4, 123.1, 114.2, 110.1, 109.4, 109.1, 102.2, 47.3. ESI-MS *m/z* 404 (M-H)<sup>-</sup>. Anal. Calcd. for C<sub>16</sub>H<sub>11</sub>N<sub>3</sub>O<sub>4</sub>S<sub>3</sub>: C, 47.39; H, 2.73; N, 10.36; Found: C, 47.45; H, 2.77; N, 10.38.

**2-(5-(4-Chlorobenzylidene)-4-oxo-2-thioxothiazolidin-3-yl)-N-(3-chlorophenyl)acetamide (RD\_08)**

The compound was synthesized according to the general procedure using *N*-(3-chlorophenyl)-2-(4-oxo-2-thioxothiazolidin-3-yl)acetamide (**RD\_02b**) (0.1 g, 0.33 mmol) and 4-chlorobenzaldehyde (0.051 g, 0.36 mmol) to afford **RD\_08** (0.097 g, 69.59 %) as pale yellow solid. M.p: 286-288 °C. <sup>1</sup>H NMR (DMSO-d<sub>6</sub>): δ<sub>H</sub> 10.59 (s, 1H), 7.96 (s, 1H), 7.81 (s, 1H), 7.71 – 7.41 (m, 7H), 5.02 (s, 2H). <sup>13</sup>C NMR (DMSO-d<sub>6</sub>): δ<sub>C</sub> 193.3, 167.1, 163.8, 142.9, 139.8, 134.0, 133.6, 133.3, 130.6, 129.1 (2C), 128.8 (2C), 127.1, 122.9, 119.9, 115.8, 47.2. ESI-MS *m/z* 422 (M-H)<sup>-</sup>. Anal. Calcd. for C<sub>18</sub>H<sub>12</sub>Cl<sub>2</sub>N<sub>2</sub>O<sub>2</sub>S<sub>2</sub>: C, 51.07; H, 2.86; N, 6.62; Found: C, 51.12; H, 2.89; N, 6.64.

***N*-(3-Chlorophenyl)-2-(5-(4-nitrobenzylidene)-4-oxo-2-thioxothiazolidin-3-yl)acetamide (RD\_09)**

The compound was synthesized according to the general procedure using *N*-(3-chlorophenyl)-2-(4-oxo-2-thioxothiazolidin-3-yl)acetamide (**RD\_02b**) (0.1 g, 0.33 mmol) and 4-nitrobenzaldehyde (0.055 g, 0.36 mmol) to afford **RD\_09** (0.104 g, 72.36 %) as pale yellow solid. M.p: 260-262 °C. <sup>1</sup>H NMR (DMSO-d<sub>6</sub>): δ<sub>H</sub> 10.61 (s, 1H), 8.37 – 7.18 (m, 9H), 4.91 (s, 2H). <sup>13</sup>C NMR (DMSO-d<sub>6</sub>): δ<sub>C</sub> 193.4, 167.2, 164.0, 147.8, 143.3, 139.7, 139.3, 134.1, 130.6, 129.8 (2C), 127.1, 124.0 (2C), 123.3, 119.2, 118.0, 47.1. ESI-MS *m/z* 432 (M-H)<sup>-</sup>. Anal. Calcd. for C<sub>18</sub>H<sub>12</sub>ClN<sub>3</sub>O<sub>4</sub>S<sub>2</sub>: C, 49.83; H, 2.79; N, 9.68; Found: C, 49.88; H, 2.82; N, 9.76.

***N*-(3-Chlorophenyl)-2-(4-oxo-2-thioxo-5-(3,4,5-trimethoxybenzylidene)thiazolidin-3-yl)acetamide (RD\_10)**

The compound was synthesized according to the general procedure using *N*-(3-chlorophenyl)-2-(4-oxo-2-thioxothiazolidin-3-yl)acetamide (**RD\_02b**) (0.1 g, 0.33 mmol) and 3,4,5-trimethoxybenzaldehyde (0.071 g, 0.36 mmol) to afford **RD\_10** (0.116 g, 73.48 %)

as pale yellow solid. M.p: 199-201 °C. <sup>1</sup>H NMR (DMSO-d<sub>6</sub>): δ<sub>H</sub> 10.53 (s, 1H), 8.01 (s, 1H), 7.49 – 6.86 (m, 6H), 4.83 (s, 2H), 3.84 (s, 6H), 3.75 (s, 3H). <sup>13</sup>C NMR (DMSO-d<sub>6</sub>): δ<sub>C</sub> 193.4, 166.7, 163.8, 153.1 (2C), 143.3, 139.8, 137.8, 134.1, 130.3, 128.5, 127.1, 123.1, 119.2, 117.3, 105.5 (2C), 60.7, 56.2 (2C), 47.0. ESI-MS *m/z* 477 (M-H)<sup>-</sup>. Anal. Calcd. for C<sub>21</sub>H<sub>19</sub>ClN<sub>2</sub>O<sub>5</sub>S<sub>2</sub>: C, 52.66; H, 4.00; N, 5.85; Found: C, 52.72; H, 3.95; N, 5.77.

**2-(5-(4-(Benzyloxy)benzylidene)-4-oxo-2-thioxothiazolidin-3-yl)-N-(3-chlorophenyl)acetamide (RD\_11)**

The compound was synthesized according to the general procedure using *N*-(3-chlorophenyl)-2-(4-oxo-2-thioxothiazolidin-3-yl)acetamide (**RD\_02b**) (0.1 g, 0.33 mmol) and 4-(benzyloxy)benzaldehyde (0.077 g, 0.36 mmol) to afford **RD\_11** (0.113 g, 69.14 %) as pale yellow solid. M.p: 224-228 °C. <sup>1</sup>H NMR (DMSO-d<sub>6</sub>): δ<sub>H</sub> 10.59 (s, 1H), 8.08 (s, 1H), 7.67 – 6.92 (m, 13H), 5.23 (s, 2H), 4.86 (s, 2H). <sup>13</sup>C NMR (DMSO-d<sub>6</sub>): δ<sub>C</sub> 193.5, 166.7, 163.8, 157.7, 144.2, 139.8, 136.2, 134.0, 130.4, 130.1 (2C), 128.9 (2C), 128.3, 127.2, 127.0, 126.8 (2C), 123.2, 119.3, 118.1, 114.3 (2C), 71.0, 47.2. ESI-MS *m/z* 494 (M-H)<sup>-</sup>. Anal. Calcd. for C<sub>25</sub>H<sub>19</sub>ClN<sub>2</sub>O<sub>3</sub>S<sub>2</sub>: C, 60.66; H, 3.87; N, 5.66; Found: C, 60.60; H, 3.82; N, 5.60.

**2-(5-(Benzo[*d*][1,3]dioxol-5-ylmethylene)-4-oxo-2-thioxothiazolidin-3-yl)-N-(3-chlorophenyl)acetamide (RD\_12)**

The compound was synthesized according to the general procedure using *N*-(3-chlorophenyl)-2-(4-oxo-2-thioxothiazolidin-3-yl)acetamide (**RD\_02b**) (0.1 g, 0.33 mmol) and piperonal (0.077 g, 0.36 mmol) to afford **RD\_12** (0.090 g, 63.52 %) as pale yellow solid. M.p: 286-288 °C. <sup>1</sup>H NMR (DMSO-d<sub>6</sub>): δ<sub>H</sub> 10.63 (s, 1H), 7.83 (s, 1H), 7.76 (s, 1H), 7.73 – 7.12 (m, 6H), 6.17 (s, 2H), 4.88 (s, 2H). <sup>13</sup>C NMR (DMSO-d<sub>6</sub>): δ<sub>C</sub> 193.2, 166.5, 163.6, 150.0, 148.4, 139.7, 133.9, 133.1, 130.5, 127.1, 127.0, 123.4, 119.4, 118.6, 117.5, 109.6, 109.3, 102.2, 46.6. ESI-MS *m/z* 431 (M-H)<sup>-</sup>. Anal. Calcd. for C<sub>19</sub>H<sub>13</sub>ClN<sub>2</sub>O<sub>4</sub>S<sub>2</sub>: C, 52.71; H, 3.03; N, 6.47; Found: C, 52.65; H, 3.05; N, 6.41.

***N*-(2-Chloro-5-(trifluoromethyl)phenyl)-2-(5-(4-chlorobenzylidene)-4-oxo-2-thioxothiazolidin-3-yl)acetamide (RD\_13)**

The compound was synthesized according to the general procedure using *N*-(2-chloro-5-(trifluoromethyl)phenyl)-2-(4-oxo-2-thioxothiazolidin-3-yl)acetamide (**RD\_02c**) (0.1 g, 0.27 mmol) and 4-chlorobenzaldehyde (0.042 g, 0.29 mmol) to afford **RD\_13** (0.117 g, 88.23 %)

as pale yellow solid. M.p: 276-278 °C. <sup>1</sup>H NMR (DMSO-d<sub>6</sub>): δ<sub>H</sub> 10.38 (s, 1H), 7.85 (s, 1H), 7.71 – 7.24 (m, 7H), 5.08 (s, 2H). <sup>13</sup>C NMR (DMSO-d<sub>6</sub>): δ<sub>C</sub> 193.1, 166.5, 164.5, 143.1, 137.9, 133.7, 133.4, 130.5, 130.3, 129.1 (2C), 128.8 (2C), 126.2, 124.2, 122.6, 119.0, 116.2, 47.3. ESI-MS *m/z* 490 (M-H)<sup>-</sup>. Anal. Calcd. for C<sub>19</sub>H<sub>11</sub>Cl<sub>2</sub>F<sub>3</sub>N<sub>2</sub>O<sub>2</sub>S<sub>2</sub>: C, 46.45; H, 2.26; N, 5.70; Found: C, 46.38; H, 2.22; N, 5.78.

***N*-(2-Chloro-5-(trifluoromethyl)phenyl)-2-(5-(4-nitrobenzylidene)-4-oxo-2-thioxothiazolidin-3-yl)acetamide (RD\_14)**

The compound was synthesized according to the general procedure using *N*-(2-chloro-5-(trifluoromethyl)phenyl)-2-(4-oxo-2-thioxothiazolidin-3-yl)acetamide (**RD\_02c**) (0.1 g, 0.27 mmol) and 4-nitrobenzaldehyde (0.045 g, 0.29 mmol) to afford **RD\_14** (0.100 g, 73.66 %) as pale yellow solid. M.p: 275-277 °C. <sup>1</sup>H NMR (DMSO-d<sub>6</sub>): δ<sub>H</sub> 10.41 (s, 1H), 8.38 – 7.56 (m, 8H), 5.05 (s, 2H). <sup>13</sup>C NMR (DMSO-d<sub>6</sub>): δ<sub>C</sub> 193.0, 166.3, 164.4, 147.7, 143.2, 138.9, 135.1, 131.5 (2C), 130.9, 130.7, 126.4, 124.5, 124.3 (2C), 122.8, 121.5, 116.0, 46.6. ESI-MS *m/z* 500 (M-H)<sup>-</sup>. Anal. Calcd. for C<sub>19</sub>H<sub>11</sub>ClF<sub>3</sub>N<sub>3</sub>O<sub>4</sub>S<sub>2</sub>: C, 45.47; H, 2.21; N, 8.37; Found: C, 45.41; H, 2.17; N, 8.31.

***N*-(2-Chloro-5-(trifluoromethyl)phenyl)-2-(4-oxo-2-thioxo-5-(3,4,5-trimethoxybenzylidene)thiazolidin-3-yl)acetamide (RD\_15)**

The compound was synthesized according to the general procedure using *N*-(2-chloro-5-(trifluoromethyl)phenyl)-2-(4-oxo-2-thioxothiazolidin-3-yl)acetamide (**RD\_02c**) (0.1 g, 0.27 mmol) and 3,4,5-trimethoxybenzaldehyde (0.058 g, 0.29 mmol) to afford **RD\_15** (0.101 g, 68.72 %) as pale yellow solid. M.p: 232-234 °C. <sup>1</sup>H NMR (DMSO-d<sub>6</sub>): δ<sub>H</sub> 10.40 (s, 1H), 7.79 (s, 1H), 7.41 – 7.25 (m, 5H), 4.98 (s, 2H), 3.83 (s, 6H), 3.76 (s, 3H). <sup>13</sup>C NMR (DMSO-d<sub>6</sub>): δ<sub>C</sub> 193.2, 168.6, 165.0, 153.2 (2C), 143.4, 138.1, 137.6, 129.7, 129.3, 129.0, 125.6, 124.2, 121.9, 118.6, 116.2, 105.2 (2C), 60.4, 56.1 (2C), 47.3. ESI-MS *m/z* 545 (M-H)<sup>-</sup>. Anal. Calcd. for C<sub>22</sub>H<sub>18</sub>ClF<sub>3</sub>N<sub>2</sub>O<sub>5</sub>S<sub>2</sub>: C, 48.31; H, 3.32; N, 5.12; Found: C, 48.26; H, 3.36; N, 5.16.

**2-(5-(4-(Benzyloxy)benzylidene)-4-oxo-2-thioxothiazolidin-3-yl)-*N*-(2-chloro-5-(trifluoromethyl)phenyl)acetamide (RD\_16)**

The compound was synthesized according to the general procedure using *N*-(2-chloro-5-(trifluoromethyl)phenyl)-2-(4-oxo-2-thioxothiazolidin-3-yl)acetamide (**RD\_02c**) (0.1 g, 0.27 mmol) and 4-(benzyloxy)benzaldehyde (0.063 g, 0.29 mmol) to afford **RD\_16** (0.097 g,

63.83 %) as pale yellow solid. M.p: 222-224 °C. <sup>1</sup>H NMR (DMSO-d<sub>6</sub>): δ<sub>H</sub> 9.98 (s, 1H), 8.03 (s, 1H), 7.68 – 7.17 (m, 12H), 5.19 (s, 2H), 5.01 (s, 2H). <sup>13</sup>C NMR (DMSO-d<sub>6</sub>): δ<sub>C</sub> 193.1, 168.6, 164.2, 157.7, 143.4, 137.4, 136.3, 130.1 (2C), 129.4, 129.1, 128.8 (2C), 127.7, 127.4, 127.2 (2C), 126.1, 124.2, 122.0, 118.6, 116.2, 114.1 (2C), 71.0, 47.2. ESI-MS *m/z* 562 (M-H)<sup>-</sup>. Anal. Calcd. for C<sub>26</sub>H<sub>18</sub>ClF<sub>3</sub>N<sub>2</sub>O<sub>3</sub>S<sub>2</sub>: C, 55.47; H, 3.22; N, 4.98; Found: C, 55.43; H, 3.27; N, 5.06.

**2-(5-(Benzo[*d*][1,3]dioxol-5-ylmethylene)-4-oxo-2-thioxothiazolidin-3-yl)-*N*-(2-chloro-5-(trifluoromethyl)phenyl)acetamide (RD\_17)**

The compound was synthesized according to the general procedure using *N*-(2-chloro-5-(trifluoromethyl)phenyl)-2-(4-oxo-2-thioxothiazolidin-3-yl)acetamide (**RD\_02c**) (0.1 g, 0.27 mmol) and piperonal (0.044 g, 0.29 mmol) to afford **RD\_17** (0.088 g, 65.43 %) as pale yellow solid. M.p: 236-238 °C. <sup>1</sup>H NMR (DMSO-d<sub>6</sub>): δ<sub>H</sub> 10.02 (s, 1H), 7.84 (s, 1H), 7.42 – 6.87 (m, 6H), 6.19 (s, 2H), 4.97 (s, 2H). <sup>13</sup>C NMR (DMSO-d<sub>6</sub>): δ<sub>C</sub> 193.2, 166.5, 164.6, 149.8, 148.4, 141.2, 138.2, 129.6, 129.2, 128.8, 126.1, 124.3, 122.7, 122.4, 119.0, 116.7, 109.7, 109.2, 102.3, 47.1. ESI-MS *m/z* 499 (M-H)<sup>-</sup>. Anal. Calcd. for C<sub>20</sub>H<sub>12</sub>ClF<sub>3</sub>N<sub>2</sub>O<sub>4</sub>S<sub>2</sub>: C, 47.96; H, 2.41; N, 5.59; Found: C, 47.89; H, 2.45; N, 5.63.

**2-(5-(4-Chlorobenzylidene)-4-oxo-2-thioxothiazolidin-3-yl)-*N*-(3,4-dichlorophenyl)acetamide (RD\_18)**

The compound was synthesized according to the general procedure using *N*-(3,4-dichlorophenyl)-2-(4-oxo-2-thioxothiazolidin-3-yl)acetamide (**RD\_02d**) (0.1 g, 0.29 mmol) and 4-chlorobenzaldehyde (0.046 g, 0.32 mmol) to afford **RD\_18** (0.113 g, 83.11 %) as buff coloured solid. M.p: 295-297 °C. <sup>1</sup>H NMR (DMSO-d<sub>6</sub>): δ<sub>H</sub> 10.21 (s, 1H), 7.85 (s, 1H), 7.70 – 7.21 (m, 7H), 4.79 (s, 2H). <sup>13</sup>C NMR (DMSO-d<sub>6</sub>): δ<sub>C</sub> 192.9, 170.1, 166.3, 143.2, 138.8, 133.6, 133.4, 131.3, 130.3, 129.2, 129.0 (2C), 128.7 (2C), 124.1, 121.3, 116.0, 46.9. ESI-MS *m/z* 456 (M-H)<sup>-</sup>. Anal. Calcd. for C<sub>18</sub>H<sub>11</sub>Cl<sub>3</sub>N<sub>2</sub>O<sub>2</sub>S<sub>2</sub>: C, 47.23; H, 2.42; N, 6.12; Found: C, 47.28; H, 2.45; N, 6.18.

***N*-(3,4-Dichlorophenyl)-2-(5-(4-nitrobenzylidene)-4-oxo-2-thioxothiazolidin-3-yl)acetamide (RD\_19)**

The compound was synthesized according to the general procedure using *N*-(3,4-dichlorophenyl)-2-(4-oxo-2-thioxothiazolidin-3-yl)acetamide (**RD\_02d**) (0.1 g, 0.29 mmol)

and 4-nitrobenzaldehyde (0.049 g, 0.32 mmol) to afford **RD\_19** (0.110 g, 79.16 %) as pale yellow solid. M.p: 277-279 °C. <sup>1</sup>H NMR (DMSO-d<sub>6</sub>): δ<sub>H</sub> 10.23 (s, 1H), 8.36 – 7.55 (m, 7H), 7.41 (s, 1H), 4.82 (s, 2H). <sup>13</sup>C NMR (DMSO-d<sub>6</sub>): δ<sub>C</sub> 193.1, 170.0, 165.8, 147.4, 143.1, 141.0, 138.5, 131.1, 130.2, 129.1, 128.8 (2C), 124.2, 123.6 (2C), 121.2, 116.2, 47.2. ESI-MS *m/z* 467 (M-H)<sup>-</sup>. Anal. Calcd. for C<sub>18</sub>H<sub>11</sub>Cl<sub>2</sub>N<sub>3</sub>O<sub>4</sub>S<sub>2</sub>: C, 46.16; H, 2.37; N, 8.97; Found: C, 46.22; H, 2.33; N, 8.92.

***N*-(3,4-Dichlorophenyl)-2-(4-oxo-2-thioxo-5-(3,4,5-trimethoxybenzylidene)thiazolidin-3-yl)acetamide (RD\_20)**

The compound was synthesized according to the general procedure using *N*-(3,4-dichlorophenyl)-2-(4-oxo-2-thioxothiazolidin-3-yl)acetamide (**RD\_02d**) (0.1 g, 0.29 mmol) and 3,4,5-trimethoxybenzaldehyde (0.064 g, 0.32 mmol) to afford **RD\_20** (0.118 g, 77.69 %) as brown solid. M.p: 215-217 °C. <sup>1</sup>H NMR (DMSO-d<sub>6</sub>): δ<sub>H</sub> 10.17 (s, 1H), 7.98 – 6.72 (m, 6H), 4.92 (s, 2H), 3.83 (s, 6H), 3.71 (s, 3H). <sup>13</sup>C NMR (DMSO-d<sub>6</sub>): δ<sub>C</sub> 193.0, 170.0, 166.4, 153.3 (2C), 143.3, 138.5, 138.1, 131.3, 130.7, 129.6, 129.1, 124.3, 121.5, 116.3, 104.1 (2C), 61.0, 56.2 (2C), 46.8. ESI-MS *m/z* 512 (M-H)<sup>-</sup>. Anal. Calcd. for C<sub>21</sub>H<sub>18</sub>Cl<sub>2</sub>N<sub>2</sub>O<sub>5</sub>S<sub>2</sub>: C, 49.13; H, 3.53; N, 5.46; Found: C, 49.17; H, 3.55; N, 5.49.

**2-(5-(4-(Benzyloxy)benzylidene)-4-oxo-2-thioxothiazolidin-3-yl)-*N*-(3,4-dichlorophenyl)acetamide (RD\_21)**

The compound was synthesized according to the general procedure using *N*-(3,4-dichlorophenyl)-2-(4-oxo-2-thioxothiazolidin-3-yl)acetamide (**RD\_02d**) (0.1 g, 0.29 mmol) and 4-(benzyloxy)benzaldehyde (0.069 g, 0.32 mmol) to afford **RD\_21** (0.107 g, 68.43 %) as pale yellow solid. M.p: 219-221 °C. <sup>1</sup>H NMR (DMSO-d<sub>6</sub>): δ<sub>H</sub> 10.21 (s, 1H), 7.96 – 6.92 (m, 13H), 5.22 (s, 2H), 4.93 (s, 2H). <sup>13</sup>C NMR (DMSO-d<sub>6</sub>): δ<sub>C</sub> 193.2, 170.1, 166.5, 158.2, 143.2, 138.5, 136.4, 131.2, 130.6, 130.2 (2C), 129.1, 128.8 (2C), 127.7, 127.4, 127.2 (2C), 124.1, 121.3, 116.2, 114.2 (2C), 71.0, 46.7. ESI-MS *m/z* 528 (M-H)<sup>-</sup>. Anal. Calcd. for C<sub>25</sub>H<sub>18</sub>Cl<sub>2</sub>N<sub>2</sub>O<sub>3</sub>S<sub>2</sub>: C, 56.71; H, 3.43; N, 5.29; Found: C, 56.66; H, 3.40; N, 5.20.

**2-(5-(Benzo[*d*][1,3]dioxol-5-ylmethylene)-4-oxo-2-thioxothiazolidin-3-yl)-*N*-(3,4-dichlorophenyl)acetamide (RD\_22)**

The compound was synthesized according to the general procedure using *N*-(3,4-dichlorophenyl)-2-(4-oxo-2-thioxothiazolidin-3-yl)acetamide (**RD\_02d**) (0.1 g, 0.29 mmol)

and piperonal (0.049 g, 0.32 mmol) to afford **RD\_22** (0.100 g, 72.29 %) as pale yellow solid. M.p: 285-287 °C. <sup>1</sup>H NMR (DMSO-d<sub>6</sub>): δ<sub>H</sub> 10.42 (s, 1H), 7.81 (s, 1H), 7.74 (s, 1H), 7.68 – 6.92 (m, 5H), 6.13 (s, 2H), 4.90 (s, 2H). <sup>13</sup>C NMR (DMSO-d<sub>6</sub>): δ<sub>C</sub> 193.0, 167.1, 166.2, 150.0, 148.3, 145.3, 138.2, 131.3, 130.4, 129.0, 128.6, 124.4, 122.7, 121.1, 116.2, 111.7, 108.7, 101.3, 46.8. ESI-MS *m/z* 466 (M-H)<sup>-</sup>. Anal. Calcd. for C<sub>19</sub>H<sub>12</sub>Cl<sub>2</sub>N<sub>2</sub>O<sub>4</sub>S<sub>2</sub>: C, 48.83; H, 2.59; N, 5.99; Found: C, 48.88; H, 2.64; N, 6.04.

### **3-(5-(4-Chlorobenzylidene)-4-oxo-2-thioxothiazolidin-3-yl)-N-(thiazol-2-yl)propanamide (RD\_23)**

The compound was synthesized according to the general procedure using 3-(4-oxo-2-thioxothiazolidin-3-yl)-N-(thiazol-2-yl)propanamide (**RD\_02e**) (0.1 g, 0.34 mmol) and 4-chlorobenzaldehyde (0.053 g, 0.38 mmol) to afford **RD\_23** (0.103 g, 72.76 %) as brown solid. M.p: 288-290 °C. <sup>1</sup>H NMR (DMSO-d<sub>6</sub>): δ<sub>H</sub> 12.24 (s, 1H), 7.83 (s, 1H), 7.69 – 7.19 (m, 6H), 4.36 – 4.33 (t, *J* = 5.7 Hz, 2H), 2.86 – 2.82 (t, *J* = 5.8 Hz, 2H). <sup>13</sup>C NMR (DMSO-d<sub>6</sub>): δ<sub>C</sub> 193.2, 168.7, 164.1, 158.2, 142.8, 133.8, 133.5, 133.2, 129.2 (2C), 128.6 (2C), 113.5, 109.2, 45.3, 32.2. ESI-MS *m/z* 408 (M-H)<sup>-</sup>. Anal. Calcd. for C<sub>16</sub>H<sub>12</sub>ClN<sub>3</sub>O<sub>2</sub>S<sub>3</sub>: C, 46.88; H, 2.95; N, 10.25; Found: C, 46.93; H, 2.97; N, 10.21.

### **3-(5-(4-Nitrobenzylidene)-4-oxo-2-thioxothiazolidin-3-yl)-N-(thiazol-2-yl)propanamide (RD\_24)**

The compound was synthesized according to the general procedure using 3-(4-oxo-2-thioxothiazolidin-3-yl)-N-(thiazol-2-yl)propanamide (**RD\_02e**) (0.1 g, 0.34 mmol) and 4-nitrobenzaldehyde (0.057 g, 0.38 mmol) to afford **RD\_24** (0.111 g, 76.33 %) as brown solid. M.p: 281-283 °C. <sup>1</sup>H NMR (DMSO-d<sub>6</sub>): δ<sub>H</sub> 12.18 (s, 1H), 8.20 – 7.32 (m, 7H), 4.34 – 4.30 (t, *J* = 5.5 Hz, 2H), 2.87 – 2.83 (t, *J* = 6.3 Hz, 2H). <sup>13</sup>C NMR (DMSO-d<sub>6</sub>): δ<sub>C</sub> 193.2, 168.8, 164.3, 158.4, 147.8, 143.0, 141.2, 132.7, 129.1 (2C), 123.9 (2C), 115.9, 112.3, 45.3, 31.8. ESI-MS *m/z* 419 (M-H)<sup>-</sup>. Anal. Calcd. for C<sub>16</sub>H<sub>12</sub>N<sub>4</sub>O<sub>4</sub>S<sub>3</sub>: C, 45.70; H, 2.88; N, 13.32; Found: C, 45.77; H, 2.83; N, 13.36.

### **3-(4-Oxo-2-thioxo-5-(3,4,5-trimethoxybenzylidene)thiazolidin-3-yl)-N-(thiazol-2-yl)propanamide (RD\_25)**

The compound was synthesized according to the general procedure using 3-(4-oxo-2-thioxothiazolidin-3-yl)-N-(thiazol-2-yl)propanamide (**RD\_02e**) (0.1 g, 0.34 mmol) and 3,4,5-

trimethoxybenzaldehyde (0.074 g, 0.38 mmol) to afford **RD\_25** (0.103 g, 63.72 %) as pale yellow solid. M.p: 265-267 °C. <sup>1</sup>H NMR (DMSO-d<sub>6</sub>): δ<sub>H</sub> 12.24 (s, 1H), 7.77 (s, 1H), 7.44 – 6.96 (m, 4H), 4.38 – 4.33 (t, *J* = 6.6 Hz, 2H), 3.85 (s, 6H), 3.74 (s, 3H), 2.86 – 2.82 (t, *J* = 5.8 Hz, 2H). <sup>13</sup>C NMR (DMSO-d<sub>6</sub>): δ<sub>C</sub> 193.0, 168.2, 163.8, 157.6, 153.2 (2C), 143.5, 137.5, 133.2, 128.3, 121.1, 113.4, 108.1 (2C), 60.2, 56.0 (2C), 45.5, 32.1. ESI-MS *m/z* 464 (M-H)<sup>-</sup>. Anal. Calcd. for C<sub>19</sub>H<sub>19</sub>N<sub>3</sub>O<sub>5</sub>S<sub>3</sub>: C, 49.02; H, 4.11; N, 9.03; Found: C, 48.96; H, 4.07; N, 9.10.

**3-(5-(4-(Benzyloxy)benzylidene)-4-oxo-2-thioxothiazolidin-3-yl)-N-(thiazol-2-yl)propanamide (RD\_26)**

The compound was synthesized according to the general procedure using 3-(4-oxo-2-thioxothiazolidin-3-yl)-N-(thiazol-2-yl)propanamide (**RD\_02e**) (0.1 g, 0.34 mmol) and 4-(benzyloxy)benzaldehyde (0.080 g, 0.38 mmol) to afford **RD\_26** (0.124 g, 74.36 %) as pale yellow solid. M.p: 251-253 °C. <sup>1</sup>H NMR (DMSO-d<sub>6</sub>): δ<sub>H</sub> 12.16 (s, 1H), 8.02 (s, 1H), 7.63 – 6.97 (m, 11H), 5.22 (s, 2H), 4.37 – 4.33 (t, *J* = 6.3 Hz, 2H), 2.88 – 2.84 (t, *J* = 6.3 Hz, 2H). <sup>13</sup>C NMR (DMSO-d<sub>6</sub>): δ<sub>C</sub> 193.0, 168.3, 164.0, 157.7, 157.4, 143.2, 136.3, 133.0, 130.3 (2C), 129.0 (2C), 127.8, 127.6, 127.2 (2C), 116.0, 114.3 (2C), 112.1, 70.9, 45.1, 31.9. ESI-MS *m/z* 480 (M-H)<sup>-</sup>. Anal. Calcd. for C<sub>23</sub>H<sub>19</sub>N<sub>3</sub>O<sub>3</sub>S<sub>3</sub>: C, 57.36; H, 3.98; N, 8.72; Found: C, 57.32; H, 4.02; N, 8.77.

**3-(5-(Benzo[*d*][1,3]dioxol-5-ylmethylene)-4-oxo-2-thioxothiazolidin-3-yl)-N-(thiazol-2-yl)propanamide (RD\_27)**

The compound was synthesized according to the general procedure using 3-(4-oxo-2-thioxothiazolidin-3-yl)-N-(thiazol-2-yl)propanamide (**RD\_02e**) (0.1 g, 0.34 mmol) and piperonal (0.057 g, 0.38 mmol) to afford **RD\_27** (0.097 g, 67.31 %) as brown solid. M.p: 269-271 °C. <sup>1</sup>H NMR (DMSO-d<sub>6</sub>): δ<sub>H</sub> 12.21 (s, 1H), 7.84 (s, 1H), 7.71 – 6.96 (m, 5H), 6.15 (s, 2H), 4.36 – 4.32 (t, *J* = 5.8 Hz, 2H), 2.76 – 2.74 (t, *J* = 5.7 Hz, 2H). <sup>13</sup>C NMR (DMSO-d<sub>6</sub>): δ<sub>C</sub> 193.1, 168.9, 164.3, 158.4, 149.9, 148.3, 143.4, 132.8, 128.7, 122.6, 116.2, 112.3, 111.4, 108.2, 101.3, 45.6, 32.3. ESI-MS *m/z* 418 (M-H)<sup>-</sup>. Anal. Calcd. for C<sub>17</sub>H<sub>13</sub>N<sub>3</sub>O<sub>4</sub>S<sub>3</sub>: C, 48.67; H, 3.12; N, 10.02; Found: C, 48.60; H, 3.15; N, 10.06.

**3-(5-(4-Chlorobenzylidene)-4-oxo-2-thioxothiazolidin-3-yl)-N-(3-chlorophenyl)propanamide (RD\_28)**

The compound was synthesized according to the general procedure using *N*-(3-chlorophenyl)-3-(4-oxo-2-thioxothiazolidin-3-yl)propanamide (**RD\_02f**) (0.1 g, 0.31 mmol) and 4-chlorobenzaldehyde (0.049 g, 0.35 mmol) to afford **RD\_28** (0.118 g, 86.21 %) as pale yellow solid. M.p: 260-262 °C. <sup>1</sup>H NMR (DMSO-d<sub>6</sub>): δ<sub>H</sub> 10.61 (s, 1H), 7.83 (s, 1H), 7.70 – 7.21 (m, 8H), 4.34 – 4.30 (t, *J* = 6.3 Hz, 2H), 2.75 – 2.71 (t, *J* = 6.4 Hz, 2H). <sup>13</sup>C NMR (DMSO-d<sub>6</sub>): δ<sub>C</sub> 193.0, 171.7, 166.5, 143.4, 139.9, 134.6, 133.5, 133.2, 130.3, 129.1 (2C), 128.7 (2C), 128.0, 122.1, 119.8, 116.1, 45.4, 31.9. ESI-MS *m/z* 436 (M-H)<sup>-</sup>. Anal. Calcd. for C<sub>19</sub>H<sub>14</sub>Cl<sub>2</sub>N<sub>2</sub>O<sub>2</sub>S<sub>2</sub>: C, 52.18; H, 3.23; N, 6.41; Found: C, 52.25; H, 3.28; N, 6.34.

***N*-(3-Chlorophenyl)-3-(5-(4-nitrobenzylidene)-4-oxo-2-thioxothiazolidin-3-yl)propanamide (RD\_29)**

The compound was synthesized according to the general procedure using *N*-(3-chlorophenyl)-3-(4-oxo-2-thioxothiazolidin-3-yl)propanamide (**RD\_02f**) (0.1 g, 0.31 mmol) and 4-nitrobenzaldehyde (0.052 g, 0.35 mmol) to afford **RD\_29** (0.114 g, 80.37 %) as pale yellow solid. M.p: 236-238 °C. <sup>1</sup>H NMR (DMSO-d<sub>6</sub>): δ<sub>H</sub> 10.58 (s, 1H), 8.37 – 7.25 (m, 9H), 4.37 – 4.33 (t, *J* = 6.1 Hz, 2H), 2.75 – 2.71 (t, *J* = 5.8 Hz, 2H). <sup>13</sup>C NMR (DMSO-d<sub>6</sub>): δ<sub>C</sub> 192.7, 168.7, 166.3, 147.5, 143.2, 141.4, 140.0, 134.6, 130.5, 129.0 (2C), 127.8, 123.7 (2C), 122.2, 119.9, 116.3, 45.2, 31.7. ESI-MS *m/z* 446 (M-H)<sup>-</sup>. Anal. Calcd. for C<sub>19</sub>H<sub>14</sub>ClN<sub>3</sub>O<sub>4</sub>S<sub>2</sub>: C, 50.95; H, 3.15; N, 9.38; Found: C, 51.03; H, 3.18; N, 9.44.

***N*-(3-Chlorophenyl)-3-(4-oxo-2-thioxo-5-(3,4,5-trimethoxybenzylidene)thiazolidin-3-yl)propanamide (RD\_30)**

The compound was synthesized according to the general procedure using *N*-(3-chlorophenyl)-3-(4-oxo-2-thioxothiazolidin-3-yl)propanamide (**RD\_02f**) (0.1 g, 0.31 mmol) and 3,4,5-trimethoxybenzaldehyde (0.068 g, 0.35 mmol) to afford **RD\_30** (0.114 g, 73.28 %) as pale yellow solid. M.p: 201-203 °C. <sup>1</sup>H NMR (DMSO-d<sub>6</sub>): δ<sub>H</sub> 10.60 (s, 1H), 7.81 (s, 1H), 7.56 – 6.82 (m, 6H), 4.39 – 4.35 (t, *J* = 6.3 Hz, 2H), 3.87 (s, 6H), 3.75 (s, 3H), 2.88 – 2.84 (t, *J* = 6.1 Hz, 2H). <sup>13</sup>C NMR (DMSO-d<sub>6</sub>): δ<sub>C</sub> 193.1, 169.2, 166.4, 153.4 (2C), 143.5, 140.1, 138.5, 134.7, 130.4, 129.7, 128.0, 122.1, 119.9, 116.2, 107.6 (2C), 60.1, 56.1 (2C), 45.7, 32.0. ESI-MS *m/z* 492 (M-H)<sup>-</sup>. Anal. Calcd. for C<sub>22</sub>H<sub>21</sub>ClN<sub>2</sub>O<sub>5</sub>S<sub>2</sub>: C, 53.60; H, 4.29; N, 5.68; Found: C, 53.69; H, 4.34; N, 5.75.



**3-(5-(4-(Benzyloxy)benzylidene)-4-oxo-2-thioxothiazolidin-3-yl)-N-(3-chlorophenyl)propanamide (RD\_31)**

The compound was synthesized according to the general procedure using *N*-(3-chlorophenyl)-3-(4-oxo-2-thioxothiazolidin-3-yl)propanamide (**RD\_02f**) (0.1 g, 0.31 mmol) and 4-(benzyloxy)benzaldehyde (0.074 g, 0.35 mmol) to afford **RD\_31** (0.124 g, 77.49 %) as pale yellow solid. M.p: 241-243 °C. <sup>1</sup>H NMR (DMSO-d<sub>6</sub>): δ<sub>H</sub> 10.56 (s, 1H), 8.12 (s, 1H), 7.76 – 7.18 (m, 13H), 5.20 (s, 2H), 4.34 – 4.30 (t, *J* = 5.8 Hz, 2H), 2.78 – 2.74 (t, *J* = 5.7 Hz, 2H). <sup>13</sup>C NMR (DMSO-d<sub>6</sub>): δ<sub>C</sub> 193.2, 168.8, 166.2, 157.7, 143.5, 140.1, 136.8, 134.3, 130.4, 130.0 (2C), 129.0 (2C), 128.1, 127.7, 127.4, 127.1 (2C), 121.9, 120.0, 116.1, 114.0 (2C), 70.7, 45.0, 31.2. ESI-MS *m/z* 508 (M-H)<sup>-</sup>. Anal. Calcd. for C<sub>26</sub>H<sub>21</sub>ClN<sub>2</sub>O<sub>3</sub>S<sub>2</sub>: C, 61.35; H, 4.16; N, 5.50; Found: C, 61.44; H, 4.21; N, 5.60.

**3-(5-(Benzo[*d*][1,3]dioxol-5-ylmethylene)-4-oxo-2-thioxothiazolidin-3-yl)-N-(3-chlorophenyl)propanamide (RD\_32)**

The compound was synthesized according to the general procedure using *N*-(3-chlorophenyl)-3-(4-oxo-2-thioxothiazolidin-3-yl)propanamide (**RD\_02f**) (0.1 g, 0.31 mmol) and piperonal (0.052 g, 0.35 mmol) to afford **RD\_32** (0.115 g, 81.52 %) as pale yellow solid. M.p: 231-233 °C. <sup>1</sup>H NMR (DMSO-d<sub>6</sub>): δ<sub>H</sub> 10.57 (s, 1H), 8.03 (s, 1H), 7.52 – 6.98 (m, 7H), 6.17 (s, 2H), 4.35 – 4.31 (t, *J* = 6.3 Hz, 2H), 2.86 – 2.84 (t, *J* = 6.1 Hz, 2H). <sup>13</sup>C NMR (DMSO-d<sub>6</sub>): δ<sub>C</sub> 192.8, 169.1, 166.1, 150.0, 148.5, 143.5, 140.1, 134.6, 130.5, 128.7, 127.8, 122.7, 122.2, 119.8, 116.2, 111.6, 108.5, 101.4, 45.4, 31.8. ESI-MS *m/z* 445 (M-H)<sup>-</sup>. Anal. Calcd. for C<sub>20</sub>H<sub>15</sub>ClN<sub>2</sub>O<sub>4</sub>S<sub>2</sub>: C, 53.75; H, 3.38; N, 6.27; Found: C, 53.82; H, 3.43; N, 6.35.

***N*-(2-Chloro-5-(trifluoromethyl)phenyl)-3-(5-(4-chlorobenzylidene)-4-oxo-2-thioxothiazolidin-3-yl)propanamide (RD\_33)**

The compound was synthesized according to the general procedure using *N*-(2-chloro-5-(trifluoromethyl)phenyl)-3-(4-oxo-2-thioxothiazolidin-3-yl)propanamide (**RD\_02g**) (0.1 g, 0.26 mmol) and 4-chlorobenzaldehyde (0.040 g, 0.28 mmol) to afford **RD\_33** (0.115 g, 81.52 %) as pale yellow solid. M.p: 234-236 °C. <sup>1</sup>H NMR (DMSO-d<sub>6</sub>): δ<sub>H</sub> 9.96 (s, 1H), 8.08 (s, 1H), 7.82 (s, 1H), 7.70 – 7.28 (m, 6H), 4.37 – 4.33 (t, *J* = 5.8 Hz, 2H), 2.86 – 2.82 (t, *J* = 6.1 Hz, 2H). <sup>13</sup>C NMR (DMSO-d<sub>6</sub>): δ<sub>C</sub> 193.0, 168.2, 164.1, 143.5, 137.8, 133.6, 133.3, 129.6, 129.3, 129.0 (2C), 128.7 (2C), 126.0, 124.2, 122.1, 118.9, 116.4, 45.3, 31.4. ESI-MS *m/z* 504

(M-H)<sup>-</sup>. Anal. Calcd. for C<sub>20</sub>H<sub>13</sub>Cl<sub>2</sub>F<sub>3</sub>N<sub>2</sub>O<sub>2</sub>S<sub>2</sub>: C, 47.53; H, 2.59; N, 5.54; Found: C, 47.64; H, 2.63; N, 5.60.

***N*-(2-Chloro-5-(trifluoromethyl)phenyl)-3-(5-(4-nitrobenzylidene)-4-oxo-2-thioxothiazolidin-3-yl)propanamide (RD\_34)**

The compound was synthesized according to the general procedure using *N*-(2-chloro-5-(trifluoromethyl)phenyl)-3-(4-oxo-2-thioxothiazolidin-3-yl)propanamide (**RD\_02g**) (0.1 g, 0.26 mmol) and 4-nitrobenzaldehyde (0.043 g, 0.28 mmol) to afford **RD\_34** (0.102 g, 76.63 %) as pale yellow solid. M.p: 247-249 °C. <sup>1</sup>H NMR (DMSO-d<sub>6</sub>): δ<sub>H</sub> 9.92 (s, 1H), 8.23 – 7.31 (m, 8H), 4.36 – 4.32 (t, *J* = 5.8 Hz, 2H), 2.84 – 2.80 (t, *J* = 5.7 Hz, 2H). <sup>13</sup>C NMR (DMSO-d<sub>6</sub>): δ<sub>C</sub> 193.2, 168.5, 164.5, 147.7, 143.5, 141.4, 137.6, 129.5, 129.2, 129.0 (2C), 125.9, 124.2, 123.7 (2C), 122.2, 118.9, 116.1, 45.3, 31.5. ESI-MS *m/z* 514 (M-H)<sup>-</sup>. Anal. Calcd. for C<sub>20</sub>H<sub>13</sub>ClF<sub>3</sub>N<sub>3</sub>O<sub>4</sub>S<sub>2</sub>: C, 46.56; H, 2.54; N, 8.14; Found: C, 46.65; H, 2.57; N, 8.21.

***N*-(2-Chloro-5-(trifluoromethyl)phenyl)-3-(4-oxo-2-thioxo-5-(3,4,5-trimethoxybenzylidene)thiazolidin-3-yl)propanamide (RD\_35)**

The compound was synthesized according to the general procedure using *N*-(2-chloro-5-(trifluoromethyl)phenyl)-3-(4-oxo-2-thioxothiazolidin-3-yl)propanamide (**RD\_02g**) (0.1 g, 0.26 mmol) and 3,4,5-trimethoxybenzaldehyde (0.056 g, 0.28 mmol) to afford **RD\_35** (0.118 g, 81.33 %) as pale yellow solid. M.p: 221-223 °C. <sup>1</sup>H NMR (DMSO-d<sub>6</sub>): δ<sub>H</sub> 9.88 (s, 1H), 8.08 (s, 1H), 7.76 – 6.79 (m, 5H), 4.39 – 4.35 (t, *J* = 6.1 Hz, 2H), 3.83 (s, 6H), 3.72 (s, 3H), 2.87 -2.83 (t, *J* = 5.8 Hz, 2H). <sup>13</sup>C NMR (DMSO-d<sub>6</sub>): δ<sub>C</sub> 193.2, 168.6, 164.2, 153.1 (2C), 143.4, 138.5, 137.6, 129.6, 129.4, 129.1, 125.9, 124.2, 122.3, 119.0, 116.0, 103.9 (2C), 60.6, 56.1 (2C), 45.1, 31.6. ESI-MS *m/z* 559 (M-H)<sup>-</sup>. Anal. Calcd. for C<sub>23</sub>H<sub>20</sub>ClF<sub>3</sub>N<sub>2</sub>O<sub>5</sub>S<sub>2</sub>: C, 49.24; H, 3.59; N, 4.99; Found: C, 49.32; H, 3.64; N, 5.09.

**3-(5-(4-(Benzyloxy)benzylidene)-4-oxo-2-thioxothiazolidin-3-yl)-*N*-(2-chloro-5-(trifluoromethyl)phenyl)propanamide (RD\_36)**

The compound was synthesized according to the general procedure using *N*-(2-chloro-5-(trifluoromethyl)phenyl)-3-(4-oxo-2-thioxothiazolidin-3-yl)propanamide (**RD\_02g**) (0.1 g, 0.26 mmol) and 4-(benzyloxy)benzaldehyde (0.060 g, 0.28 mmol) to afford **RD\_36** (0.118 g, 79.11 %) as pale yellow solid. M.p: 211-213 °C. <sup>1</sup>H NMR (DMSO-d<sub>6</sub>): δ<sub>H</sub> 9.97 (s, 1H), 8.10 (s, 1H), 7.78 – 7.19 (m, 12H), 5.21 (s, 2H), 4.37 – 4.33 (t, *J* = 6.9 Hz, 2H), 2.86 – 2.82 (t, *J* =

7.0 Hz, 2H).  $^{13}\text{C}$  NMR (DMSO- $d_6$ ):  $\delta_{\text{C}}$  193.1, 168.4, 164.0, 157.5, 143.3, 137.5, 136.4, 130.0 (2C), 129.6 (2C), 128.8 (2C), 127.8, 127.4, 127.0 (2C), 125.8, 124.3, 121.7, 118.4, 116.0, 113.9 (2C), 71.1, 45.2, 31.8. ESI-MS  $m/z$  576 (M-H) $^-$ . Anal. Calcd. for  $\text{C}_{27}\text{H}_{20}\text{ClF}_3\text{N}_2\text{O}_3\text{S}_2$ : C, 56.20; H, 3.49; N, 4.85; Found: C, 56.31; H, 3.53; N, 4.92.

**3-(5-(Benzo[*d*][1,3]dioxol-5-ylmethylene)-4-oxo-2-thioxothiazolidin-3-yl)-*N*-(2-chloro-5-(trifluoromethyl)phenyl)propanamide (RD\_37)**

The compound was synthesized according to the general procedure using *N*-(2-chloro-5-(trifluoromethyl)phenyl)-3-(4-oxo-2-thioxothiazolidin-3-yl)propanamide (**RD\_02g**) (0.1 g, 0.26 mmol) and piperonal (0.043 g, 0.28 mmol) to afford **RD\_37** (0.110 g, 82.73 %) as pale yellow solid. M.p: 213-215 °C.  $^1\text{H}$  NMR (DMSO- $d_6$ ):  $\delta_{\text{H}}$  9.95 (s, 1H), 8.10 (s, 1H), 7.74 (s, 1H), 7.43 – 6.96 (m, 5H), 6.15 (s, 2H), 4.30 – 4.26 (t,  $J$  = 6.4 Hz, 2H), 2.81 – 2.76 (t,  $J$  = 6.3 Hz, 2H).  $^{13}\text{C}$  NMR (DMSO- $d_6$ ):  $\delta_{\text{C}}$  193.3, 168.7, 164.1, 150.0, 148.5, 143.5, 137.8, 129.6, 129.3, 128.6, 126.0, 124.2, 122.6, 122.3, 118.9, 116.3, 111.6, 109.4, 102.2, 45.1, 31.6. ESI-MS  $m/z$  513 (M-H) $^-$ . Anal. Calcd. for  $\text{C}_{21}\text{H}_{14}\text{ClF}_3\text{N}_2\text{O}_4\text{S}_2$ : C, 48.98; H, 2.74; N, 5.44; Found: C, 49.06; H, 2.80; N, 5.50.

**3-(5-(4-Chlorobenzylidene)-4-oxo-2-thioxothiazolidin-3-yl)-*N*-(3,4-dichlorophenyl)propanamide (RD\_38)**

The compound was synthesized according to the general procedure using *N*-(3,4-dichlorophenyl)-3-(4-oxo-2-thioxothiazolidin-3-yl)propanamide (**RD\_02h**) (0.1 g, 0.28 mmol) and 4-chlorobenzaldehyde (0.044 g, 0.31 mmol) to afford **RD\_38** (0.105 g, 78.18 %) as pale yellow solid. M.p: 253-255 °C.  $^1\text{H}$  NMR (DMSO- $d_6$ ):  $\delta_{\text{H}}$  10.28 (s, 1H), 8.03 (s, 1H), 7.83 (s, 1H), 7.70 – 7.41 (m, 6H), 4.36 – 4.32 (t,  $J$  = 6.1 Hz, 2H), 2.77 – 2.73 (t,  $J$  = 5.8 Hz, 2H).  $^{13}\text{C}$  NMR (DMSO- $d_6$ ):  $\delta_{\text{C}}$  193.1, 168.9, 164.3, 143.5, 138.2, 133.6, 133.2, 131.3, 130.7, 129.2, 128.9 (2C), 128.6 (2C), 124.4, 121.1, 116.2, 45.2, 31.9. ESI-MS  $m/z$  470 (M-H) $^-$ . Anal. Calcd. for  $\text{C}_{19}\text{H}_{13}\text{Cl}_3\text{N}_2\text{O}_2\text{S}_2$ : C, 48.37; H, 2.78; N, 5.94; Found: C, 48.44; H, 2.83; N, 6.02.

***N*-(3,4-Dichlorophenyl)-3-(5-(4-nitrobenzylidene)-4-oxo-2-thioxothiazolidin-3-yl)propanamide (RD\_39)**

The compound was synthesized according to the general procedure using *N*-(3,4-dichlorophenyl)-3-(4-oxo-2-thioxothiazolidin-3-yl)propanamide (**RD\_02h**) (0.1 g, 0.28

mmol) and 4-nitrobenzaldehyde (0.047 g, 0.31 mmol) to afford **RD\_39** (0.104 g, 75.44 %) as pale yellow solid. M.p: 226-228 °C. <sup>1</sup>H NMR (DMSO-d<sub>6</sub>): δ<sub>H</sub> 10.36 (s, 1H), 8.37 – 7.40 (m, 8H), 4.37 – 4.33 (t, *J* = 6.3 Hz, 2H), 2.78 – 2.74 (t, *J* = 6.1 Hz, 2H). <sup>13</sup>C NMR (DMSO-d<sub>6</sub>): δ<sub>C</sub> 192.8, 170.2, 166.2, 147.6, 143.1, 141.0, 138.7, 131.0, 130.3, 129.2, 128.9 (2C), 124.2, 123.7 (2C), 121.4, 115.8, 45.3, 32.0. ESI-MS *m/z* 481 (M-H)<sup>-</sup>. Anal. Calcd. for C<sub>19</sub>H<sub>13</sub>Cl<sub>2</sub>N<sub>3</sub>O<sub>4</sub>S<sub>2</sub>: C, 47.31; H, 2.72; N, 8.71; Found: C, 47.39; H, 2.78; N, 8.63.

***N*-(3,4-Dichlorophenyl)-3-(4-oxo-2-thioxo-5-(3,4,5-trimethoxybenzylidene)thiazolidin-3-yl)propanamide (RD\_40)**

The compound was synthesized according to the general procedure using *N*-(3,4-dichlorophenyl)-3-(4-oxo-2-thioxothiazolidin-3-yl)propanamide (**RD\_02h**) (0.1 g, 0.28 mmol) and 3,4,5-trimethoxybenzaldehyde (0.061 g, 0.31 mmol) to afford **RD\_40** (0.117 g, 78.14 %) as pale yellow solid. M.p: 239-241 °C. <sup>1</sup>H NMR (DMSO-d<sub>6</sub>): δ<sub>H</sub> 10.23 (s, 1H), 7.77 (s, 1H), 7.73 (s, 1H), 7.66 – 6.81 (m, 4H), 4.35 – 4.32 (t, *J* = 4.8 Hz, 2H), 3.82 (s, 6H), 3.73 (s, 3H), 2.82 – 2.78 (t, *J* = 4.7 Hz, 2H). <sup>13</sup>C NMR (DMSO-d<sub>6</sub>): δ<sub>C</sub> 193.0, 170.4, 166.3, 153.1 (2C), 143.3, 138.6, 138.1, 131.3, 130.7, 129.6, 129.2, 124.2, 121.0, 116.1, 107.8 (2C), 60.1, 56.0 (2C), 45.3, 32.1. ESI-MS *m/z* 526 (M-H)<sup>-</sup>. Anal. Calcd. for C<sub>22</sub>H<sub>20</sub>Cl<sub>2</sub>N<sub>2</sub>O<sub>5</sub>S<sub>2</sub>: C, 50.10; H, 3.82; N, 5.31; Found: C, 50.21; H, 3.76; N, 5.37.

**3-(5-(4-(Benzyloxy)benzylidene)-4-oxo-2-thioxothiazolidin-3-yl)-*N*-(3,4-dichlorophenyl)propanamide (RD\_41)**

The compound was synthesized according to the general procedure using *N*-(3,4-dichlorophenyl)-3-(4-oxo-2-thioxothiazolidin-3-yl)propanamide (**RD\_02h**) (0.1 g, 0.28 mmol) and 4-(benzyloxy)benzaldehyde (0.066 g, 0.31 mmol) to afford **RD\_41** (0.126 g, 81.38 %) as pale yellow solid. M.p: 254-256 °C. <sup>1</sup>H NMR (DMSO-d<sub>6</sub>): δ<sub>H</sub> 10.21 (s, 1H), 7.98 (s, 1H), 7.82 (s, 1H), 7.69 – 6.93 (m, 11H), 5.21 (s, 2H), 4.37 – 4.33 (t, *J* = 6.1 Hz, 2H), 2.74 – 2.70 (t, *J* = 5.8 Hz, 2H). <sup>13</sup>C NMR (DMSO-d<sub>6</sub>): δ<sub>C</sub> 193.0, 170.4, 166.4, 157.7, 143.5, 138.2, 136.8, 131.3, 130.6, 130.3 (2C), 129.1, 128.9 (2C), 127.7, 127.4, 127.2 (2C), 124.5, 121.1, 116.3, 114.3 (2C), 70.9, 45.2, 31.6. ESI-MS *m/z* 542 (M-H)<sup>-</sup>. Anal. Calcd. for C<sub>26</sub>H<sub>20</sub>Cl<sub>2</sub>N<sub>2</sub>O<sub>3</sub>S<sub>2</sub>: C, 57.46; H, 3.71; N, 5.15; Found: C, 57.39; H, 3.75; N, 5.07.

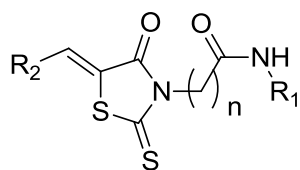
### **3-(5-(Benzo[*d*][1,3]dioxol-5-ylmethylene)-4-oxo-2-thioxothiazolidin-3-yl)-*N*-(3,4-dichlorophenyl)propanamide (RD\_42)**

The compound was synthesized according to the general procedure using *N*-(3,4-dichlorophenyl)-3-(4-oxo-2-thioxothiazolidin-3-yl)propanamide (**RD\_02h**) (0.1 g, 0.28 mmol) and piperonal (0.047 g, 0.31 mmol) to afford **RD\_42** (0.100 g, 72.61 %) as pale yellow solid. M.p: 251-253 °C. <sup>1</sup>H NMR (DMSO-*d*<sub>6</sub>): δ<sub>H</sub> 10.18 (s, 1H), 7.85 (s, 1H), 7.74 (s, 1H), 7.66 – 6.96 (m, 5H), 6.14 (s, 2H), 4.35 – 4.31 (t, *J* = 5.8 Hz, 2H), 2.73 – 2.69 (t, *J* = 5.7 Hz, 2H). <sup>13</sup>C NMR (DMSO-*d*<sub>6</sub>): δ<sub>C</sub> 193.1, 170.3, 166.3, 150.1, 148.8, 143.5, 138.2, 131.3, 130.7, 129.2, 128.6, 124.5, 122.8, 121.1, 116.2, 111.7, 108.7, 101.4, 45.2, 31.9. ESI-MS *m/z* 480 (M-H)<sup>-</sup>. Anal. Calcd. for C<sub>20</sub>H<sub>14</sub>Cl<sub>2</sub>N<sub>2</sub>O<sub>4</sub>S<sub>2</sub>: C, 49.90; H, 2.93; N, 5.82; Found: C, 50.01; H, 2.89; N, 5.86.

#### **5.4.4 *In vitro* Mycobacterium tuberculosis InhA inhibition assay, antimycobacterial potency and cytotoxicity studies of the synthesised molecules**

All the synthesized derivatives were first evaluated for their *in vitro* *Mycobacterium tuberculosis* InhA inhibitory potency as steps towards the derivation of structure-activity relationships and hit optimization. The compounds were further subjected to a whole cell screening against *Mycobacterium tuberculosis* H37Rv strain to understand their bactericidal potency using the agar dilution method and later the safety profile of these molecules were evaluated by checking the *in vitro* cytotoxicity against RAW 264.7 cell line (mouse macrophage) at 50 μM concentration by MTT assay, and the results are tabulated in **Table 5.11**.

**Table 5.11:** *In vitro* biological evaluation of the synthesized derivatives **RD\_03** – **RD\_42**.

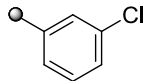
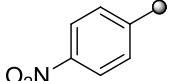
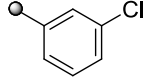
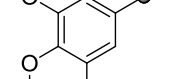
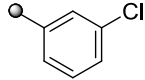
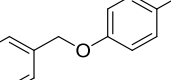
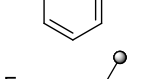
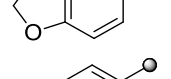
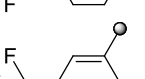
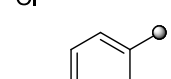
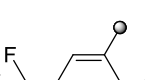
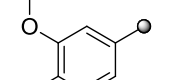
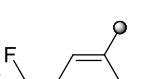
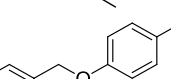
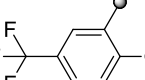
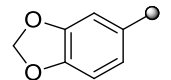
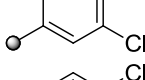
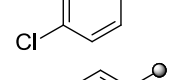
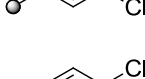
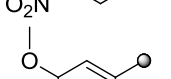
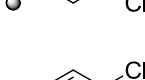
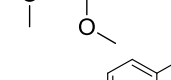
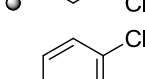
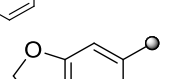
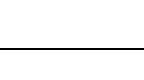
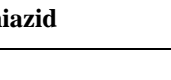




| Comp  | n | R <sub>1</sub> | R <sub>2</sub> | % of InhA inhibition at 10 μM <sup>a</sup> (IC <sub>50</sub> in μM) | MIC (μM) <sup>b</sup> |                | Cytotoxicity <sup>c</sup> (% inhib at 50 μM) |
|-------|---|----------------|----------------|---|-----------------------|----------------|--|
|       |   |                |                |   | MTB                   | MTB (Piperine) |  |
| RD_03 | 1 |                |                | 35.41±1.83  | 7.89                  | 1.97           | 31.00  |
| RD_04 | 1 |                |                | 30.12±1.66  | 30.75                 | 15.38          | 28.31  |
| RD_05 | 1 |                |                | 46.12±2.35  | 27.68                 | 13.84          | 36.61  |
| RD_06 | 1 |                |                | 20.12±0.73  | 53.47                 | 26.73          | 35.95  |
| RD_07 | 1 |                |                | 31.06±0.89  | 30.82                 | 7.70           | 41.22  |
| RD_08 | 1 |                |                | 60.12±0.92 (8.02±0.54)  | 3.68                  | 0.92           | 28.27  |
| RD_09 | 1 |                |                | 32.12±0.88  | 7.20                  | 3.59           | 30.67  |
| RD_10 | 1 |                |                | 48.12±0.55  | 13.05                 | 6.52           | 26.79  |
| RD_11 | 1 |                |                | 39.68±0.87  | 6.31                  | 3.15           | 34.80  |
| RD_12 | 1 |                |                | 30.12±1.2   | 28.87                 | 14.44          | 31.17  |
| RD_13 | 1 |                |                | 72.36±0.58 (6.86±0.46)  | 25.44                 | 6.36           | 27.74  |
| RD_14 | 1 |                |                | 50.12±0.89 (10.22±0.65)   | 6.23                  | 0.78           | 30.48  |

Contd...

| Comp  | n | R <sub>1</sub> | R <sub>2</sub> | % of InhA inhibition at 10 μM <sup>a</sup> (IC <sub>50</sub> in μM) | MIC (μM) <sup>b</sup> |                | Cytotoxicity <sup>c</sup> (% inhib at 50 μM) |
|-------|---|----------------|----------------|---|-----------------------|----------------|--|
|       |   |                |                |   | MTB                   | MTB (Piperine) |  |
| RD_15 | 1 |                |                | 69.12±0.93<br>(7.88±0.49)   | 2.85                  | 0.71           | 32.86  |
| RD_16 | 1 |                |                | 60.45±0.86<br>(8.42±0.55)   | 2.77                  | 1.38           | 41.98  |
| RD_17 | 1 |                |                | 52.12±0.65<br>(10.19±0.62)  | 24.95                 | 24.95          | 38.52  |
| RD_18 | 1 |                |                | 70.14±1.82<br>(7.12±0.38)   | 27.31                 | 13.65          | 35.10  |
| RD_19 | 1 |                |                | 58.14±0.66<br>(8.90±0.61)   | 26.69                 | 26.69          | 29.84  |
| RD_20 | 1 |                |                | 48.12±2.43  | 24.35                 | 6.09           | 28.77  |
| RD_21 | 1 |                |                | 46.43±1.91  | 0.74                  | 0.37           | 24.77  |
| RD_22 | 1 |                |                | 58.12±0.88<br>(9.06±0.64)   | 26.75                 | 13.37          | 44.30  |
| RD_23 | 2 |                |                | 52.16±0.65<br>(9.97±0.58)   | 7.62                  | 3.81           | 37.97  |
| RD_24 | 2 |                |                | 50.12±1.83<br>(10.23±0.66)  | 3.71                  | 0.93           | 40.07  |
| RD_25 | 2 |                |                | 38.12±0.82  | 3.35                  | 0.84           | 32.37  |
| RD_26 | 2 |                |                | 46.12±1.92  | 6.49                  | 3.24           | 26.94  |
| RD_27 | 2 |                |                | 48.62±0.79  | 7.45                  | 1.86           | 33.09  |
| RD_28 | 2 |                |                | 39.12±1.54  | 3.57                  | 0.89           | 23.01  |

Contd...

| Comp  | n | R <sub>1</sub>  | R <sub>2</sub>  | % of InhA inhibition at 10 μM <sup>a</sup> (IC <sub>50</sub> in μM) | MIC (μM) <sup>b</sup> |                | Cytotoxicity <sup>c</sup> (% inhib at 50 μM) |
|-------|---|---|---|---|-----------------------|----------------|--|
|       |   |   |   |   | MTB                   | MTB (Piperine) |  |
| RD_29 | 2 |    |    | 40.62±1.82  | 1.74                  | 0.87           | 28.09  |
| RD_30 | 2 |    |    | 38.12±2.32  | 3.16                  | 3.16           | 37.29  |
| RD_31 | 2 |    |    | 36.60±0.93  | 3.06                  | 1.53           | 32.93  |
| RD_32 | 2 |    |    | 49.12±2.33  | 6.99                  | 6.99           | 38.13  |
| RD_33 | 2 |    |    | 56.12±1.55 (8.67±0.47)  | 6.18                  | 3.09           | 36.99  |
| RD_34 | 2 |   |   | 52.14±1.24 (10.21±0.59)   | 1.51                  | 0.76           | 29.97  |
| RD_35 | 2 |  |  | 49.07±0.81  | 5.57                  | 2.78           | 37.78  |
| RD_36 | 2 |  |  | 46.70±0.94  | 21.66                 | 21.66          | 17.61  |
| RD_37 | 2 |  |  | 44.33±1.82  | 0.76                  | 0.38           | 23.11  |
| RD_38 | 2 |  |  | 36.05±1.92  | 6.62                  | 3.31           | 32.07  |
| RD_39 | 2 |  |  | 30.12±1.52  | 3.23                  | 3.23           | 28.29  |
| RD_40 | 2 |  |  | 29.87±0.55  | 2.96                  | 1.48           | 31.93  |
| RD_41 | 2 |  |  | 40.61±1.44  | 5.75                  | 2.87           | 35.13  |
| RD_42 | 2 |  |  | 20.52±1.32  | 12.98                 | 6.49           | 39.99  |
|       |   |   | <b>Isoniazid</b>  |   | 0.72                  | NT             | NT   |

Contd...



| Comp n | R <sub>1</sub> | R <sub>2</sub>    | % of InhA inhibition at 10 μM <sup>a</sup> (IC <sub>50</sub> in μM) | MIC (μM) <sup>b</sup> |                | Cytotoxicity <sup>c</sup> (% inhib at 50 μM) |
|--------|----------------|-------------------|---|-----------------------|----------------|--|
|        |                |                   |   | MTB                   | MTB (Piperine) |  |
|        |                | <b>Ethambutol</b> |   | 7.64                  | NT             | NT   |
|        |                | <b>Rifampicin</b> |   | 0.15                  | NT             | NT   |
|        |                | <b>Ofloxacin</b>  |   | 2.16                  | NT             | NT   |

IC<sub>50</sub>, 50% inhibitory concentration; MTB, *Mycobacterium tuberculosis*; MIC, minimum inhibitory concentration; NT, not tested

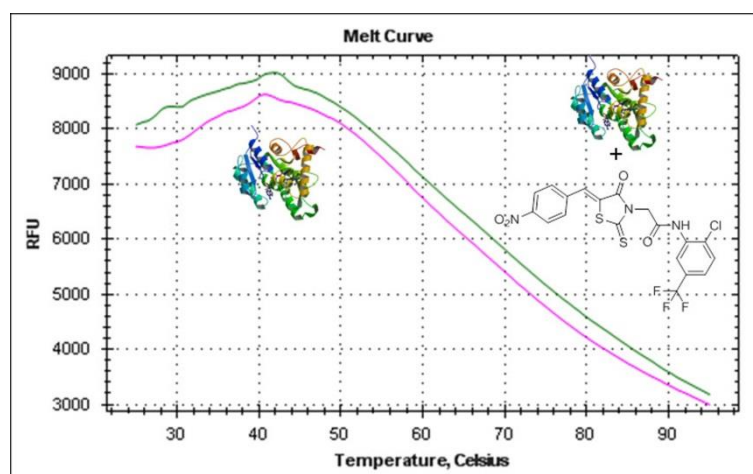
<sup>a</sup>MTB InhA enzyme inhibition activity

<sup>b</sup>*In vitro* activity against MTB H37Rv

<sup>c</sup>Against RAW 264.7 cells

#### 5.4.5 Evaluation of protein interaction and stability using biophysical characterization experiment

The most active compound from this series was further investigated using biophysically using DSF. In our study, compound **RD\_13** showed significant positive T<sub>m</sub> shift of 0.5 °C confirming the stability of the protein-ligand complex as shown in **Figure 5.37**.



**Figure 5.37:** DSF experiment for compound **RD\_13** (protein-ligand complex, green) showing an increase in the thermal shift of 0.5 °C compared with the native InhA protein (pink). Protein T<sub>m</sub> 38.90 °C and protein with ligand T<sub>m</sub> 39.40 °C.

#### 5.4.6 Discussion

Most of the synthesized compounds (except **RD\_06** and **RD\_42**) showed the percentage inhibition in the range of 72.36 - 29.87 % at 10 μM. Thirteen compounds (**RD\_08**, **RD\_13** -

**RD\_19, RD\_22 - RD\_24** and **RD\_33 - RD\_34** ) showed more than 50 % inhibition and were subsequently tested for their IC<sub>50</sub>. In order to arrive at SAR of rhodanine derivatives, the rhodanine scaffold was derivatized at position N<sub>3</sub> with varying length of carbon side chain and C<sub>5</sub>. The effects of various substituents at these positions were explored.

The first subset of compounds (**RD\_03 - RD\_07** and **RD\_23 - RD\_27**) contained 2-thiazolyl group as R<sub>1</sub> attached to N<sub>3</sub> position of rhodanine through a carbon side chain (n=1,2) while various substituted aryl groups were at R<sub>2</sub> position as shown in **Table 5.11**. The 4-chlorophenyl group substituent at R<sub>2</sub> position (compound **RD\_03** and **RD\_23**) displayed satisfactory InhA inhibitory activity. Compounds containing the 3,4,5-trimethoxyphenyl group substitution at R<sub>2</sub> position (compound **RD\_05** and **RD\_25**) provided moderate InhA inhibitory activity, whereas 4-nitrophenyl group at R<sub>2</sub> position (compound **RD\_04** and **RD\_24**) provided less to moderate InhA inhibitory activity depending upon length of carbon side chain. Additionally, benzo[*d*][1,3]dioxol-5-yl group substitution (compound **RD\_07** and **RD\_27**) was somewhat more favoured than 4-(benzyloxy)phenyl group at the R<sub>2</sub> position (compound **RD\_06** and **RD\_26**). In this subset, compounds with two-carbon side chain (n=2) resulted in better *in vitro* InhA inhibitory potency in the range of 52.16 to 38.12 % inhibition at 10 μM than similar compounds with one carbon side chain (n=1).

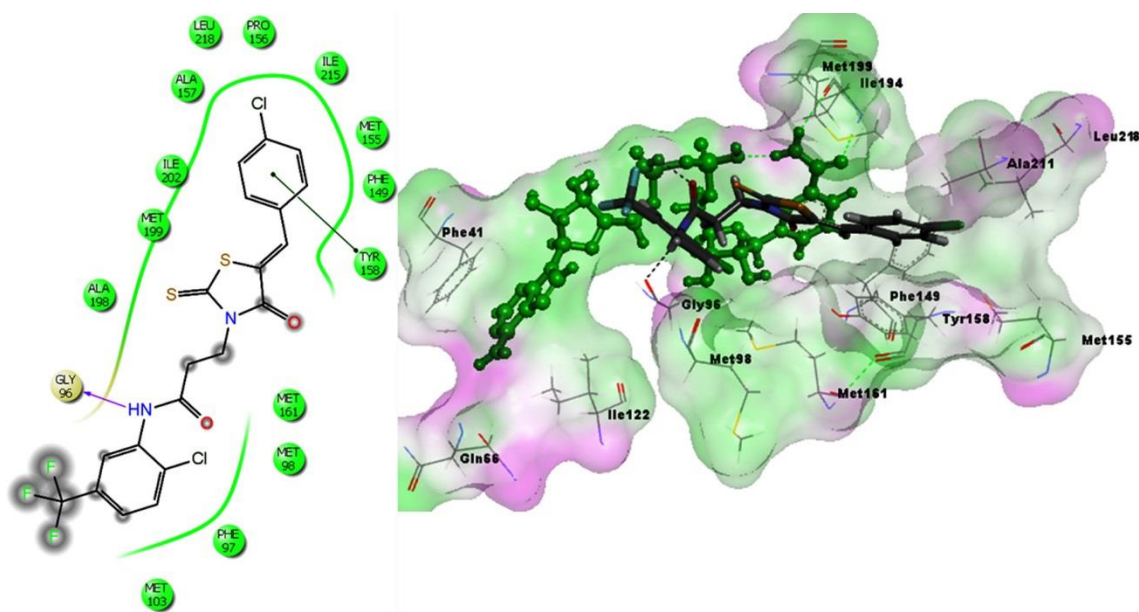
In the second subset of compounds (**RD\_08 - RD\_12** and **RD\_28 - RD\_32**), the effect of 3-chlorophenyl group substituent at R<sub>1</sub> attached to N<sub>3</sub> position of rhodanine through varying length of carbon side chain (n=1,2) was investigated to understand the effect of same aryl substituents at R<sub>2</sub> position. The 4-chlorophenyl group substituent as R<sub>2</sub> with R<sub>1</sub> attached through one carbon side chain (n=1) (compound **RD\_08**) displayed good InhA inhibition potency with IC<sub>50</sub> of 8.02 μM, but change in length of carbon side chain (n=2) resulted in reduced activity (compound **RD\_28**). At R<sub>2</sub> position, benzo[*d*][1,3]dioxol-5-yl group substitution (compound **RD\_32**) was preferred with two-carbon side chain (n=2) as that of 3,4,5-trimethoxyphenyl group substitution (compound **RD\_10**) with one carbon side chain (n=1). Also, compounds with 4-nitrophenyl and 4-(benzyloxy)phenyl group substitution at R<sub>2</sub> position displayed satisfactory InhA inhibition (compounds **RD\_09, RD\_11, RD\_29** and **RD\_31**). The length of the carbon side chain (n=1,2), depending on the overall structure of the compound, had a variable impact on the activities of compounds from this subset.

In the third subset of compounds (**RD\_13 - RD\_17** and **RD\_33 - RD\_37**), R<sub>1</sub> consisted of 2-chloro-5-trifluoromethylphenyl group and R<sub>2</sub> was substituted with various aryl groups same

as previous two subsets. In general, compounds with one carbon side chain ( $n=1$ ) displayed promising InhA inhibition potency with  $IC_{50}$  in the range of 6.86 to 10.22  $\mu\text{M}$ , whereas similar compounds with two-carbon side chain ( $n=2$ ) inhibited 56.12 - 44.33 % InhA at 10  $\mu\text{M}$ . Compound **RD\_13** emerged as the most potent molecule from this series with  $IC_{50}$  of  $6.86\pm 0.46$   $\mu\text{M}$ . It was noted that 4-chlorophenyl group substituent was more preferred than 4-nitrophenyl group at  $R_2$  position whereas introduction of benzo[*d*][1,3]dioxol-5-yl group at same position resulted in slightly reduced activity.

In the fourth subset of compounds (**RD\_18 - RD\_22** and **RD\_38 - RD\_42**), the effect of 3,4-dichlorophenyl group substituent at  $R_1$  attached to  $N_3$  position of rhodanine through variable length of carbon side chain ( $n=1,2$ ) was investigated to understand the effect of same aryl substituents at  $R_2$  position. The length of the carbon side chain ( $n=1,2$ ), had a varying impact on the activities of compounds from this subset, where compounds with one carbon side chain displayed 70.14 - 46.43 % inhibition of InhA and compounds with two-carbon side chain resulted in reduced enzyme activity. In general, 4-chlorophenyl- and 4-nitrophenyl group substituents at  $R_2$  position were more preferred than other substituents from this subset of compounds.

The docking results suggested that the formation of hydrogen bonds and hydrophobic interactions with the active site were predicted to be the most important factors affecting the inhibitory potency of these compounds. The predicted binding pose of the most active compound (**RD\_13**) revealed that the observed improved potency arises due to the extensive hydrophobic interactions predicted to be formed with the side chains of Tyr158, Phe149, Pro193, Ile215, Leu218, Met103, Ala198, Met98 and Met161 amino acid residues (**Figure 5.38**). The molecule oriented in a similar manner to that of crystal ligand retaining hydrogen bonding with hydroxyl ribose group of the  $\text{NAD}^+$  which was earlier demonstrated to be crucial for activity and specificity observed at the enzyme level, and probably serves as the key feature that governs the orientation of the compound within the active site. The binding energy of the compound **RD\_13** was found to be -7.87 kcal/mol. The *pi-pi* interaction formed between the 2-chloro-5-trifluoromethylphenyl ring of **RD\_13** and Phe97 resulted into good activity, and the additional hydrogen-bond interactions is observed with amino acid residues Gly96 helped the molecule to fit into the active site of protein.



**Figure 5.38:** Binding pose and interaction pattern of most active compound **RD\_13**.

The overall trend in enzyme inhibition activity showed that substitution at R<sub>1</sub> position with 2-chloro-5-trifluoromethylphenyl group was more favoured than 3-chlorophenyl group, whereas substitution with 2-thiazolyl- and 3,4-dichlorophenyl group gave mixed results. In case of R<sub>2</sub> position, substitution with electron withdrawing groups such as 4-chlorophenyl- and 4-nitrophenyl groups was more preferred than with electron donating groups such as 3,4,5-trimethoxyphenyl-, 4-(benzyloxy)phenyl- and benzo[*d*][1,3]dioxol-5-yl groups. The length of the carbon side chain (n=1,2), had a variable impact on the activities of compounds depending on the overall structure of the compound.

All synthesized compounds were also evaluated *in vitro* for their activity against *Mycobacterium tuberculosis* H37Rv (ATCC27294) using an agar dilution method with drug concentrations from 25 to 0.195 µg/mL in duplicates and the results are presented in **Table 5.11**. All synthesized compounds showed activity against *Mycobacterium tuberculosis* with MIC ranging from 0.74 to 53.46 µM. Twenty six out of forty synthesized compounds exhibited *Mycobacterium tuberculosis* MIC of <10 µM whereas fourteen compounds (**RD\_08**, **RD\_15** - **RD\_16**, **RD\_21**, **RD\_24** - **RD\_25**, **RD\_28** - **RD\_31**, **RD\_34**, **RD\_37** and **RD\_39** - **RD\_40**) inhibited *Mycobacterium tuberculosis* with MIC of <5 µM. Compounds **RD\_21** and **RD\_37** showed most promising *Mycobacterium tuberculosis* MIC of 0.74 and 0.76 µM respectively. Many of the synthesized compounds exhibited potent inhibition of *Mycobacterium tuberculosis* despite less potency in the enzyme inhibition study, suggesting that the compounds might be targeting enzyme other than InhA or acting in a non-specific

manner. In general, compounds with 3-chlorophenyl- and 2-thiazolyl group as R<sub>1</sub> substituent attached to N<sub>3</sub> position of rhodanine through a two-carbon side chain (n=2) showed better MIC than similar compounds with one carbon side chain (n=1). In case of substitution at R<sub>2</sub> position, substitution with 4-chlorophenyl-, 4-nitrophenyl- and 3,4,5-trimethoxyphenyl group was more favoured than with 4-(benzyloxy)phenyl- and benzo[d][1,3]dioxol-5-yl group.

Efflux mechanisms contribute in a major way to intrinsic resistance to drugs which could be due to one or more efflux pumps working alone or in co-ordination, therefore in present work we have carried out the *Mycobacterium tuberculosis* screening of the synthesized compounds in presence of a reported efflux pump inhibitor piperine (8 µg/mL). In most cases MIC decreased 2 to 4 fold when compared to absence of an efflux pump inhibitor. Compounds **RD\_21** and **RD\_37** showed *Mycobacterium tuberculosis* MIC of 0.37 and 0.38 µM respectively in the presence of piperine.

All the compounds were further tested for cytotoxicity in a RAW 264.7 cell line (mouse leukemic monocyte macrophage) at 50 µM. All tested compounds were not cytotoxic (less than 50 % inhibition at 50 µM) to RAW 264.7 cells and their percentage growth inhibitions were reported in **Table 5.11**.

All the synthesized derivatives were further evaluated for their predicted ADMET properties using the QikProp3.5 module of Schrodinger software. All compounds showed excellent membrane permeability but their predicted association with hERG toxicity may limit their further scope for optimization and development (as shown in **Table 5.12**). Also, many compounds showed violation of Lipinski rule of five mainly because of higher QPlogPo/w values and molecular weight (>500). The most active compound from this series **RD\_13** was predicted to have highly lipophilic nature and showed higher QPlogPo/w.

**Table 5.12:** QikProp analysis of the ADMET properties of the synthesized derivatives **RD\_03 – RD\_42.**

| <b>Comp</b>  | <b>QPlogPo/w<sup>a</sup></b> | <b>QPlogHERG<sup>b</sup></b> | <b>QPPCaco<sup>c</sup></b> | <b>QPlogBB<sup>d</sup></b> | <b>QPPMDCK<sup>e</sup></b> | <b>Percent Human Oral Absorption<sup>f</sup></b> | <b>Rule of Five<sup>g</sup></b> |
|--------------|------------------------------|------------------------------|----------------------------|----------------------------|----------------------------|--|---------------------------------|
| <b>RD_03</b> | 4.51                         | -5.90                        | 875.74                     | -0.43                      | 5583.07                    | 100.00   | 0                               |
| <b>RD_04</b> | 3.25                         | -5.91                        | 104.73                     | -1.68                      | 227.76                     | 82.11  | 0                               |
| <b>RD_05</b> | 4.20                         | -5.66                        | 875.90                     | -0.83                      | 2107.99                    | 100.00   | 0                               |
| <b>RD_06</b> | 6.00                         | -7.30                        | 1138.31                    | -0.73                      | 3701.43                    | 100.00   | 1                               |
| <b>RD_07</b> | 3.43                         | -5.46                        | 875.95                     | -0.55                      | 2263.33                    | 100.00   | 0                               |
| <b>RD_08</b> | 5.33                         | -6.54                        | 1712.66                    | -0.02                      | 10000.00                   | 100.00   | 1                               |
| <b>RD_09</b> | 4.12                         | -6.54                        | 204.37                     | -1.33                      | 720.54                     | 92.45  | 0                               |
| <b>RD_10</b> | 5.10                         | -6.27                        | 1708.96                    | -0.41                      | 6631.44                    | 100.00   | 1                               |
| <b>RD_11</b> | 6.78                         | -8.14                        | 1709.23                    | -0.48                      | 7155.53                    | 100.00   | 1                               |
| <b>RD_12</b> | 4.36                         | -6.13                        | 1709.25                    | -0.16                      | 7152.24                    | 100.00   | 0                               |
| <b>RD_13</b> | 6.12                         | -6.26                        | 1737.42                    | 0.19                       | 10000.00                   | 100.00   | 1                               |
| <b>RD_14</b> | 4.91                         | -6.27                        | 207.70                     | -1.11                      | 2113.48                    | 84.21  | 1                               |
| <b>RD_15</b> | 5.91                         | -6.03                        | 1736.32                    | -0.20                      | 10000.00                   | 93.60  | 2                               |
| <b>RD_16</b> | 7.58                         | -7.88                        | 1739.80                    | -0.27                      | 10000.00                   | 100.00   | 2                               |
| <b>RD_17</b> | 5.14                         | -5.87                        | 1736.40                    | 0.06                       | 10000.00                   | 89.09  | 2                               |
| <b>RD_18</b> | 5.76                         | -6.45                        | 1712.08                    | 0.11                       | 10000.00                   | 100.00   | 1                               |
| <b>RD_19</b> | 4.55                         | -6.45                        | 204.32                     | -1.21                      | 1497.87                    | 94.96  | 0                               |
| <b>RD_20</b> | 5.52                         | -6.17                        | 1708.54                    | -0.28                      | 10000.00                   | 91.23  | 2                               |
| <b>RD_21</b> | 7.21                         | -8.03                        | 1708.75                    | -0.35                      | 10000.00                   | 100.00   | 2                               |
| <b>RD_22</b> | 4.78                         | -6.05                        | 1708.82                    | -0.03                      | 10000.00                   | 100.00   | 0                               |
| <b>RD_23</b> | 4.84                         | -6.14                        | 665.90                     | -0.66                      | 4329.27                    | 100.00   | 0                               |
| <b>RD_24</b> | 3.59                         | -6.16                        | 79.62                      | -1.94                      | 176.54                     | 81.97  | 0                               |
| <b>RD_25</b> | 4.51                         | -5.88                        | 665.78                     | -1.05                      | 1636.79                    | 100.00   | 0                               |
| <b>RD_26</b> | 6.31                         | -7.77                        | 665.98                     | -1.17                      | 1753.36                    | 100.00   | 1                               |
| <b>RD_27</b> | 3.89                         | -5.75                        | 826.22                     | -0.64                      | 2588.34                    | 100.00   | 0                               |

Contd...

| Comp  | QPlogPo/w <sup>a</sup> | QPlogHERG <sup>b</sup> | QPPCaco <sup>c</sup> | QPlogBB <sup>d</sup> | QPPMDCK <sup>e</sup> | Percent Human Oral Absorption <sup>f</sup> | Rule of Five <sup>g</sup> |
|-------|------------------------|------------------------|----------------------|----------------------|----------------------|--|---------------------------|
| RD_28 | 5.60                   | -6.71                  | 1288.32              | -0.25                | 10000.00             | 100.00                                     | 1                         |
| RD_29 | 4.40                   | -6.72                  | 154.02               | -1.59                | 525.64               | 91.84                                      | 0                         |
| RD_30 | 5.39                   | -6.46                  | 1288.25              | -0.65                | 4855.24              | 100.00                                     | 1                         |
| RD_31 | 7.07                   | -8.29                  | 1312.22              | -0.72                | 5298.22              | 100.00                                     | 2                         |
| RD_32 | 4.62                   | -6.32                  | 1288.20              | -0.38                | 5218.66              | 100.00                                     | 0                         |
| RD_33 | 6.49                   | -6.49                  | 1423.51              | 0.02                 | 10000.00             | 95.47                                      | 2                         |
| RD_34 | 5.29                   | -6.51                  | 170.15               | -1.32                | 1933.38              | 71.93                                      | 2                         |
| RD_35 | 6.27                   | -6.28                  | 1414.94              | -0.37                | 10000.00             | 94.15                                      | 2                         |
| RD_36 | 7.95                   | -8.07                  | 1423.86              | -0.45                | 10000.00             | 100.00                                     | 2                         |
| RD_37 | 5.52                   | -6.16                  | 1415.70              | -0.11                | 10000.00             | 89.74                                      | 2                         |
| RD_38 | 6.03                   | -6.61                  | 1287.86              | -0.13                | 10000.00             | 100.00                                     | 1                         |
| RD_39 | 4.83                   | -6.62                  | 153.97               | -1.48                | 1092.67              | 94.36                                      | 0                         |
| RD_40 | 5.82                   | -6.36                  | 1287.77              | -0.52                | 10000.00             | 90.77                                      | 2                         |
| RD_41 | 7.49                   | -8.17                  | 1287.94              | -0.60                | 10000.00             | 100.00                                     | 2                         |
| RD_42 | 5.05                   | -6.23                  | 1287.78              | -0.26                | 10000.00             | 100.00                                     | 1                         |

<sup>a</sup>Predicted octanol/water partition coefficient logP (acceptable range: -2.0 to 6.5)

<sup>b</sup>Predicted IC<sub>50</sub> value for blockage of hERG K<sup>+</sup> channels.(below -5)

<sup>c</sup>Predicted apparent Caco-2 cell permeability in nm/sec (<25 poor; >500 great)

<sup>d</sup>Predicted brain/blood partition coefficient (-3.0 to 1.2)

<sup>e</sup>Predicted apparent MDCK cell (model for blood-brain barrier) permeability in nm/s. (< 25 poor, > 500 great)

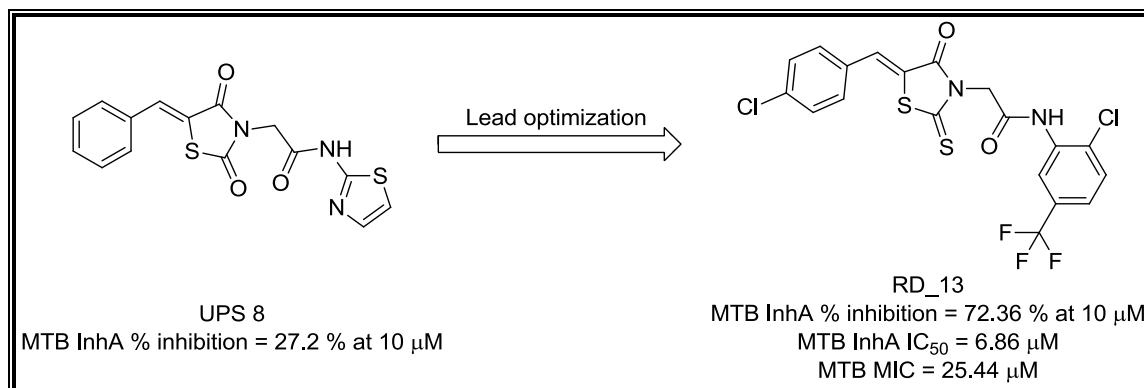
<sup>f</sup>Percent human oral absorption (< 25% is poor and > 80% is high)

<sup>g</sup>Rule of 5 violation (mol\_MW < 500, QPlogPo/w < 5, donorHB ≤ 5, acptHB ≤ 10) (concern above 1)

#### 5.4.7 Highlights of the study

A series of forty rhodanine derivatives was synthesized and screened against *Mycobacterium tuberculosis* InhA as well as drug sensitive *Mycobacterium tuberculosis* strains. In our study, most of the synthesized compounds showed better InhA inhibition as compared to lead molecules, and **RD\_13** (*N*-(2-chloro-5-(trifluoromethyl)phenyl)-2-(5-(4-chlorobenzylidene)-4-oxo-2-thioxothiazolidin-3-yl)acetamide) was found to be the most potent compound with IC<sub>50</sub> of 6.86 μM against *Mycobacterium tuberculosis* InhA, inhibited drug sensitive

*Mycobacterium tuberculosis* with MIC of 25.44  $\mu\text{M}$  and was non-cytotoxic at 50  $\mu\text{M}$  (**Figure 5.39**). The interaction with protein and enhancement of protein stability in complex with compound **RD\_13** was further confirmed biophysically by using DSF.



**Figure 5.39:** Chemical structure and biological activity of the most active compound **RD\_13**.



TB has returned as one of the most dangerous infectious diseases of the modern times with the epidemic of acquired immune deficiency syndrome (AIDS) in the 1980s. The TB that we face today is not exactly the same disease of the past. Decades of widespread clinical application of antibiotics has resulted in the emergence of drug resistant strains of *Mycobacterium tuberculosis* which along with some other factors has resulted in rapid insurgence of multidrug-resistant (MDR), extensively drug-resistant (XDR), or more recently, totally drug-resistant (TDR)-TB. This has rendered the presently available anti-tubercular drug regimen inadequate to address the many inherent and emerging challenges of treatment. Mycobacterial type II fatty acid biosynthesis (FASII) pathway and in particular InhA (2-*trans*-enoyl-acyl carrier protein reductase) is an essential but underexploited target for anti-tubercular drug discovery and thus holds an immense potential for the development of novel agents that are not impacted by target-mediated cross-resistance associated with previously reported drugs such as Isoniazid.

Earlier, the virtual screening efforts of our research group resulted in the identification of several hits belonging to more than eight chemo-types which demonstrated 10-38 % inhibition against InhA at 10  $\mu$ M. The quest for more potent molecules encouraged us to utilize such moderately active hits as a structural framework to construct a library for developing a strong structure-activity relationship profile, and to achieve mycobacterial cellular potency through improved InhA inhibition. These leads were taken up for hit expansion by chemical synthesis and a total of 123 molecules from 4 different series/leads as InhA inhibitors were synthesized and characterized in our laboratory.

All 123 synthesized derivatives were first evaluated for their *in vitro* *Mycobacterium tuberculosis* InhA inhibitory potency as step towards the derivation of structure-activity relationships and hit optimization. Also, some of the active compounds from each series of chemical class were further evaluated for protein interaction and stability using biophysical technique, differential scanning fluorimetry (DSF). The compounds were further subjected to a whole cell screening against *Mycobacterium tuberculosis* H37Rv strain to understand their bactericidal potency using the agar dilution method, and later the safety profile of these molecules were evaluated by checking the *in vitro* cytotoxicity against RAW 264.7 cell line

(mouse macrophage) by MTT assay. Also, all the synthesized derivatives were further evaluated for their predicted ADMET properties using the QikProp3.5 module of Schrodinger software for their drug-likeness from pharmaceutical point of view.

In 2-(2-oxobenzo[*d*]oxazol-3(2*H*)-yl)acetamide series, compound **BX\_25** (2-(6-Nitro-2-oxobenzo[*d*]oxazol-3(2*H*)-yl)-*N*-(5-nitrothiazol-2-yl)acetamide) emerged as the most active compound displaying 82.43 % inhibition of *Mycobacterium tuberculosis* InhA at 10  $\mu$ M with an IC<sub>50</sub> of 5.12  $\mu$ M, inhibited drug sensitive *Mycobacterium tuberculosis* with MIC of 17.11  $\mu$ M and was non-cytotoxic at 100  $\mu$ M. Compound **BX\_31** (2-(6-Nitro-2-oxobenzo [*d*]oxazol-3(2*H*)-yl)-*N*-(6-nitrobenzo[*d*]thiazol-2-yl)acetamide) was identified as most potent antimycobacterial compound with *Mycobacterium tuberculosis* MIC of 3.75  $\mu$ M in the presence of efflux pump inhibitors verapamil and piperine.

In 2-(4-oxoquinazolin-3(4*H*)-yl)acetamide series, compound **QN\_17** (2-(6-Chloro-2-methyl-4-oxoquinazolin-3(4*H*)-yl)-*N*-phenylacetamide) was found to be the most active compound exhibiting 88.12 % inhibition of InhA at 10  $\mu$ M with an IC<sub>50</sub> of 3.12  $\mu$ M. It inhibited drug sensitive *Mycobacterium tuberculosis* with MIC of 4.76  $\mu$ M and was non-cytotoxic at 100  $\mu$ M. Compound **QN\_33** (*N*-(6-Nitrobenzo[*d*]thiazol-2-yl)-2-(4-oxoquinazolin-3(4*H*)-yl)acetamide) was recognised as most potent antimycobacterial compound with *Mycobacterium tuberculosis* MIC of 1.02  $\mu$ M in the presence of piperine.

In 4-amino-1,5-dimethyl-2-phenyl-1*H*-pyrazol-3(2*H*)-one series, compound **PR\_15** (1-(1,5-Dimethyl-3-oxo-2-phenyl-2,3-dihydro-1*H*-pyrazol-4-yl)-3-(4-methoxyphenyl)urea) was identified as the most potent molecule displaying 93.12 % inhibition of *Mycobacterium tuberculosis* InhA at 10  $\mu$ M with an IC<sub>50</sub> of 2.96  $\mu$ M, inhibited drug sensitive *Mycobacterium tuberculosis* with MIC of 8.86  $\mu$ M and was non-cytotoxic at 50  $\mu$ M. Compounds **PR\_10** (*N*-(1,5-Dimethyl-3-oxo-2-phenyl-2,3-dihydro-1*H*-pyrazol-4-yl)-3-phenylpropanamide) and **PR\_16** (1-Benzyl-3-(1,5-dimethyl-3-oxo-2-phenyl-2,3-dihydro-1*H*-pyrazol-4-yl)urea) were considered to be most potent antimycobacterial compounds with *Mycobacterium tuberculosis* MIC of 0.58  $\mu$ M in the presence of piperine.

In 5-arylalkylidene-2-(4-oxo-2-thioxothiazolidin-3-yl)acetamide/propanamide series, **RD\_13** (*N*-(2-Chloro-5-(trifluoromethyl)phenyl)-2-(5-(4-chlorobenzylidene)-4-oxo-2-thioxothiazolidin-3-yl)acetamide) was found to be the most potent compound exhibiting 72.36 % inhibition of InhA at 10  $\mu$ M with an IC<sub>50</sub> of 6.86  $\mu$ M against *Mycobacterium*

*tuberculosis* InhA, inhibited drug sensitive *Mycobacterium tuberculosis* with MIC of 25.44  $\mu$ M and was non-cytotoxic at 50  $\mu$ M. Compounds **RD\_21** (2-(5-(4-(Benzyloxy)benzylidene)-4-oxo-2-thioxothiazolidin-3-yl)-*N*-(3,4-dichlorophenyl) acetamide) and **RD\_37** (3-(5-(Benzo[*d*][1,3]dioxol-5-yl)methylene)-4-oxo-2-thioxothiazolidin-3-yl)-*N*-(2-chloro-5-(trifluoromethyl)phenyl)propanamide) were considered to be most potent antimycobacterial compounds with *Mycobacterium tuberculosis* MIC of 0.37 and 0.38  $\mu$ M respectively in the presence of efflux pump inhibitor piperine.

In conclusion, the class of compounds described here besets a collection of promising lead compounds for further optimization and development to yield best novel drugs aimed to combat ever-present and ever-increasing mycobacterial infections. The study also provides the basis for further chemical optimization of these potent inhibitors as potential anti-tubercular agents.

## Future perspectives

---

The bacterial type II fatty acid biosynthesis pathways are absent in humans but essential in mycobacteria for synthesis of mycolic acids, suggesting that it provides potential targets for the development of novel anti-tubercular agents. The present study focused on developing promising *Mycobacterium tuberculosis* InhA direct inhibitors as potential anti-tubercular agents, thus offers an excellent opportunity to address the ever increasing problem of mycobacterial resistance and to develop an effective treatment for TB.

The study describes the development of four chemically diverse series of molecules as potential InhA direct inhibitors. The molecules reported here displayed considerable *in vitro* enzyme inhibition and potency against *Mycobacterium tuberculosis* H37Rv strain. Although these results are encouraging, lead optimization is still needed to build an efficient pharmacokinetic and a pharmacodynamics profile, and to achieve an adequate safety profile to ensure that the dose to humans would be in an acceptable range.

The advancement of any of the candidate molecules presented in this thesis along a drug development track will require a substantial investment in medicinal chemistry, preclinical and clinical studies.

## References

---

Alibert S., Pages J-M. Efflux pump inhibitors in bacteria. *Expert Opin. Ther. Pat.* **2007**, *17*, 883-888.

am Ende C.W., Kundson S.E., Liu N., Childs J., Sullivan T.J., Boyne M., Xu H., Knudson D.L., Johnson F., Peloquin C.A., Slayden R.A., Tonge P.J. Synthesis and *in vitro* antimycobacterial activity of B-ring modified diaryl ether InhA inhibitors. *Bioorg. Med. Chem. Lett.* **2008**, *18*, 3029-3033.

Andries K., Verhasselt P., Guillemont J., Göhlmann H.W., Neefs J.M., Winkler H., Gestel J.V., Timmerman P., Zhu M., Lee E., Williams P., Chaffoy D., Huitric E., Hoffner S., Cambau E., Truffot-Pernot C., Lounis N., Jarlier V. A diarylquinoline drug active on the ATP synthase of *Mycobacterium tuberculosis*. *Science* **2005**, *307*, 223-227.

Argyrou A., Vetting M.W., Blanchard J.S. New insight into the mechanism of action of and resistance to isoniazid: interaction of *Mycobacterium tuberculosis* enoyl-ACP reductase with INH-NADP. *J. Am. Chem. Soc.* **2007**, *31*, 9582-9583.

Ballell Pages L., Castro Pichel J., Fernandez Menendez R., Fernandez Velando E.P., Gonzalez Del Valle S., Mendoza Losana A., Wolfendale M.J. (Pyrazol-3-yl)-1,3,4-thiadiazole-2-amine and (Pyrazol-3-yl)-1,3,4-thiazole-2-amine compounds. PCT publication No. WO 2010/118852 A1, **2010**.

Banerjee A., Dubnau E., Quemard A., Balasubramanian V., Um K.S., Wilson T., Collins D., de Lisle G., Jacobs Jr. W.R. inhA, a gene encoding a target for isoniazid and ethionamide in *Mycobacterium tuberculosis*. *Science* **1994**, *263*, 227-230.

Banerjee S.K., Bhatt K., Rana S., Misra P., Chakraborti P.K. Involvement of an efflux system in mediating high level of fluoroquinolone resistance in *Mycobacterium smegmatis*. *Biochem. Biophys. Res. Commun.* **1996**, *226*, 362-368.

Baulard A.R., Betts J.C., Engohang-Ndong J., Quan S., McAdam R.A., Brennan P.J., Locht C., Besra G.S. Activation of the pro-drug ethionamide is regulated in mycobacteria. *J. Biol. Chem.* **2000**, *275*, 28326-28331.

Bell I.M., Selnick H.G., Stump C.A. Bicyclic anilide heterocyclic CGRP receptor antagonists. U.S. Patent No. 8,173,655. Filed 8 May **2012**.

Bernstein J., Lott W.A., Steinberg B.A., Yale H.L. Chemotherapy of experimental tuberculosis. V. Isonicotinic acid hydrazide (nydrazid) and related compounds. *Am. Rev. Tuberc.* **1952**, *65*, 357-364.

Bhatt A., Fujiwara N., Bhatt K., Gurucha S.S., Kremer L., Chen B., Chan J., Porcelli S.A., Kobayashi K., Besra G.S., Jacobs Jr. W.R. Deletion of *kasB* in *Mycobacterium tuberculosis* causes loss of acid-fastness and subclinical latent tuberculosis in immunocompetent mice. *Proc. Natl. Acad. Sci. USA* **2007**, *104*, 5157-5162.

Bonnac L., Gao G.Y., Chen L., Felczak K., Bennett E.M., Xu H., Kim T., Liu N., Oh H., Tonge P.J., Pankiewicz K.W. Synthesis of 4-phenoxybenzamide adenine dinucleotide as NAD analogue with inhibitory activity against enoyl-ACP reductase (InhA) of *Mycobacterium tuberculosis*. *Bioorg. Med. Chem. Lett.* **2007**, *17*, 4588-4591.

Boyne M.E., Sullivan T.J., am Ende C.W., Lu H., Gruppo V., Heaslip D., Amin A.G., Chatterjee D., Lenaerts A., Tonge P.J., Slayden R.A. Targeting fatty acid biosynthesis for the development of novel chemotherapeutics against *Mycobacterium tuberculosis*: evaluation of A-ring-modified diphenyl ethers as high-affinity InhA inhibitors. *Antimicrob. Agents Chemother.* **2007**, *51*, 3562-3567.

Brennan P.J., Nikaido H. The envelope of mycobacteria. *Annu. Rev. Biochem.* **1995**, *64*, 29-63.

Broussy S., Bernardes-Génisson V., Quémard A., Meunier B., Bernadou J. The first chemical synthesis of the core structure of the benzoylhydrazine-NAD adduct, a competitive inhibitor of the *Mycobacterium tuberculosis* enoyl reductase. *J. Org. Chem.* **2005**, *70*, 10502-10510.

Broussy S., Coppel Y., Nguyen M., Bernadou J., Meunier B. <sup>1</sup>H and <sup>13</sup>C NMR Characterization of Hemiamidal Isoniazid-NAD(H) Adducts as Possible Inhibitors Of InhA Reductase of *Mycobacterium tuberculosis*. *Chem. Eur. J.* **2003**, *9*, 2034-2038.

Campbell E.A., Korzheva N., Mustaev A., Murakami K., Nair S., Goldfarb A., Darst S.A. Structural mechanism for rifampicin inhibition of bacterial RNA polymerase. *Cell* **2001**, *104*, 901-912.

Carter A.P., Clemons W.M., Brodersen D.E., Morgan-Warren R.J., Wimberly B.T., Ramakrishnan V. Functional insights from the structure of the 30S ribosomal subunit and its interactions with antibiotics. *Nature* **2000**, *407*, 340-348.

Castro Pichel J., Fernandez Menendez R., Fernandez Velando E.P., Gonzalez Del Valle S., Mallo-Rubio A. 3-Amino-Pyrazole Derivatives Useful Against Tuberculosis. PCT publication No. WO 2012/049161 A1, **2012**.

Chan E.D., Strand M.J., Iseman M.D. Treatment outcomes in extensively resistant tuberculosis. *New Engl. J. Med.* **2008**, *359*, 657-659.

Clark-Curtiss J.E., Haydel S.E. Molecular genetics of *Mycobacterium tuberculosis* pathogenesis. *Annu. Rev. Microbiol.* **2003**, *57*, 517-549.

Cohen J. Approval of novel TB drug celebrated-with restraint. *Science* **2013**, *339*, 130-130.

Coker R.J. Review: Multidrug-resistant tuberculosis: public health challenges. *Trop. Med. Int. Health* **2004**, *9*, 25-40.

Cole S.T., Brosch R., Parkhill J., Garnier T., Churcher C., Harris D., Gordon S.V., Eiglmeier K., Gas S., Barry III C.E., Tekaia F., Badcock K., Basham D., Brown D., Chillingworth T., Connor R., Davies R., Devlin K., Feltwell T., Gentles S., Hamlin N., Holroyd S., Hornsby H., Jagels K., Krogh A., McLean J., Moule S., Murphy L., Oliver K., Osborne J., Quail M.A., Rajandream M.A., Rogers J., Rutter S., Seeger K., Skelton J., Squares R., Squares S., Sulston J.E., Taylor K., Whitehead S., Barrell B.G. Deciphering the biology of *Mycobacterium tuberculosis* from the complete genome sequence. *Nature* **1998**, *393*, 537-544.

Corbett E.L., Watt C.J., Walker N., Maher D., Williams B.G., Raviglione M.C., Dye C. The growing burden of tuberculosis: global trends and interactions with the HIV epidemic. *Arch. Intern. Med.* **2003**, *163*, 1009-1021.

Crick D.C., Mahapatra S., Brennan P.J. Biosynthesis of the arabinogalactan-peptidoglycan complex of *Mycobacterium tuberculosis*. *Glycobiology* **2001**, *11*, 107R-118R.

Daffe M., Draper P. The envelope layers of mycobacteria with reference to their pathogenicity. *Adv. Microb. Physiol.* **1998**, *39*, 131-203.

Debarber A.E., Mdluli K., Bosman M., Bekker L.G., Barry III C.E. Ethionamide activation and sensitivity in multidrug-resistant *Mycobacterium tuberculosis*. *Proc. Natl. Acad. Sci. U.S.A.* **2000**, *97*, 9677-9682.

Delaine T., Bernardes-Génisson V., Quémard A., Constant P., Meunier B., Bernadou J. Development of isoniazid-NAD truncated adducts embedding a lipophilic fragment as potential bi-substrate InhA inhibitors and antimycobacterial agents. *Eur. J. Med. Chem.* **2010**, *45*, 4554-4561.

Delaine T., Bernardes-Génisson V., Stigliani J.L., Gornitzka H., Meunier B., Bernadou J. Ring-Chain Tautomerism of Simplified Analogues of Isoniazid-NAD (P) Adducts: an Experimental and Theoretical Study. *Eur. J. Org. Chem.* **2007**, *10*, 1624-1630.

Deraeve C., Dorobantu I.M., Rebbah F., Le Quémener F., Constant P., Quémard A., Bernardes-Génisson V., Bernadou J., Pratviel G. Chemical synthesis, biological evaluation and structure-activity relationship analysis of azaisoindolinones, a novel class of direct enoyl-ACP reductase inhibitors as potential antimycobacterial agents. *Bioorg. Med. Chem.* **2011**, *19*, 6225-6232.

Dessen A., Quemard A., Blanchard J.S., Jacobs Jr. W.R., Sacchettini J.C. Crystal structure and function of the isoniazid target of *Mycobacterium tuberculosis*. *Science* **1995**, *267*, 1638-1641.

Dickinson J.M., Mitchison D.A. Experimental models to explain the high sterilizing activity of rifampin in the chemotherapy of tuberculosis. *Am. J. Respir. Crit. Care Med.* **1981**, *159*, 1580-1584.

Dorman S.E., Chaisson R.E. From magic bullets back to the Magic Mountain: the rise of extensively drug-resistant tuberculosis. *Nat. Med.* **2007**, *13*, 295-298.

Dubnau E., Chan J., Raynaud C., Mohan V.P., Laneelle M.A., Yu K., Quemard A., Smith I., Daffe M. Oxygenated mycolic acids are necessary for virulence of *Mycobacterium tuberculosis* in mice. *Mol. Microbiol.* **2000**, *36*, 630-637.

Encinas L., O'Keefe H., Neu M., Remuiñán M.J., Patel A.M., Guardia A., Davie C.P., Perez-Macias N., Yang H., Convery M.A., Messer J.A., Perez-Herran E., Centrella P.A., Alvarez-Gomez D., Clark M.A., Huss S., O'Donovan G.K., Ortega-Muro F., McDowell W.,



Castaneda P., Arico-Muendel C.C., Pajk S., Rullas J., Angulo-Barturen I., Alvarez-Ruiz E., Mendoza-Losana A., Ballell Pages L., Castro-Pichel J., Evindar G. Encoded library technology as a source of hits for the discovery and lead optimization of a potent and selective class of bactericidal direct inhibitors of *Mycobacterium tuberculosis* InhA. *J. Med. Chem.* **2014**, *57*, 1276-1288.

Flynn J.L., Chan J. Tuberculosis: Latency and Reactivation. *Infect. Immun.* **2001**, *69*, 4195-4201.

Fox W., Ellard G.A., Mitchison D.A. Studies on the treatment of tuberculosis undertaken by the British Medical Research Council tuberculosis units, 1946-1986, with relevant subsequent publications. *Int. J. Tuberc. Lung Dis.* **1999**, *3*, S231-S279.

Franzblau S.G., Witzig R.S., McLaughlin J.C., Torres P., Madico G., Hernandez A., Degnan M.T., Cook M.B., Quenzer V.K., Ferguson R.M., Gilman R.H. Rapid, low-technology MIC determination with clinical *Mycobacterium tuberculosis* isolates by using the microplate Alamar Blue assay. *J. Clin. Microbiol.* **1998**, *36*, 362-366.

Gerlier D., Thomasset N. Use of MTT colorimetric assay to measure cell activation. *J. Immunol. Methods* **1986**, *94*, 57-63.

Girling D.J. The role of pyrazinamide in primary chemotherapy for pulmonary tuberculosis. *Tubercle* **1984**, *65*, 1-4.

Glickman M.S., Cox J.S., Jacobs Jr. W.R. A novel mycolic acid cyclopropane synthetase is required for cording, persistence, and virulence of *Mycobacterium tuberculosis*. *Mol. Cell* **2000**, *5*, 717-727.

Glickman M.S., Jacobs Jr. W.R. Microbial pathogenesis of *Mycobacterium tuberculosis*: dawn of a discipline. *Cell* **2001**, *104*, 477-485.

Goldman P., Vagelos P.R. The specificity of triglyceride synthesis from diglycerides in chicken adipose tissue. *J. Biol. Chem.* **1961**, *236*, 2620-2623.

Green K.D., Garneau-Tsodikova S. Resistance in tuberculosis: what do we know and where can we go?. *Front. Microbiol.* **2013**, *4*, 1-7.

Hafner R., Cohn J.A., Wright D.J., Dunlap N.E., Egorin M.J., Enama M.E., Muth K., Peloquin C.A., Mor N., Heifets L.B. Early bactericidal activity of isoniazid in pulmonary tuberculosis. *Am. J. Respir. Crit. Care Med.* **1997**, *156*, 918-923.

Haydel S.E. Extensively drug-resistant tuberculosis: a sign of the times and an impetus for antimicrobial discovery. *Pharmaceuticals* **2010**, *3*, 2268-2290.

Hazbon M.H., Brimacombe M., Bobadilla Del Valle M., Cavatore M., Guerrero M.I., Varma-Basil M., Billman-Jacobe H., Lavender C., Fyfe J., Garcia-Garcia L., Leon C.I., Bose M., Chaves F., Murray M., Eisenach K.D., Sifuentes-Osornio J., Cave M.D., Ponce de Leon A., Alland D. Population genetics study of isoniazid resistance mutations and evolution of multidrug-resistant *Mycobacterium tuberculosis*. *Antimicrob. Agents Chemother.* **2006**, *50*, 2640-2649.

He X., Alian A., Ortiz de Montellano P.R. Inhibition of the *Mycobacterium tuberculosis* enoyl acyl carrier protein reductase InhA by arylamides. *Bioorg. Med. Chem.* **2007**, *15*, 6649-6658.

He X., Alian A., Stroud R., Ortiz de Montellano P.R. Pyrrolidine carboxamides as a novel class of inhibitors of enoyl acyl carrier protein reductase from *Mycobacterium tuberculosis*. *J. Med. Chem.* **2006**, *49*, 6308-6323.

Heath R.J., Rubin J.R., Holland D.R., Zhang E., Snow M.E., Rock C.O. Mechanism of triclosan inhibition of bacterial fatty acid synthesis. *J. Biol. Chem.* **1999**, *274*, 11110-11114.

Hoffmann C., Leis A., Niederweis M., Plitzko J.M., Engelhardt H. Disclosure of the mycobacterial outer membrane: cryo-electron tomography and vitreous sections reveal the lipid bilayer structure. *Proc. Natl. Acad. Sci. USA* **2008**, *105*, 3963-3967.

Hopewell P.C., Pai M., Maher D., Uplekar M., Raviglione M.C. International standards for tuberculosis care. *Lancet Infect. Dis.* **2006**, *6*, 710-725.

Hugonnet J.E., Blanchard J.S. Irreversible inhibition of the *Mycobacterium tuberculosis* beta-lactamase by clavulanate. *Biochemistry* **2007**, *46*, 11998-12004.

Johansen S.K., Maus C.E., Plikaytis B.B., Douthwaite S. Capreomycin binds across the ribosomal subunit interface using tlyA-encoded 2'-O-methylations in 16S and 23S rRNAs. *Mol. Cell* **2006**, *23*, 173-182.

Jones D., Metzger H.J., Schatz A., Waksman S.A. Control of gram-negative bacteria in experimental animals by streptomycin. *Science* **1994**, *100*, 103-105.

Kamsri P., Punkvang A., Saparpakorn P., Hannongbua S., Irle S., Pungpo P. Elucidating the structural basis of diphenyl ether derivatives as highly potent enoyl-ACP reductase inhibitors through molecular dynamics simulations and 3D-QSAR study. *J. Mol. Modell.* **2014**, *20*, 1-12.

Khan S., Nagarajan S.N., Parikh A., Samantaray S., Singh A., Kumar D., Roy R.P., Bhatt A., Nandicoori V.K. Phosphorylation of enoyl-acyl carrier protein reductase InhA impacts mycobacterial growth and survival. *J. Biol. Chem.* **2010**, *285*, 37860-37871.

Khodair A.I. A Convenient Synthesis of 2-Arylidene-5H-thiazolo(2,3-b)quinazoline-3,5(2H)-diones and Their Benzoquinazoline Derivatives. *J. Org. Chem.* **2002**, *39*, 1153-1160.

Kini S.G., Bhat A.R., Bryant B., Williamson J.S., Dayan F.E. Synthesis, antitubercular activity and docking study of novel cyclic azole substituted diphenyl ether derivatives. *Eur. J. Med. Chem.* **2009**, *44*, 492-500.

Koch R. Classics in infectious diseases. The etiology of tuberculosis: Robert Koch. Berlin, Germany. *Rev. Infect. Dis.* **1982**, *4*, 1270-1274.

Koul A., Arnoult E., Lounis N., Guillemont J., Andries K. The challenge of new drug discovery for tuberculosis. *Nature* **2011**, *469*, 483-490.

Kumar A., Siddiqi M.I. CoMFA based de novo design of pyrrolidine carboxamides as inhibitors of enoyl acyl carrier protein reductase from *Mycobacterium tuberculosis*. *J. Mol. Modell.* **2008**, *14*, 923-935.

Kumar U.C., BVS S.K., Mahmood S., D. Sriram, Kumar-Sahu P., Pulakanam S., Ballell L., Alvarez-Gomez D., Malik S., JARP S. Discovery of novel InhA reductase inhibitors: application of pharmacophore-and shape-based screening approach. *Future Med. Chem.* **2013**, *5*, 249-259.

Kuo M.R., Morbidoni H.R., Alland D., Sneddon S.F., Gourlie B.B., Staveski M.M., Leonard M., Gregory J.S., Janjigian A.D., Yee C., Musser J.M., Kreiswirth B., Iwamoto H., Perozzo R., Jacobs Jr. W.R., Sacchettini J.C., Fidock D.A. Targeting tuberculosis and malaria through inhibition of Enoyl reductase: compound activity and structural data. *J. Biol. Chem.* **2003**, 278, 20851-20859.

Labby K.J. and Garneau-Tsodikova S. Strategies to overcome the action of aminoglycoside-modifying enzymes for treating resistant bacterial infections. *Future Med. Chem.* **2013**, 5, 1285-1309.

Lattmann P., Lattmann E., Singh H. Novel ureido-and amido-pyrazolone derivatives. U.S. Patent Application 10/558,787. Filed May 27, **2004**.

Lechartier B., Rybniker J., Zumla A., Cole S. Tuberculosis drug discovery in the post-post-genomic era. *EMBO Mol. Med.* **2014**. Published online Jan 8. DOI: 10.1002/emmm.201201772.

Levy C.W., Roujeinikova A., Sedelnikova S., Baker P.J., Stuitje A.R., Slabas A.R., Rice D.W., Rafferty J.B. Molecular basis of triclosan activity. *Nature* **1999**, 398, 383-384.

Li F., Feng Y., Meng Q., Li W., Li Z., Wang Q., Tao F. An efficient construction of quinazolin-4(3H)-ones under microwave irradiation. *Arkivoc* **2007**, 1, 40-50.

Lu H., Tonge P.J. Inhibitors of FabI, an enzyme drug target in the bacterial fatty acid biosynthesis pathway. *Acc. Chem. Res.* **2008**, 41, 11-20.

Lu X.Y., You Q.D., Chen Y.D. Recent progress in the identification and development of InhA direct inhibitors of *Mycobacterium tuberculosis*. *Min. Rev. Med. Chem.* **2010**, 10, 182-193.

Luckner S.R., Liu N., am Ende C.W., Tonge P.J., Kisker C. A slow, tight binding inhibitor of InhA, the enoyl-acyl carrier protein reductase from *Mycobacterium tuberculosis*. *J. Biol. Chem.* **2010**, 285, 14330-14337.

Makarov V., Manina G., Mikusova K., Mollmann U., Ryabova O., Saint-Joanis B., Dhar N., Pasca M.R., Buroli S., Lucarelli A.P., Milano A., De Rossi E., Belanova M., Bobovska A., Dianiskova P., Kordulakova J., Sala C., Fullam E., Schneider P., McKinney J.D., Brodin P.,

Christophe T., Waddell S., Butcher P., Albrethsen J., Rosenkrands I., Brosch R., Nandi V., Bharath S., Gaonkar S., Shandil R.K., Balasubramanian V., Balganesht T., Tyagi S., Grosset J., Riccardi G., Cole S.T. Benzothiazinones kill *Mycobacterium tuberculosis* by blocking arabinan synthesis. *Science* **2009**, *324*, 801-804.

Malone L., Schurr A., Lindh H., McKenzie D., Kiser J.S., Williams J.H. The effect of pyrazinamide (Aldinamide) on experimental tuberculosis in mice. *Am. Rev. Tuberc.* **1952**, *65*, 511-518.

Marrakchi H., Lan elle M.A., Daff  M. Mycolic acids: structures, biosynthesis, and beyond. *Chem. Biol.* **2014**, *21*, 67-85.

Matviiuk T., Rodriguez F., Saffon N., Mallet-Ladeira S., Gorichko M., de Jesus Lopes Ribeiro A.L., Pasca M.R., Lherbet C., Voitenko Z., Baltas M. Design, chemical synthesis of 3-(9H-fluoren-9-yl)pyrrolidine-2,5-dione derivatives and biological activity against enoyl-ACP reductase (InhA) and *Mycobacterium tuberculosis* *Eur. J. Med. Chem.* **2013**, *70*, 37-48.

McClure W.R., Cech C.L. On the mechanism of rifampicin inhibition of RNA synthesis. *J. Biol. Chem.* **1978**, *253*, 8949-8956.

McKee T., Sowadski J., Suto R., Tibbitts T. Pin1-modulating compounds and methods of use thereof. U.S. Patent Application 10/379,410, Filed March 3, **2003**.

McMurry L.M., McDermott P.F., Levy S.B. Genetic evidence that InhA of *Mycobacterium smegmatis* is a target for triclosan. *Antimicrob. Agents Chemother.* **1999**, *43*, 711-713.

McMurry L.M., Oethinger M., Levy S.B. Triclosan targets lipid synthesis. *Nature* **1998**, *394*, 531-532.

McNeil M., Daffe' M., Brennan P.J. Location of the mycolyl ester substituents in the cell walls of mycobacteria. *J. Biol. Chem.* **1991**, *266*, 13217-13223.

Mendgen T., Steuer C., Klein C.D. Privileged scaffolds or promiscuous binders: a comparative study on rhodanines and related heterocycles in medicinal chemistry. *J. Med. Chem.* **2012**, *55*, 743-753.

Menendez C., Gau S., Lherbet C., Rodriguez F., Inard C., Pasca M.R., Baltas M. Synthesis and biological activities of triazole derivatives as inhibitors of InhA and antituberculosis agents. *Eur. J. Med. Chem.* **2011**, *46*, 5524-5531.

Migliori G.B., De Iaco G., Besozzi G., Centis R., Cirillo D.M. First tuberculosis cases in Italy resistant to all tested drugs. *Euro. Surveill.* **2007**, *12*, E070517- E070517.

More U.A., Joshi S.D., Aminabhavi T.M., Gadad A.K., Nadagouda M.N., Kulkarni V.H. Design, synthesis, molecular docking and 3D-QSAR studies of potent inhibitors of enoyl-acyl carrier protein reductase as potential antimycobacterial agents. *Eur. J. Med. Chem.* **2014**, *71*, 199-218.

Morlock G.P., Metchock B., Sikes D., Crawford J.T., Cooksey R.C. ethA, inhA, and katG loci of ethionamide-resistant clinical *Mycobacterium tuberculosis* isolates. *Antimicrob. Agents Chemother.* **2003**, *47*, 3799-3805.

Mukherjee J.S., Rich M.L., Socci A.R., Joseph J.K., Virú F.A., Shin S.S., Furin J.J., Becerra M.C., Barry D.J., Kim J.Y., Bayona J., Farmer P., Fawzi M.C., Seung K.J. Programmes and principles in treatment of multidrug-resistant tuberculosis. *Lancet* **2004**, *363*, 474-481.

Murphy D.J., Brown J.R. Identification of gene targets against dormant phase *Mycobacterium tuberculosis* infections. *BMC Infect. Dis.* **2007**, *7*, 84-99.

Nguyen M., Quemard A., Broussy S., Bernadou J., Meunier B. Mn(III) pyrophosphate as an efficient tool for studying the mode of action of isoniazid on the InhA protein of *Mycobacterium tuberculosis*. *Antimicrob. Agents Chemother.* **2002**, *46*, 2137-2144.

Niesen F.H., Berglund H., Vedadi M. The use of differential scanning fluorimetry to detect ligand interactions that promote protein stability. *Nat. Protoc.* **2007**, *2*, 2212-2221.

Ning W., Zhu J., Zheng C., Liu X., Song Y., Zhou Y., Zhang X., Zhang L., Sheng C., Lv J. Fragment-Based Design of Novel Quinazolinon Derivatives as Human Acrosin Inhibitors. *Chem. Biol. Drug Des.* **2013**, *81*, 437-441.

Ohishi Y., Mukai T., Nagahara M., Yajima M., Kajikawa N., Miyahara K., Takano T. Preparations of 5-alkylmethylidene-3-carboxymethylrhodanine derivatives and their aldose reductase inhibitory activity. *Chem. Pharm. Bull.* **1995**, *38*, 1911-1919.

Ojha A., Anand M., Bhatt A., Kremer L., Jacobs Jr. W.R., Hatfull G.F. GroEL1: a dedicated chaperone involved in mycolic acid biosynthesis during biofilm formation in mycobacteria. *Cell* **2005**, *123*, 861-873.

Palomino J.C., Martin A. Drug Resistance Mechanisms in *Mycobacterium tuberculosis*. *Antibiotics* **2014**, *3*, 317-340.

Pan P., Knudson S.E., Bommineni G.R., Li H.J., Lai C.T., Liu N., Garcia-Diaz M., Simmerling C., Patil S.S., Slayden R.A., Tonge P.J. Time-Dependent Diaryl Ether Inhibitors of InhA: Structure-Activity Relationship Studies of Enzyme Inhibition, Antibacterial Activity, and *in vivo* Efficacy. *ChemMedChem* **2014**, *9*, 776-791.

Pan P., Tonge P.J. Targeting InhA, the FASII enoyl-ACP reductase: SAR studies on novel inhibitor scaffolds. *Curr. Top. Med. Chem.* **2012**, *12*, 672-693.

Pankiewicz K.W., Lesiak K., Zatorski A., Goldstein B.M., Carr S.F., Sochacki M., Majumdar A., Seidman M., Watanabe K.A. The Practical Synthesis of a Methylenebisphosphonate Analogue of Benzamide Adenine Dinucleotide: Inhibition of Human Inosine Monophosphate Dehydrogenase (Type I and II) 1. *J. Med. Chem.* **1997**, *40*, 1287-1291.

Parida S.K., Axelsson-Robertson R., Rao M.V., Singh N., Master I., Lutckii A., Keshavjee S., Andersson J., Zumla A., Maeurer M. Totally-drug resistant tuberculosis and adjunct therapies. *J. Intern. Med.* **2014**. Published online Jan 18. DOI:10.1111/joim.12264.

Parikh S.L., Xiao G., Tonge P.J. Inhibition of InhA, the enoyl reductase from *Mycobacterium tuberculosis*, by triclosan and isoniazid. *Biochemistry* **2000**, *39*, 7645-7650.

Pauli I., dos Santos R.N., Rostirolla D.C., Martinelli L.K., Ducati R.G., Timmers L.F., Basso L.A., Santos D.S., Guido R.V.C., Andricopulo A.D., Norberto de Souza O. Discovery of new inhibitors of *Mycobacterium tuberculosis* InhA enzyme using virtual screening and a 3D-pharmacophore-based approach. *J. Chem. Inf. Modell.* **2013**, *53*, 2390-2401.

Pethe K., Bifani P., Jang J., Kang S., Park S., Ahn S., Jiricek J., Jung J., Jeon H.K., Cecjetto J., Christophe T., Lee H., Kempf M., Jackson M., Lenaerts A.J., Pham H., Jones V., Seo M.J., Kim Y.M., Seo M., Seo J.J., Park D., Ko Y., Choi I., Kim R., Kim S.Y., Lim S., Yim S-A., Nam J., Kang H., Kwon H., Oh C-T., Cho Y., Jang Y., Kim J., Chua A., Tan B.H., Nanjundappa M.B., Rao S.P.S., Barnes W.S., Walker J.R., Alonso S., Lee S., Kim J., Oh S.,

Oh T., Nehrbass U., Han S-J., No Z., Lee J., Brodin P., Cho S.N., Nam K., Kim J. Discovery of Q203, a potent clinical candidate for the treatment of tuberculosis. *Nat. Med.* **2013**, *19*, 1157-1160.

Rajendran V., Sethumadhavan R. Drug resistance mechanism of PncA in *Mycobacterium tuberculosis*. *J. Biomol. Struct. Dyn.* **2013**, *32*, 209-221.

Ramaswamy S.V., Reich R., Dou S.J., Jasperse L., Pan X., Wanger A., Quitugua T., Graviss E.A. Single nucleotide polymorphisms in genes associated with isoniazid resistance in *Mycobacterium tuberculosis*. *Antimicrob. Agents Chemother.* **2003**, *47*, 1241-1250.

Ramirez M.S., Tolmasky M.E. Aminoglycoside modifying enzymes. *Drug Resist. Updat.* **2010**, *13*, 151-171.

Rawat R., Whitty A., Tonge P.J. The isoniazid-NAD adduct is a slow, tight-binding inhibitor of InhA, the *Mycobacterium tuberculosis* enoyl reductase: adduct affinity and drug resistance. *Proc. Natl. Acad. Sci. U.S.A.* **2003**, *100*, 13881-13886.

Roujeinikova A., Levy C.W., Rowsell S., Sedelnikova S., Baker P.J., Minshull C.A., Mistry A., Colls J.G., Camble R., Stuitje A.R., Slabas A.R., Rafferty J.B., Pauptit R.A., Viner R., Rice D.W. Crystallographic analysis of triclosan bound to enoyl reductase. *J. Mol. Biol.* **1999**, *294*, 527-535.

Rozwarski D.A., Grant G.A., Barton D.H., Jacobs Jr. W.R., Sacchettini J.C. Modification of the NADH of the isoniazid target (InhA) from *Mycobacterium tuberculosis*. *Science* **1998**, *279*, 98-102.

Rozwarski D.A., Vilcheze C., Sugantino M., Bittman R., Sacchettini J.C. Crystal structure of the *Mycobacterium tuberculosis* enoyl-ACP reductase, InhA, in complex with NAD<sup>+</sup> and a C16 fatty acyl substrate. *J. Biol. Chem.* **1999**, *274*, 15582-15589.

Sani M., Houben E.N., Geurtsen J., Pierson J., de Punder K., van Zon M., Wever B., Piersma S.R., Jimenez C.R., Daffe M., Appelmelk B.J., Bitter W., van der Wel N., Peters P.J. Direct visualization by cryo-EM of the mycobacterial capsular layer: a labile structure containing ESX-1-secreted proteins. *PLoS Pathog.* **2010**, *6*, e1000794:1-10.



Shanthi V., Ramanathan K. Identification of potential inhibitor targeting enoyl-acyl carrier protein reductase (InhA) in *Mycobacterium tuberculosis*: a computational approach. *3 Biotech* **2014**, *4*, 253-261.

Shirude P.S., Madhavapeddi P., Naik M., Murugan K., Shinde V., Nandishaiah R., Bhat J., Kumar A., Hameed S., Holdgate G., Davies G., McMiken H., Hegde N., Ambady A., Venkatraman J., Panda M., Bandodkar B., Sambandamurthy V.K., Read J.A. Methyl-Thiazoles: A novel mode of inhibition with the potential to develop novel inhibitors targeting InhA in *Mycobacterium tuberculosis*. *J. Med. Chem.* **2013**, *56*, 8533-8542.

Silva P.E., Bigi F., Santangelo M.P., Romano M.I., Martin C., Cataldi A., Ainsa J.A. Characterization of P55, a multidrug efflux pump in *Mycobacterium bovis* and *Mycobacterium tuberculosis*. *Antimicrob. Agents Chemother.* **2001**, *45*, 800-804.

Singh M., Jadaun G.P.S., Srivastava R.K., Chauhan V., Mishra R., Gupta K., Nair S., Chauhan D.S., Sharma V.D., Venkatesan K., Katoch V.M. Effect of efflux pump inhibitors on drug susceptibility of ofloxacin resistant *Mycobacterium tuberculosis* isolates. *Indian J. Med. Res.* **2011**, *133*, 535-540.

Sivaraman S., Zwahlen J., Bell A.F., Hedstrom L., Tonge P.J. Structure-activity studies of the inhibition of FabI, the enoyl reductase from *Escherichia coli*, by triclosan: kinetic analysis of mutant FabIs. *Biochemistry* **2003**, *42*, 4406-4413.

Sotgiu G., Centis R., D'Ambrosio L., Alffenaar J.W.C., Ager H.A., Caminero J.A., Castiglia P., De Lorenzo S., Ferrera G., Koh W.J., Scheter G.F., Shim T.S., Singla R., Skrahina A., Spanevello A., Udvardi Z.F., Villar M., Zampogna E., Zellweger J.P., Zumla A., Migliori G.B. Efficacy, safety and tolerability of linezolid containing regimens in treating MDR-TB and XDR-TB: systematic review and meta-analysis. *Eur. Respir. J.* **2012**, *40*, 1430-1442.

Stigliani J.L., Arnaud P., Delaine T., Bernardes-Génisson V., Meunier B., Bernadou J. Binding of the tautomeric forms of isoniazid-NAD adducts to the active site of the *Mycobacterium tuberculosis* enoyl-ACP reductase (InhA): A theoretical approach. *J. Mol. Graphics Modell.* **2008**, *27*, 536-545.

Stocker F.B. and Evans A.J. Synthesis of 6-aryl-4,5-dibenzamido-1,2,3,6-tetrahydropyridines. *J. Org. Chem.* **1990**, *55*, 3370-3373.

- Stoffels K., Mathys V., Fauville-Dufaux M., Wintjens R., Bifani P. Systematic analysis of pyrazinamide-resistant spontaneous mutants and clinical isolates of *Mycobacterium tuberculosis*. *Antimicrob. Agents Chemother.* **2012**, *56*, 5186-5193.
- Sullivan T.J., Truglio J.J., Boyne M.E., Novichenok P., Zhang X., Stratton C.F., Li H.J., Kaur T., Amin A., Johnson F., Slayden R.A., Kisker C., Tonge P.J. High affinity InhA inhibitors with activity against drug-resistant strains of *Mycobacterium tuberculosis*. *ACS Chem. Biol.* **2006**, *1*, 43-53.
- Takayama K., Kilburn J.O. Inhibition of synthesis of arabinogalactan by ethambutol in *Mycobacterium smegmatis*. *Antimicrob. Agents Chemother.* **1989**, *33*, 1493-1499.
- Takayama K., Wang C., Besra G.S. Pathway to synthesis and processing of mycolic acids in *Mycobacterium tuberculosis*. *Clin. Microbiol. Rev.* **2005**, *18*, 81-101.
- Takayama K., Wang L., David H.L. Effect of isoniazid on the *in vivo* mycolic acid synthesis, cell growth, and viability of *Mycobacterium tuberculosis*. *Antimicrob. Agents Chemother.* **1972**, *2*, 29-35.
- Takiff H.E., Salazar L., Guerrero C., Philipp W., Huang W.M., Kreiswirth B., Cole S.T, Jacobs Jr. W.R., Telenti A. Cloning and nucleotide sequence of *Mycobacterium tuberculosis* gyrA and gyrB genes and detection of quinolone resistance mutations. *Antimicrob. Agents Chemother.* **1994**, *38*, 773-780.
- Telenti A., Philipp W.J., Sreevatsan S., Bernasconi C., Stockbauer K.E., Wieles B., Musser J.M., Jacobs Jr. W.R. The emb operon, a gene cluster of *Mycobacterium tuberculosis* involved in resistance to ethambutol. *Nat. Med.* **1997**, *3*, 567-570.
- Timmins G.S., Deretic V. Mechanisms of action of isoniazid. *Mol. Microbiol.* **2006**, *62*, 1220-1227.
- Tonge P.J., Kisker C., Slayden R.A. Development of modern InhA inhibitors to combat drug resistant strains of *Mycobacterium tuberculosis*. *Curr. Top. Med. Chem.* **2007**, *7*, 489-498.
- Udwadia Z.F., Amale R.A., Ajbani K.K., Rodrigues C. Totally drug-resistant tuberculosis in India. *Clin. Infect. Dis.* **2012**, *54*, 579-581.

Vannelli T.A., Dykman A., de Montellano P.R.O. The antituberculosis drug ethionamide is activated by a flavoprotein monooxygenase. *J. Biol. Chem.* **2002**, *277*, 12824-12829.

Velayati A.A., Masjedi M.R., Farnia P., Tabarsi P., Ghanavi J., Ziazarifi A.H., Hoffner S.E. Emergence of new forms of totally drug-resistant tuberculosis bacilli: super extensively drug-resistant tuberculosis or totally drug-resistant strains in iran. *Chest* **2009**, *136*, 420-425.

Vezeris N., Truffot-Pernot C., Aubry A., Jarlier V., Lounis N. Fluoroquinolone-containing third-line regimen against *Mycobacterium tuberculosis* in vivo. *Antimicrob. Agents Chemother.* **2003**, *47*, 3117-3122.

Vilchèze C., Jacobs Jr. W.R. The mechanism of isoniazid killing: clarity through the scope of genetics. *Annu. Rev. Microbiol.* **2007**, *61*, 35-50.

Vilcheze C., Morbidoni H.R., Weisbrod T.R., Iwamoto H., Kuo M., Sacchettini J.C., Jacobs Jr. W.R. Inactivation of the *inhA*-encoded fatty acid synthase II (FASII) enoyl-acyl carrier protein reductase induces accumulation of the FASI end products and cell lysis of *Mycobacterium smegmatis*. *J. Bacteriol.* **2000**, *182*, 4059-4067.

Villemagne B., Crauste C., Flipo M., Baulard A.R., Déprez B., Willand N. Tuberculosis: the drug development pipeline at a glance. *Eur. J. Med. Chem.* **2012**, *51*, 1-16.

Wachino J., Shibayama K., Kimura K., Yamane K., Suzuki S., Arakawa Y. RmtC introduces G1405 methylation in 16S rRNA and confers high-level aminoglycoside resistance on Gram-positive microorganisms. *FEMS Microbiol. Lett.* **2010**, *311*, 56-60.

Wall M.D., Oshin M., Chung G.A., Parkhouse T., Gore A., Herreros E., Cox B., Ducan K., Evans B., Everett M., Mendoza A. Evaluation of *N*-(phenylmethyl)-4-[5-(phenylmethyl)-4,5,6,7-tetrahydro-1*H*-imidazo[4,5-*c*]pyridin-4-yl]benzamide inhibitors of *Mycobacterium tuberculosis* growth. *Bioorg. Med. Chem. Lett.* **2007**, *17*, 2740-2744.

Wang F., Langley R., Gulten G., Dover L.G., Besra G.S., Jacobs Jr. W.R., Sacchettini J.C. Mechanism of thioamide drug action against tuberculosis and leprosy. *J. Exp. Med.* **2007**, *204*, 73-78.

Wehrli W. Rifampin: mechanisms of action and resistance. *Rev. Infect. Dis.* **1983**, *5*, S407-S411.

Whitesitt C.A., Simon R.L., Reel J.K., Sigmund S.K., Phillips M.L., Shadle J.K., Heinz L.J., Koppel G.A., Hunden G.A., Hunden D.C., Lifer S.L., Berry D., Ray J., Little S.P., Liu X., Marshall W.S., Panetta J.A. Synthesis and structure-activity relationships of benzophenones as inhibitors of cathepsin D. *Bioorg. Med. Chem.* **1996**, *6*, 2157-2162.

Wilming M., Johnsson K. Spontaneous formation of the bioactive form of the tuberculosis drug isoniazid. *Angew. Chem. Int. Ed.* **1999**, *38*, 2588-2590.

Winder F.G.; Collins P.B.; Whelan D. Effects of ethionamide and isoxyl on mycolic acid synthesis in *Mycobacterium tuberculosis* BCG. *J. Gen. Microbiol.* **1971**, *66*, 379-380.

World Health Organization Global Tuberculosis Report, 2013.  
[http://apps.who.int/iris/bitstream/10665/91355/1/9789241564656\\_eng.pdf](http://apps.who.int/iris/bitstream/10665/91355/1/9789241564656_eng.pdf)

Yuan Y., Zhu Y., Crane D.D., Barry III C.E. The effect of oxygenated mycolic acid composition on cell wall function and macrophage growth in *Mycobacterium tuberculosis*. *Mol. Microbiol.* **1998**, *29*, 1449-1458.

Zatorski A., Watanabe K.A., Carr S.F., Goldstein B.M., Pankiewicz K.W. Chemical Synthesis of Benzamide Adenine Dinucleotide: Inhibition of Inosine Monophosphate Dehydrogenase (Types I and II) 1. *J. Med. Chem.* **1996**, *39*, 2422-2426.

Zhang D., Lu Y., Liu K., Liu B., Wang J., Zhang G., Zhang H., Liu Y., Wang B., Zheng M., Fu L., Hou Y., Gong N., Lv Y., Li C., Cooper C.B., Upton A.M., Yin D., Ma Z., Huang H. Identification of less lipophilic riminophenazine derivatives for the treatment of drug-resistant tuberculosis. *J. Med. Chem.* **2012**, *55*, 8409-8417.

Zhang Y., Mitchison D. The curious characteristics of pyrazinamide: a review. *Int. J. Tuberc. Lung Dis.* **2003**, *7*, 6-21.

Zignol M., Hosseini M.S., Wright A., Weezenbeek C.L., Nunn P., Watt C.J., Williams B.G., Dye C. Global incidence of multidrug-resistant tuberculosis. *J. Infect. Dis.* **2006**, *194*, 479-85

Zuber B., Chami M., Houssin C., Dubochet J., Griffiths G., Daffe´ M. Direct visualization of the outer membrane of mycobacteria and corynebacteria in their native state. *J. Bacteriol.* **2008**, *190*, 5672-5680.

Zumla A.I., Gillespie S.H., Hoelscher M., Philips P.P., Cole S.T., Abubakar I., McHugh T.D., Schito M., Marurer M., Nunn A.J. New antituberculosis drugs, regimens, and adjunct therapies: needs, advances, and future prospects. *Lancet Infect. Dis.* **2014**, *14*, 327-340.

## Appendix

---

### List of Publications

**Pedgaonkar G.S.**, Sridevi J.P., Kumar V.U.J., Saxena S., Devi P.B., Renuka J., P. Yogeewari, Sriram D. Development of 2-(4-oxoquinazolin-3(4*H*)-yl)acetamide derivatives as novel enoyl-acyl carrier protein reductase (InhA) inhibitors for the treatment of tuberculosis. *Eur. J. Med. Chem.* **2014**, *86*, 613-627. DOI: 10.1016/j.ejmech.2014.09.028.

**Pedgaonkar G.S.**, Sridevi J.P., Kumar V.U.J., Saxena S., Devi P.B., Renuka J., P. Yogeewari, Sriram D. Development of benzo[*d*]oxazol-2(3*H*)-ones derivatives as novel inhibitors of *Mycobacterium tuberculosis* InhA. *Bioorg. Med. Chem.* **2014**. DOI: 10.1016/j.bmc.2014.08.031. [In Press]

**Pedgaonkar G.S.**, Sridevi J.P., Kumar V.U.J., Saxena S., Devi P.B., Renuka J., P. Yogeewari, Sriram D. Development of 4-amino-1,5-dimethyl-2-phenyl-1*H*-pyrazol-3(2*H*)-one derivatives as novel inhibitors of *Enoyl acyl carrier protein reductase* (InhA) from *Mycobacterium tuberculosis*. [Communicated to *Bioorg. Med. Chem. Lett.*]

**Pedgaonkar G.S.**, Sridevi J.P., Kumar V.U.J., Saxena S., Devi P.B., Renuka J., P. Yogeewari, Sriram D. Development of Rhodanine Derivatives as Novel Inhibitors of *Mycobacterium tuberculosis* InhA. [Communicated to *Arch. Pharm. Chem. Life Sci.*]

### Paper presented at International Conference

**Pedgaonkar G.S.**, Kumar V.U.J., Sridevi J.P., P. Yogeewari, Sriram D. Development of novel substituted benzoxazolinone derivatives as potential anti-tubercular agents, 2<sup>nd</sup> UK-India MedChem Congress, 22-23 March 2013, Hyderabad.

## **BIOGRAPHY OF PEDGAONKAR GANESH SITARAM**

Mr. Pedgaonkar Ganesh Sitaram completed his Bachelor of Pharmacy from Dr. Babasaheb Ambedkar Marathwada University Aurangabad, Maharashtra, and Master of Pharmacy in Pharmaceutical chemistry from Swami Ramanand Teerth Marathwada University, Nanded, Maharashtra. He has about 2 years of academic experience in teaching at Shree Bhagwan college of Pharmacy, Aurangabad, Maharashtra from 2009-2011. He has been appointed as a DST INSPIRE Fellow at Birla Institute of Technology and Science, Pilani, Hyderabad campus from 2012-2014 under the supervision of Prof. D. Sriram. He has published four scientific papers in well-renowned international journals (two from previous work and two from current work) and also presented papers at international conferences.

## **BIOGRAPHY OF Professor D. SRIRAM**

D. Sriram is presently working in the capacity of Professor at Department of Pharmacy, Birla Institute of Technology and Science, Pilani, Hyderabad campus. He received his Ph.D. in 2000 from Banaras Hindu University, Varanasi. He has been involved in teaching and research for last 15 years. He has 235 peer-reviewed research publications to his credit. He has collaborations with various national and international organizations such as Karolinska Institute, Sweden; National Institute of Immunology, New Delhi; Institute of Science and Technology for Tuberculosis, PA, Brazil etc. He was awarded the Young Pharmacy Teacher of the year award of 2006 by the Association of Pharmacy Teachers of India. He received ICMR Centenary year award in 2011. He has guided 6 Ph.D. students and 14 students are pursuing Ph.D. currently. His research is funded by agencies like the UGC, CSIR, ICMR, DBT and DST.